Non-Invasive Detection of Internal Potato Defects for Reduction of Food Loss in The Fresh Produce Supply Chain

Edward Flint Hill-King

Lancaster Environment Centre

This dissertation is submitted for the degree of Doctor of Philosophy

May 2025

1 Abstract

Author: Edward Flint Hill-King

Title: Non-invasive detection of internal potato defects for reduction of food loss in the fresh produce supply chain

The potato (*Solanum tuberosum*) is the most important non-grain vegetable in the world, playing a major role in human nutrition worldwide. Half of all potato grown, however, does not reach the fork of the consumer. Food waste and losses represent a substantial challenge to potato supply chains, as well as to global food systems in general. Food waste and losses negatively impact the world in a variety of ways, contributing to food insecurity, environmental degradation and economic losses.

A leading cause of potato waste and losses is tuber defects, which result in produce failing to meet safety, storage or consumer standards. While defects with external symptoms are effectively screened for via optical grading lines, many defects exhibit only internal defects, which is a barrier to their detection. Internal defects are widely screened for by solely destructive means; novel non-destructive approaches are needed to improve the detection and screening of internal potato defects.

Work carried out in this thesis investigates the potential for non-invasive non-destructive approaches to detect internal potato defects to address the challenges they pose to the fresh potato supply chain. This research uncovers promising avenues of non-invasive non-destructive detection of internal potato defects, applying optical and electrical spectroscopy. NIR reflectance spectroscopy successfully provided a means of detecting blackheart and spraing in intact potatoes. Blackheart was also successfully detected with a novel approach to impedance spectroscopy. In addition to these findings this work develops an exciting novel method for extending the shelf-life of fresh produce such as tomatoes to reduce losses in homes, retail and transit.

It is a mistake to think you can solve any major problems just with potatoes – Douglas Adams

This research endeavours to assist potatoes, that they may help solve some of the greatest problems of our age.

2 Table of Contents

3 Table of tables

4 Table of figures

5 Acknowledgements

I would like to thank all those who have made this project possible. My internal supervisors: Professor Martin McAinsh, and Doctor Mike Roberts have continuously been of immense support throughout the duration of this degree. I have also received advice and provision of a NIRvascan ASP-NIR-M-Reflect spectrometer from my external supervisor: Professor Frank Martin.

Generous funding from BBSRC and The Waitrose Partnership have supported both me and my research. Burgess Farms, who supply potatoes to Waitrose, have been invaluable partners, providing expertise and study specimens. I would like to thank in particular Caroline Williams and Brogan Connolly from Burgess Farms for their correspondence and support.

I express gratitude towards Louise Hill-King (LHK Ltd.) for proofreading and maternal support, as well as Michael Hill-King for assistance during the application phase, with special thanks to Eva Jones for her moral support and patience.

For lab support and loan of a CO_2 valve control system I thank Doctor Geoff Holroyd, Maureen Harrison for support with the plant growth facilities and Professor Ian Dodd for advice on potato growth. Finally, I would like to thank Will Medd for leading a series of writing retreats funded by the Waitrose CTP.

6 Author's Declaration

I declare that the work contained in this thesis is my own. This work has not been submitted substantially in the same form for award of another higher degree. This thesis does not exceed the word limit of 80,000 words excluding preceding and proceeding material; the main body of this thesis contains 45,389 words.

The manuscript in Appendix 1 has been submitted for publication to *Plants People and Planet*, and is currently under peer review.

1 Chapter 1: Introduction

1.1 Project overview

Food waste and losses occur at key stages of the fresh produce supply chain (Corrado & Sala, 2018): growth, storage, distribution, retail and consumption. This project examines the potential of novel non-invasive approaches to vegetable defect detection to tackle food waste and loss challenges from farm to fork using the potato (*Solanum tuberosum*) as an example. Potatoes are the most important non-grain vegetable in the world, cultivated in over 100 countries worldwide (International Potato Center, 2024), with global annual yield exceeding 370 billion tonnes (Mishra, 2024). Additionally, potatoes have a long history intertwined with the cultures that have cultivated and consumed them (see Appendix 1 for a manuscript describing an analysis of our changing relationship with the potato, viewed through the lens of art history).

1.1.1 Food waste and losses

Food waste and losses describe food that is grown but does not reach human consumption (Omolayo, et al., 2021). This can be in the form of losses in yield, losses during the supply chain, losses during processing, or waste at the retail, consumer and preparation level (Urugo et al., 2024). Food loss specifically refers to pre-consumer losses, and food waste to waste at the end of the supply chain by consumers or retail (Parfitt et al., 2010; Stancu et al., 2016). The first World Food Conference in 1974 set the target to half the then 15% rate of food waste and loss as a means of addressing world hunger (Parfitt et al., 2010); 50 years later we have instead doubled this rate to 30% (FAO, 2011; Scialabba, 2015). Estimates for global food waste and losses per person range between 194 and 389 kg per annum (Corrado & Sala, 2018). Food waste and losses have considerable impact on the world as they increase the need for agricultural output without increasing food supply, contributing to food insecurity (Munesue et al., 2015) and environmental degradation (Munesue et al., 2015) and causing economic losses (Slorach et al., 2019). The United Nations (UN) Sustainable Development Goal (SDG) 12.3 calls for a 50% reduction in food waste and losses between 2015 and 2030 (UN General Assembly, 2015), although insufficient progress has been made towards achieving this goal (UN Environment Programme, 2024).

1.1.2 Food insecurity and world hunger

Global hunger is a worryingly increasing issue (Abbas et al., 2025). The State of Food Security and Nutrition in the World (SOFI) publication reports that the number of people classified as hungry grew by 150 million between 2019 and 2021 to 828 million (World Health Organization, 2022), and 2 billion people were without access to safe, nutritious and sufficient food in 2019 [Food and Agriculture Organization of the United Nations (FAO), 2020]. While progress has been made towards ending world hunger, there has been stagnation in recent years as hunger continues to worsen in many regions, and 9 million people a year die from hunger (WHH, Concern Worldwide & IFHV, 2024).

The UN SDGs call for ending food insecurity and world hunger, while limiting the impacts upon food systems of anthropogenic climate change (UN, 2015; Crippa, 2021). Climate change is a key driver of global hunger and food insecurity (Abbas et al., 2025; Muluneh, 2021); it is therefore imperative that food system challenges are tackled without exacerbating environmental impacts. Sustainable and efficient food systems are concerned not only with high yield but efficiency at all stages of the supply chain (Eriksen, 2009). Food waste and losses occurring throughout the supply chain pose a major challenge to food security, particularly impacting those in lower-income regions (Gatto & Chepeliev, 2024) where there are also many other food security challenges such as poverty, political instability, urbanisation, population growth and trade barriers, for example, in Nigeria (Fawole et al., 2015) and South Africa (Battersby-Lennard et al., 2009). Reducing food waste and losses can therefore improve the effective output of food systems without requiring additional agricultural inputs in supply chains that are already under stress. Ripple et al. (2020), along with 11,258 signatories, has called for a drastic reduction in food waste in order to address the serious threats of climate change on food systems. However, global food waste and food losses continue to worsen (Wang et al., 2025), whilst the demand for food continues to increase, driven by the rise in the global population. The UN predicts the global population will reach 9.7 billion by 2050, and peak at ~10 billion by 2100 (Pison, 2019), with the population rising the most in developing regions (Fox, 2013) where issues of food insecurity are most severe, making food waste even more of a critical issue in these regions (Urugo et al., 2024).

1.1.3 Environmental impacts of food waste and losses

Agriculture has substantial environmental impacts, which are exacerbated by the elevated agricultural output required to meet the demand of the growing global population given the high rates of waste and loss in food production systems (Kohli et al., 2024). Degradation of land and water, and biodiversity loss due to agriculture (Foley et al., 2011) all have devastating consequences for the natural environment, resulting in significant impacts for ecosystem services and humanity (Midler, 2022, Tan et al., 2022). Disruption of water cycles impacts access to fresh water (Gleick & Cooley, 2021; Mishra, 2023), including that for crop watering (Gleick & Cooley, 2021). Watering of crops is a major demand for fresh water, with 20%–30% of the Earth's available surface water used for irrigation, accounting for ~90% of anthropogenic freshwater consumption (Rosa, 2022), although only around half of that water is used for crop growth due to inefficiency in distribution and application of water (Cassman et al., 2005). In addition, food waste and losses greatly increase the water consumption of agriculture, representing a quarter of all water used by agriculture (World Resources Institute, 2019).

Agriculture is the single largest land use globally, occupying 38% of Earth's ice-free terrestrial surface, 26% by pasture and 12% by cropland (Foley et al. 2011). Of that cropland, 62% is for human food, 35% for animal feed and 3% for other uses such as seed, energy and industrial products (Foley et al. 2011). Growth in cropland has been slowing due to agricultural intensification greatly increasing output her hectare (Hu et al., 2020). However, agricultural intensification has had substantial environmental impacts (Matson et al., 1997). Furthermore, 23% of cropland is used to grow food that is wasted or lost (Kummu, et al., 2012), equivalent to all cropland in Africa (Teigiserova et al., 2020).

Each stage of the supply chain contributes to the carbon footprint of our food systems (Scialabba, 2015), thus losses and waste further along the supply chain come at a greater environmental cost, which is further accentuated by waste at the consumer stage having the greatest carbon footprint of all stages of the supply chain (Scialabba, 2015). Where in the supply chain waste and losses primarily occur is dependent on regional income, with waste mostly occurring during the later stages of the supply chain

in higher-income countries and towards the early stages of the supply chain in lower-income countries (Kummu et al., 2012; Scialabba, 2015; Stancu et al., 2016). Different food waste and loss reduction strategies may be therefore differently suited to differing economies as a result of this.

The FAO estimates food waste to have an annual carbon emission of 3.6 $GtCO_2$ equivalents, not including the emissions of agricultural deforestation or other land use change, or 4.4 $GtCO_2$ equivalents per year including land use change (Scialabba, 2015). Carbon emission reductions have fallen disappointingly short of the targets laid out in the Paris agreement, member states only achieving a 2.6% reduction compared to the 43% reduction needed to limit warming to 1.5°C (UNFCCC Secretariat, 2024). Growing food that is not eaten constitutes 10% of the greenhouse gas emissions of wealthy countries (Stuart, 2009), therefore tackling food waste and losses could make major contributions to meeting carbon targets. The overwhelming impacts of agriculture on the environment and the unsustainability of our current food systems necessitate drastic reductions in food waste and losses to meet growing nutritional needs amongst a worsening environmental catastrophe.

1.1.4 Economic cost of food waste and losses

Food waste and losses have substantial economic impact (Venkat, 2011). Reductions in food waste and losses have great potential for savings for both households and supply chain members (Campoy-Muñoz et al., 2017). There has been a large global increase in food prices in recent years as part of the "cost of living crisis" (Robinson, 2023), with global food commodity prices 33% higher than before the COVID-19 pandemic (English & Tobi, 2023). Cost of imported food products in the UK grew twice as fast as domestic food products during this time (English & Tobi, 2023). However, in the UK, 70% of the potatoes consumed are grown domestically (Department for Environment, Food & Rural Affairs, 2024) positioning the potato as a reliable food source during this cost-of-living crisis.

The cost of food is a major contributor to the creation of food deserts (Janatabadi et al., 2024). Reduction of food losses and waste may therefore help with food accessibility during the cost-of-living crisis, especially for economically disadvantaged households, who are most affected by rising food prices (Meadows et al., 2024; Robinson, 2023). Although food commodity prices have begun to fall in the UK, this hasn't been reflected in retail prices (English & Tobi, 2023), suggesting reductions in consumer food waste may economically benefit consumers faster than reductions in food losses earlier in the supply chain. Whilst reduction in food waste and losses will undoubtedly have many economic benefits, agriculture is of great importance to rural economies (Sinabell, 2009). Post-harvest reductions in loss and waste may have the effect of reducing demand for a crop, posing challenges to rural communities and economies who are often highly dependent on agriculture in both developing and developed regions (Gowda et al., 2018; Loizou et al., 2019).

1.1.5 Waste in the potato supply chain

The year 2008 was declared the year of the potato by the UN to promote the potato as a tool for tackling poverty and world hunger (Lutaladio & Castaldi, 2009). Potatoes are well suited to many developing regions where land is scarce but labour is abundant providing not only essential nutrition but a source of income for escaping the poverty trap (Hussain, 2016). Potatoes are also vital to nutrition amongst high income regions (Goffart et al., 2022, Pllana et al., 2018).

1.1.6 Scale, source and impact of waste

Fresh produce constitutes a major contributor to retail food waste (Brancoli, 2017; Scholz, 2015). However, due to the low-production impact of fresh produce compared to other food stuffs such as bread, or especially beef, fresh produce only amounts to a small proportion of the environmental impact of retail food waste (Brancoli, 2017). Despite retail posing a site of high losses for fresh produce in general, the longevity and robustness of the potato delivers very low retail losses, accounting for only 2% of total potato losses (Tsolakis & Kumar, 2019; Willersinn, 2017). This suggests the potato is a crop well suited to the current climate of retail waste, and that research is required to tackle the 98% of potato losses and waste that occur at other stages of the supply chain.

Most of the potato that is grown in the UK never reaches the fork. Estimates of UK potato crop losses are as high as two-thirds (WRAP, 2012). Approximately 53%–55% of fresh potato production in Switzerland is lost, along with 41%–46% of processing potato stock (Willersinn et al., 2015). According to Willersinn et al.'s case study of Switzerland, of every 100 kg of potatoes grown, 53 kg are wasted (Willersinn & Mouron, 2017). Based on Willersinn et al.'s 2015 study of the Swiss potato supply chain, around half of all potato losses result from failure to meet safety, consumer or storage suitability standards (Willersinn et al., 2015), food safety accounting for 25%–34% of this waste. Failure to meet quality standards includes the occurrence of potato defects, which are injuries or pathologies that lower the quality of produce. Potato defects can either be external, such as greening, bruising, scabs and surface rots, or internal, such as necrosis, internal rots and cavitation. Defects therefore play a substantial role in waste and losses in the potato supply chain.

1.1.7 Role of defects in potato waste

Defects develop at all stages of the supply chain (Hermansyah & Romli, 2025; Kathayat & Rawat, 2019; Tort et al., 2022), so addressing defects throughout the supply chain is essential to enabling sustainable and efficient food systems. Blackheart is a common internal potato defect that usually occurs during storage when atmospheric CO_2 levels become elevated, lowering O_2 levels (Davis, 1926; Kiaitsi, 2015). Blackheart can also occur in wet hypoxic soils or when elevated tuber temperatures increase the respiration rate above that supported by available oxygen (Chapman, 2018). Consumer complaints regarding blackheart are most prevalent in late winter and spring (Kiaitsi, 2015), when potato supply is from storage, suggesting that most blackheart occurs during this stage of the supply chain. Blackheart causes necrotic damage within the pith and cortex of the tuber, resulting in blackened internal tissue, the namesake of the defect. Blackheart usually shows no external symptoms, leading to difficulty in non-destructive detection and screening. Blackheart is responsible for 25%–30% of consumer potato complaints (Kiaitsi, 2015), and as defects are a major driver of household food waste (Makhal et al., 2021), this customer dissatisfaction likely translates to waste. Another defect of internal necrosis is spraing. Unlike blackheart, spraing is a biotic defect caused by the Tobacco Rattle and mop-top viruses (Mølgaard & Nielsen, 1996). Similarly to blackheart, spraing typically exhibits no external symptoms (Thybo et al., 2004) posing a challenge to non-destructive detection.

Pest damage is also a major cause of potato defects (Gao et al., 2024). While many forms of pest damage are externally detectable such as slug damage, burrowing insect damage like wireworm can be challenging to detect. Wireworms (the larvae of click beetles), are especially detrimental to potatoes as they introduce pathogens into the tuber including *Rhizoctonia solani* which causes dry core (Keiser, 2012). Wireworm and drycore cause devastating losses of 7% of organic whole potato stock, drycore being the primary reason organic potatoes fail to meet quality standards as well as having substantial impacts on conventional potatoes (Keiser 2012).

Detecting potato defects is vital to their management for environmental, economic and food systems motives. Grading of potatoes allows for the highest quality produce to be sold at the highest margin and to uphold quality standards, while selling lower quality

produce to the appropriate markets and applications. Waste repurposing is important to waste and losses management (Sarma et al., 2024). Potato waste is repurposed for a variety of applications such as biogas, biochar and slurry (Maroušek et al., 2020). Repurposing of waste is thus still a form of waste as agricultural inputs are not translated into efficient energetic or nutrient outputs. Waste repurposing, however, is out of the scope of this project, where this research focuses on reduction of waste and losses.

1.2 Current approaches to potato defect screening

Screening of defects is essential for providing quality produce and managing the storage, distribution, and retail of potatoes to minimise the economic and quality impacts of defects. Potato defect screening can, however, be a substantial source of waste and undervaluing of produce. Current approaches to potato defect detection are divided into destructive sample testing (Heinemann, 1996; Pedreschi, 2016; Razmjooy, 2012), and online optical grading (Pedreschi et al., 2015; Wang et al., 2016). Optical grading is effective at identifying external defects, although defects that show no external symptoms are elusive to these approaches. Internal defects are screened for destructively, a sample of each truckload transported from farm to storage/sorting facility is cut open to grade the shipment. While this method is effective at ascertaining the rate and severity of internal defects of a shipment, due to its destructive nature it cannot be used to assess individual intact tubers. This results in potatoes being wasted, as when a shipment contains an unacceptable rate of defective tubers, the entire shipment receives that grading and may be wasted or used for lower value applications. Therefore, non-destructive approaches to internal potato defect detection would enable individual tubers to be screened. This could be applied to shipments that fail to meet quality control requirements to sort out defective potatoes and lower the rate of defects in the shipment to an acceptable level.

Consumer preferences and standards make serious contribution to waste and losses of fresh produce (Gracia & Gomez, 2020). This occurs at the consumer levels of the supply chain, at retail and in private homes, but also at earlier stages of the supply chain where consumer standards are enforced pre-retail. Many vegetable defects detract from the attractiveness of produce without posing any significant health hazard to the consumer,

for example blackheart in potatoes. However, such cosmetic defects can have considerable impact on household waste as they are perceived as ugly or distasteful to consumers (Makhal et al., 2021). While many potato defects do not pose a hazard to the consumer, biotic defects can render potatoes and other produce unsafe for human consumption, such as rots. Screening for biotic defects can be especially important as biotic defects may pathogenically spread through storage facilities without effective management (Mumia, 2017). Detection of both cosmetic and hazardous defects are important as both contribute to waste and losses. Shifts in consumer attitudes and culture towards variation in produce appearance may be effective for reducing waste of cosmetically defective food (Makhal et al., 2021). Nevertheless, even if consumer attitudes shift, screening of these defects will still be important as they may reflect disorders that affect the plant in other important ways. The zebra chip disease, for example, has only a cometic effect on the tubers but causes plant disease, reducing yield (Wenninger & Rashed, 2024).

1.3 Optical spectroscopy in vegetable screening

One approach that can be applied for non-destructive screening of potato and other vegetable defects is optical spectroscopy (Dospatliev et al., 2013). Optical spectroscopy is the study of how electromagnetic radiation interacts with a sample at differing frequencies. Two forms of spectroscopy, reflectance and transmittance, are most commonly used in vegetable assessment. However, other methods such as RAMAN spectroscopy see occasional research (Xu et al., 2023). Reflectance spectroscopy positions a light source and detector on the same side of the sample, such that the light received by the detector has been reflected off the sample. The detector measures frequency composition of the reflected light, which is compared to the composition of the light source, such that the absorbance of the sample at each wavelength within the band of the source can be calculated. This produces an “absorbance spectrum” were absorbance (or inversely reflectance) is plotted along the frequency axis. Transmittance spectroscopy differs from reflectance as the source and detector are positioned on opposing sides of the sample, such that light reaching the detector has been transmitted through the sample. Transmittance also produces an absorbance spectrum along the frequency axis.

Absorbance spectra give chemometric insights into the composition of the sample as differing chemicals bonds, bends and molecular vibrations absorb differing frequencies of light (Weyer & Lo, 2002). Absorbance spectra of samples can be compared to the spectra of known compounds to estimate the presence and concentration of that compound in the sample, and peaks within a sample's absorbance spectra can be compared to peaks associated with specific compounds or chemical properties. In the case of vegetable screening, absorbance spectra can be compared between vegetables with known quality parameters, such as the presence or absence of a given defect. Spectra of vegetables with unknown quality parameters can be compared to datasets of vegetable spectra to estimate the quality parameters of that vegetable. Reflectance spectroscopy has practicality advantages over transmittance spectroscopy when applied to industry or the field, as reflectance spectroscopy can be operated in a point-and-shoot manner, including handheld units.

Both near-infrared (NIR) and mid-infrared (MIR) spectroscopy are emerging as vegetable assessment technologies (Escuredo, 2021; Su et al., 2021). The terms NIR and MIR describe the bandwidth of the light source and detector used. NIR spectroscopy has seen widespread interest for determination of micronutritional content (Ren et al., 2025) from destructive potato samples, such as phosphate content (Thygesen et al., 2001) and carotenoid content (Bonierbale et al., 2009), as well as phenolic anthocyanin and antioxidant capacity (López-Maestresalas, 2016). In addition to macronutritional values such as carbohydrate content (Brunt & Drost, 2010; Chen et al., 2004; Haase, 2011, Ren et al., 2025), protein content (Brunt & Drost, 2010; Fernández-Ahumada et al., 2006), and lipid content (Ni et al., 2011). Optical spectroscopy is well suited for vegetable quality assessment as it can be fast and accurate without damage or contamination of samples (López et al., 2013). There is growing interest in optical spectroscopy for non-invasive screening of potato and other crops (Su et al., 2017); both reflectance and transmittance spectroscopy are emerging as a non-destructive approach to internal potato defect detection (Imanian et al., 2021; Semyalo et al., 2024). Research into applications of NIR spectroscopy for non-destructive vegetable assessment is being conducted with a variety of produce, including starchy vegetables similar to potato-like sweet potato (Kudenov et al., 2021) and cassava (Bantadjan et al.,

2020), as well as other vegetables such as chestnuts (Hu et al., 2017; Lui et al., 2011; Moscetti et al., 2014), squash (Torres et al., 2019), apples (Si et al., 2022), tomatoes (Ścibisz et al., 2011; Si et al., 2022) and melon (Li et al., 2019). Promising non-destructive results are emerging for defects like blackheart (Guo et al., 2024) and zebra chip disease (Liang et al., 2018); however, the range of defects with non-destructive results is limited, with most progress in the field being determination of nutritional content. In addition to postharvest applications, spectroscopy could be applied pre-harvest to detect warning signs of defect-forming plant pathology. For example, spectroscopy has proved to be an effective and fast method of characterising pathogenic plant diseases via leaf spectra (Sankaran et al., 2010).

1.4 Electrical impedance spectroscopy in vegetables

In contrast to optical spectroscopy, another approach to vegetable assessment is electrical spectroscopy. Impedance describes electrical losses of an AC signal through a system, comprising two constituents: resistance, R, and reactance, X. Resistance represents electrical energy dissipated as heat, whereas reactance represents energy stored inductively and capacitively. Impedance, denoted as Z, is a complex value, with resistance as the real part, and reactance the imaginary part (Equation 1.1).

$$Z = R + jX \quad [1.1]$$

Bioimpedance is the impedance of a biological sample or system. Biological systems are heterogeneous and comprise many differing fluids, tissues and membranes. This complex multiphase structure creates a complex frequency response to an electrical signal. At low frequencies in plant matter, the intercellular fluid provides lower impedance than cells themselves, whereas at higher frequencies the cells impede current less than intercellular fluids (Abdelrahman et al., 2021).

Electrical impedance spectroscopy (EIS) is an analytical tool where electrical excitation signals are passed through a sample to study the relationships between electrical parameters such as impedance, phase, amplitude or input frequency (Cheng et al., 2022). Research has been conducted into the applications of EIS to fruit and vegetable quality assessment (Ibba, 2021; Li et al., 2019a; Cheng et al., 2022), including work on potatoes measuring moisture content (Ando et al., 2014) and assessing freeze–thaw damage (Feng, 2021; Zhang, 1992). Impedance spectroscopy has been used to assess the microstructural properties of intact potatoes to study changes that occur during heating above 50°C (Fuentes et al., 2014). However, existing work on potato assessment via electrical methods has been limited, only applied to a narrow range of properties, and not applicable to defect screening. Destructive sample processing (Sobotka et al., 2006; Zhang et al., 1990) and invasive electrodes (Cabrera-López & Velasco-Medina, 2019) limit the applicability of current methods to industrial potato defect detection. There has also been limited translation from lab experimentation to industrial field deployment (Ibba, 2021). Further novel research is required to progress food system

applications of EIS; research will be conducted in this thesis into the potential of electrical methods for non-invasively detecting model potato defects.

1.4.1 Equivalent circuits of plant tissue

While analysis by EIS data is often performed by Nyquist plots (Lui, 2006; Cabrera-López & Velasco-Medina, 2019), complex plane plots or frequency domain plots, another analytical method is to model the observed electrical behaviour of the sample with an equivalent circuit. The Hayden model (Figure 1.1 a) is the most commonly used equivalent circuit in plant EIS, based on the structure of a single cell (Hayden et al., 1969). The model breaks down the cell into three subsystems: extracellular fluid; the cell wall; and intracellular fluid. Other elements are considered negligible and not included in this model. Both the external and internal cellular fluids are modelled with a single resistor. Due to the higher resistance of the cell wall, it forms a Faradaic interface with the more conductive cellular fluids, and thus is modelled by a resistor and capacitor in parallel. Experimental results have shown the membrane resistance to be sufficiently high to remove it from the model; this is known as the simplified Hayden model (Azzarello et al., 2012). Some simplifications for intact produce also remove the intracellular resistance, leaving only a resistor and capacitor in parallel (Rehman et al., 2011). Some modern techniques explore fractional element versions of the simplified Hayden model, where the capacitive element is replaced by a fractional order element. Rather than the Laplace domain impedance of Sc^{-1} of an ideal capacitor, fractional order elements have an impedance of S^{α}, where α is a real number (Bošković et al., 2017). While fractional order models provide better fit to observed results, they are less biologically interpretable (Ibba, 2021). Equivalent circuit models allow for the values of the equivalent elements to be estimated and used for comparison between samples or to inform the underlying mechanisms behind observed electrical properties.

Another equivalent circuit that has been used in plant tissue EIS research is the Randle's circuit (Jesus et al., 2006) (Figure 1.1 b). The Randle's circuit models a Faradaic reaction to an electrochemical interface with semi-infinite diffusion. The circuit consists of an electrolyte resistance, a charge transfer resistance, a double-layer capacitance and a Warburg impedance. The Warburg impedance is a constant phase component that models diffusion. Electrolyte resistance represents the ohmic

resistance of electrolytes in the system and is in series with the rest of the circuit. The charge transfer resistance represents the ohmic resistance due to the energy requirement to transfer a charge from one body to another. A Warburg element models diffusion in a dielectric, point charges diffusing to the surface of a body due to Maxwellian relaxation.

While fractional order models like the Randle's circuit or fractional variants of the Hayden model offer better fit to observed results, the better biological interpretability of integer order models like the Hayden model makes them well suited for vegetable assessment (Ibba, 2021). Abstract and black box data can be acquired without an equivalent circuit, so fractional models may not offer additional benefits to this project. The Hayden model was chosen for this research, as the model is based on biological structures it can be more easily altered to model damaged tissue and offers greater interpretability than other models.

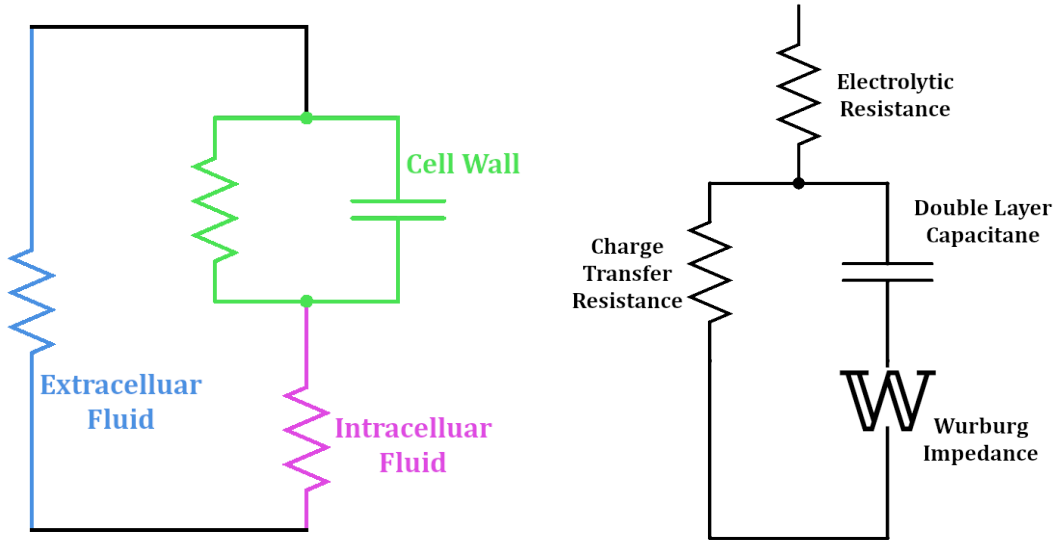

Figure 1.1 Equivalent circuits of plant tissue.
a: Randle's equivalent circuit of plant matter. b: Simplified Hayden equivalent circuit of plant cell.

1.5 Summary

Food waste and losses are a serious growing issue with substantial impacts on humanity, the environment and the economy. Rates of food waste and losses are especially high in the potato, one of the most globally crucial crops. Novel approaches are needed to reduce food waste and losses; spectroscopy, both optical and electrical, may be valuable techniques for lowering waste and losses of potato.

1.6 Aims and objectives of project

The overall aim of this project is to investigate non-destructive approaches to detecting internal potato defects for reduction of food waste and losses. The objectives of this project are as follows:

1. Investigate whether non-invasive techniques can be used to detect internal potato defects
2. Develop experimental models of internal potato defects and defect development
3. Investigate whether non-invasive techniques can detect model defect analogues
4. Develop novel approaches to food waste and losses reduction based on this research

2 Chapter 2: Pre-harvest prediction of tuber defects during plant growth

2.1 Introduction

Population growth and climate change pose a challenge to global food systems (Hall et al., 2017; Muluneh, 2021; Ray et al., 2022). Total global food demand is projected to grow between 35% and 56% by 2050 compared with 2010 (van Dijk et al., 2021), whilst the temperature rise due to climate change is predicted to reach 2.1-3.2°C. Potatoes are one of the most important crops in the world, cultivated in all continents bar Antarctica. Increases in global temperatures are modelled to reduce global potato yield by 18-32% without cultivar and planting time adaption or 9-18% with these adaptations (Hijmans, 2003). Wild relatives of domestic potatoes that provide an important gene pool for breeding pathogen and stress resistances are also highly threatened by climate change (Hussain, 2016). In addition, this rise in temperature will increase crop water demand (Lobell, 2013) and the resulting environmental impact on crop production.

Potatoes are valued for their water use efficiency (WUE) (Nasir & Toth, 2022), as well as high production rate and nutritional value positioning them as especially valuable in economically underdeveloped nations (Islam et al., 2022). Nevertheless, potato plants and tubers are exposed to abiotic and biotic stresses throughout growth. Weather conditions and soil quality affect the health of a potato plant (Escuredo et al., 2018; Aliche et al., 2018), influencing tuber quality (Wang et al., 2012; Adams & Stephenson, 1990). Hypoxic soils or pest and pathogen damage also directly influence the development of tuber defects (Parker & Howard, 2001; Chandel et al., 2022). Additionally, despite having a higher WUE than other important crops such as rice, wheat and corn, potatoes have poor drought tolerance (Nasir & Toth, 2022). Potato yields are threatened by susceptibility to drought impacting potato plant and tuber health (Obidiegwu et al., 2015) and posing a barrier to efficient production (Awasthi & Verma, 2017). Climate change poses a risk of more severe and frequent drought in many agricultural regions (Yuan et al., 2023), increasing the potential impact of drought-associated defects on food systems.

Pressures on existing cultivated land require a substantial increase in the efficiency of food production systems to meet the growing global demand for food. Currently three-quarters of terrestrial non-ice land is used for human use (Erb et al., 2007), and further expansion would lead to catastrophic environmental impacts (Erb et al., 2016) threatening key ecosystem services for humanity (Eriksen, 2009). Agricultural intensification and management improvements are therefore essential to meet future food demands (Mauser et al., 2015; Erb et al., 2016). However, increases in food system efficiency do not solely consist of improvements in yield but also improvements throughout the entire food system supply chain, such as storage, transit and management (Eriksen, 2009).

Pre-harvest prediction of defect development may inform the management and reduction of waste in early stages of the supply chain. Early diagnosis and intervention are crucial to preventing disease spread and reducing plant and crop damage (Ampatzidis et al., 2017). Crop walking is one of the most important jobs in vegetable production to identify symptoms of stress, disease or herbivore infestation. Regular walking of the crop means problems are quickly identified and can be appropriately tackled (CALU, 2011). However, visual inspections of plants by human observers for disease identification are time-consuming, costly, and prone to error. Furthermore, not all defects may present early symptoms. Losses could potentially be reduced through early harvest of tubers if they are predicted to develop defects later in growth, assuming that total healthy tuber mass of an early harvest exceeds that of a defective later harvest, with market demand for early potatoes. Detection of contagious defects pre-harvest may also help to avoid spread in transit or storage, mitigating further waste.

Imaging techniques have been of interest over the past few years, using both visible and non-visible wavelengths, to automate or enhance conventional crop inspection (Yang et al., 2024; Khan et al., 2022). Assessment of plant health at the canopy scale has been greatly enabled by remote sensing and hyperspectral imaging, such as evaluating normalised difference vegetation index, a measure of greenness (Gascon et al., 2016), via unmanned aerial vehicles (Wang et al., 2015) and use of space-borne instruments such as the Advanced Very High Resolution Radiometer (Yang et al., 2012). Resolution is a key limitation of these approaches, posing a barrier to individual plant assessment.

Near-infrared (NIR) spectroscopy is emerging as a method of proximal crop health assessment, accurately estimating leaf macronutrient levels (Prananto et al., 2020) and soil nutrient levels (van Groenigen et al., 2003).

This chapter assesses the potential of pre-harvest NIR spectroscopy for predicting post-harvest outcomes such as yield, and the rate and severity of defects. Specifically, since drought causes major challenges for producers during potato cultivation (Kikuchi et al., 2015) drought will be used as a model stress in potato plants to increase the frequency and severity of defects.

2.1.1 Aims and objectives

The overall aim of this chapter is to investigate whether pre-harvest NIR spectra of potato plant leaves can be used to predict post-harvest outcomes such as yield or occurrence and severity of tuber defects through the following four objectives:

- Establish a growth system for potato plants grown from seed tubers, to allow the NIR monitoring of both leaves and developing tubers *in situ* during the imposition of drought stress
- Investigate the relationship between tuber defects and environmental conditions
- Investigate the relationship between pre-harvest NIR spectra and environmental conditions
- Determine whether pre-harvest NIR spectra provide a predictor of post-harvest outcomes.

2.2 Methods

2.2.1 Plant growth

Twenty-four potato plants were grown from tubers in 18.5 L pots filled with ~10 kg of John Innes No.2 compost, with 30g of Westland organic potato feed (Westland, Yeovil, Somerset, England) per pot, in a controlled glasshouse. Pots were 30 cm in diameter at the rim, 26 cm diameter at the base, and 30 cm tall. Hinged windows of 15×10 cm were cut into each pot, such that subterranean tubers could be accessed pre-harvest (Figure 2.1). Plants were divided into two groups: drought stressed (DS) and well-watered (WW). Both groups were watered every other day to saturation, till the imposition of the differential watering regimen, which began once flowers emerged in more than half of all plants, which occurred on day 35. Subsequently, pots continued to be watered every other day such that they achieved a set post-watering pot mass, WW to 12 kg and DS to 11 kg. The differential watering regimen ran for 45 days, ceasing at the occurrence of an unexpected heatwave to prevent premature plant death.

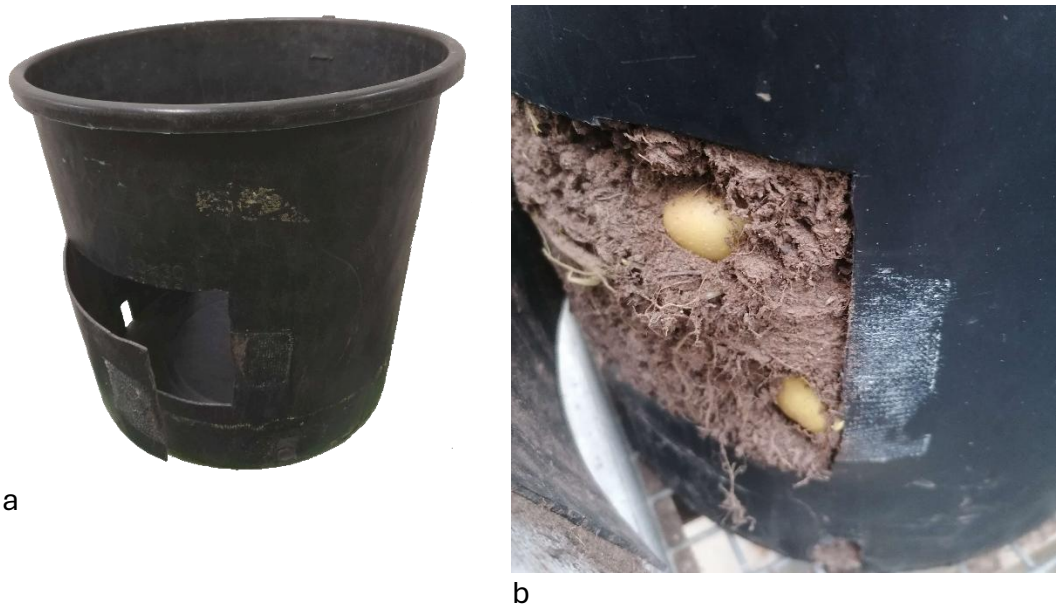

a b

Figure 2.1 Plant pots used for potato growth Plant pots used for potato growth.
a: Plant pot used for this experiment, with cut-in window. b: Potatoes in pot accessible via window, duct tape used to seal window when closed.

Pots were positioned in two 3×4 grids, one for each treatment group. Both groups were shuffled fortnightly to mitigate edge effects, in accordance with the sequence in Table 3.1 to ensure no pot remained in the same row or column following the shuffle, or moved back to its previous row, and no pot moved from one far end of the bench to the other in a single shuffle. Both control and drought followed the same sequence, where each pot rotated through the numbered locations in order, with different starting points.

Table 2.1 Pot position rotation sequence.

1	4	10	7
5	2	8	11
9	12	6	3

A HortiMaX system (Ridder Synopta version 5, Hortisystems UK Limited, West Sussex, UK.) was used to record glasshouse conditions, including temperature and humidity. Weather data were acquired from the Lancaster University Hazelrigg weather station at 54.01432460410117, −2.7756734271284094 (approx. 1 km from the glasshouse where the experiment was conducted, at 30 m higher elevation).

2.2.2 NIR spectroscopy

(See appendix 3 for a brief overview of the fundamentals of reflectance spectroscopy)

NIR absorbance leaf spectra were regularly recorded throughout plant growth, as well as tuber spectra later in growth, using a handheld NIR spectrometer device: NIRvascan ASP-NIR-M-Reflect (Allied Scientific Pro, Gatineau, Quebec, Canada) and DLP NIRscan Nano GUI software (Texas instruments, Dallas, Texas, USA). To allow use of both hands while carefully scanning leaves, a foot pedal system was devised to control the spectrometer. For this system a keyboard sustain foot pedal was connected to an Arduino Due microcontroller (Arduino, Monza, Italy) to convert the binary signal into a USB signal for communication with a Python program, which simulated mouse clicks on the spectrometer software's window, and appropriately named each scan with plant number, scan number and day number for categorisation and importation of data to MATLAB.

Only apical leaves larger than 5 cm wide were used for spectral data collection. This size was chosen as leaves below this size could not be easily scanned with the handheld spectrometer. Spectral data collection started once the earliest leaves reached 5 cm in width, on 29 March 2023. This was subsequently referred to as “day 0”, and all day numbers are relative to this date. Plants that had not yet produced large enough leaves were withheld from data collection till they had sufficiently grown but retained the same day 0. For each spectral data collection, five apical leaves on each plant were chosen at random but spaced roughly evenly around the plant. Each of these leaves were scanned five times, randomly distributed across the leaf, with each scan being a mean of six readings at each location.

NIR tuber spectra were recorded with near-surface tubers, or via openable windows fitted into each pot before planting (Figure 2.1, 2.2). Near-surface tubers were accessed by carefully brushing compost with a paintbrush and re-covering in a thin layer of compost after recording (Figure 2.2). Whilst it is common practice in potato farming to pile more compost around plants to cover protruding tubers, this was not done for tubers that naturally protruded above the compost level to avoid changing the mass of the pots or introducing an inconsistent treatment. The date of first detectable tuber emergence was recorded.

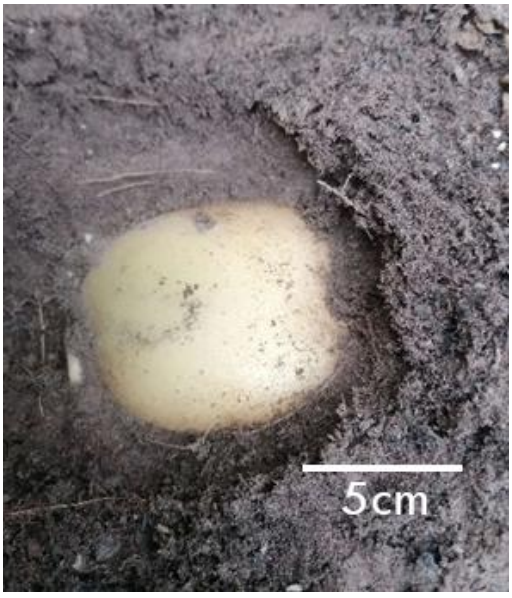

Figure 2.2 Tuber exposed at surface for data collection.

2.2.3 Plant harvest

Upon harvest, all tubers ≥30 g were inventoried, recording the plant of origin, mass and defect symptoms of each tuber. Total yields in mass and number of tubers were also recorded for each plant. Defect symptoms were scored by eye using a 0–3 scale, where 0 reflects no visible defect and 1–3 represent levels of increasing severity: 1 – barely visible; 2 – defect present; and 3 – defect severe. Defects and symptoms that were recorded were:

- Scabs on tuber skin
- Scurf: shiny film-like skin, usually resulting from the fungus “silver scurf” (*Helminthosporium solani*)
- Greening of tuber skin
- Flaccidity of tuber from turgor pressure loss
- Rot, including all forms of rot
- Lenticular spots due to lenticel enlargement: increases infection risk and reduces marketability.

Tubers were subsequently stored for 1 year in a controlled environment room (~65% relative humidity, 16 h at ~150 $\mu molm^{-2}s^{-1}$ Photosynthetically-active radiation, ~22°C/~20°C day/night) to test for differential spoilage and prediction of spoilage via spectroscopy. Defect severities were recorded at the end of this period using the 0–3 scale, and the mass of tubers recorded. Tubers were weighed again after dechitting to determine total sprout mass.

2.2.4 Porometry

Leaf stomata are pores through which gas exchange and transpiration occur, opening and closing of leaf stomata control the rate of gas exchange and transpiration. How open or closed stomata are is termed “stomatal conductance”, measured in $mmolm^{-2}s^{-1}$.

Stomatal conductance was measured using an AP4 porometer (Delta-T Devices Ltd, Burwell, Cambridge, UK). Only apical leaves larger than 5 cm were used for porometry data collection. Measurements were made at similar times of day at approximately noon.

2.3 Results

2.3.1 Stomatal conductance showed a marked response to drought and temperature

Potato plants were grown for ~160 days, with differential watering treatment imposed for 45 days. Leaf spectra were recorded from the first emergence of leaves wider than 5 cm (day 0) until day 101, and tuber spectra were recorded from day 70 to day 111. Tubers were harvested on day 145. Figure 2.3 shows the stomatal conductance of WW and DS plants at day 75. As expected, the stomatal conductance of DS was significantly lower than WW (T-test P=0.0224), confirming that differential watering treatment resulted in differential drought stress (Luan, 2002). However, glasshouse temperature, as recorded by the HortiMaX system, showed an unexpected peak between days 75 and 80, due to a heatwave, with temperatures approaching 40°C (Figure 2.4) imposing an additional heat stress on plants for a period of 15 days. Stomatal conductance was remeasured after the heatwave, on day 96, showing a significant reduction in stomatal conductance in DS plants (T-test P=0.0043) (Figure 2.3). However, the stomatal conductance of both WW and DS groups was similar to that of DS at day 75, indicating that the stomata of both WW and DS had closed in response to the increased soil drying during the heatwave. Two-way analysis of variance (ANOVA) was performed on stomatal conductance with two binary categorical factors of watering treatment and pre or post heatwave. Both factors were found to have significant impact, with a P value of P=0.009258 for pre or post heatwave, and P=0.01221 for watering condition; there was also significant interaction, with a P value of P=0.02251.

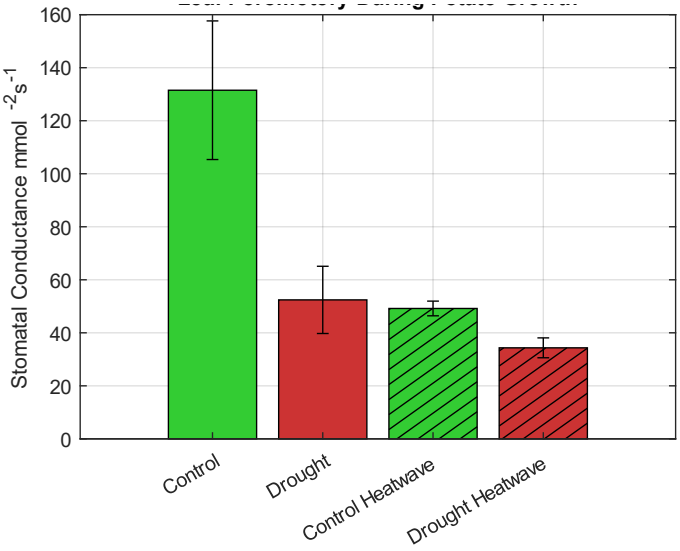

Figure 2.3 Stomatal conductance of apical leaves, between drought-stressed (DS) and well-watered (WW) potato plants, both before (day 75) and after heatwave (day 96). Day 75, n=24; day 96, n=17. Error bars denote standard error of mean.

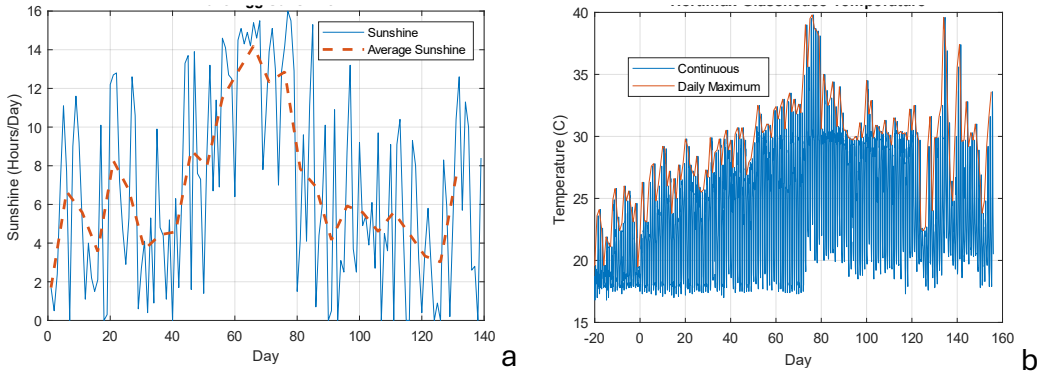

Figure 2.4 Glasshouse temperature and local sunshine during growth of potato plants.
*Average sunshine computed via sliding Hamming window. Day 0 refers to day of first spectrometric readings (*29 March 2023*), plants grown till day 111. a: Daily hours of sunshine during plant growth; blue denotes continuous readings, orange dotted line denotes average. b: Glasshouse atmospheric temperature during plant growth; blue denotes continuous readings, orange line denotes daily maxima.*

2.3.2 The effect of drought stress on tuber number and tuber defects

One hundred and forty-one tubers of greater than 30 g mass were harvested; tubers under 30 g were excluded from this experiment. Figure 2.5a shows that WW produced 45.2% higher yield by mass, on average, than DS (Welch's T-test, P=0.0047). Mean tuber

mass was also significantly greater in WW (Welch's T-test P= 0.0235) (Figure 2.5b). Greater yield by mass in control plants is largely due to greater average tuber mass, as the number of tubers produced, on average, was not significantly higher (Welch's T-test P= 0.1643) (Figure 2.5c).

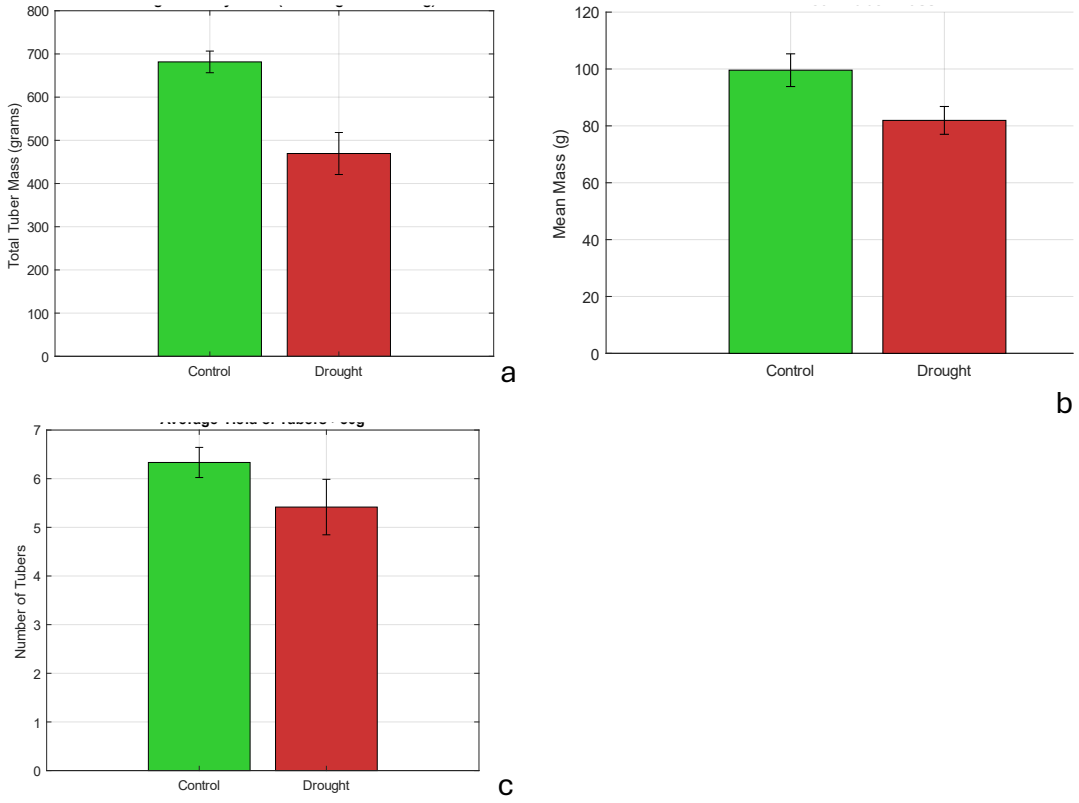

Figure 2.5 Yield of potato plants from well-watered and drought-stressed plants grown for ~160 days, excluding tubers under 30 g.
a: Mean yield per plant by total mass of tubers produced in g. b: Mean mass of individual potato tubers. c: Mean number of tubers per plant. Error bars depict standard error of mean. n=135 (70 well-watered, 65 drought), 12 plants per group. Error bars denote standard error of mean.

Both the frequency and severity of defects observed postharvest varied between the different classes of defect (Figure 2.6). There was one only incident of spraing observed, but as no statistically relevant data could be generated from a single observation, spraing was removed from the inventory. WW exhibited a higher incidence and severity of rot than DS, but there was no significant difference for any other recorded defects (Table 2.2). Growth medium moisture is likely a factor in the prevalence of wet rot, as well as other rots (Fiers, 2011), which could explain the higher incidence of rot within

WW. However, whilst "rot" was collated into a single category and the majority of observed rots were wet rot it is likely that this also includes rots of a number of different kinds.

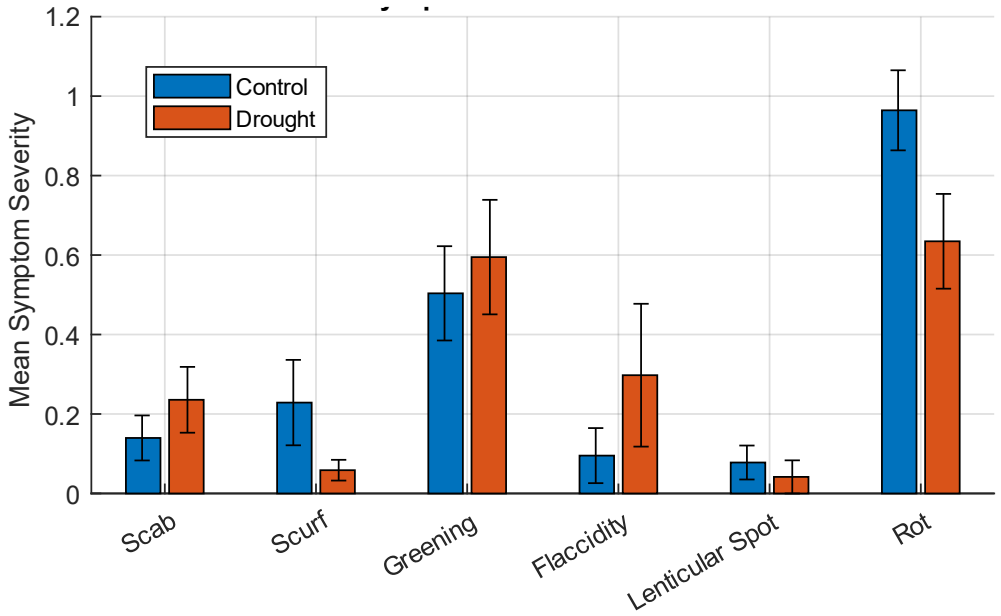

Figure 2.6 Mean potato defect symptom severity of listed defects between well-watered and drought-stressed plants.
Error bars depict standard error of mean. Symptom severities score by eye on 0-3 scale. Scab: scabs on tuber skin, Scurf: shiny film like skin, usually resulting from the fungus "silver scurf" (Helminthosporium solani), Greening: greening of tuber skin, Flaccidity: tuber flaccidity from loss of turgor pressure, Lenticular Spot: lenticular spots due to lenticel enlargement, increases infection risk and reduces marketability. Rot: all forms of rotting. n=135 (70 well-watered, 65 drought), 12 plants per group. Error bars denote standard error of means.

Table 2.2 Welch's T-tests on significance of difference in mean severity of potato tuber defects between well-watered and drought-stressed plants. Bold values denote significance (P<0.05).

	P	Higher group
Scab	0.1804	—
Scurf	0.0620	—
Greening	0.0799	—
Flaccid	0.4113	—
Spot	0.3918	—
Rot	**0.0252**	Well-watered

Pearson's correlations were used to investigate the relationships between differing defects, as well as other post-harvest outcomes, such as yield or average tuber mass. Correlations between defects were calculated using defect scores of individual tubers (Table 2.3a), although for correlations with variables specific to a plant rather than tuber, such as yield, mean tuber defect scores for each plant were used (Table 2.4). To test whether relationships between defects are consistent between WW and DS groups, correlations were calculated within each group separately (Tables 2.3b and 2.3c, respectively).

Table 2.3 Pearson's correlation matrices of defects and tuber mass data.

Mass: tuber mass (g); Scab: scabs on tuber skin; Scurf: shiny film-like skin, usually resulting from the fungus "silver scurf" (Helminthosporium solani); Green: greening of tuber skin; Flaccid: tuber flaccidity from loss of turgor pressure; Rot: all forms of rotting; Spot: lenticular spots due to lenticel enlargement, increases infection risk and reduces marketability. P and R refer to the probability and correlation coefficients of Pearson's correlation. a: Correlations using values of individual tubers from both well-watered and drought-stressed plants. b: Correlations using values of individual tubers from only well-watered plants. c: Correlations using values of individual tubers from only drought-stressed plants. Bold values denote significance (P<0.05). n=135 (70 well-watered, 65 drought-stressed), 12 plants per group. Error bars denote standard error of mean.

a

R / P	Mass	Scab	Scurf	Green	Flaccid	Rot	Spot
Mass	—	0.2461	0.0478	0.0484	−0.1366	−0.0658	0.1644
Scab	**0.0034**	—	0.0523	−0.0029	0.0228	−0.0647	−0.1619
Scurf	0.5745	0.5322	—	−0.1291	0.1536	−0.0556	−0.1064
Green	0.5715	0.9726	0.1229	—	−0.1404	−0.1471	0.3288
Flaccid	0.1076	0.7853	0.0651	0.0932	—	0.4421	−0.0832
Rot	0.4401	0.4391	0.5068	0.0785	**2.6×10^{-8}**	—	0.1670
Spot	0.0522	0.0517	0.2029	**0.0001**	0.3201	**0.0447**	—

b

R / P	Mass	Scab	Scurf	Green	Flaccid	Rot	Spot
Mass	—	0.3758	-0.0396	0.1090	−0.0222	−0.0478	0.1007
Scab	**0.0008**	—	0.1899	−0.1574	0.2380	−0.0634	−0.1498
Scurf	0.7341	0.0959	—	−0.1252	0.3522	−0.0798	−0.1483
Green	0.3485	0.1688	0.2746	—	−0.1950	−0.1585	0.3779
Flaccid	0.8494	**0.0359**	**0.0016**	0.0871	—	0.3164	−0.0374
Rot	0.6818	0.5815	0.4876	0.1658	**0.0048**	—	0.3020
Spot	0.3870	0.1904	0.1951	**0.0006**	0.7454	**0.0072**	—

c

R / P	Mass	Scab	Scurf	Green	Flaccid	Rot	Spot
Mass	—	0.1717	0.1721	0.0466	−0.2504	−0.1620	0.1941
Scab	0.1749	—	−0.1084	0.0933	−0.1373	−0.0562	−0.1438
Scurf	0.1739	0.3828	—	−0.0963	−0.0714	−0.0292	−0.1265
Green	0.7166	0.4561	0.4417	—	−0.1221	−0.1209	0.3610
Flaccid	**0.0460**	0.2679	0.5661	0.3288	—	0.7096	−0.1096
Rot	0.2009	0.6514	0.8145	0.3337	**2×10^{-11}**	—	−0.1485
Spot	0.1243	0.2455	0.3078	**0.0029**	0.3772	0.2303	—

Table 2.4 Pearson's correlation matrices of defects and tuber mass data, correlations using means for each plant including both well-watered and drought-stressed.

Mass: tuber mass (g); Scab: scabs on tuber skin; Scurf: shiny film-like skin, usually resulting from the fungus "silver scurf" (Helminthosporium solani); Green: greening of tuber skin; Flaccid: tuber flaccidity from loss of turgor pressure; Rot: all forms of rotting; Spot: lenticular spots due to lenticel enlargement, increases infection risk and reduces marketability; Emerge, days before first visible tubers emerge; N: yield in number of tubers >30 g. P and R refer to the probability and correlation coefficients of Pearson's correlation. Bold values denote significance (P<0.05). n=135 (70 well-watered, 65 drought-stressed), 12 plants per group. Error bars denote standard error of mean.

R / P	Avg. mass	N	Scab	Scurf	Green	Flaccid	Rot	Spot	Emerge
Avg. mass	—	0.1576	−0.0120	0.1112	0.0817	−0.4707	−0.0157	0.2465	0.2143
N	0.4621	—	0.0718	0.1095	0.1845	−0.7295	−0.1489	0.4523	0.2413
Scab	0.9556	0.7390	—	0.2260	0.0412	−0.0240	−0.2333	−0.4292	−0.3370
Scurf	0.6050	0.6104	0.2882	—	−0.3221	0.1474	0.1818	−0.1702	−0.3871
Green	0.7043	0.3880	0.8484	0.1248	—	−0.3694	−0.4089	0.4917	0.3906
Flaccid	**0.0203**	**0.0001**	0.9114	0.4918	0.0756	—	0.2053	−0.4943	−0.3946
Rot	0.9419	0.4875	0.2726	0.3951	**0.0473**	0.3358	—	0.0066	0.0249
Spot	0.2456	**0.0265**	**0.0364**	0.4266	**0.0147**	**0.0141**	0.9755	—	0.3825
Emerge	0.4087	0.3059	0.1859	0.1248	0.1211	0.1170	0.9244	0.1297	—

There is a strong negative correlation between flaccidity and yield by number of tubers (Pearson's correlation coefficient, R=−0.7295, P=0.0001). However, Figure 2.7 shows that most tubers were turgid, with only four flaccid, showing that this correlation suggests that plants with higher yields produce flaccid tubers less frequently as opposed to plants with higher yields producing tubers of higher turgidity. DS plants had a higher incidence of flaccid tubers, which is consistent with tubers becoming flaccid when turgor pressure becomes lower as a result of drought stress (Bethke et al., 2009).

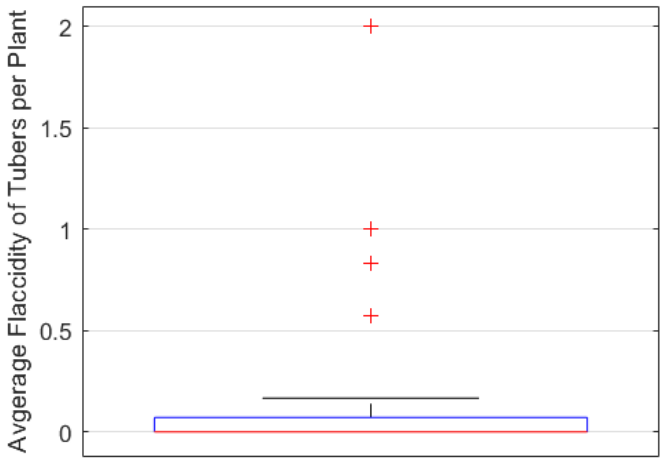

Figure 2.7 Flaccidity of potato tubers at harvest from both well-watered and drought-stressed plants.
Flaccidity scored on 0–3 scale, where 0 is turgid. n=141.Outliers denoted with red crosses. n=135 (70 well-watered, 65 drought-stressed), 12 plants per group. Error bars denote standard error of mean. Red line denotes median, blue line denotes the upper quartile, black bar denotes upper extreme, and red crosses (+) denote outliers.

There is a significant P value for the correlation between spotting and greening in both WW and DS tubers, 0.0006 and 0.0029, respectively, with coefficients suggesting weak correlation: 0.3779 and 0.3610, respectively. As defect scores are integers from 0 to 3, the data are best plotted as a matrix of incidence rather than a scatter graph and colour coded as a heatmap for visualising this relationship (Figure 3.8), where the number in each cell indicates the population with x and y values corresponding to that cell in the grid. Such that the spotting 1, greening 0 cell of Figure 2.8 shows 32 tubers had both a spotting severity of 1 and a greening severity of 0. This incidence matrix reveals that it is common for both defects to have low severities; however, if there is greening there is almost always also spotting.

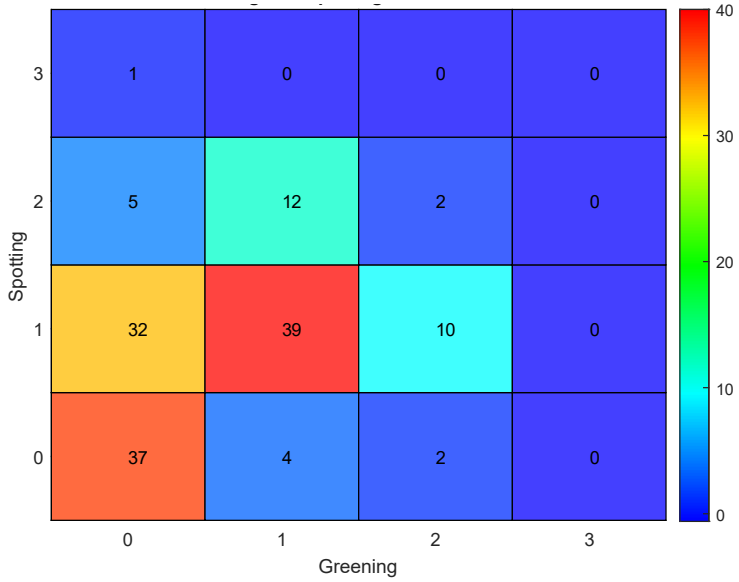

Figure 2.8 Incidence matrix of 0–3 severity scores of greening and lenticular spots.
Cells indicate the number of tubers that exhibited the corresponding greening and spotting severities.
n=144. Red indicates high coincidence and blue low coincidence.

A significant correlation between flaccidity and rot was observed in both WW and DS tubers (Table 2.3 b and c), with a stronger correlation within DS tubers (Table 2.3 c). However, incidence matrices reveal these correlations to be misleading (Figure 3.9), as the number of tubers exhibiting both defects is very small, with most tubers free of both.

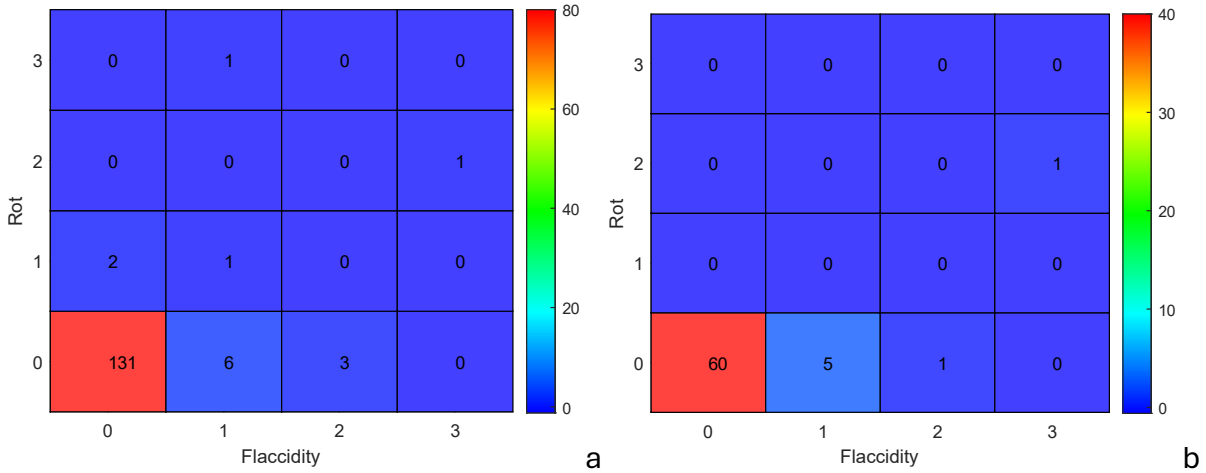

Figure 2.9 Incidence matrix of 0–3 severity scores of flaccidity and rot in potato tubers at harvest.
Cells indicate the number of tubers that exhibited the corresponding greening and spotting severities. Red indicates high coincidence and blue low coincidence. a: All tubers from both drought-stressed and well-watered plants (n=145). b: Tubers only from drought-stressed plants (n=67).

2.3.3 Pre-harvest leaf spectra and post-harvest tuber spectra as predictors of post-harvest spoilage

Peaks in leaf spectra were identified at 929 nm, 1191 nm, 1442 nm and 1627 nm (weak) (Figure 2.10; see Table 2.7 for full details on peaks found with tuber and leaf spectra). First differential does not reach zero at 1627 nm but corresponds to a large upward peak towards zero.

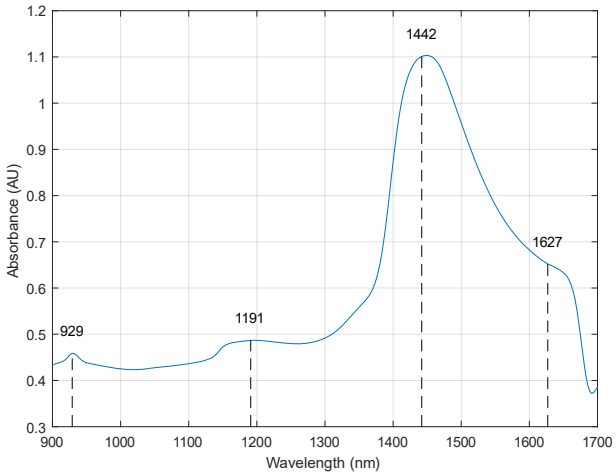

Figure 2.10 NIR spectra of potato plant leaves during plant growth. Peaks determined via zeros of first differential at 929 nm, 1191 nm, 1442 nm and 1627 nm (weak). Mean of 5678 spectra, each comprising 6 readings.

Leaf spectra were used to train statistical and machine learning models for prediction of post-harvest outcomes, such as yield or the rate of occurrence and severity of tuber defects. A Gaussian Support Vector Machine (SVM) model trained on leaf spectra was able to classify plants as either WW and DS, with varying accuracy, throughout plant growth ranging between 73.8% and 93.8%, depending on the stage of growth (Figure 2.11). However, leaf spectra proved not to be a good predicter of tuber mass, flaccidity or defects; no statistically significant results were obtained using classification algorithms, regressions (Table 2.5), and time-series neural networks.

Table 2.5 Rational Quadratic Gaussian Process Regression with principal component analysis of leaf spectra second differential for prediction of post-harvest tuber outcomes.
Mass: tuber mass (g); Flaccid: tuber flaccidity from loss of turgor pressure; Scab: scabs on tuber skin; Scurf: shiny film-like skin, usually resulting from the fungus "silver scurf" (Helminthosporium solani); Green: greening of tuber skin; Rot: all forms of rotting; Spot: lenticular spots due to lenticel enlargement, increases infection risk and reduces marketability, Emerge, days before first visible tubers emerge; N: yield in number of tubers >30 g.

Response variable	**R^2**	**RMSE**	**Range**	**RMSE (%)**
Average mass (g)	0.06	17.896	52–132.8	22.15
Average flaccidity	0.11	0.4006	0–2	20.03
Average greening	0.05	0.4324	0–1.33	32.51
Average scab	0.04	0.2420	0–0.8	30.25
Average scurf	0.05	0.2855	0–1.67	17.10
Average spot	0.04	0.3883	0–1.43	27.15
Yield (>30 g tubers only)	0.11	1.2731	1–8	15.91

Second differential absorbance was used for training all classifier models using optical spectra, unless specified otherwise. Second differentials are used as they offer better peak separation than zeroth and first differential. The signal to noise ratio however lowers with each differentiation, to limit the amplification of noise, smooth differentials were approximated using the 'irswm' function in the captain toolbox (Taylor et al., 2007) for MATLAB. Use of second differential is a method commonly used for analysis of spectra in the literature (Hsieh & Lee, 2005; Krausz, 2013; Mao et al., 2016).

Tubers were stored for one year post-harvest in a controlled environment room (~65% relative humidity, 16 h at ~150 $\mu molm^{-2}s^{-1}$ PAR, ~22°C/~20°C at day/night) to investigate whether spoilage and defect development in storage can be predicted from pre-harvest leaf spectra or post-harvest tuber spectra. Figure 2.11 shows there was no significant difference in mass loss between tubers from WW and DS tubers (T-test P=0.1705), suggesting postharvest or intraplant factors had a greater impact on potato shrivelling than pre-harvest factors. Mass loss was highly variant within plants, supporting the suggestion that post-harvest factors are more important than pre-harvest factors (Figure 2.12).

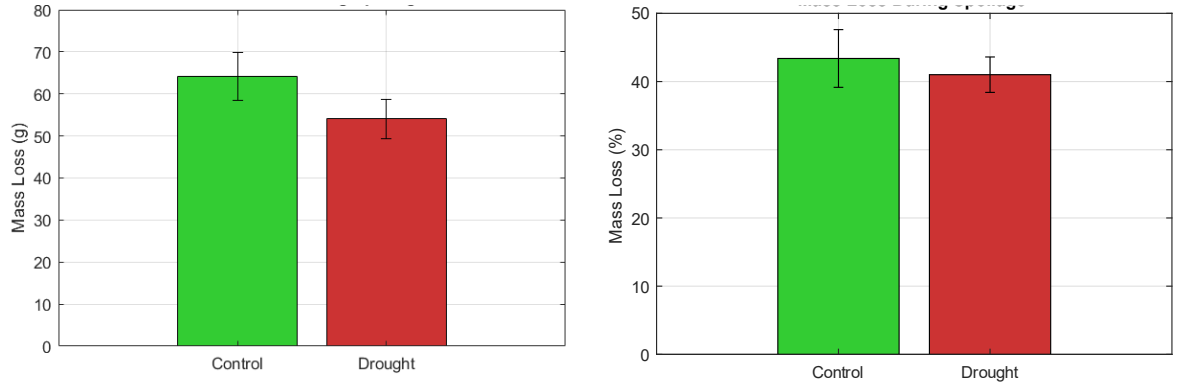

a b

Figure 2.11 Mass loss of potato tubers during post-harvest storage period of circa one year.
a: Absolute mass loss in grams. b: Relative mass loss in percentage of starting mass. Green (Control) denotes tubers from well-watered plants, red (drought) denotes tubers from drought-stressed plants. n=74 (35 well-watered, 39 drought-stressed). Error bars denote standard error of mean.

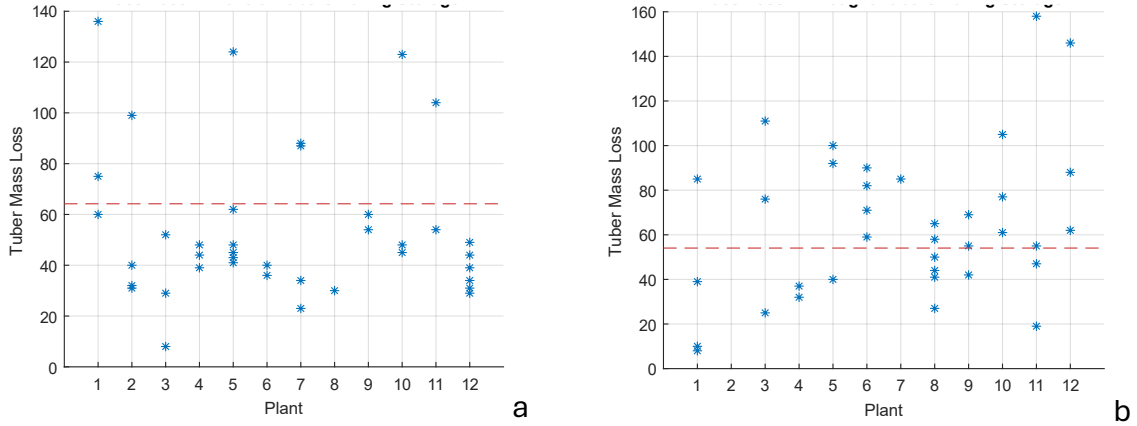

a b

Figure 2.12 Mass loss of individual potato tubers from each plant after circa one year post-harvest storage.
Dotted line represents the mean for each group. Mass was measured in grams. a: Tubers from well-watered plants. b: Tubers from drought-stressed plants.

2.3.4 Development of a novel measure of spectral separation

Classification algorithms have great utility in machine learning and for testing the potential of screening approaches. However, they have limited utility for assessing separation of grouped data over time, due to differences between algorithms and

parameters, issues with mismatched populations and randomness in heuristics optimisation. Figure 2.13 shows that classification algorithms are affected by the ratio between groups within the training data, as lopsided groups allow for accuracy to be increased by biasing towards the larger group, often requiring data from the larger group to be excluded to balance the training set. The need for validation reduced the effective population size, which may be problematic for smaller datasets. Different classification algorithms give differing classification accuracies, and heuristic algorithms give differing results each time the training is repeated. The size of training data also influences the accuracy of classification algorithms. These challenges limit the objectivity of classification algorithms as a measure of separation, although classification algorithms are a powerful and essential tool.

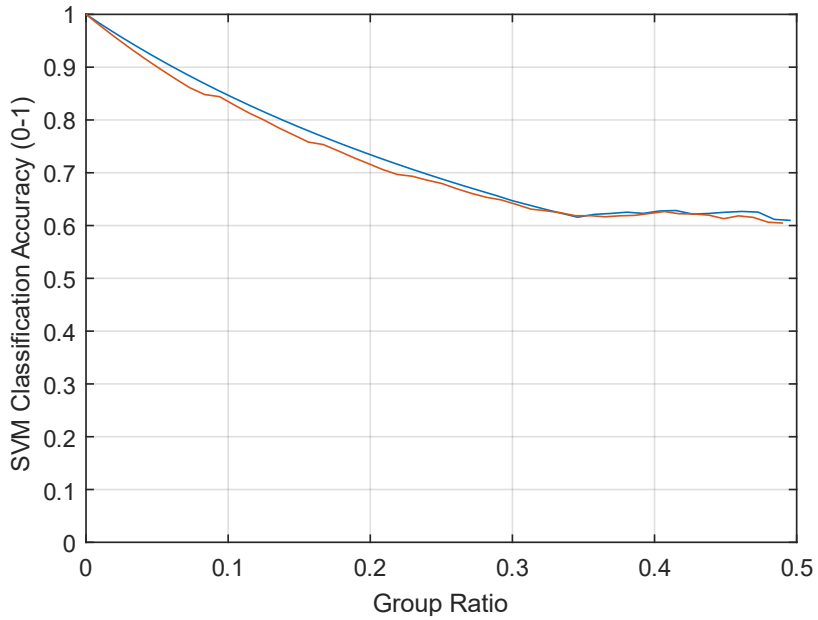

Figure 2.13 Classification accuracy of Gaussian SVM classifier for determining between NIR leaf spectra of well-watered and drought-stressed potato plants over time of plant growth.
Accuracy compared with ratio between population size of well-watered and drought-stressed plant spectra. Blue denotes all well-watered plant data with varying amounts of data from drought-stressed plants, red denotes all drought-stressed plant data with varying amounts of data from well-watered plants.

As an objective means to ascertain spectral separation between WW and DS plants varies over time, the Euclidian distance between means in a normalised principal component space was used. The Mahalanobis distance is the distance of a point from

the mean of a distribution in a transformed principal component space, measured in unitless standard deviations (Mahalanobis,1936), in a similar fashion to how z-score measures the distance of x from the mean of a standardly distributed variable. Taking inspiration from the Mahalanobis distance, the distance between the means of two different groups, rather than the distance to the mean, was used and this measure is hereafter referred to as “co-Mahalanobis distance”. While the sum of individual wavelength differences between mean spectra could be used as a simpler measure of separation, this would give equal weighting to both relevant and irrelevant wavelengths, as well as not taking the magnitude of absorbance at each wavelength into account, biasing higher peaks or more absorbent regions of the spectrum. While classification algorithms can be affected by group size ratios and randomisation in heuristic optimisation algorithms, co-Mahalanobis distance is not affected by group ratio, or heuristics.

To calculate this co-Mahalanobis distance, PCA was performed on all spectra including both WW and DS. A space was constructed from the (Principal Components) PCs that explain >95% of variance, and axes were standardised such that the standard deviation of each axis was 1. All spectra were transformed onto this space and the Euclidian distance between group centre of masses was calculated. This was plotted over time to explore if intergroup spectral difference was associated with other variables such as environmental conditions or physiological development. Figure 2.14 shows that classification accuracy of a Gaussian SVM closely correlates with co-Mahalanobis distance, as expected. This indicates that co-Mahalanobis distance can be used as an objective measure of separation that is relevant to classification, as it indicates how well the data can be classified without the variance between algorithms or repeats of a heuristic.

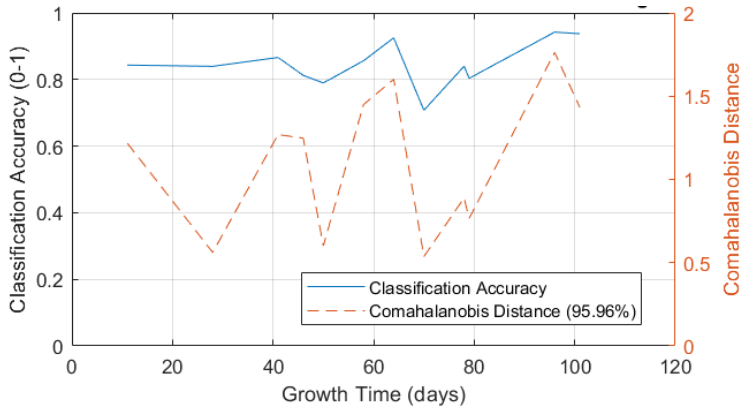

Figure 2.14 Gaussian Support Vector Machine classification accuracy of plant group from leaf spectra over time, paired with co-Mahalanobis distance between leaf spectra of drought-stressed and well-watered potato plants.

Co-Mahalanobis distance was calculated for tubers from WW and DS plants from day 70, when tubers accessible for data collection first appeared, until day 111. However, due to the subterranean location of pre-harvest tubers, tuber spectra could only be recorded from a total of 17 plants, 10 WW and 7 DS plants. The beginning of tuber data collection was asynchronous between plants as different plants had tubers emerge on different days across the 41-day measurement period. Figure 2.15 shows that there is no clear change in co-Mahalanobis distance between WW and DS tubers. This may be due at least in part to the asynchronous tuber emergence, which caused the sample size on day 70 to be low, 12 scans compared to the 334 scans on day 111, thus having low statistical power.

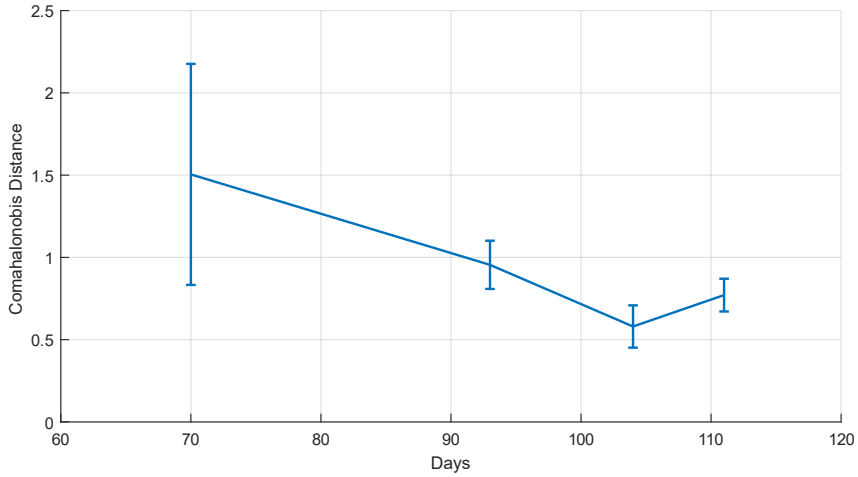

Figure 2.15 Co-Mahalanobis distance between tuber spectra from well-watered and drought-stressed plants.
Error bars represent standard error. Number of scans for each time slice: day 70: 12 scans; day 93: 168 scans; day 104: 207 scans; day 111: 334 scans. Error bar represents the Euclidean norm of the errors for both principal components used.

2.3.5 The effects of glasshouse humidity on co-Mahalanobis distance and pot mass

Humidity within the glasshouse increased markedly at ~day 80 (Figure 2.16 a). This coincides with the hose watering of both WW and DS treatments to saturation at the end of the 5-day heatwave on day 80. Pre-watering pot masses are an indicator of evapotranspiration; however, there is no relationship between glasshouse humidity and pre-watering pot masses prior to day 80 (Figure 2.16 b), as confirmed by Pearson's correlation coefficient (WW: R=0.0978, P=0.7394; DS: R=0.4043, P=0.1517). As pot mass recording ceased on day 80 due to this emergency watering regimen, the relationship between pot mass and humidity across this boundary of watering regimen cannot be quantified. This limits the time range over which this relationship can be studied and whether there was influence from the heatwave, although it is known that pot mass and soil moisture significantly increased at this point as all pots were watered to compost saturation.

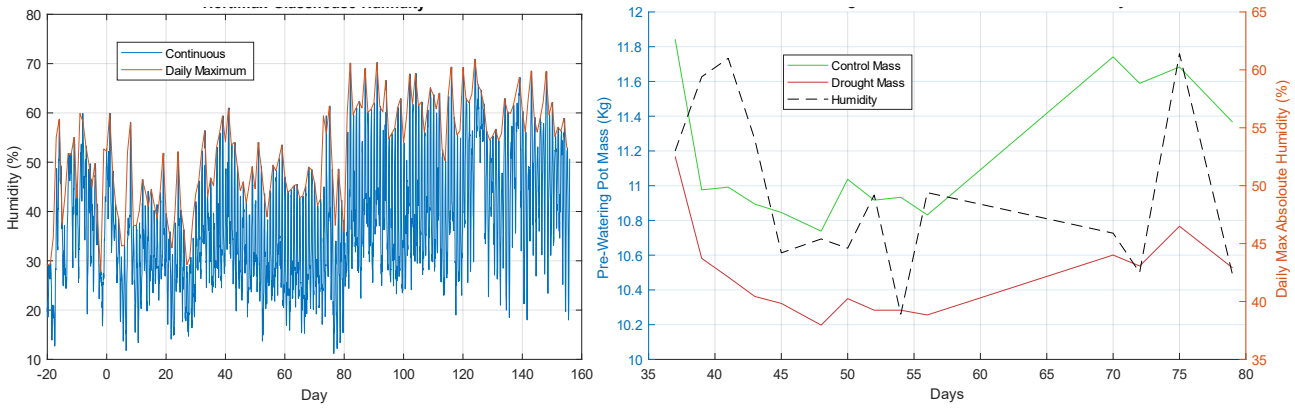

a b

Figure 2.16 Atmospheric absolute humidity in glasshouse during potato growth measured by HortiMaX system.
a: Humidity over time, blue denotes continuous readings, orange denotes daily maxima. b: Mean mass of plants pots pre-watering and glasshouse absolute humidity daily maxima. Only days with watering data displayed in b. n=24, 12 plants per group.

Glasshouse humidity does, however, correlate weakly with co-Mahalanobis distance between WW and DS leaf spectra (Figure 2.17), with a Pearson's correlation coefficient (R) of 0.5565 (P=0.0984). There is a lack of correlation between pre-watering pot masses and glasshouse humidity (Figure 2.16 b) or temperature, this may be due to a time delay as one takes time to influence the other.

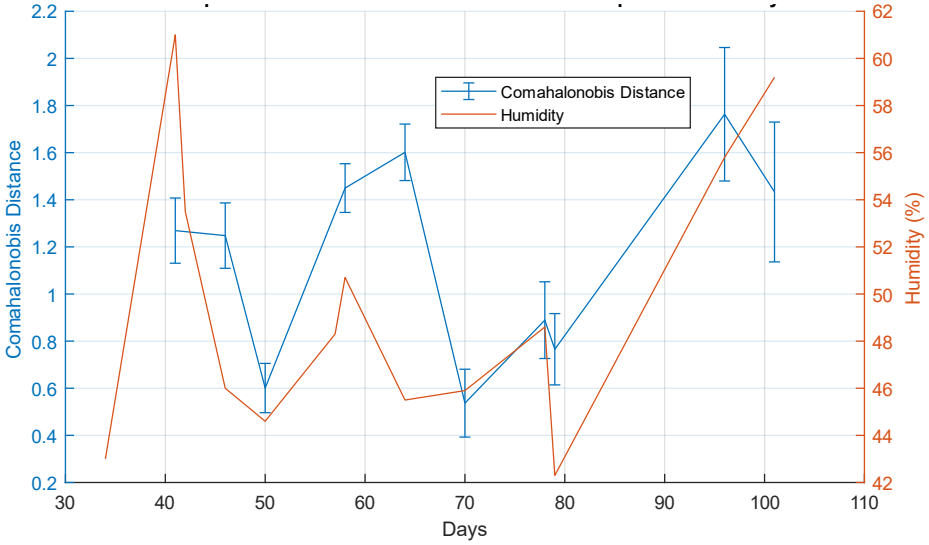

Figure 2.17 Co-Mahalanobis distance between NIR leaf spectra of drought-stressed and well-watered plants with down-sampled atmospheric absolute humidity of glasshouse during potato plant growth.
Blue denotes co-Mahalanobis distance, orange denotes humidity. Error bars denote standard error of mean. Maxima of daily humidity readings used.

WW and DS pot masses were strongly correlated (R=0.8764, P=1.8×10^{-5}, Pearson's correlation coefficient) showing the difference in treatment was consistent. Difference in pre-watering pot masses (Figure 2.18) provides evidence, in addition to differences observed in stomatal conductance (Figure 2.3), that the differential water treatment was effective in imposing differential drought stress on plants.

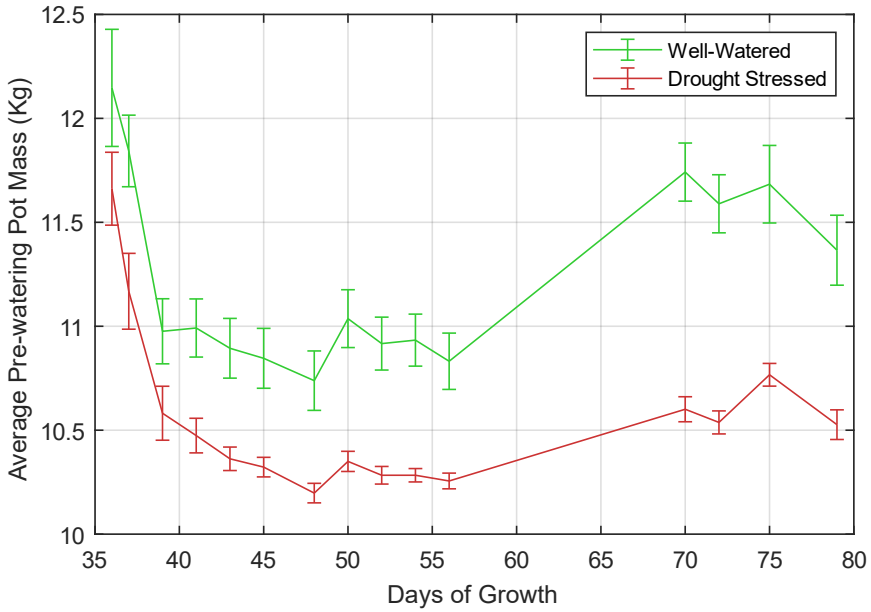

Figure 2.18 Pre-watering pot masses during potato plant growth for both well-watered and drought-stressed plants. Green denotes well-watered and red denotes drought-stressed. Error bars represent standard error of mean. n=24 (12 well-watered, 12 drought-stressed).

2.3.6 Tuber spectra prediction

Tuber spectra were not effective for prediction of post-harvest tuber defect scores (Table 2.6). Spectra are recorded by plant, whereas tuber defects are recorded by tuber, thus the predictive power of spectra for tuber defects is limited as the spectra for each plant will include spectra from different tubers. A tree classifier was trained using the classifier learner app in MATLAB R2024b (MathWorks, Portola Valley, California, USA) to classify between second differential tuber spectra PCs of WW and DS tubers. This model failed to accurately classify between WW and DS tubers, with only 63.6% accuracy. Gaussian process regression models were trained with tuber spectra for predicting average tuber defect scores of the associated plant (Table 2.6). The model was trained using the "fitrpg" (fit regression gaussian process) function in MATLAB R2024b, with a constant basis function, rational quadratic kernel function, isotropic kernel and standardisation and PCA enabled. Tuber quality metrics associated with each spectra vary at multiple scales, the tuber scale, plant scale and plant group scale, thus the rational quadratic kernel was chosen as it is effective at modelling data that varies and multiple scales (Zhang et al., 2018). Scab was the only defect with a significant R^2 value, at 0.86 (Table 2.6). Figure 2.19 reveals the fit to be very poor,

however, with only seven outlier datapoints fitting the model showing there is no significant fit.

Table 2.6 Rational Quadratic Gaussian Process Regression with PCA of tuber spectra second differential for prediction of post-harvest tuber defect severity scores, determined by eye on a 0–3 scale.
Mass: tuber mass (g); Flaccidity: tuber flaccidity from loss of turgor pressure; Green: greening of tuber skin; Scab: scabs on tuber skin; Rot: all forms of tuber rot; Scurf: shiny film-like skin, usually resulting from the fungus "silver scurf" (Helminthosporium solani); Spot: lenticular spots due to lenticel enlargement, increases infection risk and reduces marketability; Yield: amount of tuber harvested >30 g mass. R^2 from validation used, RMSE (%) is the RMSE as a percentage of the range in values. n=135 (70 well-watered, 65 drought-stressed), 12 plants per group. Error bars denote standard error of mean.

Response variable	R^2	RMSE	Range	RMSE (%)
Average mass (g)	0.14	15.66	63.2–132.8	22.5
Average flaccidity	0.18	0.2664	0–1	26.6
Average greening	0.09	0.4128	0–1.33	31.0
Average scab	**0.86**	0.1018	0–0.8	12.7
Average rot	0.04	0.1368	0–0.5	27.4
Average scurf	0.21	0.2777	0–1.67	16.6
Average spot	0.15	0.2733	0.333–1.429	24.9
Yield (by tuber count)	0.03	0.9544	4–8	23.9
Yield (by mass)	0.12	115.28	268–771	22.9
Scan day	0.23	7.407	70–111	18.1

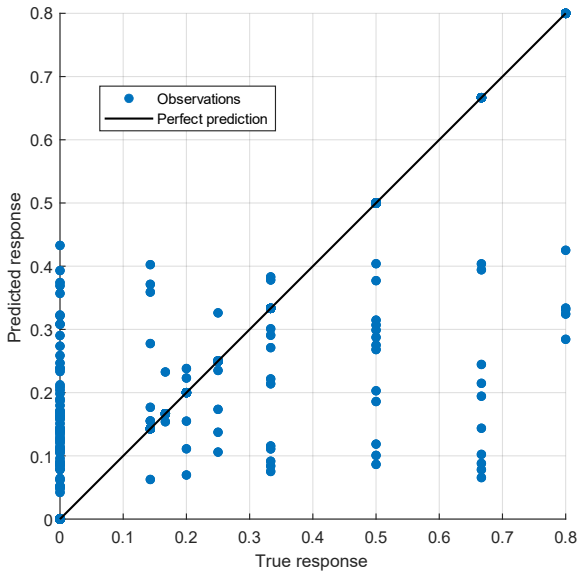

Figure 2.19 Quadratic Gaussian process regression of tuber second differential spectra with PCA for prediction of average tuber scab severity by plant.

Peaks in tuber spectra were identified via zeros of the first differential (Figure 2.20); peaks were found at 929 nm, 969 nm, 1191 nm, 1442 nm and 1697 nm.

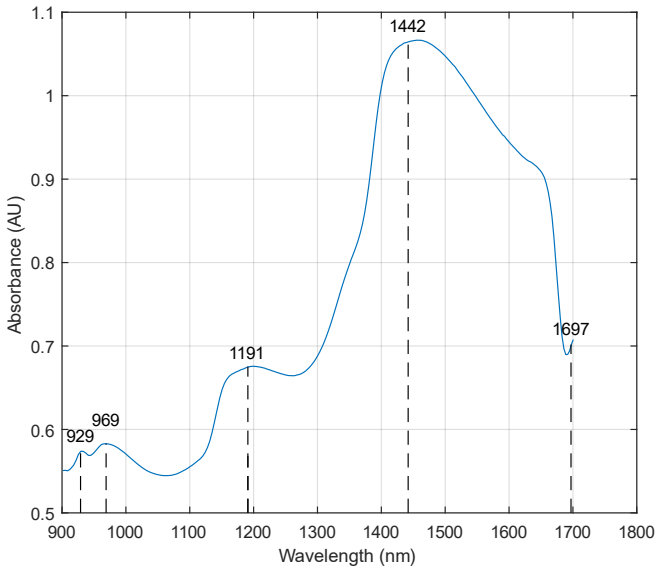

Figure 2.20 NIR absorbance spectra of pre-harvest potato tubers; peaks identified via zeros of first differential.
Mean average of 722 spectra, each comprising the average of 6 readings.

Intervals in wavelengths between readings vary from 2.9 nm to 5.2 nm, with greater intervals at lower wavelengths (Figure 2.21); therefore, wavelength of peaks may differ slightly from their true wavelength, with a non-uniform quantization error due to limited and varying resolution.

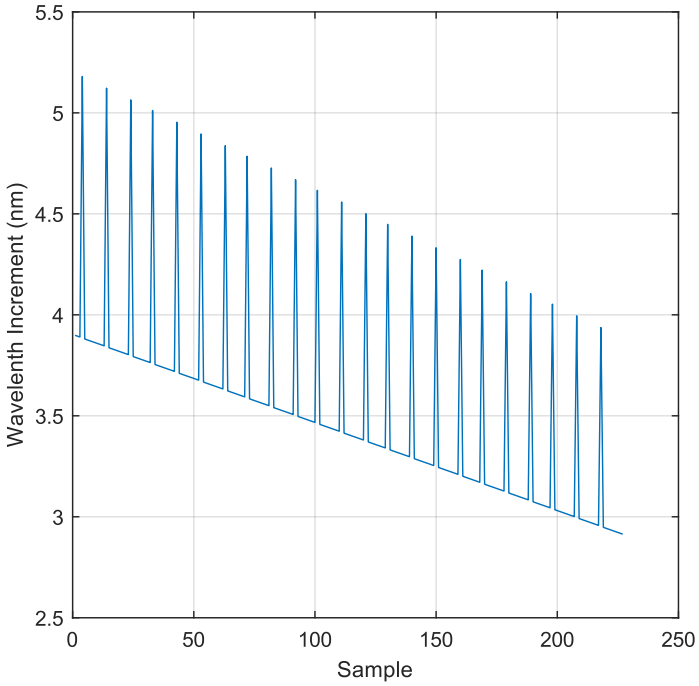

Figure 2.21 Increments in wavelength between samples in NIR spectra.
Wavelength ranges from 900 to 1700 nm.

The band recorded in this data, 900–1700 nm, primarily comprises second or higher overtones, with some first overtones above 1400 nm (Yadav et al., 2015). Compounds, functional groups and bonds associated with each of the peaks observed in tuber spectra (Figure 2.19) are detailed in Table 2.7.

Table 2.7 Correlates for each NIR absorbance peak in tuber spectra.

Peak wavelength	**Chemical correlates in literature**	**Related compounds**
929 nm (10,764 cm^{-1})	Overtone C-H of methylene group in lipids (Khodabux et al., 2007).	Triglyceride
969 nm (10,320 cm^{-1})	Overtone of the O-H stretch in water (Khodabux et al., 2007).	Water
1191 nm (8396 cm^{-1})	C-H associated with protein (Ingle et al., 2016), second overtone C-H stretch (Esposito et al., 2024; He et al., 2019). C-H stretch mode and overtone (Khodabux et al., 2007). Glucose O-H 1195 nm (Kyprianidis & Skvaril, 2017).	Glucose
1442 nm (6935 cm^{-1})	O-H first overtone of starch ~1420 nm (Lohumi et al., 2014). First overtone hydroxyl starches (1400–1600 nm) (Kyprianidis & Skvaril, 2017). Crystalline sucrose O-H stretch 1443–1440 nm (López et al., 2017). Cannot accurately distinguish sugars with this peak, as it is associated with many sugars (Kyprianidis & Skvaril, 2017). Water ~1450 nm (Khodabux et al., 2007). Fatty acids (Holman, 1956).	Starch, sugar
1697 nm (5893 cm^{-1})	1600-1800 nm due to straight carbon chain and cis double bonds of fatty acids (Sato, 1991). 1680 nm vibration of C-H bonds bound to cis-unsaturation (Holman & Edmondson, 1956; Sato et al., 1991). Acetic acid (Holman & Edmondson, 1956). Starch 1700nm (Osborne et al., 1993).	Fatty acids, Starch

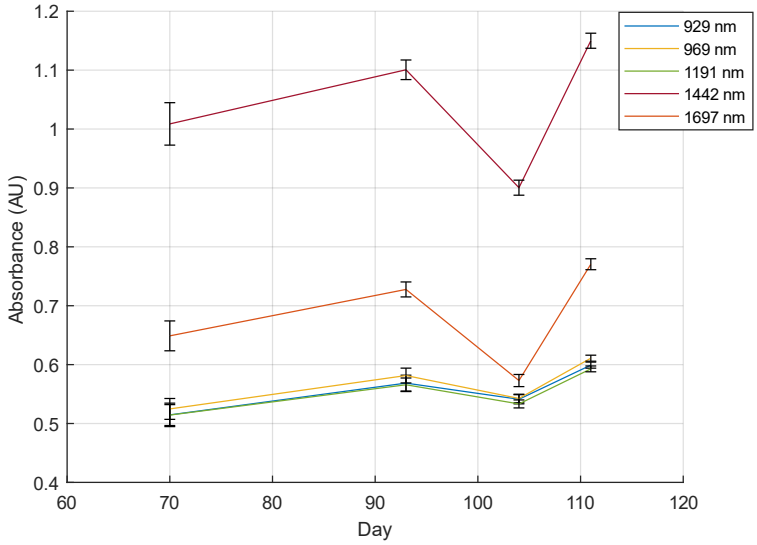

Figure 2.22 Absorbance at key peaks of potato tuber NIR spectra during growth.

There was no significant change in co-Mahalanobis distance of tuber spectra throughout the pre-harvest tuber spectra recording periods (days 70 to 11) (Figure 2.22), expect for a dip at day 104.

There was large variance in tuber defect severity scored between tubers within the same plant (Figure 2.23). Scab, scurf, flaccidity and rot showed significant P values for testing whether there is significant difference between interplant and intraplant variances in tuber defect severity scores via one-way ANOVA (Table 2.8). Pre-harvest tuber spectra were recorded on a plant-by-plant basis, not on a specific-tuber basis. This large variance limits the degree to which connecting non-specific spectra can be associated with the defect severity scores of individual tubers. Despite large variances between tubers within the same plant, interplant variances were greater than intraplant variances in all defects except flaccidity (Table 2.8). Interplant variances dominating scurf, with a P value of 3.016×10^{-3}, may be due to scurf being caused by a soil-borne fungus, *Helminthosporium solani* (Johnson & Cummings, 2015). As each plant had individual pots of compost, soil-borne pathogen exposure was shared between tubers of the same plants, but not between plants to the same extent.

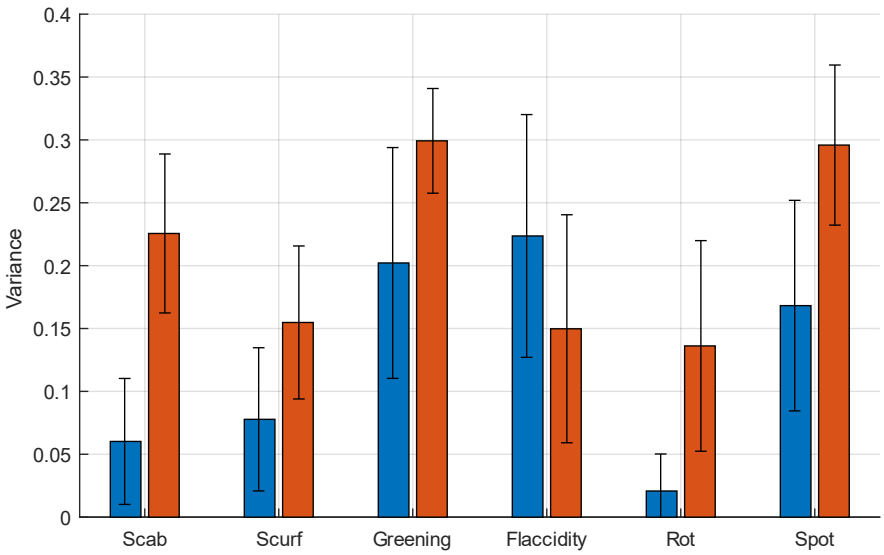

Figure 2.23 Variance of tuber defect scores.
Orange denotes variances between mean defect scores of each plant, blue denotes mean variance of defect scores between individual tubers within plants. Error bars represent standard error of mean. Scab: scabs on tuber skin; Scurf: shiny film-like skin, usually resulting from the fungus "silver scurf" (Helminthosporium solani); Green: greening of tuber skin; Flaccidity: tuber flaccidity from loss of turgor pressure; Rot: all forms of tuber rot; Spot: lenticular spots due to lenticel enlargement, increases infection risk and reduces marketability. n=135 (70 well-watered, 65 drought-stressed), 12 plants per group. Error bars denote standard error of mean.

Table 2.8 One-way ANOVA test for difference between interplant and intraplant variance in potato tuber defect severity scores. Scab: scabs on tuber skin; Scurf: shiny film-like skin, usually resulting from the fungus "silver scurf" (Helminthosporium solani); Green: greening of tuber skin; Flaccidity: tuber flaccidity from loss of turgor pressure; Rot: all forms of tuber rot; Spot: lenticular spots due to lenticel enlargement, increases infection risk and reduces marketability. Bold values denote significance (P<0.05).

Defect	**One-way ANOVA P value**	**Higher variance**
Scab	**4.755×10^{-11}**	Interplant
Scurf	**3.016×10^{-3}**	Interplant
Greening	0.0856	Interplant
Flaccidity	**0.0057**	Intraplant
Rot	**0.0011**	Interplant
Spot	0.6741	Interplant

Linear regression was used to test whether leaf and tuber spectra could predict storage mass loss; however, both datasets provided insignificant R^2 values of 0.01 and −0.01, respectively. This suggests that post-harvest factors may play a greater role in storage spoilage; these post-harvest factors will be explored in later chapters.

2.4 Discussion

2.4.1 Differential watering regimen

Tuber yield by both mass and number was greater in WW plants (Figure 2.5). This was expected since drought during tuberisation results in fewer stolons per stem, decreasing yield (Eiasu et al., 2007). Tuber defect severity scores were similar between WW and DS plants (Figure 2.6), which may be due to the heatwave and the subsequent emergency watering regimen. Accessible tubers first emerged on day 70, 10 days prior to the beginning of the heatwave, and continued emerging till day 111, so that formed tubers in both groups post-tuberisation were exposed to similar levels of heat stress. Both drought and elevated growth-medium moisture are known to cause potato tuber defects (Obidiegwu et al., 2015). Heat stress impacts potato plants to varying degrees depending on duration, intensity, water availability, soil nutrients and cultivar (Ghosh et al., 2000; Yencho et al., 2008; Zhang et al., 2020). Both WW and DS groups used the same cultivar (Orchestra), and the same compost and fertiliser so initial soil nutrients can be assumed equal. Intensity and duration of heat stresses was equal between groups as they were grown together in the same glasshouse. This is consistent with the present results, in which the combination of heat stress and drought stress as a result of the heatwave experienced during the experiments have culminated in similar levels of defects in both WW and DS groups. However, water availability was significantly different throughout the differential watering treatment, which may explain the observed difference yield between WW and DS plants (Figure 2.5).

2.4.2 Stomatal conductance

Stomatal conductance in both WW and DS plants was significantly reduced by a heatwave (Figure 2.3), where glasshouse temperatures reached 40°C (Figure 2.4). Elevated temperature is known to cause stomata to open (Urban et al., 2017). However, higher temperatures also increase plant water demand (Lobell et al., 2013), imposing drought stress as water demand may exceed water uptake. This creates a balance between closing of stomata due to drought stress and opening of stomata due to elevated temperature (Bjerring Jensen et al., 2024), where drought stress-induced stomatal closing can dominate stomatal responses (Zhou, 2017), which would result in

the drought-induced stomatal closure response observed in both WW and DS following the heatwave.

2.4.3 Correlation between tuber greening and lenticular spots

A correlation between greening and lenticular spots was observed (Table 2.3, Figure 2.8). This may be a reflection of both being common and mild defects, rather than suggesting a causal relationship. Whilst mild greening was common as no further compost was added to pots during growth, exposing surface tubers to light, lenticular spot formation is known to be promoted by high growth-medium moisture causing lenticular proliferation (Adams, 1975). This suggests that the emergency watering regimen post heatwave may have imposed sufficiently moist growth-medium conditions to widely promote lenticular spot development in plants of both treatment groups. Interestingly, DS plants produced fewer surface-accessible tubers. Drier soils cause potato root length to be greater (Nasir & Toth, 2022), which has the potential to cause tubers to form deeper, thereby increasing the average tuber depth, resulting in a reduced percentage of tubers exhibiting greening in dry soils, which also do not promote lenticular spots (Adams, 1975). However, there was no significant difference between average severity of greening or lenticular spots between WW and DS plants, suggesting that the effects of the emergency watering regimen outweigh the effects of any differential rooting depth between the treatment groups.

2.4.4 Leaf spectra

The relationship between glasshouse humidity and leaf spectra co-Mahalanobis distance may perhaps be a result of stomatal conductance responding to atmospheric humidity and this altering the internal carbon dioxide concentration (C_i) of leaves differentially between WW and DS plants. Under conditions of low relative humidity, stomata close, resulting in an increase in C_i (Driesen et al., 2020). Tahmasbian and Morgan (2021) showed that vis-NIR spectroscopy can be used to determine total carbon concentration in ground wheat; the band 400–550 nm offered the most accurate determination, although less accurate determination could be achieved with 1451–1600 nm. Spectra in this chapter were recorded in the bandwidth 900–1700 nm, which includes the band at 1451–1600 nm identified by Tahmasbian and Morgan. PCA of second differential leaf spectra from WW plants provided weak separation between pre

and post heatwave in the band 1451–1600 nm identified by Tahmasbian and Morgan in 2021 (Figure 2.23 b,d), where pre-heatwave datapoints were separate from post-heatwave datapoints. Days 55–70 were used as the pre-heatwave period and days 75–90 the post-heatwave period, the heatwave occurring from days 75 to 80. Therefore, Figure 2.23 suggests that alterations in leaf C_i due to changes in stomatal conductance, contributing to differences in total carbon, may explain some of the relationship observed between leaf spectra and atmospheric humidity. Cotrozzi et al. (2017) produced a model for estimating leaf water potential using reflectance spectroscopy in the 950–2400 nm bandwidth. Leaf water potential varies under drought stress (Martínez-Vilalta & Garcia-Forner, 2017), so may explain some of the observed changes in leaf spectra under drought conditions.

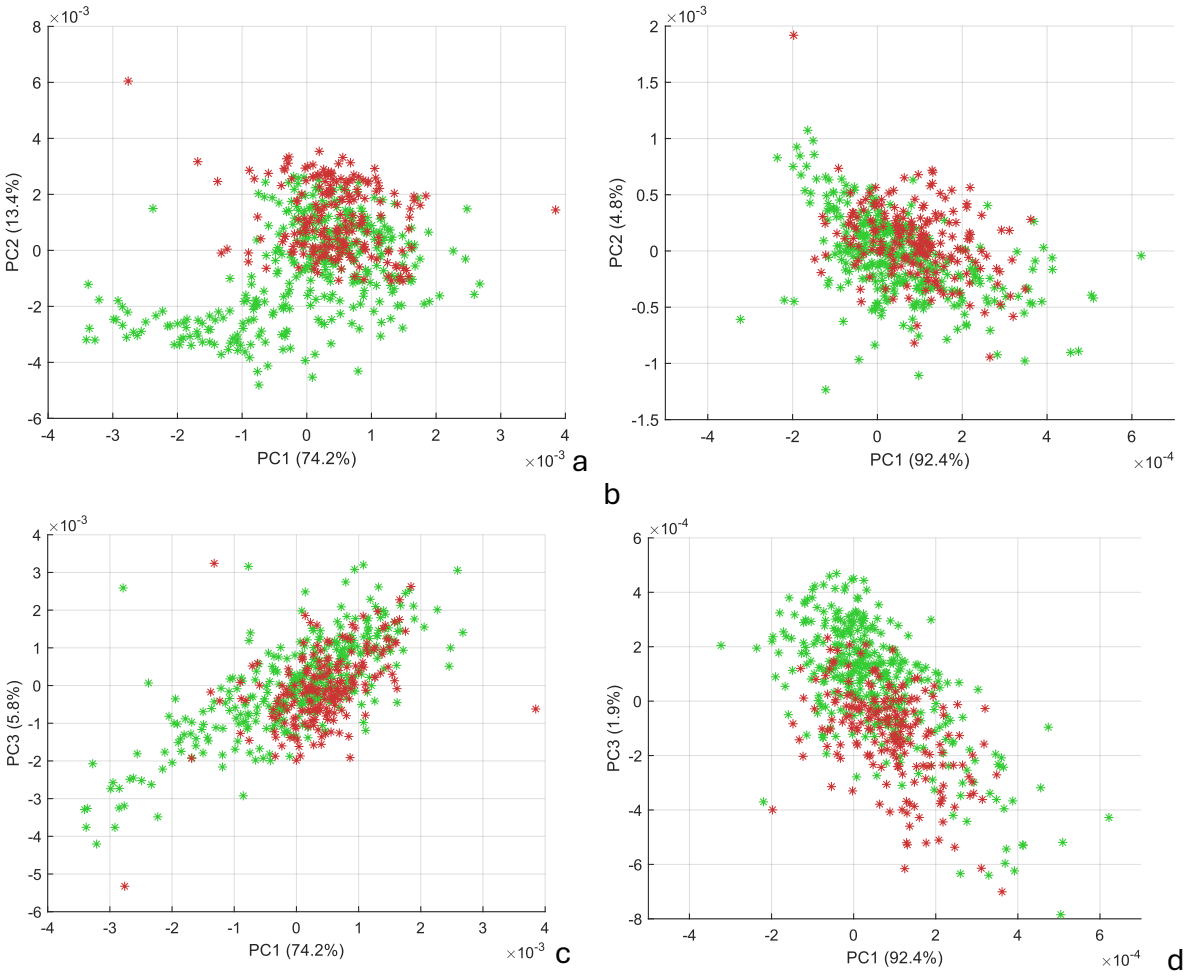

Figure 2.24 Principal Component Analysis of NIR potato leaf spectra during growth, pre and post heatwave stress.
Full bandwidth 900–1700 nm, carbon content bandwidth 1451–1600 nm. a: Full bandwidth PC1 vs PC2. b: Carbon concentration bandwidth PC1 vs PC2. c: Full bandwidth PC1 vs PC3. d: Carbon concentration bandwidth PC1 vs PC3. Green denotes pre-heatwave (days 55–70), red denotes post heatwave (days 75–90). n=560 (360 pre-heatwave, 200 post heatwave).

2.5 Conclusions

The present data suggest that NIR leaf spectra may not perform well for prediction of post-harvest tuber outcomes in potato and thus may not provide an additional tool for assisting crop walkers to identify early signs of defect development in potato plants. However, it is important to note that this study only explored heat and drought stresses, so the results cannot be extrapolated to other stresses such as nutrient deficiency, pollutants or pathogens. Nevertheless, these data do show the potential of pre-harvest NIR leaf spectra as a tool for assessing the effects of weather upon a crop.

The pot window system worked effectively for enabling subterranean tuber data collection during growth. Use of a handheld spectrometer with the foot pedal system was effective for scanning leaves without introducing unnecessary mechanical damage or need for assistance.

Importantly, large intraplant variance between tubers was observed (Figure 3.22). Given that leaf spectra are specific to a plant without any specific bearing on individual tubers, this may be a driving factor for the lack of relationship between pre-harvest leaf spectra and post-harvest tuber outcomes.

Co-Mahalanobis distance demonstrated utility as an analytical tool for exploring how categorically grouped spectra differ over time. This enabled analysis of how environmental stimuli differentially affected WW and DS plants (Figure 3.16). Accuracy of simple classification algorithms such as SVM using only two principal components, correlates strongly with co-Mahalanobis distance between spectra; however, classifications involving cascading classifiers examining hundreds of features may not be as well tied to co-Mahalanobis distance; this approach would be inappropriate for image processing, for example.

Neither pre-harvest leaf spectra nor pre-harvest tuber spectra could predict post-storage mass loss, suggesting that post-harvest factors may play a greater role in defect development during storage. This issue will be explored in Chapter 5, which will consider storage factors and defects that develop during the storage phase of the fresh potato supply chain.

3 Chapter 3: Defect development during storage and the potential for early detection or prognosis

3.1 Introduction

Food waste and losses are a growing global issue (Wang et al., 2025), increasing by a quarter between 2004 and 2014 (Gatto & Chepeliev, 2024). This represents a significant resource burden in agrifood systems, increasing their carbon footprint (Wang, 2025). The global carbon footprint of food waste and losses exceeds the carbon footprint of any country bar China and the United States (Scialabba, 2015). In addition to environmental pressures, food waste impacts food security, especially in low-income countries (Gatto & Chepeliev, 2024). Food insecurity and undernourishment are affecting more people as populations and environmental degradation increase such that the number of chronically undernourished people grew by 38 million to 815 million between 2015 and 2016 (Wijesinha-Bettoni & Mouillé, 2019). Losses in food are matched by considerable losses in market value, with 936 billion USD worth of food being wasted or lost in 2012, with another 411 billion USD in social cost of resulting greenhouse gases (Scialabba, 2015).

Potatoes are a globally important crop, rising in consumption in Asia and Africa (Wijesinha-Bettoni & Mouillé, 2019), where the challenges of food insecurity are most prevalent (Kabasa & Sage, 2009). The United Nations declared 2008 the year of the potato, recognising the crop's vital role in food security and alleviating poverty (Lutaladio & Castaldi, 2009). Tuber defects, both internal and external, are a significant contributor to potato waste and losses, with approximately half of total potato losses resulting from failure to meet quality standards, either for food safety or consumer preference (Willersinn et al., 2015). Thus, better management and prevention of potato defects is key to reducing losses in the potato supply chain, and their resulting environmental and humanitarian consequences.

Understanding how defect development can be detected is vital to their prevention and management. Identifying and detecting signs of early defect development during storage could enable evasive action to be taken to mitigate food losses. A common non-pathological potato defect that develops post-harvest during storage is blackheart

(Chapman, 2018), characterised by a visible darkened region of necrotic damage in the interior of affected tubers (Figure 3.1). The incidence of blackheart is increasing within the UK potato industry, and the ability of blackheart to develop in retail or consumer homes, and to go undetected till consumption, may obscure the true impact of this disease on crops (Terry, 2015). Blackheart typically occurs during potato storage when atmospheric CO_2 concentrations become too high, leading to atmospheric O_2 levels becoming too low (Davis, 1926; Kiaitsi, 2015). Storage facilities are kept well-ventilated to avoid this, at cool temperatures, typically 3°C–5°C, which lowers respiration rate and slows the development of blackheart as cells consume less oxygen per unit time (Hopkins, 1924).

Figure 3.1 Cross-section of potato afflicted with blackheart in the shape of a black heart.

The mechanisms of blackheart are poorly understood (Kiaitsi, 2015). Chapman (2018) suggests blackheart is induced by a low ATP:ADP ratio resulting from insufficient oxygen, whilst Kiaitsi (2015) proposes blackheart development is influenced by sugar and phenolic content. Necrosis involved in blackheart reduces subcellular compartmentalisation, increasing the availability of tyrosine, which when acted upon by tyrosinase produces melanic substances in the centre of the tuber (Davis, 1926). The importance of tyrosinase in the development of blackheart stems from early research by Bartholomew (Bartholomew, 1913; Bartholomew, 1914) and has persisted in the literature until recently. Although this established view has recently been challenged (Chapman, 2018), if tyrosinase activity is related to blackheart severity this could nevertheless provide a means of assessing the severity of blackheart or “pre-

blackheart" before visible darkening develops. However, destructive testing of this sort is wasteful, increasing food losses, as well as resulting in healthy potatoes being handled as defective when their shipment fails quality control. Therefore, non-destructive detection techniques could be harnessed to reduce food waste, whilst the ability to detect which individual potatoes in a failed shipment are defective or healthy would enable the saving of healthy potatoes.

3.1.1 Data analysis methods

3.1.1.1 Subspace ensemble classifier

Ensemble classifiers comprise multiple classifiers, whose predictions are combined into consensus. In the case of subspace ensembles, each subclassifier is trained on a focused subset of predictors called a "subspace", subspaces were chosen randomly in this chapter. "Majority voting" was used to combine predictions where the overall prediction of the ensemble is formed by the modal unweighted predictions of the subspace classifiers. Subspaces were generated randomly from the predictors. Linear discriminant classifiers were used for the subspace classifiers of the ensemble. Subspace ensemble classifiers were trained using the classifier learner app in MATLAB R2024a (MathWorks, Natick, Massachusetts, USA).

3.1.1.2 Linear least squares regression

Linear least squares (LLS) regression is a method of linear regression where the sum of squares of errors (or residuals in some cases) is minimised to fit a linear model to data. LLS was performed using the regression learner app in MATLAB R2024a.

3.1.1.3 Support vector machine

A support vector machine (SVM) is a binary classification method where a boundary formed by a hyperplane is fitted between the members of the two classes.

3.1.1.4 Gaussian process regression

Whereas other regression models typically produce a line or spline of best fit through a space of known data points, Gaussian process regression (GPR) produces a posterior normal distribution *f(y)* to model the uncertainty around unknown points within that space. Means of *f(y)* are a function of the known data points *f(x)*, and the covariance matrix of the *x* values of the unknown datapoints transposed by a kernel function. Where a kernel function describes the separation between *x* values to govern the

influence each known data point has over a given unknown data point, an exponential kernel function was used in this experiment.

3.1.1.5 Principal component analysis

Principal component analysis (PCA) is a multivariate reduction algorithm where the eigen vectors of the covariance matrix of datapoints within a hyperspace are used as latent variables to transform the datapoints onto. How much of the variance of points within the unreduced hyperspace is explained by each latent variable or "principal component" (PC) is represented by the eigen value corresponding to the eigen vector. PCs are indexed by decreasing eigen value magnitude or "explainability", such that the PC with the greatest explainability is "PC1".

3.1.1.6 Correlation coefficients

Pearson's correlation coefficient is a measure of linear correlation between two random variables. Pearson's correlation coefficient is computed by dividing the covariance of the two random variables by the sum of their standard deviations.

Classification models produce a table of predicted classes and actual classes called a "confusion matrix". Matthews correlation coefficient (MCC), sometimes referred to as the phi coefficient, is a correlation test for binary values and can be computed from a confusion matrix. Fisher's exact test (FET) was used to provide an accompanying P value for confusion matrices.

3.2 Aim and objectives

The overall aim of this chapter is to investigate whether non-destructive techniques can be used to detect blackheart development during potato storage. The objectives of this chapter are:

- Establish a model system for studying the effects of simulated blackheart-inducing storage conditions
- Investigate the potential for NIR spectroscopy for early detection of blackheart during storage
- Investigate whether tyrosinase activity is an accurate measure of blackheart severity

3.3 Materials and methods

3.3.1 Plant material and treatments

3.3.1.1 Long-term high-CO_2 and low-temperature treatment

Potatoes of the "Orchestra" variety were stored in a controlled environment cabinet (Sanyo, Osaka, Japan) at 2000 ppm CO_2, 5°C, in the dark, equivalent to suboptimal industrial storage conditions that lead to blackheart developing in potato tubers (Figure 3.2). Ideally industrial potato storage is actively ventilated to prevent elevation of CO_2 (Cunnington, 2023). Whilst potato storage temperature varies by application (Khanal & Uprety, 2014), 5°C is towards the lower end of potato storage temperatures and was chosen to avoid the development of pathogenic defects that may confound results. Additionally, this temperature was low enough to avoid spoilage without causing frosting issues with the refrigeration system of the controlled environment cabinet.

The Sanyo growth cabinet was fitted with a CO_2 vapour withdrawal cylinder and proportional-integral-derivative (PID) CO_2 valve control system. An atmospheric logger was placed inside the cabinet to validate CO_2 levels reported by the control system. The room this system was located in was fitted with a CO_2 monitor and alarm so any hazardous leakage could be detected and resolved.

Figure 3.2 High-CO_2 longitudinal storage system comprising a Sanyo controlled environment cabinet (Sanyo), CO_2 vapour withdrawal cylinder, valve control system and secondary CO_2 meter.

Potatoes were removed from the cabinet fortnightly in random groups of five and replaced by a new group of five potatoes. Prior to entry into the cabinet, potatoes were stored in a well-ventilated cold storage room at 5°C. All potatoes in this experiment were of single origin from the same farm and harvested at the same time to ensure total potato ages were comparable. The Orchestra variety was chosen both for its resistance to pre-harvest disease (Agricrops, 2020) and consistency with other experiments in this thesis. Resistance to pre-harvest disease minimises confounding factors from defects other than those studied in this chapter. Small differences can be found between differing varieties of potato, so using Orchestra across multiple experiments, where compatible, increases the comparability of these results.

3.3.1.2 Short-term very high-CO_2 and elevated-temperature treatment

Potatoes of the Orchestra variety were exposed to very high CO_2 and 25°C temperature treatment in a purpose-built rapid anaerobic chamber (RAC) system designed for rapidly inducing blackheart in intact potato tubers. This comprised an airtight 3.5 L

plastic container (16.5 cm x 24 cm x 9 cm) fitted with a gas inlet and outlet valves, and an Arduino Uno (Arduino) microcontroller for monitoring conditions. A Grove ME2-O2-Φ20 O_2 sensor (Seeed Studios, Shenzhen, China) and a Grove SCD30 CO_2, temperature and humidity sensor module (Seeed Studios) was fitted inside the RAC for logging and display via the Arduino Uno.

The RAC was flushed with CO_2 from a vapour withdrawal cylinder to reach almost 100% CO_2, and reflushed every 48 h to maintain anoxic conditions. Condensation was also removed with a paper towel when reflushing. A horticultural heating mat placed underneath the box regulated the temperature of the air within the chamber to 25°C. The thermometer of the heating mat's controller was mounted inside the chamber to ensure the temperature being regulated was the internal air temperature. The Grove SCD30 provided a second thermometer to ensure the temperature was as desired and for logging purposes. Samples were supported on a grid to avoid contact with any puddled condensation and direct contact with the heat source.

Prior to treatment, all potatoes were stored in a well-ventilated cold storage room at 5°C. Before treatment, potatoes were gently washed by hand with water, sponge and paper towels, and acclimatised at room temperature for 24 h. Control potatoes were washed and acclimatised at room temperature in the same way as treated potatoes but did not receive any further treatment.

3.3.2 NIR spectroscopy and electrical data collection

NIR spectra were gathered using a handheld NIR spectrometer device: NIRvascan ASP-NIR-M-Reflect (Allied Scientific Pro, Gatineau, Quebec, Canada) and DLP NIRscan Nano GUI software (Texas instruments, Dallas, Texas, USA), with use of the foot pedal system devised in Chapter 2. NIR spectra were recorded from tubers prior to them being placed into the controlled environment cabinet. Before scanning, tubers were removed from cold storage and left on a lab bench for 24 h to acclimatise to room temperature. Post-storage spectra were also recorded after 24 h of room temperature acclimatisation.

Electrical data were recorded immediately after spectra were collected, both pre and post-storage, to avoid electrode residue affecting spectra, although care was taken to avoid and clean any residue before storage in the controlled environment cabinet. Electrical data were recorded by passing 10 V sine and square waves through the intact potatoes in series via medical stick-on electrodes (Healthcare World, London, England) and recording the output voltage with a Hantek DSO510P oscilloscope (Hantek, Shandong, China) at differing input frequencies. Sine wave outputs were measured as peak to peak (PP). Both root-mean-square (RMS) and PP voltage were recorded for square waves, as reactances alter the waveform of square waves, as seen by the output waveforms in Figure 3.3, all of which are from square wave inputs of differing frequencies. Altering waveform changes the RMS-to-PP ratio, as different waveforms have different RMS voltages at equivalent PP voltage (Cartwright, 2007). Voltage was recorded at the following frequencies of sine wave: 10 Hz, 100 Hz, 800 Hz, 1 kHz, 3 kHz, 5 kHz, 100 kHz, 1 MHz, 3 MHz, 5 MHz, 8 MHz, 10 MHz, 13 MHz, 15 MHz, 18 MHz, 20 MHz, 23 MHz, and 25 MHz. Voltage was recorded for square waves at the same frequencies, up to a maximum of 5 MHz imposed by hardware limitations. Waves were generated with a TENMA 72-3555 function/arbitrary waveform generator (TENMA, Akabane, Tokyo, Japan).

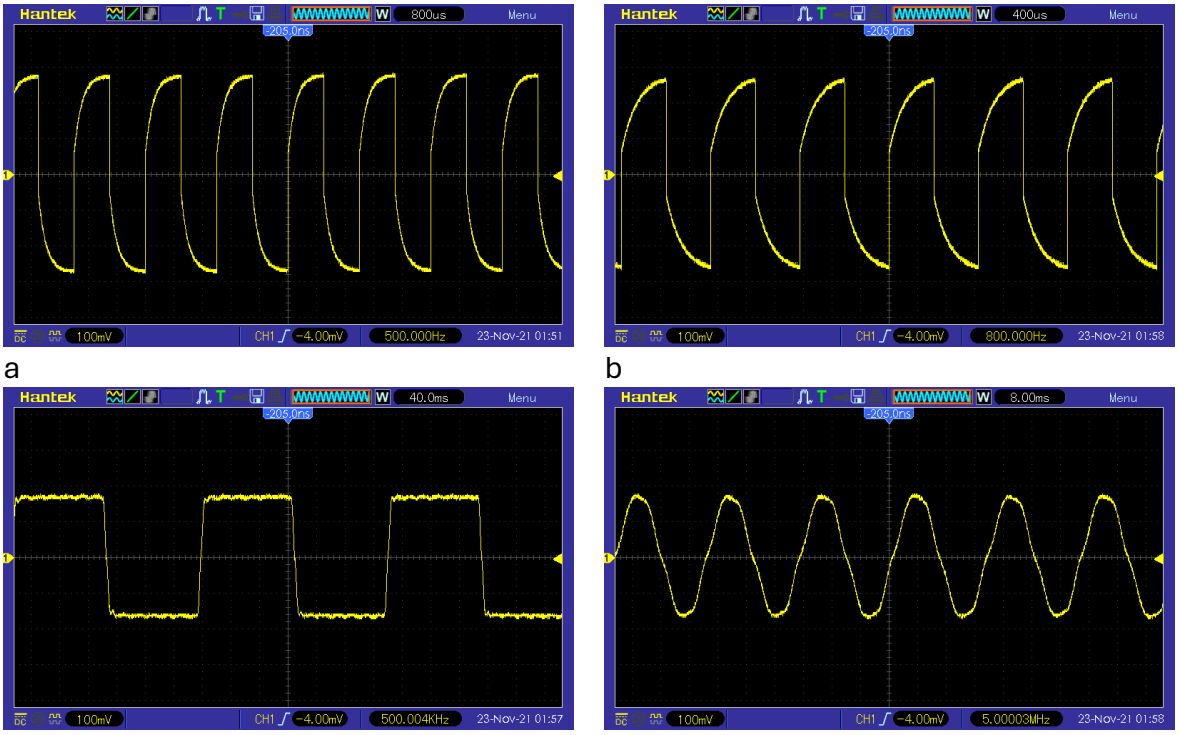

Figure 3.3 Output signals from passing 10 V square waves through an intact potato in series.
a: 500 Hz, b: 800 Hz, c: 500 kHz, d: 5 MHz. Screen captures taken on a Hantek DSO510P oscilloscope.

3.3.3 Blackheart assessment

3.3.4 Tyrosinase assay

Tyrosinase activity was measured using a spectrophotometer to measure the rate at which absorbance at 470 nm increased over time within a potato extract assay (Partington & Bolwell, 1996). Lengthwise slices 3 mm thick were cut from the middle of each potato to produce a cross-section including the pith. Slices were individually blended with a T1500 (Ystral, Ballrechten-Dottingen, Germany) in 15 mL of extraction buffer and centrifuged at 4000 rpm at 5°C in a Harrier R (MSE, Cholet, France) to separate the solid matter, then stored on ice prior to analysis. 200 µL of the resulting extract was then combined with 1 mL of assay buffer and immediately placed in a Novaspec II spectrophotometer (Pharmacia LKB, Pfizer, New York City, USA), and the absorbance recorded every 30 s for 5 min.

3.3.4.1 Extraction buffer:

50 mM phosphate buffer, pH 6.5

1 mM EDTA

0.1% (v/v) Triton X-100

5% (w/v) PVPP (polyvinylpolypyrrolidone)

3.3.4.2 Assay buffer:

50 mM phosphate buffer

0.1% SDS

10 mM L-DOPA (3,4-dihydroxyphenylalanine)

3.3.5 Cross-sectional area imaging

Tubers were bisected along their length from hip to tip; both halves were then dabbed dry with a paper towel and photographed. Photos were edited in an image manipulation program (GIMP 2.0, GIMP Development Team). A MATLAB script was used to isolate the potatoes from the red background, quadratically increase image contrast and calculate the portion of potato cross-section exhibiting blackening.

3.3.6 Data analysis

GPR and linear regressions were performed using the regression learner app in MATLAB R2024a (MathWorks). The classification learner app in MATLAB R2024a was used to train the SVM using the quadratic programming soft-margin minimalisation setting "L1QP". PCA was performed using the 'pca' function in MATLAB R2024a; however, PCA for classification and regression analysis was performed using the PCA tool in the classification and regression learner apps in MATLAB R2024a with 95% explainability.

All P and R values for Pearson's correlation coefficient in this chapter were calculated using the "corrcoef" function in MATLAB R2024a. MCC was computed for this chapter using the confusion matrices of classifier's results using Equation 1 with the variables in Table 1; this was implemented as a simple MATLAB script. *x* and *y* denote two random variables, in our use case these random variables are the actual values of a binary class and the values predicted by a classifier.

Table 3.1 Confusion matrix for MCC calculation, where x and y are random binary variables describing the predicted values and real values of the response variable of a classifier.

	y=1	*y*=0	total
x=1	n_{11}	n_{10}	$n_{1\bullet}$
x=0	n_{01}	n_{00}	$n_{0\bullet}$
total	$n_{\bullet 1}$	$n_{\bullet 0}$	n

$$\phi = \frac{n_{11}n_{00} - n_{10}n_{01}}{\sqrt{n_{1\bullet}n_{0\bullet}n_{\bullet 0}n_{\bullet 1}}} [1]$$

To provide a corresponding P-value for confusion matrices, FET was used, implemented via the 'fishertest' function in MATLAB R2024a.

3.4 Results

3.4.1 Blackheart development in potatoes is minimal at 2000 ppm CO_2 and 5°C

Five tubers of the 162 stored in the high-CO_2 environment developed blackheart during this experiment, with ranging severity; see Figure 3.4. One tuber exhibiting blackheart also developed pink rot (Figure 3.4 b), and one blackheart tuber developed cavitation (Figure 3.4 e).

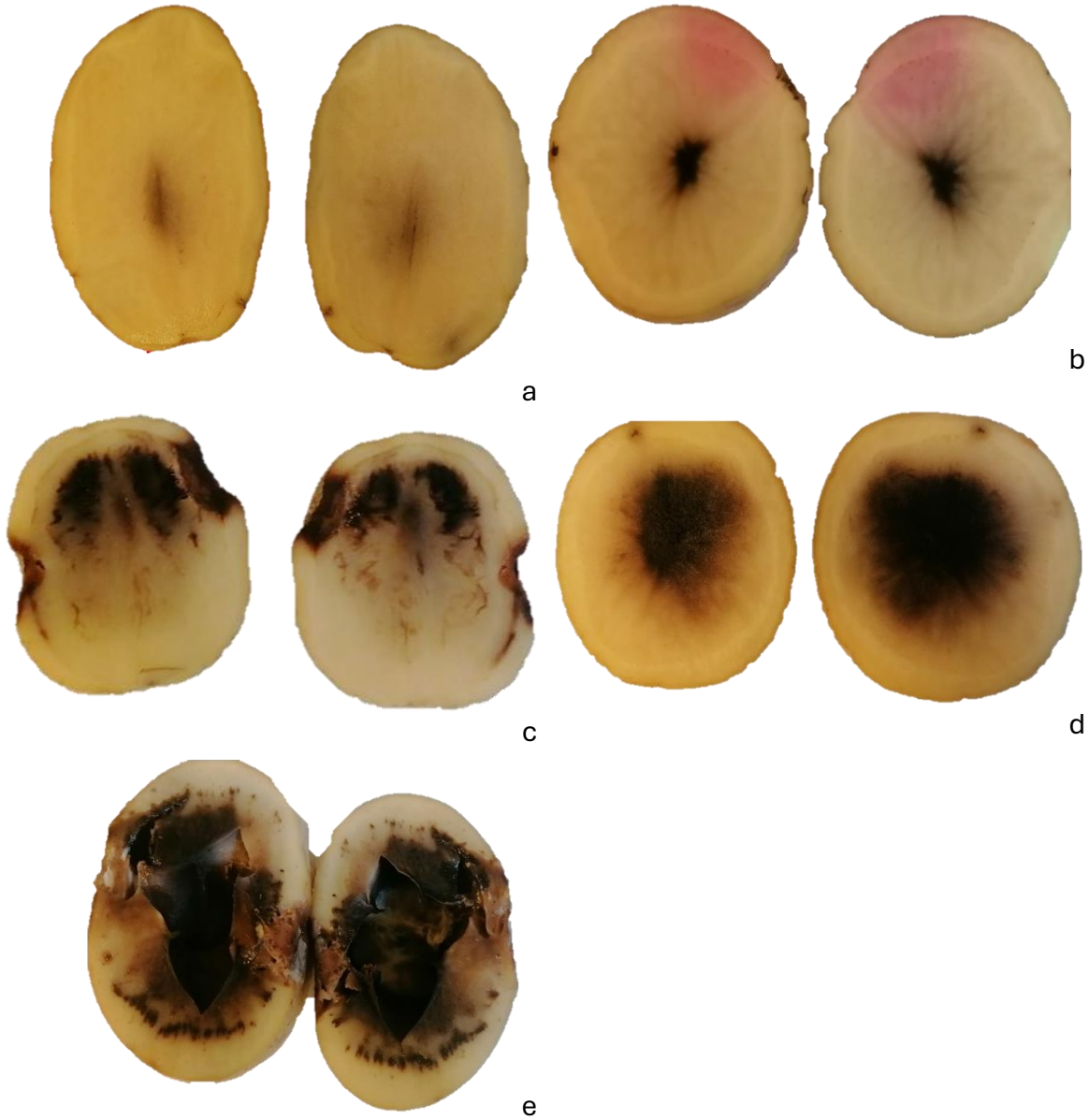

Figure 3.4 Cross-sectional images of potato defects after storage treatment. a–e: Potatoes affected by blackheart after 60 weeks in 2000 ppm CO_2 storage at 5°C. b: also affected by pink rot. e: exhibits cavitation sometimes seen in blackheart, although other causes such as hollow heart are common.

3.4.2 Long-term 2000 ppm CO_2 storage at 5°C is associated with changes in potato electrical impedance

Impedance of potatoes was measured by passing oscillations of differing frequency through the potatoes and plotting output voltage against frequency. These output voltages were altered after storage in the high-CO_2 environment for 2–62 weeks, demonstrating the potential of electrical impedance for the non-destructive assessment of the effects of storage upon fresh potatoes.

The replacement of a faulty connector, used to connect the function generator to the sample, resulted in a marked change in voltage curve data after this change. For this reason, only electrical data recorded after this point were included in the analysis. Sixty-nine tubers had useable electrical data both pre and post storage. There was little visible separation in electrical impedance spectroscopy data between pre-storage and post-storage (Figure 3.5 a–c), although there were frequencies at which high variance or inter-group separation was visible, especially within the 5kHz–5MHz band (Figure 3,5 a–c), although there was high variance at 10 Hz in square PP (Figure 3.5 c).

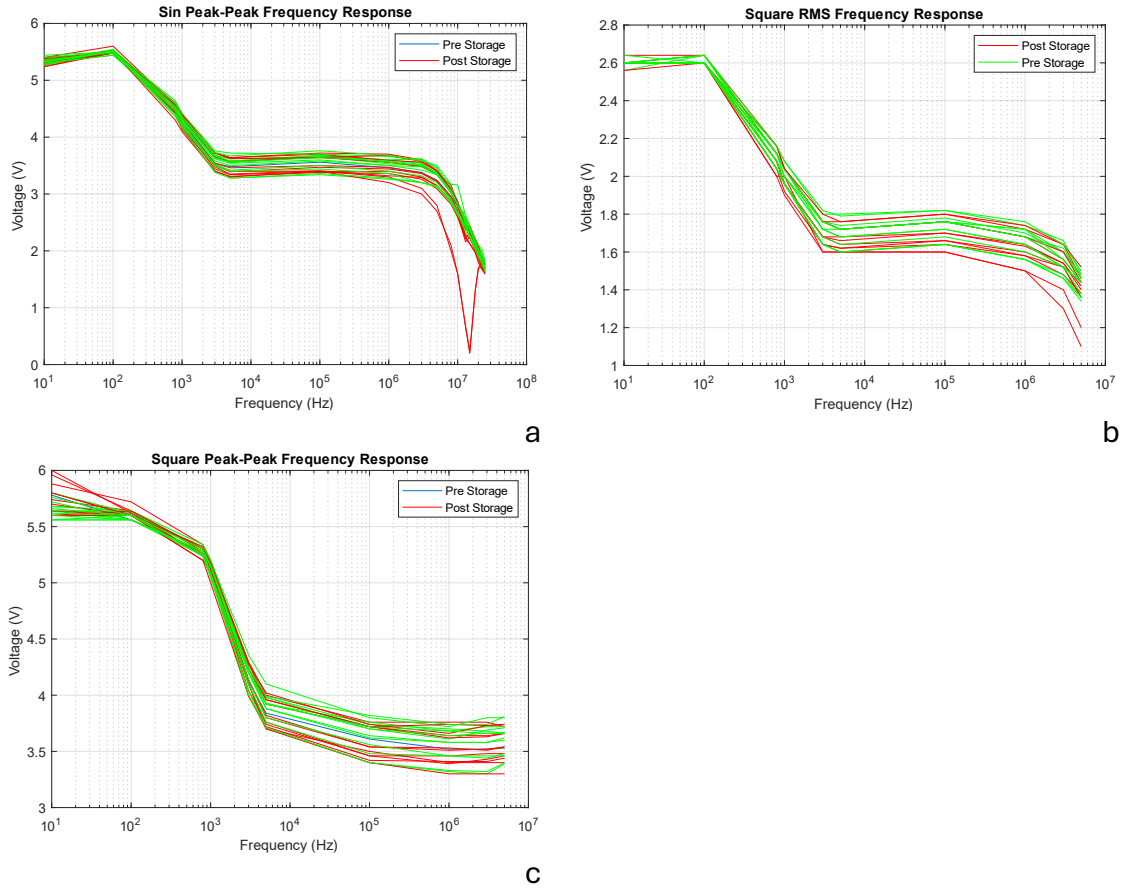

Figure 3.5 Output voltages against frequency when passing electrical sweeps through intact potatoes, pre and post 2000 ppm CO_2 storage and 5°C treatment a: Sin signal PP output voltage, b: Square wave signal RMS output voltage, c: Square wave signal PP output voltage. n=12 (12 pre-storage, 12 post-storage).

Given that variance and inter-group separation of voltage readings were spread across multiple features, a subspace ensemble classifier was trained on a concatenation of sin, PP square and RMS square data. Ensemble classifiers are made up of smaller classifiers trained on corresponding subspaces of the full feature space; classification of the combined model is performed by majority vote of the subclassifiers. Classification accuracy of 82.6% (MCC R=0.6313) was achieved with 5-fold validation and *n*=69 (Figure 3.6). Although significant given the FET P-value of 2.07×10^{-7}, these results may be exaggerated by overtraining due to the small '*n*' numbers.

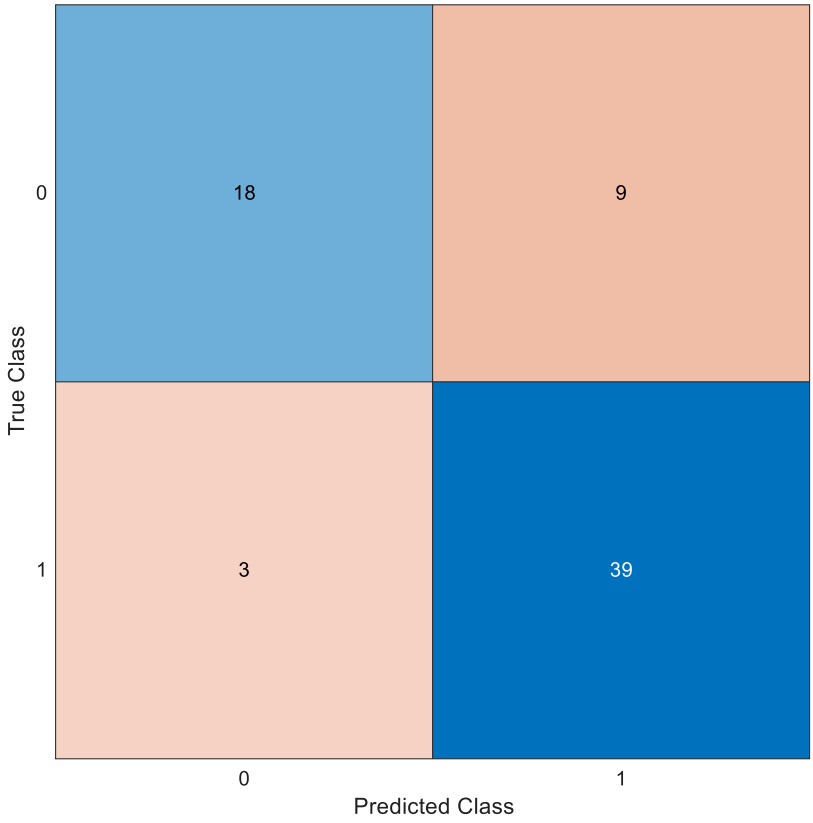

Figure 3.6 Confusion matrix for subspace ensemble of linear discriminant classifiers for classifying between pre and post storage using all 38 features, 82.6%, n=69, 5-fold validation.
Numbers in each cell denote the number of samples that were assigned to each predicted class and their corresponding true classes. Colour denotes population of each cell, where orange denotes a low population and blue a high population.

The ensemble classifier (Figure 3.6) having provided prediction between the categorical variable of pre or post storage, an LLS regression was trained for prediction of the continuous variable storage time in the 2000 ppm CO_2 environment to test whether the extent of the effects of storage can be detected via changes in electrical impedance as opposed to the binary presence of such effects. This continuous model yielded poor results, with an RMSE of 10.495 (62.9% of true value mean) (Figure 3.7 a); however, fascinatingly, differentiating the voltage curves provides better peak separation, and as a result much better linear regression results for predicting 2000 ppm CO_2 storage time (Figure 3.7 b). First-order differential provides an RMSE of 7.8207 (46.3% of actual value mean). While second-order differentials offer better peak separation than first-order differentiation, numerical differentiation, used due to the low resolution of the data, amplifies noise, resulting in a poorer regression using second-differential data with R^2=0.34 and RMSE=8.8307 (52.3% of actual value mean).

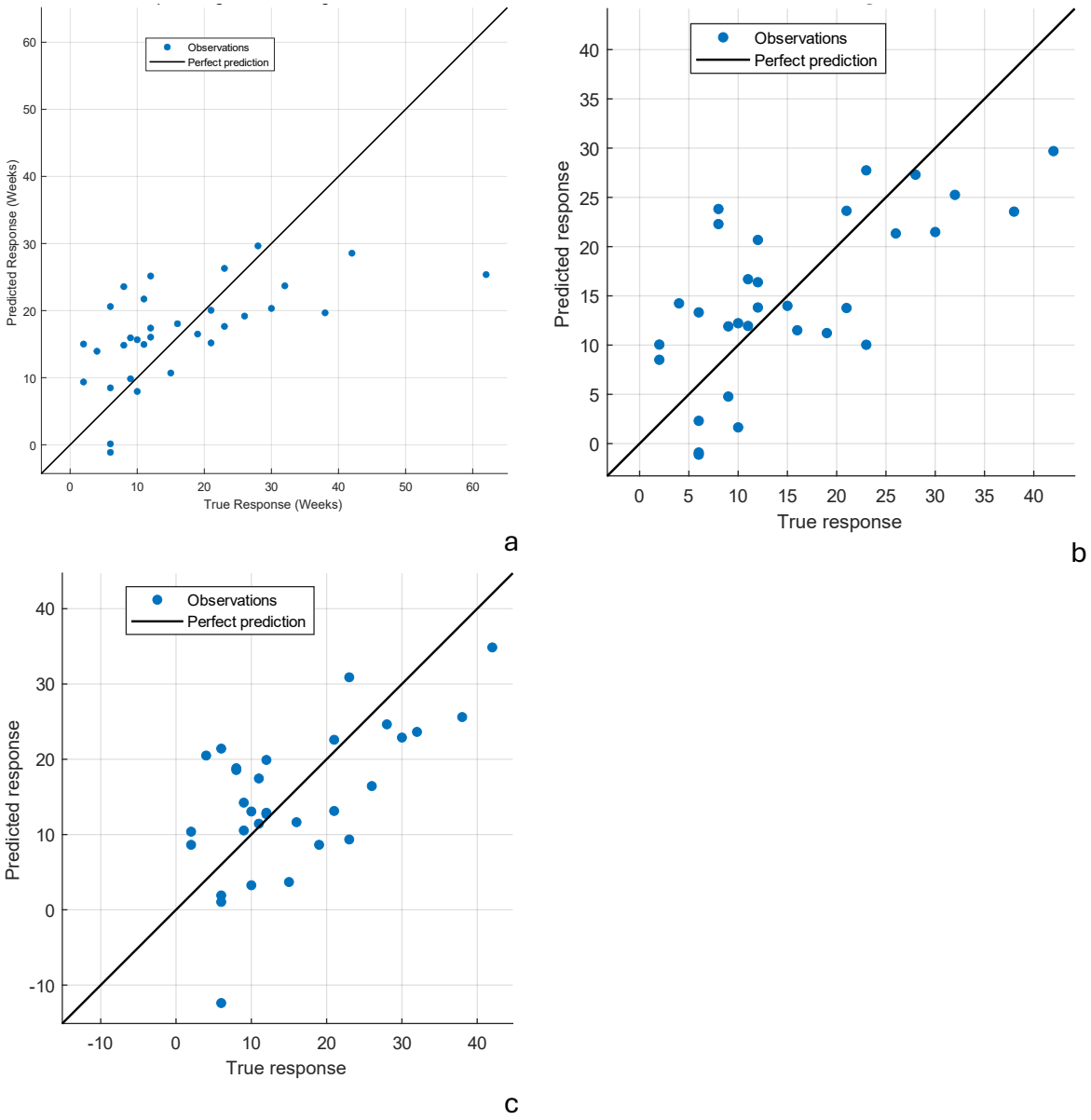

Figure 3.7 Efficient LLS regression of electrical data with potato storage time in weeks. Electrical data comprise output PP and RMS voltages when passing electrical voltages of varying frequencies and waveforms through intact potatoes. Data differentiated to different orders to separate peaks. n=32, mean actual value = 16.875. R^2 and root-mean-square error (RMSE) values reflect validation, 5-fold validation used. a: Zeroth differential R^2=0.36, RMSE=10.495. b: First differential R^2=0.47, RMSE=7.8207. c: R^2=0.34, RMSE=8.8307.

3.4.3 Investigating the potential of NIR spectroscopy for early detecting effects of 2000 ppm CO_2 storage

Tuber spectra from potatoes pre and post 2000 ppm storage produced similar peaks to those observed in tuber spectra in Chapter 2 (Figures 3.8 and 2.19, respectively), with peaks identified at 973 nm, 1191 nm, 1459 nm and 1694 nm (see Table 2.7 for associated compounds for each peak).

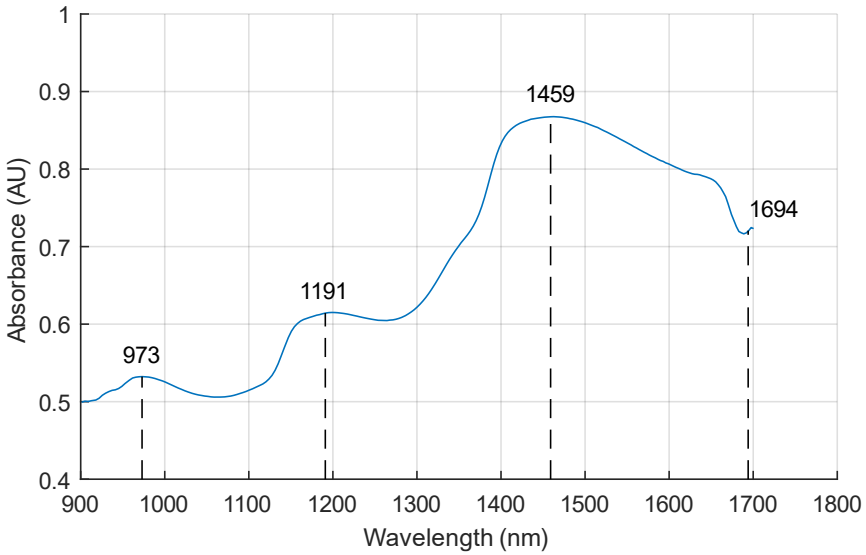

Figure 3.8 Mean NIR absorbance of potatoes both pre and post storage in a 2000 ppm 5°C environment, peaks denoted by dashed lines. n=521; each spectrum is the average of 6 scans.

To test whether storage in the long-term 2000 ppm CO_2 environment induced physiological or chemical changes detectable via NIR absorbance spectra, a subspace ensemble of 30 linear discriminant classifiers were trained on the first four PCs of 302 second-differential spectra with 5-fold validation (Figure 3.9), 151 recorded pre-storage and 151 recorded post-storage. Potatoes were stored for 19 weeks at 2000 ppm CO_2 and 5°C, on average, with a standard deviation of 14 weeks. Pre- and post-storage spectra were classified with 75.4% accuracy (Figure 3.9). The confusion matrix in Figure 3.9 shows how many potatoes were pre or post storage, and how many of each group were classified correctly. Figure 3.9 yields an MCC coefficient of R=0.493 and an FET of $P=9.1\times10^{-18}$.

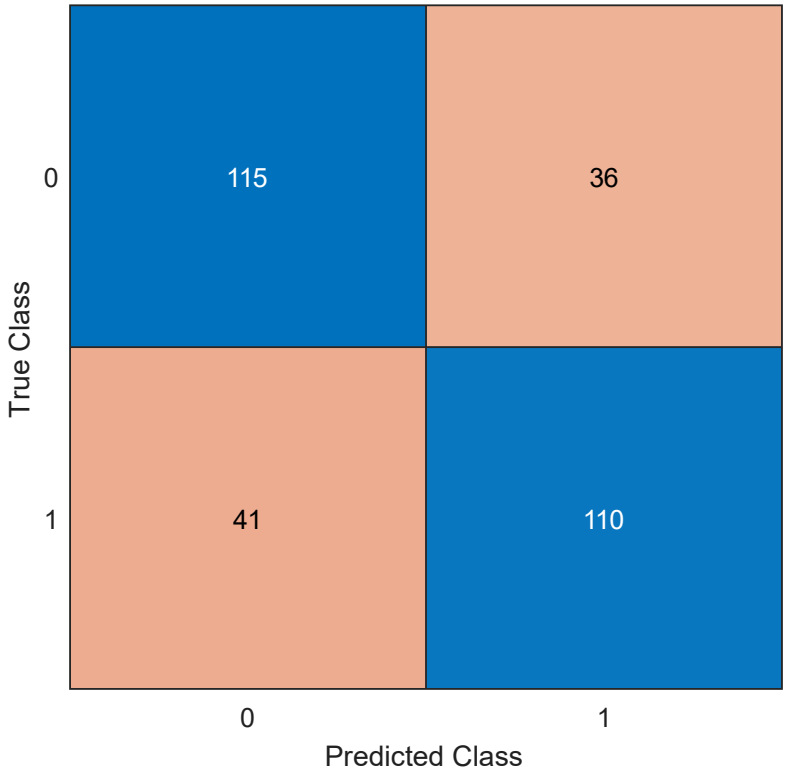

Figure 3.9 Ensemble subspace linear discriminant classifier confusion matrix for classifying between the second-differential NIR absorbance spectra of intact potatoes before and after storage in a 2000 ppm CO_2 5°C environment. First 4 PCs of NIR absorbance spectra used. 75.4%, 30 classifiers, n=302, 5-fold validation. Numbers in each cell denote the number of samples that were assigned to each predicted class and their corresponding true classes. Colour denotes population of each cell, where orange denotes a low population and blue a high population.

The classifier in Figure 3.9 does not distinguish between short and long 2000 ppm CO_2 storage times. Therefore, to test whether NIR spectra can be utilised to detect the extent of physiological or chemical changes from varying durations of 2000 ppm CO_2 storage, spectra were divided into binary groups of above and below median high-CO_2 storage time and used to train an SVM classifier with 5-fold validation. The SVM performed very poorly, with a classification accuracy of only 62.7% (Figure 3.10 b) (*n*=402). As values either side of the median can be very similar, creating weakly separated categories for classification, the upper and lower thirds were also used to train a quadratic SVM; this performed with a 71% accuracy (Figure 3.10 d) (*n*=269). To test whether observed changes are specific to the high-CO_2 storage environment, two more SVM classifiers were trained using data collection date as response variable. Since before entering the

experiment, tubers were all kept in well-ventilated cold storage, data collection date reflects total storage time independent of environment. These SVM models had similar performance to the high-CO_2 storage time models, with 68.1% (Figure 3.10 a) (*n*=521), for median based grouping, and 69.9% (Figure 3.10 c) (*n*=346), for upper and lower thirds grouping.

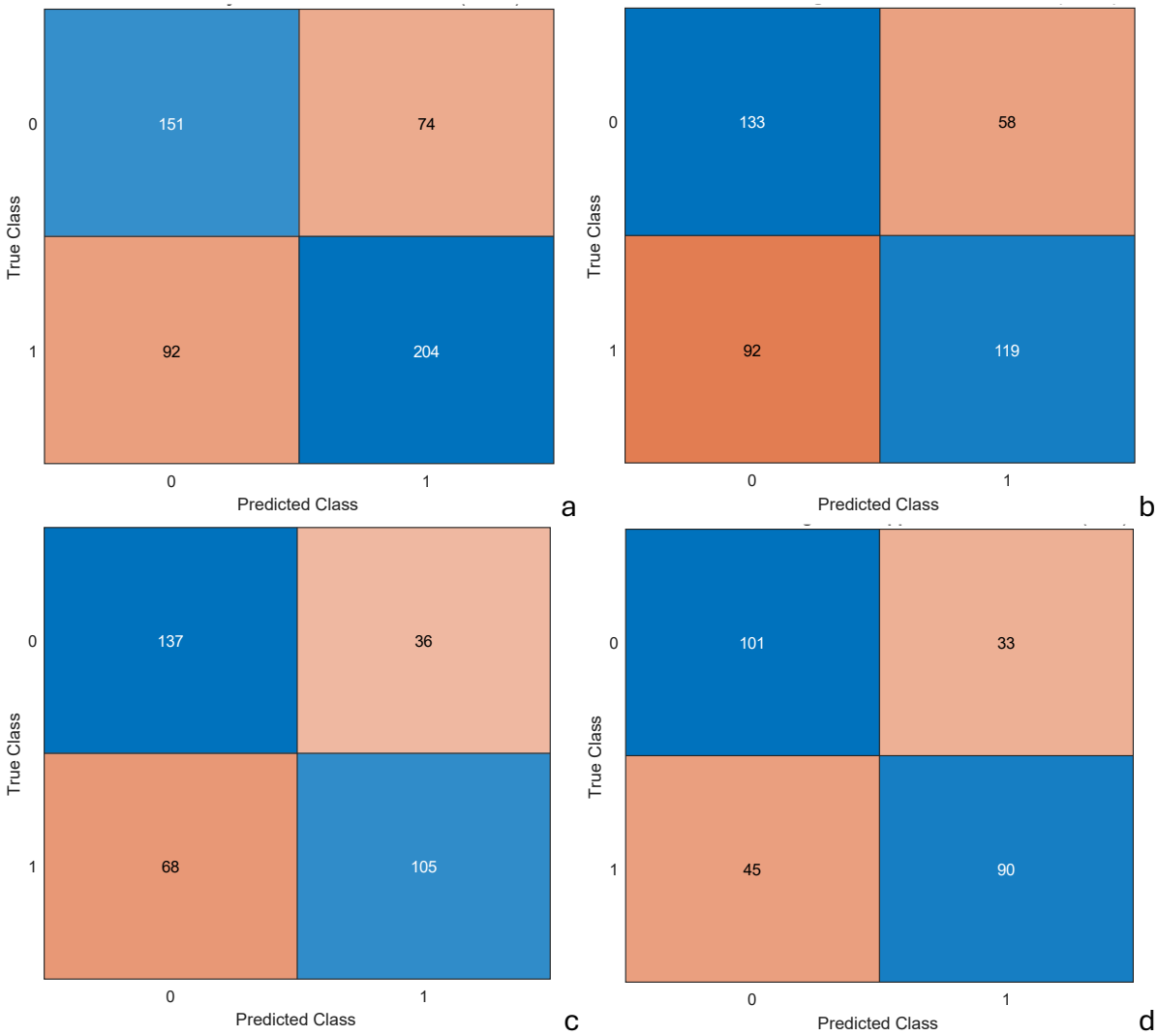

Figure 3.10 Confusion matrices for quadratic SVM classifiers trained on NIR spectra to predict storage time bracket; median used for dividing halves.
a: Classification between upper and lower halves of day of data recording, 68.1% accuracy, n=521, MCC R=0.3577, FET P=3.29×10^{-16}. b: Classification between upper and lower halves of storage time, 62.7% accuracy, n=402, MCC R=0.2619, FET P=1.55×10^{-7}. c: Classification between upper and lower thirds of data recording day, 69.9% accuracy, n=346, MCC R=0.4058, FET P=4.02×10^{-14}. d: Classification between upper and lower thirds of storage time, 71% accuracy, n=269, MCC R=0.4219, FET P=3.6×10^{-12}. Numbers in each cell denote the number of samples that were assigned to each predicted class and their corresponding true classes. Colour denotes population of each cell, where orange denotes a low population and blue a high population.

Interestingly, while spectra provided binary classification between pre and post storage (Figure 3.9), and between upper and lower thirds of storage time (Figure 3.10 d), spectra did not provide prediction of continuous 2000 CO_2 5°C storage time (Figure 3.11). GPR with an exponential kernel function was trained with PCs of second-differential NIR spectra to predict 2000 ppm CO_2 5°C storage time in weeks (Figure 3.10), yielding an RMSE of 13.444, which is 70.2% of the mean storage time. The difference in results between binary classification (Figures 3.10 and 3.9) and continuous regression (Figure 3.11) suggests that biological variance between potatoes affects the impact of elevated 2000 ppm CO_2 storage upon those potatoes.

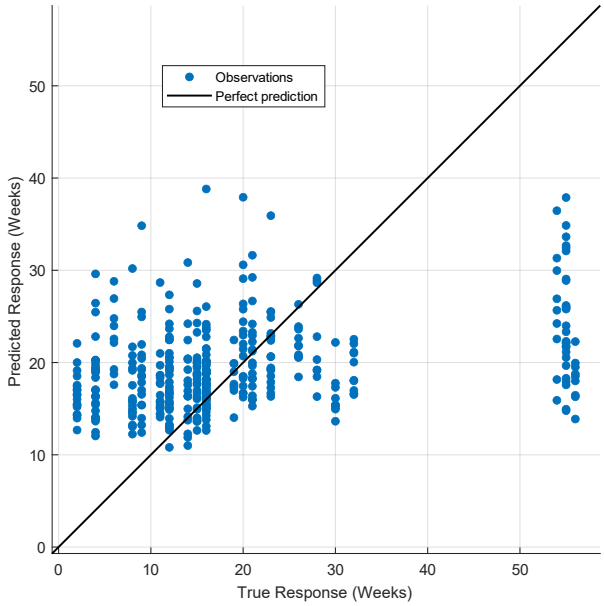

Figure 3.11 NIR second-differential storage time GPR with exponential kernel function, R^2=0.12, mean=19.321, RMSE=13.554, n=402.

3.4.4 Tyrosinase activity is not linked to blackheart severity

Tuber tyrosinase activity was compared with cross-sectional blackheart area; all five tubers that exhibited visible blackheart were included. There was no observed correlation between tyrosinase activity and cross-sectional blackheart area (Figure 3.12).

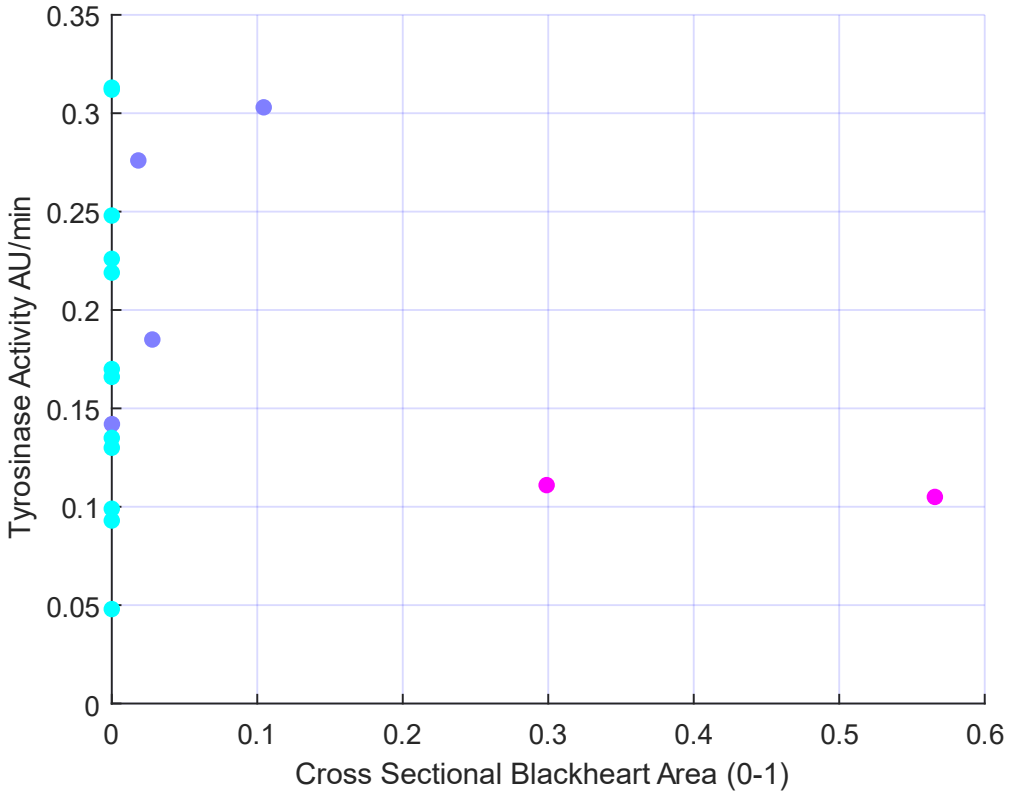

Figure 3.12 Tyrosinase activity in potato tuber samples against blackheart cross-sectional area, n=17. Colours reflect blackheart severity, where blue is no blackheart, purple some visible blackheart, and pink severe blackheart.

Given the small number of tubers that developed blackheart in the long-term high-CO_2 treatment, a new RAC system was constructed with the aim of rapidly inducing blackheart by exposing tubers to more extreme conditions: very high (~100%) CO_2 and 25°C. Although these conditions do not accurately simulate an industrially realistic scenario, they provide a more amenable experimental model for inducing defects in tubers and for examining the correlation between tyrosinase activity, blackheart symptoms and the potential of NIR spectroscopy for the non-destructive detection of blackheart.

The combination of very high CO_2 and 25°C in the RAC induced visible blackheart in 42% of tubers within 10–14 days, providing a greater sample size of blackheart-affected tubers for analysis. Tyrosinase assays were performed on blackheart and control untreated tubers taken from cold storage, washed and acclimatised at room temperature for 24 h. Cross-sectional blackheart area was again recorded, and tubers grouped by their severity level, with mild below 50% cross-sectional area of blackheart,

and severe above 50%. There was no significant difference in tyrosinase activity between healthy tubers and mild blackheart tubers (Welch's T-test P=0.4369). Severe blackheart tubers exhibited a lower tyrosinase activity, although because the severe group comprised only two tubers, the result was not statistically significant (Welch's T-test P=0.2243).

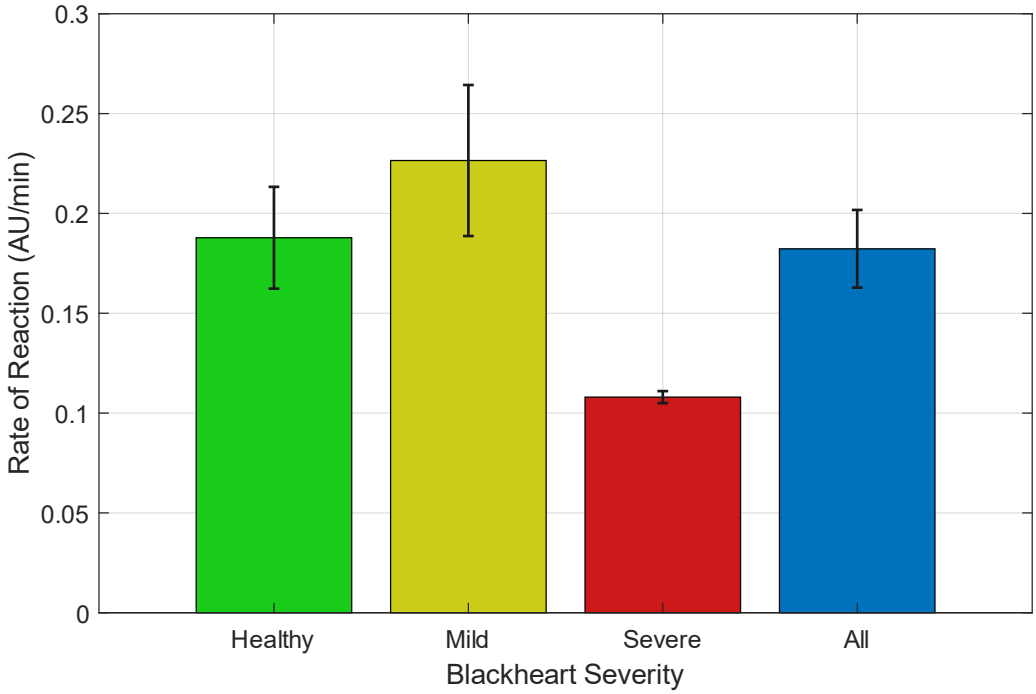

Figure 3.13 Reaction rate of tyrosinase in potato samples from potato tubers with varying blackheart severity.
Blackheart severity determined via percentage cross-sectional area of darkened region. Mild severity indicates <50% cross-sectional area affected by blackheart, whereas severe severity indicates >50% cross-sectional area affected by blackheart. n=19 (11 healthy, 6 mild, 2 severe). Potatoes treated for 14 days at 25°C in an anoxic chamber flushed with 100% CO_2 every 48 h. Error bars denote standard error of means.

3.4.5 Developing a non-destructive measure for chitting quantification

Given the success of the very high CO_2 and 25°C RAC treatment in promoting blackheart development, the long-term high-CO_2 storage treatment was repeated on another set of potatoes with harsher conditions for more frequent and severe blackheart induction. Potatoes were stored in the same controlled-environment cabinet as before, but at 15°C and 2000–3000 ppm CO_2, for 60 days. Whilst this experiment was not continued to completion due to technical issues resulting in excessive potato sprouting (Figure 3.14), the chitted potatoes were used to develop a non-destructive method of quantifying total chitting. This was subsequently used to test the hypothesis that larger tubers produce more total chitting.

Figure 3.14 Photo of sprouted potatoes in growth cabinet, potatoes stored for 60 days at 25°C at 2000–3000 ppm CO_2.

Whilst chitting can be measured destructively by removing all chits and weighing them, this is unsuitable for time-course experiments, where non-destructive means are required. To this end, a parameter termed the chitting coefficient (CC) was developed, which was calculated by multiplying the number of sprouts by the length of the longest sprout in metres. Branches on sprouts were counted as sprouts. Only sprouts and branches 2.5 cm or longer or with purple colouration were included, in order to

distinguish between significant sprouts and insignificant nubs in an objective and consistent manner.

$$k_{chitting} = Max\ Length \times NSprouts$$

Number of sprouts can be considered a proxy for total cross-sectional sprout area; it is not a proxy for volume as number of spouts (NSprouts) and sprout length are not significantly correlated (Figure 3.15 a). Measuring only the longest length may not linearly reflect average length but is fast and practical. The product of this length and area provides a pseudo-volume to represent total chitting. There was no correlation between maximum sprout length and number of sprouts (see Figure 3.15 a), R=0.1372, P=0.2797 (Pearson correlation coefficient), suggesting there is little redundancy within their product.

Tuber mass does not correlate with longest sprout length (Figure 3.15 b); however, the other component of CC, number of sprouts, is correlated with tuber mass (Figure 3.15 c), R=0.9995, P=0.0204 (Pearson's Correlation Coefficient). However, the product of these two measures, CC, is strongly correlated with tuber mass (Figure 3.15 d) with a Person Correlation Coefficient of R=0.8836 and $P=4.21\times10^{-22}$. Using exponential GPR to predict CC from mass, an R^2 value of 0.77 is reached for the validation set, with an RMSE of 4.49.

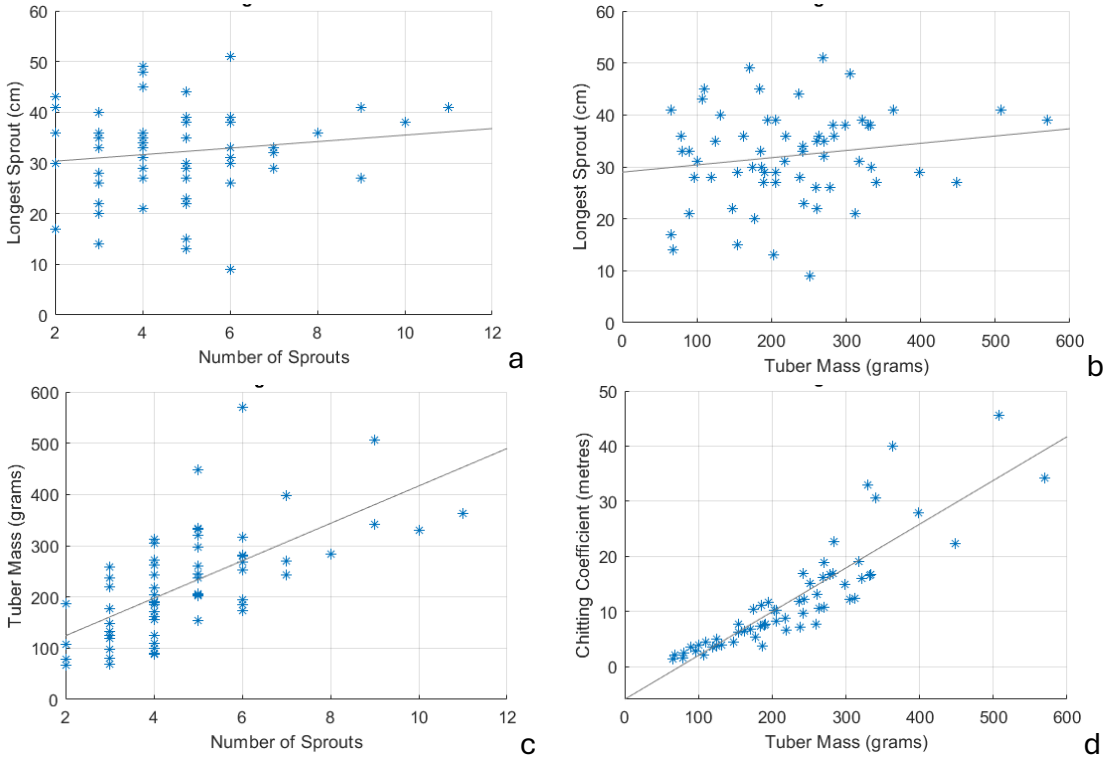

Figure 3.15 CC and component parts of tubers sprouted in 3000 ppm CO_2 15°C dark environment.
a: Longest sprout length (cm) against number of sprouts on tuber. b: Tuber mass (grams) against number of sprouts on tuber. c: Longest sprout length (cm) against tuber mass (grams). d: CC (metres) against tuber mass (g), n=64.

3.5 Discussion

The aim of this study was to investigate whether electrical and optical methods can be used to non-invasively detect internal potato defects as they develop during storage, with a focus on blackheart as the model defect. Tubers stored in 2000 ppm CO_2 at 5°C exhibited changes in both surface NIR spectra and electrical properties, positioning both optical and electrical approaches as potential techniques for detecting internal defects during storage.

NIR spectra were successfully used to classify between spectra recorded pre and post storage in the 2000 ppm CO_2 environment (Figure 3.9) with 75.4% accuracy and an MCC of R=0.493 and a FET of $P=9.1\times10^{-18}$. Similar classification accuracies, as well as MCC R values, were found for models classifying between short and long storage time in 2000 ppm CO_2 environment, and models trained to predict between short and long total storage time including both in cold storage before high CO_2 treatment and storage in the elevated CO_2 environment (Figure 3.10). Classification between upper and lower thirds of total storage time yielded MCC R=0.4058, FET $P=4.02\times10^{-14}$, similar values were achieved for 2000 ppm CO_2 storage time with MCC R=0.4219, FET $P=3.6\times10^{-12}$. Total storage times can be compared as all samples used were of single origin from the same harvest. These results suggest the observed changes in spectra and electrical properties are non-specific to an elevated CO_2 environment, factors such as water content (Chourasia et al., 2005) and sugar content (Kumar et al., 2004) are known to change during storage and can affect NIR spectra (Kyprianidis & Skvaril, 2017; Lui et al., 2011). While these data suggest the 2000 ppm 5°C treatment failed to impose a significant blackheart-inducing stress on the potatoes, both NIR spectra and electrical impedance have shown promise for assessing storage effects on intact potatoes.

Since this experiment was conducted, advancements in blackheart detection have been published (Guo et al., 2024; Wei et al., 2024). Guo et al. (2024) demonstrated that Vis-NIR spectroscopy can be used to detect early blackheart online in storage and sorting facilities. Wei et al. (2024) integrated Vis-NIR transmittance spectroscopy with machine vision for accurate online blackheart detection. These recent advancements demonstrate the poignancy and timeliness of this research. Recent advancements have been focused on the Vis-NIR bandwidth, wider than the NIR bandwidth used in this

chapter, and have mainly focused on symptomatic blackheart, whereas the potatoes used in this chapter overwhelmingly lacked visible symptoms upon dissection. The RAC system successfully and reliably induced blackheart; spectra will be recorded on more severe blackheart induced potatoes with the RAC system in the following chapter to investigate how the approach explored in this chapter can be applied to detecting symptomatic blackheart.

While optical spectra elucidate biochemical properties of samples, electrical impedance relates to biophysical properties of samples. Electrical impedances of potatoes were recorded to investigate whether changes in biophysical properties during elevated CO_2 storage represent significant enough shifts in electrical properties to enable detection of the effects of elevated CO_2 storage in a non-destructive manner.

The LLS regression model in Figure 3.7 uses storage time as the response variable; however, the severity of the effects of storage time may vary independently from time with biological variance between replicates. As the potatoes studied in this model did not exhibit visible blackheart, the severity of storage effects are not known; however, treatment in the RAC demonstrated tubers with identical storage stresses yield variable blackheart severity (Figure 3.13), suggesting there is great variance between replicates.

There is moderate correlation of R^2=0.47 between predicted storage time and actual storage time for the linear regression model trained on output voltages (Figure 3.7 b). The connection between the storage time and electrical properties suggested by these data are further supported by the classification results in Figure 3.6. The subspace ensemble discriminant model in Figure 3.6 classified between short and long storage times with 82.6% accuracy. As most tubers did not develop blackheart, this change in impedance may be due to other factors. Water loss is well documented in potato storage (Chourasia et al., 2005; Grudzińska and Mańkowski, 2018) and water content affects electrical impedance (Ando et al., 2014; Zhang et al., 2024).

The relationship between tyrosinase activity and blackheart was studied as a potential destructive method for assessing the severity of pre-symptomatic blackheart. While seminal work by Bartholomew (1913; 1914) and Davis (1926) placed great emphasis on the importance of tyrosinase in blackheart development, the data in this chapter

support Chapman's (2018) refutation of the long-held claims of Bartholomew and Davis. Figures 3.11, 3.12 and 3.13 demonstrate there is no correlation between tyrosinase activity and the severity of blackheart determined by cross-sectional area. These data suggest tyrosinase cannot be used as a measure of blackheart severity in potato.

Potatoes stored at 2000–3000 ppm at 15°C for 60 days developed substantial chitting (Figure 3.14). These potatoes were used to develop a measure of chitting, CC, that can be practically measured without removing any sprouts. CC showed strong correlation with tuber mass (Figure 3.15 d), demonstrating the potential for this non-destructive measure. The non-destructiveness and practicality of CC may position it as ideal for longitudinal experiments, where non-destructive methods allow for the preservation of the sample population.

Number of chits is dependent on tuber mass (Figure 3.15 b); this observation is supported by Dardić & Dimitrić (2009). Wurr (1978) reported that total chit length and pre-sprouting tuber mass are linearly related, although this measure is more time-intensive and potentially destructive than CC. Previous work on chit length was performed on tubers with early chitting ready for planting, the longest chit measured by Wurr (1978) as 36.5 mm. Chit length studied in this chapter was very extreme, with tuber maxima ranging from 9 to 52 cm long. The strong correlation found between CC and tuber mass may not translate to smaller chits.

3.6 Conclusion

The low rate of blackheart development in this study supports that low temperatures may play an important role in blackheart prevention. While the partially elevated 2000 ppm CO_2 environment represented a mild industrially realistic storage environment, the RAC proved to be an effective experimental model for severe blackheart development.

Both NIR spectra and electrical impedance were altered by elevated CO_2 storage, providing two separate methods of assessing impacts of storage on potato quality. As optical spectra reflect chemistry, and impedances reflect physiological properties, an integrated approach combining both methods could be a powerful means for detecting the effects of storage and defect development.

The severity of blackheart-inducing stresses studied in this chapter were mild, evidenced by only five tubers developing visible blackheart after long-term storage. The following chapter will develop this research, studying more severe stresses using the RAC system developed in this chapter for investigating the relationship between tyrosinase and blackheart. In addition to severe blackheart stresses, stresses analogous to other important and challenging defects will be explored.

4 Chapter 4: Non-invasive detection of internal potato defects

4.1 Introduction

4.1.1 Potato sorting and quality control

Quality control at potato distribution and storage facilities is essential for four core motives: (1) public health considerations, ensuring produce is safe to handle, store and consume; (2) customer satisfaction, maintaining consumer trust in high-quality produce, and avoiding food waste and economic losses from consumer rejection of defective produce; (3) contamination, reducing the spread of pathogenic defects in storage facilities (Mumia et al., 2017), through screening prior to storage; and (4) distribution/application – potato usage, such as fresh produce, processed crisps, vodka production or industrial use, is informed by potato quality, such that tubers are of the quality demanded by their application. For example, baking potato family packs demand the highest standards, while lower-quality potatoes can be used for applications with more tolerance like vodka. Some varieties are specifically bred to have properties ideal for these often lower-value applications, such as reduced water mass for dehydrated potato production (Singh et al., 2023).

Potato sorting and storage facilities generally employ two kinds of potato quality control: manual destructive testing (Heinemann et al., 1996; Pedreschi et al., 2016; Razmjooy et al., 2012) and automated optical sorting (Díaz et al., 2025; Hassankhani & Navid, 2012). Manual destructive testing is used to check for frequency of internal defects within a sample of each truckload of potatoes arriving at the facility. The industrial partner in the present research, Burgess Farms (https://burgessfarms.co.uk/), uses a 20 kg sample per approximately 20 tonne truckload. These checks are executed by humans (Heinemann et al., 1996; Pedreschi et al., 2016; Razmjooy et al., 2012), destructively cutting open the samples and recording the incidence rate of each internal defect. Optical grading machines identify external defects via computer vision and sort potatoes appropriately (Díaz et al., 2025; Hassankhani & Navid, 2012). These optical grading machines, however, are limited to only externally visible defects, making destructive quality control also necessary. Furthermore, destructive quality control is

done immediately after washing the truckload of potatoes, whereas optical grading is done as part of the automated sorting process.

Truckloads of potatoes fail destructive quality control if the frequency and severity of internal defects exceed accepted thresholds; these thresholds vary by retailer or processer. Due to the destructive nature of this process, only an average of the truckload is known, not the quality of individual tubers. However, defects can occasionally be mass dependent, allowing shipments to be sorted by size, and size groups to be handled differently. Nevertheless, there is still great uncertainty about which tubers are defective or healthy, resulting in healthy or high-quality potatoes being wasted or used for lower-value applications. While the environmental impacts of abject waste are clear, there are also environmental impacts of potatoes being used for lower-value applications than necessary. Agricultural inputs, such as fertiliser, pesticides, water, etc. are used to increase produce quality (Guenthner et al., 1999; Palmer et al., 2013), thus high-quality produce used for low-value applications is wasting the retroactively unneeded inputs.

4.1.2 Model defects

4.1.2.1 Spraing

Spraing is an internal potato defect caused by the mop-top virus (*Pomovirus solani*) and tobacco rattle virus (*Tobravirus tabaci*) (Mølgaard & Nielsen, 1996), characterised by distinctive marbled streaks of necrosis through the pith and cortex of tubers (see Figure 4.1). Although not harmful to humans, it renders produce unmarketable, leading to food waste and loss of profits. Spraing is a driver of waste in potato processing and in consumer homes (Thybo et al., 2004). It is also especially industrially challenging as it exhibits no external symptoms, and internal necrosis can develop during storage (Thybo et al., 2004), making screening difficult and destructive.

Figure 4.1 Spraing in potato of the baby rose variety. Each scalebar segment represents 1 cm.

4.1.2.2 Wireworm

Wireworms, the larvae of click beetles, feed upon potato tubers, leaving narrow burrows and scars (Parker & Howard, 2001; Vernon & van Herk, 2022). Wireworm tunnels enable the penetration of *Rhizoctonia solani*, and both wireworm damage and *R. solani* infection contribute to the development of drycore (Keiser et al., 2012a). Drycore and wireworms result in substantial losses of whole potato stock (Keiser et al., 2012b). Drycore is a primary reason for organic potatoes not meeting quality standards and has a big impact on conventional and integrated potato farming (Keiser et al., 2012a). Wireworm damage is difficult to detect externally as the tunnels appear as small black dots, visually appearing similar to other surface features such as lenticels, posing a challenge for computer-vision-based defect identification systems. Perhaps non-visual methods may offer better detection and screening of wireworm damage.

4.1.3 Optical NIR and MIR spectroscopy

NIR and mid-infrared (MIR) spectroscopy are both potential avenues for non-destructive screening of internal potato defects (Escuredo et al., 2021; Su & Xue, 2021) (see Chapter 2 for detail on NIR spectroscopy). MIR differs from NIR in the bandwidth of the electromagnetic spectrum used; MIR includes higher wavelengths and often uses a wider bandwidth, sometimes encompassing the NIR band. While MIR has a wider bandwidth than NIR, and a “richer” bandwidth including more peaks, it suffers from a lesser signal-to-noise ratio. NIR is more stable and robust under variable or non-ideal conditions than MIR, which lends NIR better to the industrial environment.

4.1.4 Electrical impedance spectroscopy in vegetable assessment

Electrical impedance spectroscopy (EIS), where the electrical properties of a sample are measured at varying frequencies of input signals, may provide an alternative for screening for internal potato defects non-destructively (see Chapter 1). EIS has been applied to detecting freeze–thaw injury in potatoes (Feng, 2021; Zhang & Willison, 1992), as well as being related to moisture content (Ando et al., 2014), which is an important factor in potato quality (Elbatawi et al., 2008a), and assessing maturity of tomatoes (Li et al., 2019a). Electrical impedance has shown some promise in vegetable quality assessment including in potato (Feng, 2021; Zhang & Willison, 1992); however, current approaches have been limited in the range of vegetable defects they can detect. Many of the current approaches to electrical assessment of plant tissue are destructive, involving invasive electrodes (Zhang et al., 1990; Cabrera-López & Velasco-Medina, 2019) or cutting of samples into controlled shapes such as cubes or discs of set thickness.

4.1.5 Aim and objectives

This chapter investigates the potential for non-destructive screening for internal defects to separate truckloads of potatoes that fail destructive tests into healthy and defective tubers. The overall aim of this chapter is to investigate whether non-invasive optical (NIR/MIR) and electrical spectroscopy (EIS) techniques can be used to non-destructively detect internal defects in potato tubers. The objectives of the research were to:

- generate laboratory-induced defect analogues as an experimental model for assessing approaches to detecting internal potato defects
- test the potential for non-invasive methods for detection of defect analogues
- test the potential for non-invasive methods for detection of real defects in potatoes provided by Burgess Farms

4.2 Methods and materials

4.2.1 Spectroscopy

NIR and MIR spectroscopy (see Chapters 1 & 2) were tested for screening of potato defects, with the aim to reduce the defect rate within a truckload of potatoes such that it meets an acceptable level for quality control. An NIRscan Nano (Allied Scientific Pro, Gatineau, Quebec) was used to collect NIR data, and a Bruker Alpha II compact FT-IR Spectrometer (Billerica, Massachusetts, USA) was used for MIR data collection. Spectra were taken at 10 locations per sample, randomly distributed across the tuber surface, for both NIR and MIR. NIR spectra were averaged from six readings per location. All tubers were dissected after spectra were taken, and whether they exhibited spraing was determined by observation.

4.2.1.1 Spectroscopy optimisation

When recording spectra of an intact sample, spectra were recorded at multiple locations across the sample's surface to ensure the likely heterogeneous sample was well represented. To determine whether scans should be randomly distributed across a tuber's surface or follow a non-random distribution, spectra across tuber surfaces were mapped in 3D to investigate how NIR absorbance was distributed spatially across a tuber's surface. To this end, two pieces of software were developed:

(1) For generating map data, written in python (Python Software Foundation, Wilmington, Delaware, USA), which instructs the user where on the tuber surface to next scan and automatically labels the collected scan data for telemetry. A point field representing scan locations was saved as a CSV for importing into MATLAB alongside the labelled spectra.

(2) For converting these datasets into heatmaps and animated GIF visualisations, written in MATLAB. Imported heatmaps were structured to determine whether regionality of signals justifies any particular scan location regimens or whether random distribution is appropriate.

The Python program generated point fields of scan locations around a tuber surface and displayed a visualisation to aid in locating and sequencing scans correctly (Figure 4.2). The Mayavi library (Ramachandran & Varoquaux, 2011) was used for rendering the visual

aid (Figure 4.2 a and b). Alternatively, MATLAB was used to produce a more practical and reliable visualisation, without the debugging and crashing issues that come with using large libraries (Figure 4.2 c). An additional feature was added in the MATLAB version, with the previous scan location being highlighted in red, enabling easier and more confident location of each scan location. To enable hands-free scanning while handling samples, a foot pedal was used with this Python program to increment scan number and command scans to be recorded, adapting the system developed for Chapter 2. After each scan was recorded, a marker pen was used to mark the location on the tuber surface as reference for positioning further scan locations.

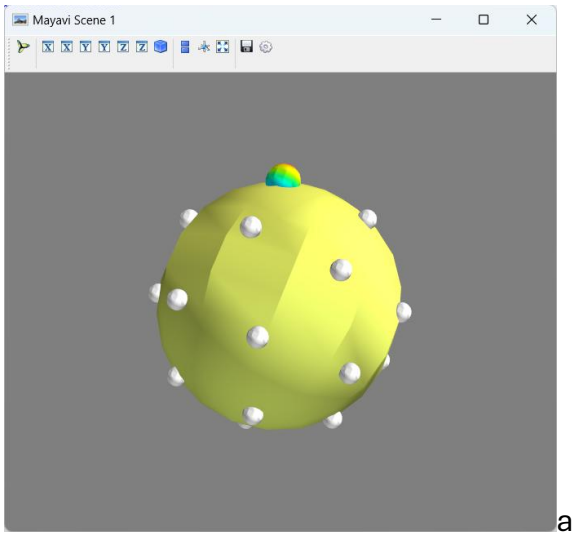

a

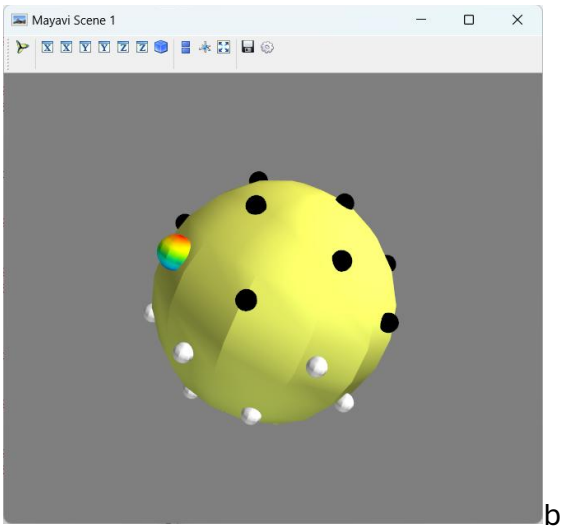

b

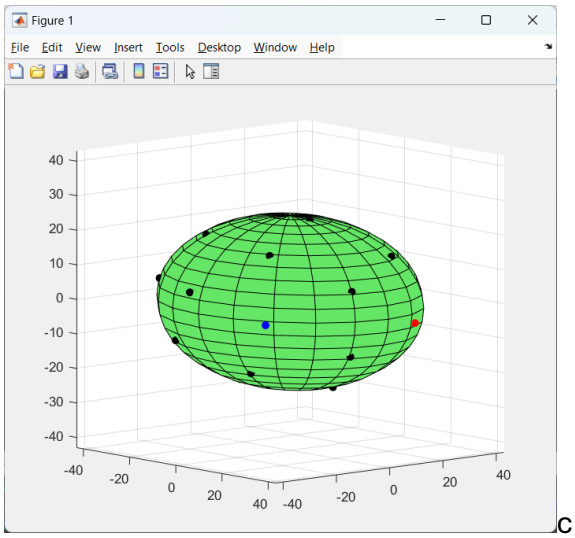

c

Figure 4.2 Potato spectra mapping visual aids.
a, b Screenshots of Python program displaying where on the tuber to scan, and where has already been scanned for easy positioning reference. Rainbow node marks current scan location, black previous scan locations, and white future scan locations. c: MATLAB visualisation program.

4.2.2 Defect analogues

Acquiring defective potatoes for research can be challenging, as they are seldom kept so cannot be bought easily on the consumer market. A 'Burgess Farms' potato facility worked with during this project were able to provide some bags of defective potatoes for experimentation. However, availability of such samples is sporadic and limited, thus often difficult for research. Laboratory-induced defects or simulated defect analogues would provide useful models for experimentation.

4.2.2.1 Wireworm holes

Ethanol-sterilised 1.4 mm diameter copper wire was used to puncture narrow 50 mm deep canals into 34 potato tubers, each tuber stabbed 10 times at 50 mm depth. Where 50 mm of penetration was not possible, the excess depth was carried over into additional stabs. Tubers were subsequently left for 3 days at room temperature on a lab bench to allow holes to dry and healing to occur. NIR spectra and electrical sweep responses were recorded both pre and post treatment.

4.2.2.2 Mechanical voids

Metal corers (6 mm diameter) were used to remove a cylindrical plug through the entire width of each potato. A 1 cm-long plug was cut from either end of the core and reinserted into the tuber and sealed with petroleum jelly to prevent shrinkage or displacement creating a void inside tubers. Voids were either left empty or filled with 3% (w/w) agar prior to resealing to provide a difference in medium between tuber and void that more accurately matches that of internal rot than an air-filled void.

4.2.2.3 Enzymatic void formation

Initially, the porosity of potato tubers for diffusing void-forming substances was assessed using methyl blue dye. Reservoirs fashioned from 5 mL pipette tips with the tips removed, giving an apical diameter of 4 mm, were inserted into 30 mm-deep pilot holes in tubers and filled with 5% (v/v) methyl blue in reverse osmosis (RO) water and secured with 3M Micropore tape (Figure 4.3). Tubers were bisected 2 days after infusion and the cross-sectional area of blue tissue was measured from the potato halves.

Figure 4.3 Potatoes with methyl blue aqueous solution reservoirs, wound sealed with Vaseline™ petroleum jelly.

Alpha-Amylase hydrolyses starch into smaller molecules and is secreted by potato pests and pathogens (Franco et al., 2002; Yarullina et al., 2016). Thus, infusion of α-amylase solution into potato tubers may be an effective method of internal potato void creation. Test tubers were divided into groups of six tubers and infused with one of six α-amylase concentrations: 0.2%, 0.4%, 0.6%, 0.8%, 1% and 5% (v/v) α-amylase (from Aspergillus oryzae) (Sigma Aldrich, St. Louis, Missouri, USA) in RO water. The size of formed voids formed was measured after 2 days as total mass loss; the starting mass was recorded after removing the pilot hole, and final mass recorded after rinsing the void with RO water to remove any broken-down material.

4.2.3 Electrical sweep response acquisition

To gather electrical sweep responses for potatoes, tubers were connected in series between a TENMA 72-3555 function/arbitrary waveform generator (TENMA, Akabane, Tokyo, Japan) and an M-Track Solo audio interface (M-Audio, Cumberland, Rhode Island, USA). Potatoes were connected via four square 5 cm × 5 cm TENS pads with self-adhesive gel (Healthcare World, London, UK). Logarithmic sweeps were generated using the TENMA 72-3555, ranging from 5 Hz to 25 MHz for sine waves, and 5 Hz to 5 MHz for triangle and square waves. The frequency limit for triangle and square waves were lower due to technical limitations. Output sweeps from the potato and a reference signal from the TENMA 72-3555 were connected to the audio interface via ¼” jack as the left and right channels of an audio signal to record unitless voltaic displacement of both channels.

The Hilbert transform was used as an alternative to Fast Fourier transformation of sweep data due to issues with noisy phase data produced by the latter. However, it must be noted that the Hilbert transform produces an abstract analytical signal, so this phase does not map directly onto physical phase. The Hilbert transform is a linear map calculated by the convolution of a function with 1/πt (Equation 4.1).

$$H(u)(t) = u(t) * \frac{1}{\pi t} \quad [4.1]$$

1/πt has no definite integral over t=0, thus the Cauchy principal value (PV) of the integral is used to reach a definite value (Kschischang, 2006) (Equation 4.2). PV is a method of obtaining values for undefined integrals by taking the limit approaching the singularity from both sides if the singularity is at a finite value, or from the finite side if the singularly occurs at an infinite value (Fox, 1957).

$$H(u)(t) = \frac{1}{\pi} p.v. \int_{-\infty}^{+\infty} \frac{u(\tau)}{t-\tau} d\tau \quad [4.2]$$

The Hilbert transform produces an analytic representation comprising real and imaginary parts from a solely real valued input signal. The Hilbert transform can be used to accurately extract instantaneous phase from narrow band oscillations without need for marker events (Boccaletti et al., 2002; Matsuki et al., 2023; Pikovsky et al., 1997), making it an appropriate and effective method for extracting the phase of sine sweeps amplitude independently (Cohen et al., 1999). Instantaneous phase of square wave sweeps was also extracted using the Hilbert transform in this thesis, as square waves have a narrow band. While potatoes act as passive low-pass or bandpass-filters (Figure 3.3), this filtering does not broaden the bandwidth of square sweeps.

The phase of a Hilbert transformed recorded sine sweep response is wrapped; this means there is discontinuity in the curve due to the circularity of phase (Figure 4.4 a) compared to the true signal (Figure 4.4 b). Between opposing spikes in the differential (Figure 4.4 c and d), integer multiples of 2π are added to the discontinuous region until the discontinuity is minimised. When this method is applied to the Hilbert phase of the measured signals the result is a smooth curve, as illustrated in Figure 4.4 e.

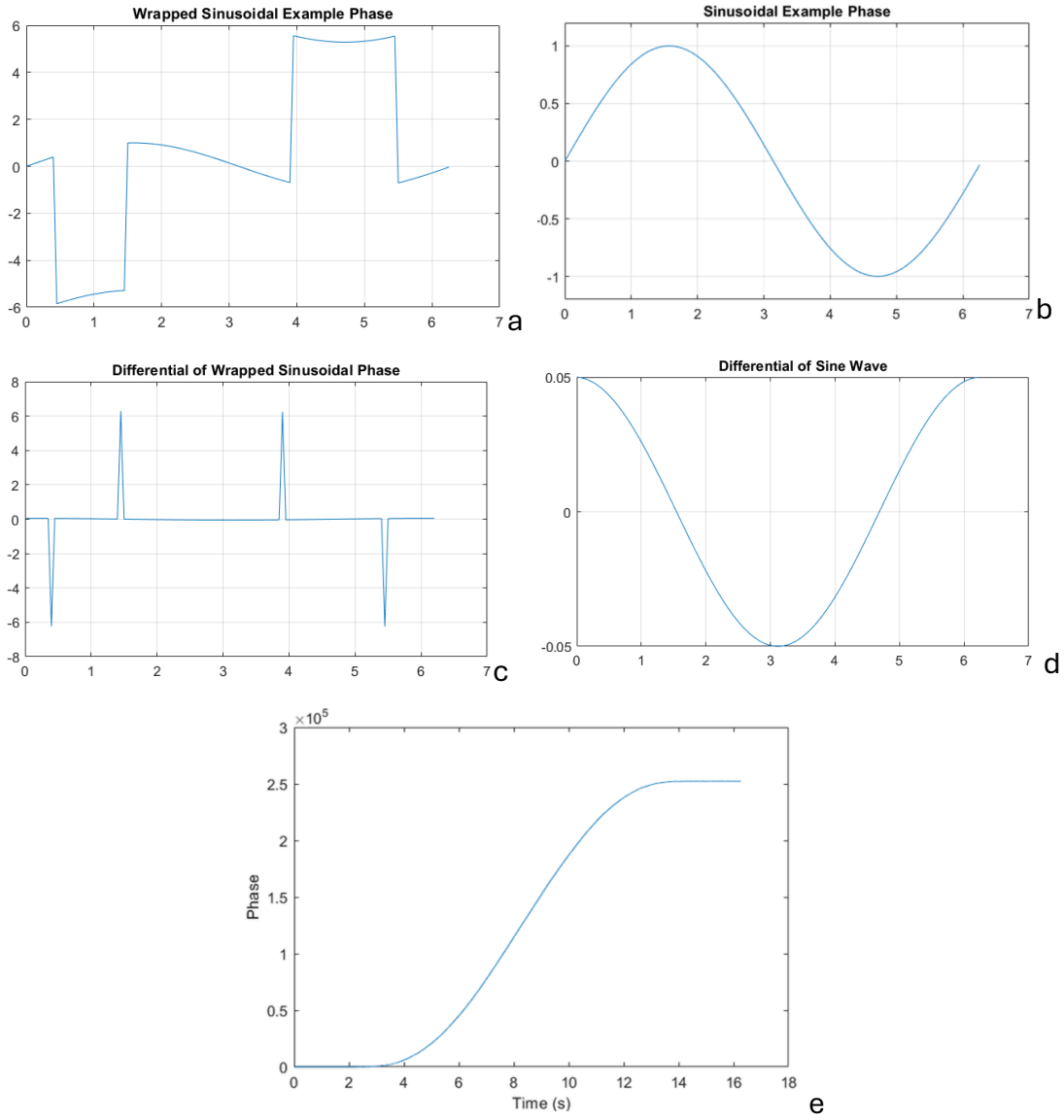

Figure 4.4 Signal unwrapping visualisations.
a: Example signal wrapped. b: Example signal, a sinusoid. c: Differential of wrapped example signal. d: Differential of example signal. e: Unwrapped phase of Hilbert-transformed electrical sweep response of potato.

By taking the frequency difference between the beginning and end of the phase shift, the rate and frequency band of the phase shift can be ascertained (Figure 4.5), as phase takes a gradual approach to the minima and maxima, and to account for noise and overshoot, the 90-90 points are used. There is a brief moment between the beginning of a recording, and the beginning of the sweep as both are triggered manually, so the initial silence is removed by removing the section of the signal before the sliding RMS exceeds a voltage threshold.

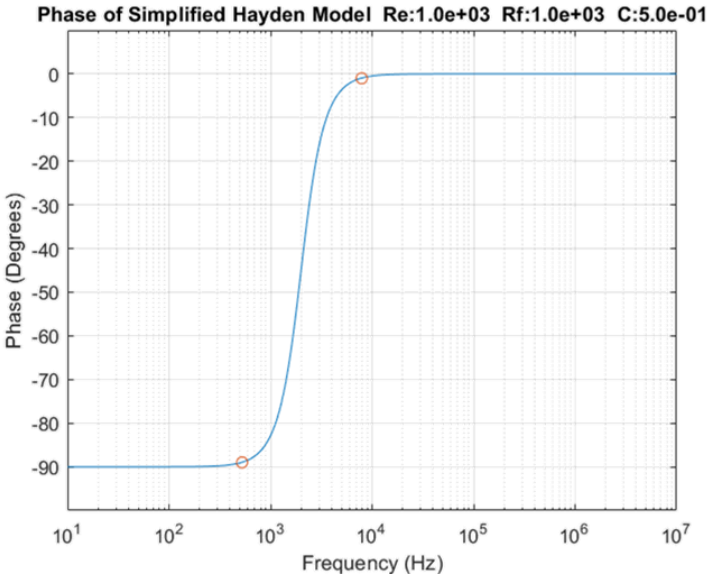

Figure 4.5 Bode plot with 90-90 points of phase shift marked.
Extracellular resistance=1kΩ, intracellular resistance=1kΩ, cell wall capacitance=0.5F, cell wall resistance=∞.

4.2.4 Rapid anaerobic chamber

Tubers were treated for 14 days in the rapid anaerobic chamber (RAC, see Chapter 2) to induce blackheart. This provided an experimental model for determining whether NIR spectroscopy and EIS can be used to non-invasively detect blackheart. The RAC was reflushed with CO_2 and condensation removed every 48 h. NIR spectra and electrical sweeps were recorded both pre- and post-RAC treatment.

4.2.4.1 Tuber respiration for studying metabolism

Increases in RAC chamber CO_2 level due to tuber respiration were used to calculate the combined respiration rate of the contained tubers using Equation 4.3, which assumes that metabolism of one glucose molecule produces six molecules of CO_2 (Divakaruni et al., 2014). The volume of the RAC chamber (V) and tubers (M) are known, as well as the CO_2 concentration (C). From this, the total CO_2, and the differential of this can be determined. CO_2 has an atomic mass of 44.1g/mol, thus there is 1.366×10^{22} molecules of CO_2 per gram of pure CO_2 gas. The internal pressure (ρ) can be assumed to be roughly one atmosphere if no CO_2 is pumped into the chamber and sealed in normal air. The volume of air inside the RAC (V−M) is the volume of the RAC (V) minus the volume of the

potatoes (M). I estimated the density of Vivaldi potatoes to be 1.05 kg/L using a displacement method; thus, we can approximate the density of all varieties of potato to 1 kg/L, and the mass of a tuber in kilograms (M) can be assumed to be its volume in litres.

$$G = \frac{1}{6t}\Delta C\rho(V - M) \quad [4.3]$$

G: glucose molecules metabolised per unit time

C: concentration of CO_2

ρ: atmospheric density

V: volume of chamber

M: total mass of tubers

t: time

4.3 Results

4.3.1 Optimisation of NIR reflectance spectra recording

When performing spectroscopy, it is important to take an appropriate number of scans, distributed across the sample in an appropriate manner. The spectral properties of individual potatoes were mapped across their surface and modelled using Python and MATLAB.

Tubers were initially modelled as polyhedra of right-angled triangle faces, the edges comprising the edges of a 26 node graph, with each node labelled with a letter of the alphabet (Figure 4.6). Each face of the polyhedron is denoted by its vertices, for example, FQW would be the triangular face with points F, Q and W as its vertices. Map values of faces are weighted as a function of the corresponding spectrum recorded within that region on the tuber surface, for the example the primary principal component can be used.

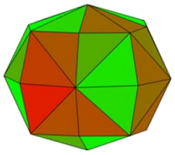

Figure 4.6 Original 26 vertex polyhedron model

This approach is limited by the geometry of the model, the number of adjacent faces each vertex has is highly heterogeneous, and there is a fixed number of vertices. Therefore, a more parametric and homogeneous model was produced, in which the nodes were distributed across the surface of a sphere rather than a polyhedral model forming a node graph (Figure 4.7 a). Potatoes exhibit morphological variation, and often deviate from a spherical form. Transformation matrices can be utilised to transform a point field representing scan locations to non-spherical forms. Simple scaling matrices can be used to stretch the model to elongate tubers (Figure 4.7 b); the field is centred around the origin to avoid translation issues. Concavity and other topological features are unlikely to have a significant impact on the deviation of the model from a tuber's true surface, so can be ignored, although they can be included in the model by multiplying the point field with a trigonometric transformation function (Figure 4.7 c).

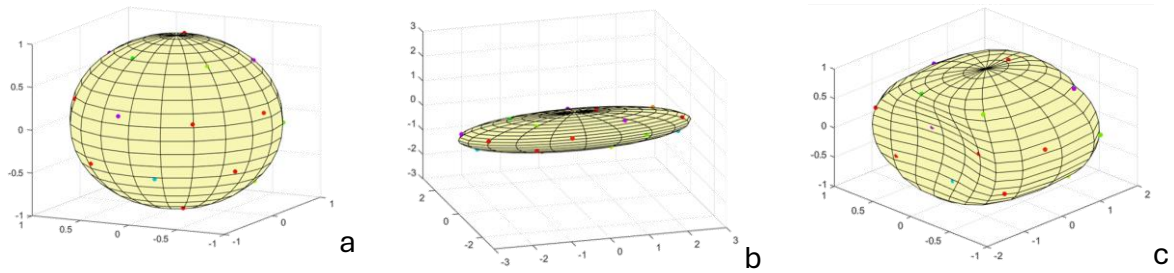

Figure 4.7 Second potato mapping system, developed in MATLAB.
a: Spherical model, b: Elongated model, c: Concave model. Colours of points denote local value of dominant principal component.

This system was refined by generating high-resolution segmented heatmaps from the point field data, and by selectively choosing the most spherical potatoes to avoid issues with shape. Colours on the heatmaps represent the local value of the dominant principal component of the spectra (Figure 4.8). The closer a datapoint is to a segment of the map, the greater influence it has over its colour. Points beyond a cutoff point are ignored. A cutoff radius of $\sqrt{2}/2$ (~0.707) in standardised coordinates, the expected distance between points, is utilised such that the segments directly under a sample reflect the true value of that sample while maximising radii of each sample's influence.

The number of segments greatly exceeds the number of data points, requiring interpolation. Four interpolation methods were tested: linear (Figure 4.8 a), quadratic (Figure 4.8 b), cubic (Figure 4.8 c), and Hamming window (Figure 4.8 d). Hamming window interpolation (Figure 4.8 d) provides smooth interpolation, and the morphology of each region is deformed by neighbouring regions rather than the fixed circular blobs of the polynomial interpolations (Figure 4.8 b and c). The Hamming interpolation is achieved by using a Hamming window translated to have a minimum of zero, such that there is no square edge to a sample's region of influence. This method can be used at high resolutions without artefacts.

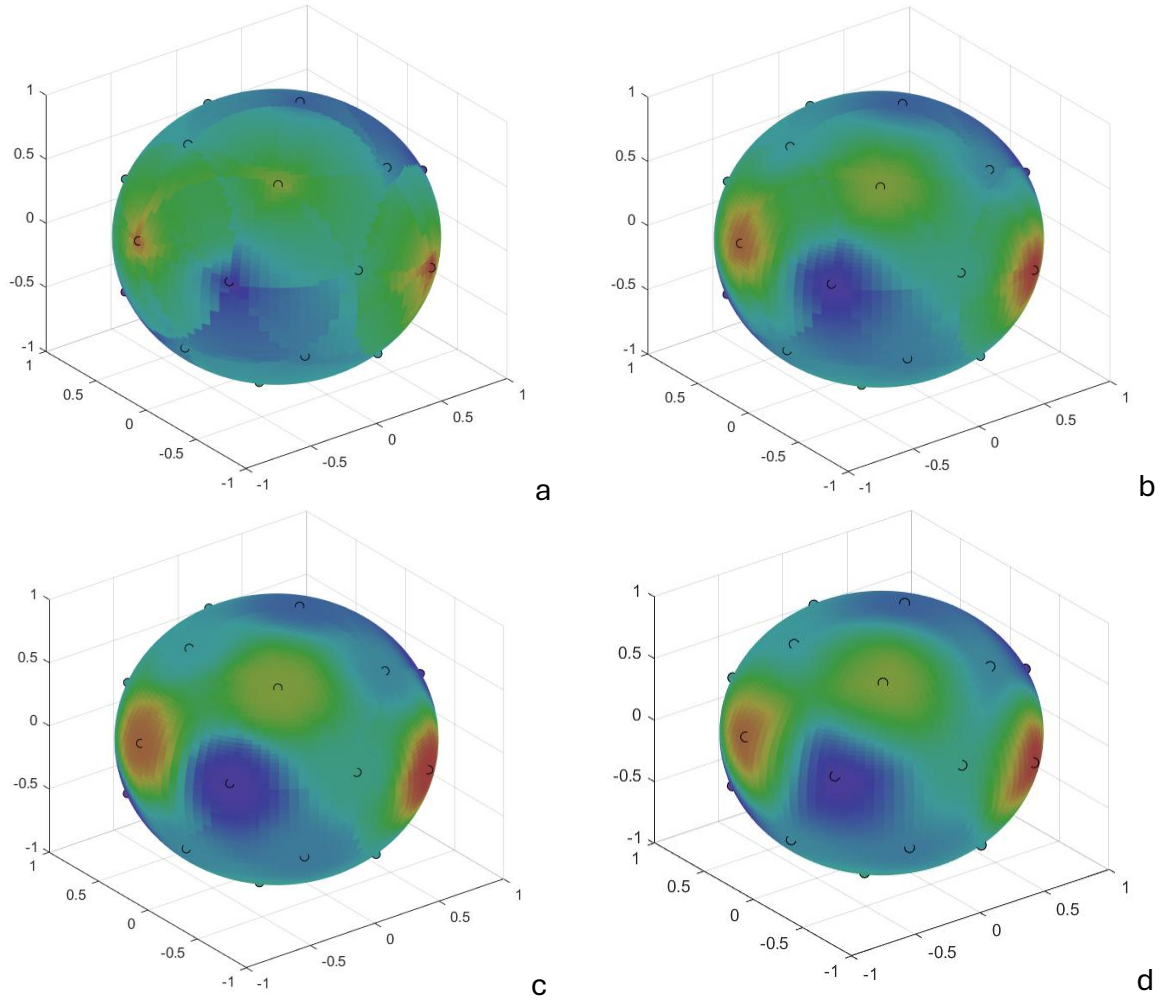

Figure 4.8 Heatmaps with varying interpolation methods; same data and perspective used for each map.
a: Linear interpolation, b: Quadratic interpolation, c: Cubic interpolation, d: Hamming interpolation.

Figure 4.9 demonstrates a smooth 800×800 segment heatmap, generated and rendered on a laptop with a Ryzen 7 processor in 21 seconds. Such maps can be rendered from a sequence of angles to produce rotating animated GIFs for full tuber visualisation (Figure 4.10).

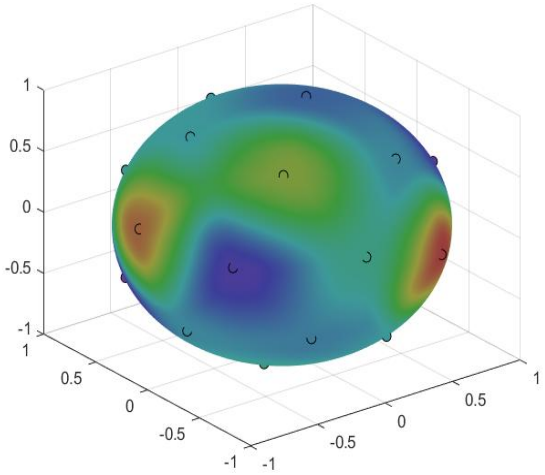

Figure 4.9 Potato surface NIR spectra first principal component heatmap with Hamming interpolation.
800×800 segments. Red reflects higher values, blue lower values.

The distance between datapoints and their respective PC1 values did not correlate (Table 4.1), suggesting the distribution of spectral features to be randomly distributed across the tuber surface. No discernible pattern is recognisable via observing heatmaps either. Therefore, based on this evidence, randomly distributed scans were used for NIR absorbance data collection on potato tubers.

Table 4.1 Correlation between distance between points on potato tuber surfaces and difference in PC1 of NIR spectra between points. Pearson's correlation used, P and R values averaged between tubers. Spherical distances reflect the distance across tuber surface, rather than Euclidean distance along a chord. Only very spherical potatoes were used to minimise error of sphere approximation.

	Correlation R	Correlation P
Euclidean Distance	−0.0589	0.2144
Surface Distance	−0.0172	0.1539

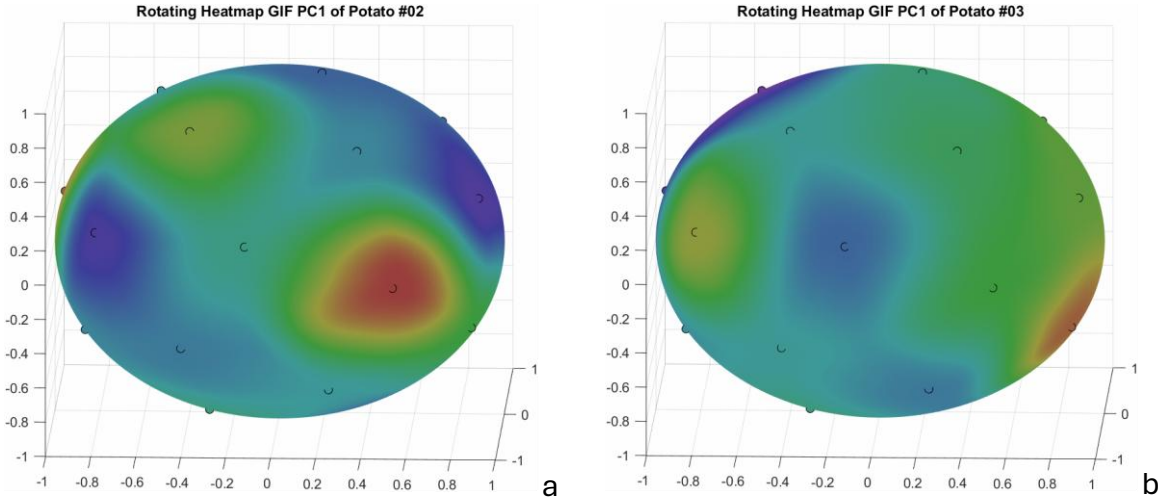

Figure 4.10 Animated heatmap rotation GIFs of potato tuber surface NIR absorbance first principal component.
If viewing in Microsoft Word, click the play button on the heatmaps to watch the animation. If viewing in PDF see supplementary files.

4.3.2 NIR spectra were successful in training tuneable screening models for spraing

Two batches of spraing effected potatoes were screened using either NIR or MIR spectroscopy. The first batch had a total of 142 tubers, 30 of which (21%) exhibited spraing determined by dissection; these tubers were used to train the NIR model. The second batch had a total of 50 tubers, 11 of which exhibited spraing (22%) this batch was used to generate an MIR dataset. Quadratic SVM classifiers with 5-fold validation were trained on both NIR (Figure 4.11 a) and MIR data (Figure 4.11 b and c). Training sets had an equal number of healthy tuber scans and spraing tuber scans to avoid bias in training. Models were trained using the classification learner app in MATLAB. The MIR models failed to classify healthy and spraing tubers with both full bandwidth [Figure 4.11 b; Fisher's exact test (FET) P=0.34] and fingerprint region of <1500 nm only (Figure 4.11 c; FET P=0.89). However, the NIR model performed better, although with a moderate accuracy of 66.4%, FET $P=7.6\times10^{-30}$. Ten MIR spectra were recorded per tuber, and each spectrum was fed into the classifier model to generate a prediction of healthy or spraing. Individual spectra provided poor classification, so majority voting, where the modal prediction from all 10 spectra of a given tuber is used as the tuber's prediction in a democratic fashion, was used, however this also produced a poor classification accuracy of only 56.4%.

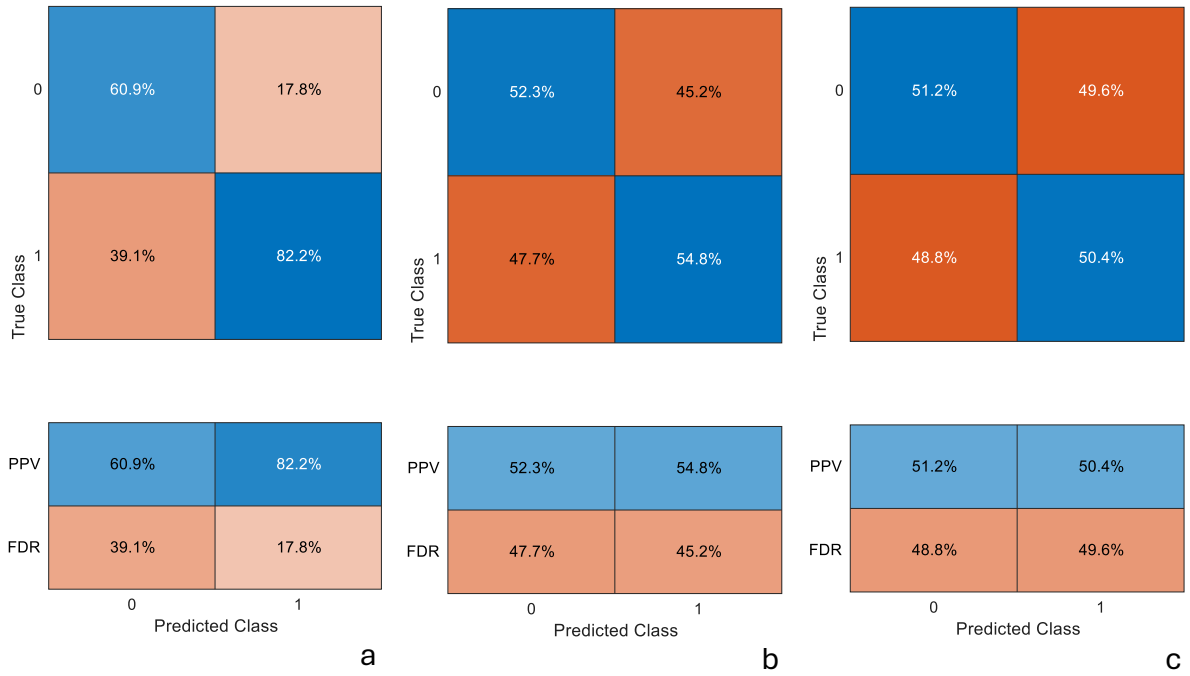

Figure 4.11 Confusion matrices for quadratic support vector machine models with 5-fold validation trained on training sets with equal number of control and spraing spectra.
a: NIR, n=640 (320 spectra per group), Matthews correlation coefficient (MCC) R=0.4411, Fisher's exact test (FET) P=7.6×10^{-30}, b: MIR n=212 (106 spectra per group) MCC R=0.0710, FET P=0.3338, c: MIR fingerprint region only <1500 nm, n= 212 (106 spectra per group) MCC R=0.0160, FET P=0.8903.

Although the models in Figure 4.11 have low accuracy, for an industrial application the metric of success is not classification accuracy, but rather percentage of post-screening tubers that are defective. With screening the raw dataset to reduce percentage of tubers defective as the objective, quadratic tree models with varying relative error costs were trained, putting greater error costs onto false negatives. This was also performed on MIR data for comparison. Table 4.2 shows that tree classifiers trained on NIR spectra successfully screen for spraing and reduce the rate of spraing post-screening. Although a higher error cost for false negatives reduces the classification accuracy (Table 4.2), the rate of spraing after screening is improved. Therefore, there is a trade-off between classification accuracy and percentage of spraing potatoes removed; this trade-off needs to be balanced to minimise the percentage of post-screening tubers that are defective whilst minimising loss of healthy potatoes due to misclassification. In contrast, tree classifiers trained on MIR data (Table

4.3 a) failed to significantly lower the post-screening defect rate at all relative error costs. To test whether the smaller *n* of MIR data was a limiting factor on performance, the same models were trained again using all MIR spectra, treating each scan as a replicant; these models also failed to lower the post-screening defect rate (Table 4.3 b).

Table 4.2 Screening of spraing in intact potatoes with tree classifier trained on PCA of NIR spectra (900–1700 nm) with varying error costs.

Error cost for false positives is constant; relative error cost refers to error cost of false negatives as multiple of false-positive error cost. Passed defective is the rate of spraing in the potatoes classified as healthy (false). n=142, mean of 10 spectra used for each tuber.

Relative error cost	**Healthy removed**	**Spraing removed**	**Classification accuracy**	**Passed defective**
1	4 (3.7%)	19 (63.3%)	89.4%	9.2%
2	7 (6.3%)	23 (76.6%)	87.3%	6.5%
3	19 (17%)	28 (93.3%)	85.2%	2.1%
4	17 (15.2%)	28 (93.3%)	86.6%	2.1%
5	35 (31.3%)	30 (100%)	75.4%	0%
6	35 (31.3%)	30 (100%)	75.4%	0%

Table 4.3 Screening of spraing in intact potatoes with tree classifier trained on PCA of MIR spectra (347–4000 nm) with varying error costs.

Error cost for false positives is constant; relative error cost refers to error cost of false negatives as multiple of false-positive error cost. Passed defective is the rate of spraing in the potatoes classified as healthy (false). a: Mean of 10 spectra used for each tuber, n=50, 11/50 (22%) initially defective, b: All spectra, n=500, 107/500 (21.4%) initially defective.

Relative error cost	**Healthy removed**	**Spraing removed**	**Classification accuracy**	**Passed defective**
1	4 (10.3%)	2 (18.2%)	74%	20.5%
2	15 (38.5%)	1 (9.1%)	50%	29.4%
3	15 (38.5%)	4 (36.4%)	56%	22.6%
4	19 (48.7%)	2 (18.2%)	44%	31.0%
5	19 (48.7%)	3 (27.3%)	46%	28.6%
6	20 (51.3%)	3 (27.3%)	44%	29.6%

a

Relative error cost	**Healthy removed**	**Spraing removed**	**Classification accuracy**	**Passed defective**
1	52 (13.3%)	18 (17.0%)	71.8%	88 (20.7%)
2	91 (23.3%)	25 (23.6%)	65.3%	81 (21.3%)
3	118 (30.3%)	35 (33.0%)	61.9%	71 (20.7%)
4	124 (31.8%)	47 (44.3%)	63.1%	59 (20.7%)
5	142 (36.4%)	37 (39.4%)	57.5%	69 (21.8%)
6	154 (39.5%)	38 (35.8%)	55.2%	68 (22.4%)

b

Classification in Tables 4.2 and 4.3, was performed by training machine learning algorithms to make predictions based on individual spectra from a potato. However, the difference between spectra from the same tuber may offer an alternative avenue of classification. The PCs of spectra vary across a tuber's surface, as seen in the heatmaps in Figures 4.9 and 4.10; these intratuber differences between spectra may offer insights into the health of a potato. To test this, Ten NIR spectra were recorded per tuber, and the PCs within the 10 scans of a given tuber were compared after performing PCA on all spectra from all tubers. There was significant difference in the skewness of the primary principal component of NIR spectra between healthy and spraing-affected potatoes (Figure 4.2), Welch's T-test P=0.005.

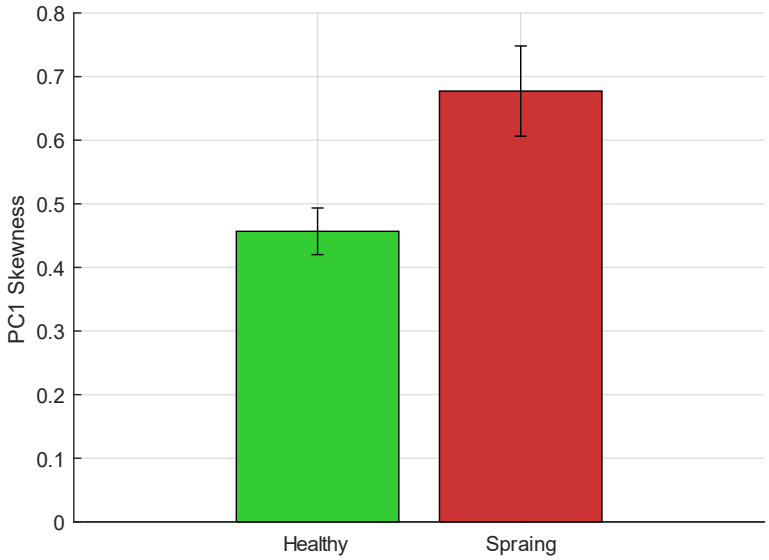

Figure 4.12 Skewness of primary principal component of NIR spectra (900–1700 nm) per potato tuber, with or without spraing.
Spraing status was determined by eye after dissection, spectra recorded on intact tubers prior to dissection. *n*=138, 106 healthy, 32 spraing. Welch's T-test P=0.005.

Significant skew was also found for MIR spectra (Welch's T-test P=0.0448). Interestingly, while spraing-affected tubers had greater positive skew for NIR PC1, the MIR PC1 of spraing-affected tubers was negatively skewed (Figure 4.13).

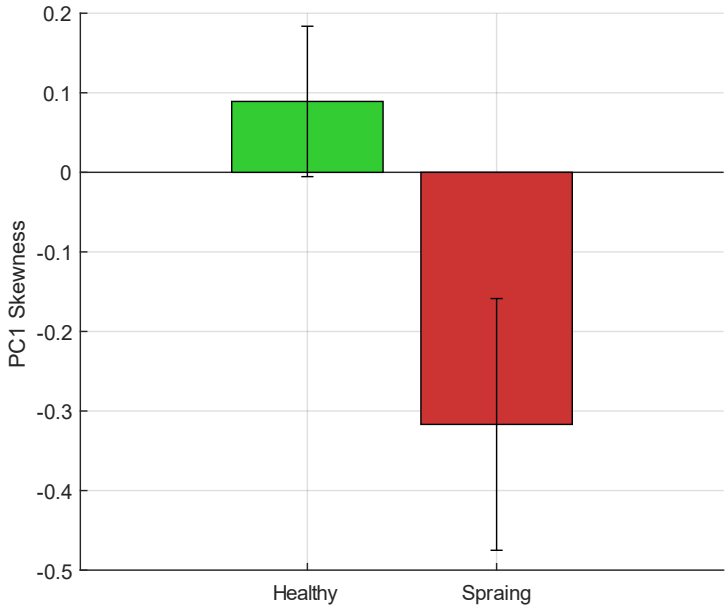

Figure 4.13 Skewness of primary principal component of MIR spectra per intact potato tuber.
Spraing tubers exhibited visible necrosis upon dissection, healthy tubers did not. Tubers of single origin. Error bars denote standard error of means.

4.3.3 Electrical sweeps of wireworm-affected tubers might provide a novel method of wireworm damage detection

Electrical sweep responses of intact potatoes were recorded pre and post wireworm damage simulation to test whether these sweep responses were altered by the treatment. This could provide a method of non-invasive detection of pest damage. There is a significant difference between the RMS output voltages of potatoes pre and post wireworm simulation ($P=9.15\times10^{-18}$, T-test) (Figure 4.14 a). However, this might not be due to the simulated wireworm damage, since Figure 4.14 b reveals the unwrapped Hilbert transform phases pre and post simulation to be almost identical. This suggests that there may be other causes to the observed voltage differential. The three-day difference in recording times could contribute to this, introducing a slight difference in the experimental set-up between the two data collections, such as a cleaner electrode, or accidental adjustment of equipment. No external sources of induction could be identified that could have caused the observed voltage change.

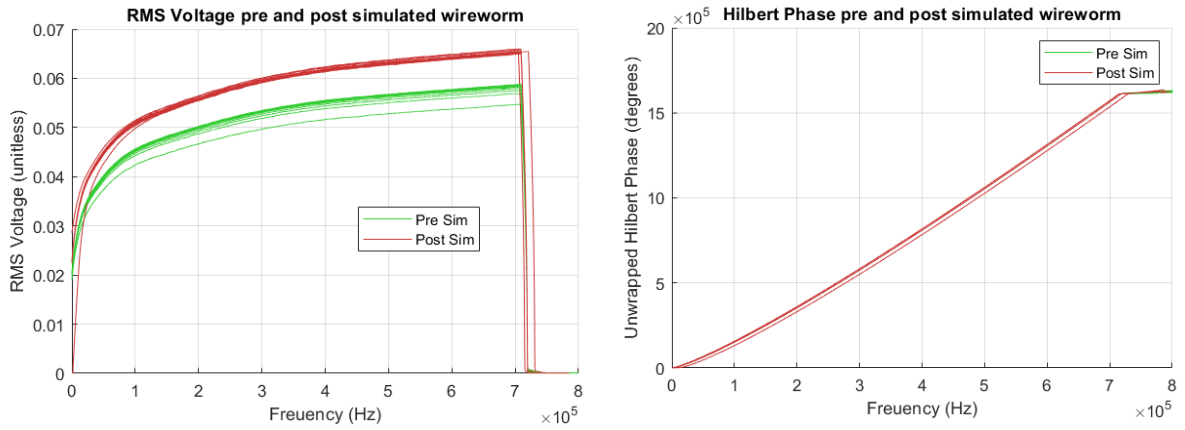

Figure 4.14 Output root mean squared (RMS) voltage and Hilbert phase of logarithmic sweeps passed through intact potatoes pre and post abiotic-simulated wireworm stress.
a: RMS voltage, b: Unwrapped phase of analytic signal after Hilbert transformation of voltaic displacement recording. Green denotes pre-simulated wireworm, red denotes post-simulated wireworm. Wireworm simulation performed via mechanical damage by 1.4 mm diameter wire.

4.3.4 α-Amylase produced inconsistent voids

Mechanically created voids experienced drying from the inside, despite external application of petroleum jelly plugs, making this an unsuccessful method of void formation (Figure 4.15 a). Methyl blue aqueous solutions successfully diffused into

tubers (Figure 4.15 b), approximately 80 % (4 mL) of the reservoir volume diffused in 24 hours, although this may have been an overestimation of the diffusion rate due to some leakage being observed. On this basis, the ability α-amylase (0.2 to 5% w/v) to generate internal tuber voids was tested (Figure 4.15 c and d). There was no correlation between α-amylase concentration and void size (Figure 4.16), with Pearson's correlation coefficient R=−0.4238, P=0.4024, and great variance within concentration groups. Due to leakage of the solution, only two tubers from the 5% concentration group could be accurately measured and the other four were rejected.

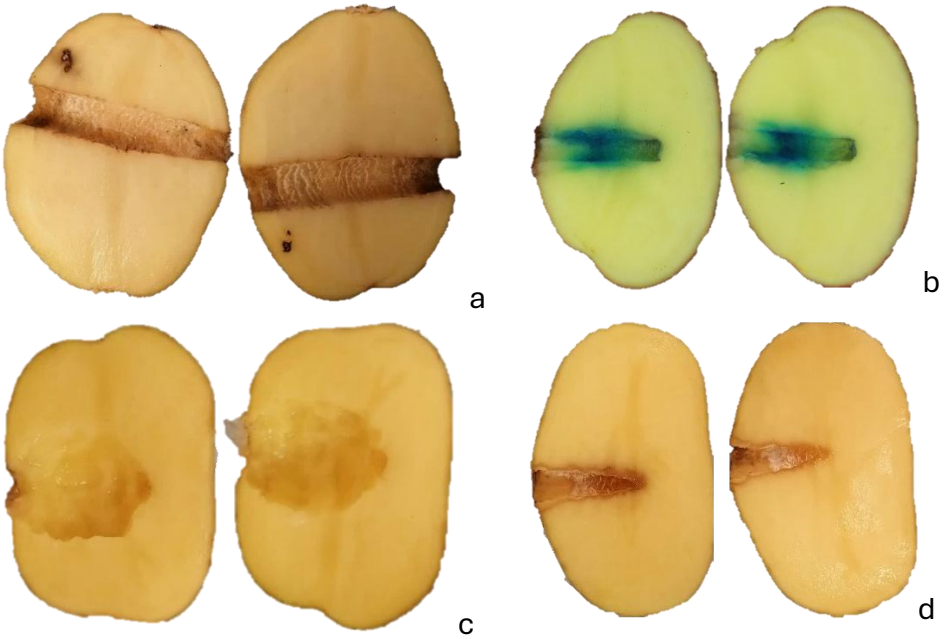

Figure 4.15 Potato voids created in lab as models for natural defects. a: Mechanical void formed with metal borer. b: Potato void stained with 10% methyl blue aqueous solution after 24 hour diffusion. c: Large void formed with 0.4% α-amylase aqueous solution. d: Small void formed with 0.2% α-amylase aqueous solution.

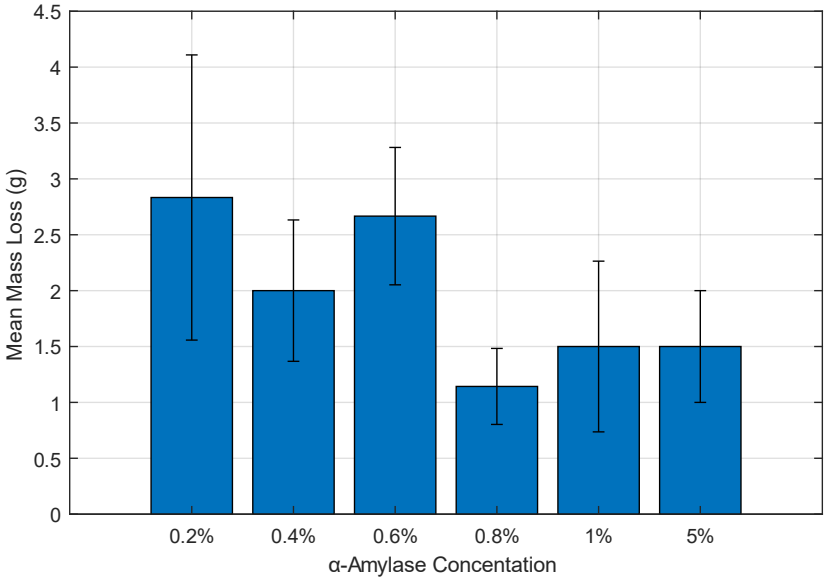

Figure 4.16 Mean mass loss of potato tubers after 24 hours of α-amylase aqueous solution infusion.
Solutions suspended in reservoirs fed into 16 mm diameter bore holes. Error bars denoted standard error of means.
n=32 (6 in each group except 5% where only 2 tubers had usable data).

4.3.5 RAC

4.3.5.1 NIR spectra change after blackheart inducing stress in the RAC

Spectra of intact tubers were recorded pre and post 14 days storage in the RAC at 25°C and saturating level of atmospheric CO_2. The second differential of these spectra computed by integrated random walk with smoothing and decimation using the "irwsm" function in the CAPTAIN toolbox (Taylor, 2007), was reduced using PCA. Spectra from healthy tubers pre RAC and tubers treated in the RAC for 14 days are separated by their second differential PCs, with the best separation using PC1 and PC3 (Figure 4.17 a), with most of the separation in PC1. There is also separation using PC1 and PC2 (Figure 4.17 b), although the separation is almost entirely in PC1, with poor separation using PC2 and PC3 (Figure 4.17 c). The separation visible in Figure 4.17 b was tested by calculating the perpendicular distance between each point and the line that bisects the groups [$(0, 2\times10^{-3})$ and $(-8\times10^{-3}, -8\times10^{-3})$]. These distances were given directionality by comparing the slope of the separation line with the slope from the line's midpoint to each point in the group. Welch's T-test was used to test whether these distances were significantly different, yielding a P value of 1.7×10^{-48}. Taking a binary value of which side

of the separating line a point falls provides a 97.6% classification accuracy, without a validation or test group.

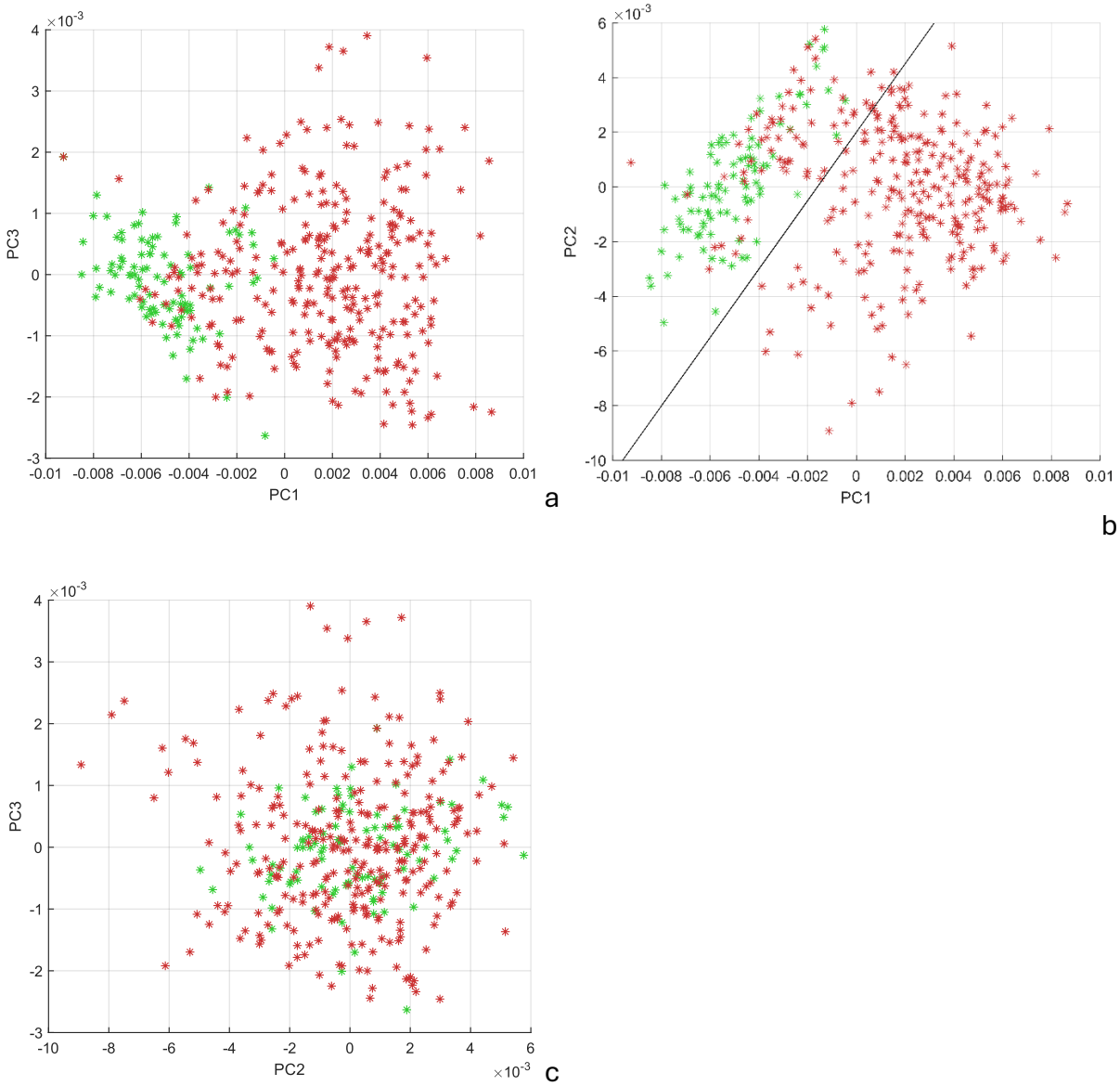

Figure 4.17 Principal components (PC) of potato tuber NIR spectra (900–1700 nm). Green markers denote spectra from healthy potatoes, and red markers denote spectra from potatoes damaged by 14 days in a hypoxic 25°C environment. Explainabilities, PC1: 68.3%, PC2: 22.5%, PC3: 5.1%. n=389).

4.3.5.2 Electrical sweep phases change after blackheart inducing stress in the RAC

Sweep responses were recorded pre and post RAC treatment for 23 potatoes. There was a marked difference between the phases in the Hilbert domain between pre and post treatment for individual tubers (Figure 4.18 a). The unwrapped phase in the Hilbert domain had a greater end value at sample 600,000 for all potatoes except one (22 out of

23; 95.7%). However, the variance in phase curves between tubers is much greater than the shift in individual tubers pre and post treatment (Figure 4.18 b), making this signal-to-noise ratio unusable for classification or defect detection.

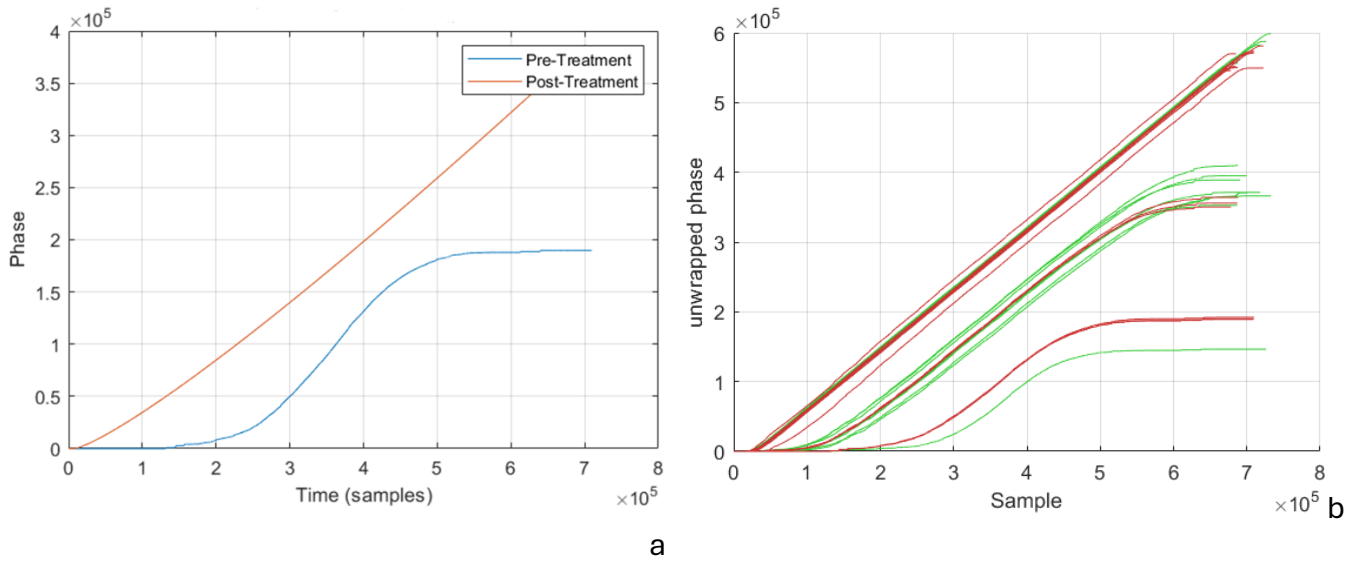

Figure 4.18 Phase of square wave logarithmic electrical sweep responses (5 Hz–5 MHz) in the Hilbert domain of potatoes pre and post 2 weeks treatment at 25°C and very high CO_2. a: Example of sweeps pre and post treatment for a single potato, n=1. b: Pre and post treatment for all tubers; green denotes untreated potatoes, whereas red denotes post-treatment potatoes, n=23.

To investigate whether this change in sweep response can be detected via a method that isn't overpowered by inter-tuber variance, the relationship between the real and imaginary parts of the Hilbert-transformed sweeps were explored. Sweeps were cropped to samples 10,000–40,000 of the 850,000 sample-long recordings (13 Hz–32 Hz of the sweep) to isolate a low frequency region where the samples per oscillation are greatest. Leading zeros were removed from the recordings prior to the isolation of this band. The real and imaginary parts were plotted against one another (Figure 4.19 a). Real components were multimodal, resulting in a vertical columns shape plot; pre-treatment tubers were observed to exhibit lower minimum values for each vertical column. To objectively test this observation, values were multiplied by 10^5 and real parts rounded to the nearest integer, such that the real part values in each vertical bar were equal. Minimum imaginary values for each vertical bar for each tuber were

recorded, and averages of minima taken for each individual tuber. Twenty-four post-treatment tubers and 19 pre-treatment tubers were recorded. Both pre- and post-treatment data sets comprised two repeats, each done on different days to ensure differences were not due to variances in experimental conditions.

Pre- and post-treatment tubers were significantly separated (Figure 4.19 b), Welch's T-test $P=1.02\times10^{-8}$. There was no difference between post-treatment tubers between repeats, Welch's T-test P=0.66. However, there was a significant difference within pre-treatment tubers between repeats, Welch's T-test P=0.0064. The difference in means pre- and post-treatment was 4.334, and 1.8674 between pre-treatment tuber repeats (Figure 4.19 c).

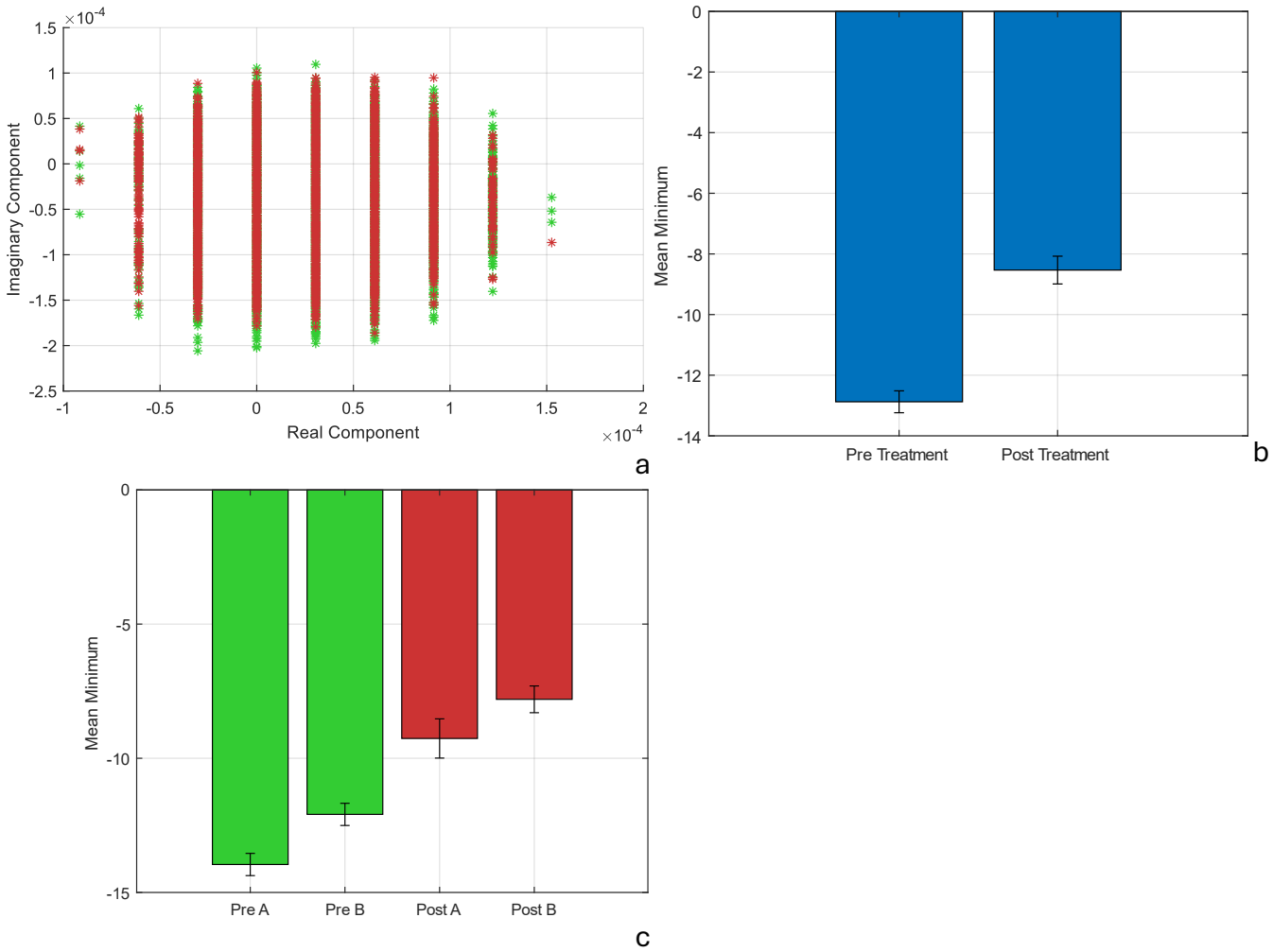

Figure 4.19 Comparison between voltaic displacement of electrical sweep responses of potatoes pre and post RAC treatment in the complex plane after Hilbert transformation.
a: Real and imaginary parts for example potato pre- and post-treatment; green markers represent pre-treatment, and red markers post-treatment. b: Mean minimum imaginary part for each

discretised real component column. P=1.02×10⁻⁸. Data for samples 10,000–40,000 used for both a and b. c: Mean minima for individual repeats.

4.3.5.3 Mechanical damage and RAC treatment increase trans-epidermal water loss and CO_2 release of potatoes

As well as differences in spectral and electrical behaviour of RAC-treated tubers, there were also differences in water loss from untreated and RAC-treated tubers measured over a period of 2.5 h using changes in the humidity of the RAC as a surrogate for trans-epidermal water loss. Data logging in the RAC revealed that the rate of humidity increase was greater with tubers treated in the RAC for 3 weeks than before treatment (Figure 4.20). This may suggest that there is a loss in epidermal integrity after treatment.

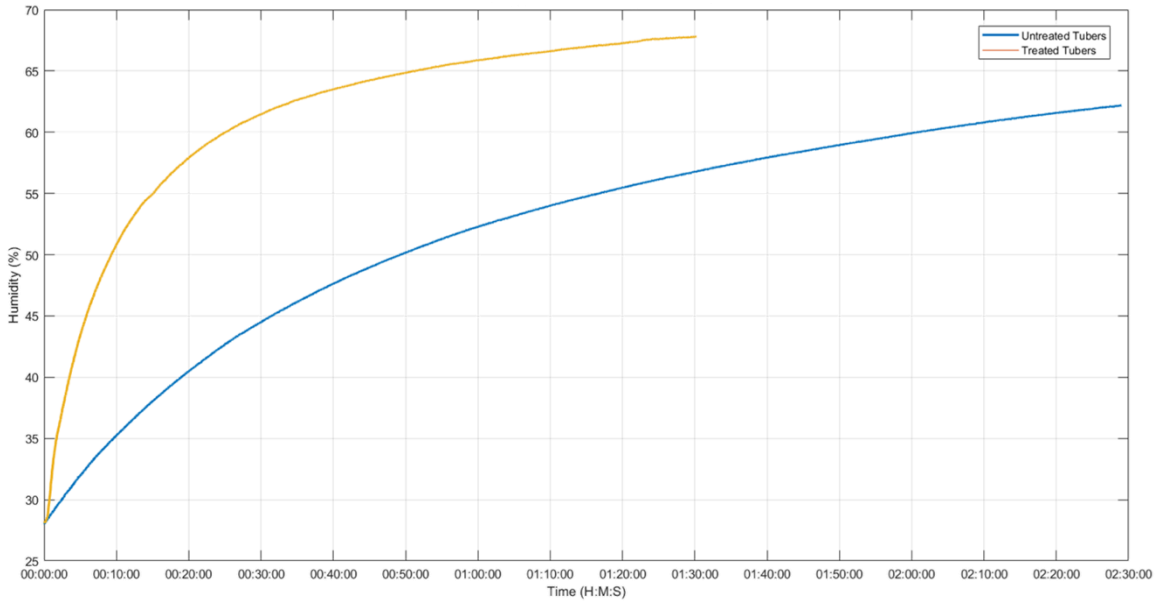

Figure 4.20 Absolute internal atmospheric humidity of 3.5 L RAC chamber over time to quantify water loss of tubers pre and post RAC treatment.
Blue line represents the mean of untreated tubers, yellow line represents RAC-treated tubers. n=23.

Changes in humidity as a surrogate for trans-epidermal water loss was also recorded for tubers with existing mechanical damage from the farm or sorting facility to test whether this observed effect may be due to loss of epidermal integrity. Trans-epidermal water loss (Figure 4.21 a), was also greater in mechanically damaged tubers with suberised wounds, suggesting that the higher rate of humidity increase observed may be due to loss of epidermal integrity. Increase in RAC CO_2 was also higher with mechanically damage tubers (Figure 4.21 b), although whether this is linked to a respiratory change was not explored.

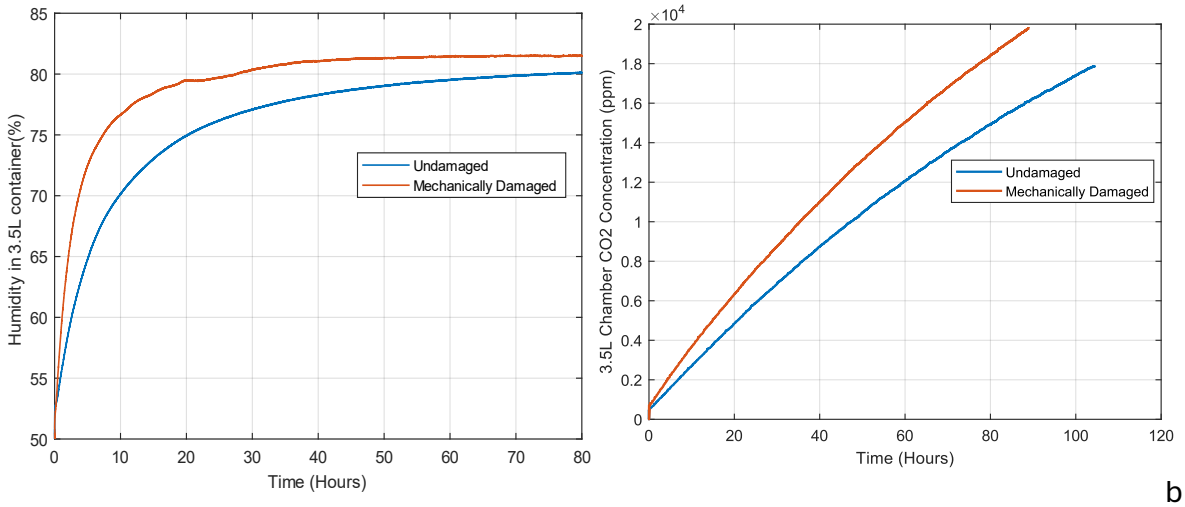

a b

Figure 4.21 Absolute humidity and CO_2 concentration in sealed 3.5 L container of potatoes to measure trans-epidermal water loss and respiration rate over time of healthy tubers compared to mechanically damaged tubers.
Mechanical damage occurred during harvest or sorting of potatoes. a: Absolute humidity, b: Atmospheric CO_2 concentration. Blue denotes healthy tubers, red denotes tubers with visible mechanical damage from farm/transit before reaching laboratory.

Tubers sealed in a 3.5 L chamber at 25°C exhibit reduced rate of CO_2 release after 12 days compared to when they were sealed, suggesting there may be a drop in metabolic rate. The chamber was flushed with normal air every 72 h and the rate at which CO_2 increased again was measured. This revealed that potatoes produce 38% less CO_2 on average (*n*=8) over 72 h after 12 days sealed at 25°C than before the 12-day treatment.

4.4 Discussion

4.4.1 Absorbance spectroscopy provides a non-invasive method of screening for spraing

Classification models using NIR spectra trained with varying relative error costs showed great success in providing a tuneable approach to effectively screen for spraing. Differing relative error costs can be utilised to tune models to necessary levels of strictness. If a threshold of 10% spraing is acceptable, then only a relative error cost of 1 is needed, and only 3.7% of healthy tubers need be wasted. However, if only 5% spraing can be tolerated, more aggressive screening from a higher relative error cost model is needed, at the cost of wasting more healthy tubers, suboptimal for higher thresholds. This approach could be applied in storage and distribution facilities. Shipments that fail to meet destructive quality control standards can be screened using a model of the appropriate relative error cost and sent back to quality control with an acceptable rate of defection. This would reduce food waste as shipments that don't meet quality standards are used for lower-value non-food uses or wasted. With only 1420 NIR spectra, performance will be exaggerated, but these results show the potential for tuneable potato screening via spectroscopy, and the applicability of NIR spectroscopy to spraing screening. These results have shown that NIR spectroscopy is more appropriate than MIR spectroscopy for spraing screening in intact potato tubers. This is likely due to NIR having a better signal-to-noise ratio; NIR spectrometers are also more stable in sub-ideal conditions, positioning them well for industrial or agricultural settings. Previous research has been conducted into non-destructive spraing detection via magnetic resonance imaging (Thybo et al., 2004), however this approaches has limited industrial applications due to high cost and slow throughput. The vast majority of literature on tackling spraing focusses on disease resistance (Brown et al., 2000; Brown et al. 2009), control of viruses which cause it (Lannetta et al., 2010; Quick et al., 2020), or the nematodes which act as vectors (Hafez et al., 2020; Holgado et al., 2012). Advancements in spraing detection are lacking and most spraing screening is performed via destructive sampling (Pérez et al., 2003). NIR spectroscopy with classifier models tuned for defect reduction rather than overall accuracy could offer a practical industrially applicable approach for spraing screening.

4.4.2 NIR spectroscopy and electrical sweep responses show promise for the detection of blackheart

As well as detecting spraing, NIR spectroscopy also showed promise for the detection of blackheart. Pre- and post-RAC treatment spectra are separated on PC plots (Figure 4.17 a and b). While no pre-RAC spectra enter the post-RAC region of the plot, there are post-RAC spectra within the pre-RAC region. This may be due to some potatoes only exhibiting mild symptoms from the RAC treatment thus being grouped with healthy tubers. The results presented in this chapter are consistent with those of recent published studies of spectroscopy-based blackheart detection (Guo et al., 2024; Wei et al., 2024). Both Guo et al. (2024) and Wei et al. (2024) made use of Visible to Near Infrared (Vis-NIR) transmittance spectroscopy, in contrast to the NIR absorbance spectroscopy utilised in this chapter. Transmittance spectroscopy may have advantages over absorbance spectroscopy for blackheart detection as light passes through the necrotic tissue, whereas absorbance spectra have lower penetration.

Alongside changes in NIR absorbance spectra, there was detectable change in the unwrapped phase of Hilbert-transformed (Johansson, 1999) tuber sweep responses after RAC treatment. However, this change is smaller than the variance between tubers (Figure 4.18), leading to a very poor signal-to-noise ratio when attempting to use this shift in phase as a means of classification. While phase in the time domain offered limited group separation, the complex plane offered much better separation. Electrical sweeps Hilbert-transformed created vertical columns in the complex plane at low frequencies (Figure 4.19 b). The minima of the real part of these columns differed significantly ($P=1.02\times10^{-8}$) between healthy tubers pre-treatment and the same tubers post-treatment at 25°C in very high CO_2 for 8 days.

A significant difference was also recorded between the minima of tubers acclimatised for 1 day after removal from cold storage and tubers acclimatised for 4 days after removal for cold storage (Figure 4.19). This difference was smaller than the observed difference between tubers pre- and post-treatment. The Hilbert transform produces an analytic signal within an abstract domain (Johansson, 1999), introducing difficulty in interpreting biological mechanisms underpinning the observed change in minima. This could be explored in the future by exploring a wider range of produce, and treatments

that impart known biochemical changes. The effects of storage at room temperature, in normal air, on this measurement may offer insights into the underlying mechanisms of the observed changes in Hilbert minima, as changes that occur during normal atmosphere storage are well documented. Water content (Chourasia et al., 2005) and sugar content (Kumar et al., 2004) vary during storage. As a conductor and major constituent of plant matter, water plays a major role in plant electrical properties; soluble sugars and starch can also affect the electrical properties of plant tissue (Qian et al., 2021). Thus, water and carbohydrates may play a role in the changes in minima observed in this experiment. Variation in water and sugar content during storage may also be a mechanism for spectral changes, as water content and sugar content are known to change during storage and can affect NIR spectra (Lui et al., 2007; Zhang & Zhang 2012).

4.4.3 Enzymatic void formation was not a viable experimental model for cavitation in potatoes

Voids formed via α-amylase aqueous solution created large voids, but inconsistency of void size rendered this approach unviable as an experimental model. This void creation approach also created uncontrolled pathogen exposure, leading to some tubers developing undesired rots such as pink rot. Insertion of the reservoir into the pilot hole altered the shape, creating a taper (Figure 4.15 b), making reinsertion of the plug for sealing not possible. It is not known whether this treatment significantly altered the chemistry of the potato in undesirable ways, either directly or by stimulating the stress responses. Such chemical changes could alter optical spectroscopy results (Zahir et al., 2022), although would be unlikely to have a significant effect on electrical spectroscopy. Whilst the potential for creating artificial voids in tubers as a model for studying the effectiveness of non-destructive approaches for detecting internal potato defects, inconsistency of void size makes repeating experiments difficult and may lead to an overly skewed void size distribution, where a flat or binomial distribution would be desirable for regression and classification respectively. Research into detection of internal potato voids such as hollow via sonic means has been conducted. Elbatawi (2008b) successfully detected hollow heart from the impact sound of potatoes falling

onto stainless steel bars. Success has also been found with hyperspectral imaging (Dacal-Neito et al., 2011).

4.4.4 Electrical sweep responses might assist in detecting wireworm damage in tubers

The data presented in this chapter provide tantalising glimpses of the potential for using alterations in the RMS envelope of electrical sweep responses for detecting wireworm damage (Figure 4.14). However, the two caveats to this are that these data are preliminary and would require repeating to confirm the results conclusively, and that they have been obtained using purely mechanical simulated wireworm damage. Real wireworm tunnels are much shallower, with the majority of tunnel damage occurring in the outer 1 cm of a potato's radius (Jonasson & Olsson, 1994). Salivary compounds (Li et al., 2019b), and pathogenic microorganisms (Keiser et al, 2012) introduced to a tuber by pests such as wireworms may also create unique stresses not detectable by this approach. The extreme burrow depth used in this model serves as a proof of concept as longer burrows are likely more easy to detect.

[REDACTED]

[REDACTED].

5 Chapter 5: [REDACTED] treatment for extending shelf-life of fast-spoiling high-value produce

5.1 Introduction

Food waste has disastrous impacts on both humanity and the Earth. Overproduction of crops and livestock brought on by waste in the supply chain leads to deterioration of soils, overuse of water, water pollution, loss of biodiversity and additional greenhouse gas emissions (Foley et al., 2011). Many of these impacts also have deleterious effects on agricultural production (Agrawal, 2005; Burney & Ramanathan, 2014; Bindraban et al., 2012). Reduction of food waste at all stages, from farm to fork, is therefore paramount to building sustainable and accessible food systems.

Defects and spoilage can occur at any stage of the fresh produce supply chain (Hermansyah & Romli, 2025; Kathayat & Rawat, 2019; Tort et al., 2022). Chapters 3–5 explored defects that develop pre-retail, such as blackheart during storage or spraing during growth, and the potential of biophysical approaches to detect and mitigate these defects. However, retail environments, consumer homes, and transit to these locations, account for a significant proportion of food waste and food deterioration, with retail and domestic food waste accounting for 5% and 42%, respectively, of food being discarded (European Commission, 2011). Fruit and vegetables are a significant contributor to retailer food wastes. Scholz et al. (2015) reported that fruits and vegetables constitute 85% of food waste mass in Swedish supermarkets, whilst Brancoli et al. (2017) reported they contribute under 30% in other Swedish supermarkets, with bread as the major waste mass contributor. In addition to a reduction in food waste contributing to food security (Paraschivu, 2022), managing these losses is especially important as access to fresh produce is a key concern for consumers, with 60% of UK consumers and 70% of US consumers saying their most important consideration when deciding food shopping location is “access to the best-quality fresh food” (Wyman, 2013).

5.1.1 Environmental impact of packaging

Packaging can play a valuable role in maintaining the quality of produce and for managing waste and reducing spoilage of fresh produce at the retail, transport and consumer stages of the supply chain (Karanth et al., 2023). Packaging offers protection

for fresh produce from mechanical damage (Al-Dairi et al., 2022; Karanth et al., 2023). Modified atmosphere packaging is a packaging technique where gases different in content or concentration to normal air are sealed within packaging; nitrogen, oxygen and CO_2 are typically employed (Floros & Matsos, 2005). Gases are sealed using plastic films, often partially permeable to slowly naturalise the internal atmosphere (Qu et al., 2022).

Modified atmosphere packaging is used to manage the physiology of the produce itself and its pathogens, encouraging ripening or lowering metabolic and respiration rates to slow spoilage (Kandasamy, 2022). Controlled atmosphere storage is used to manage produce physiology pre-retail through the same mechanisms (Mullan & McDowell, 2011). Modified atmosphere packaging is a chronic stimulus maintained until the packaging is opened, requiring appropriate packaging such as polyvinyl chloride, polyethylene terephthalate, polypropylene or polyethylene (Mangaraj et al., 2009), all of which pose environmental hazards with low rates of recycling (Abbasi et al., 2023; Akinro et al., 2012; Alsabri et al., 2022; Ye et al., 2017), typically making use of films that are not recycled by the consumer. Polyvinyl chloride is becoming more recyclable, although it has considerable environmental impact (Ye et al., 2017) and is often disposed of into landfill or the ocean (Jiang et al., 2023).

5.1.2 Extending shelf-life

[REDACTED]. This effect was observed both on tubers treated for an extended period of [REDACTED], and those treated for a shorter period of [REDACTED], resulting in the metabolic rate dropping by almost half. This suggests that [REDACTED] treatment could therefore increase shelf-life, reducing food waste, and raises the intriguing possibility that [REDACTED] treatments may be employed in this manner to reduce the dependence on modified atmosphere packaging further down the supply chain. This would come with the advantages of less restriction on packaging design, perhaps with the elimination of some packaging, and maintaining desired physiological effects after the packaging has been opened. In addition, foodborne microbes within and on the vegetable will also be subject to [REDACTED] treatment, which may alter vegetable–pathogen interactions and have beneficial effects for shelf-life of vegetables. This

chapter will explore the potential of [REDACTED] treatment prior to packaging to achieve shelf-life extension of fresh produce.

5.1.3 Tomatoes as model produce

Losses in the tomato supply chain are high, especially in Africa (Arah et al., 2015a). Therefore, tomato was chosen as the model crop to study the potential [REDACTED], to reduce wastage, with grapes also tested to assess the universality of the effects observed. Tomatoes offer the benefit of having a consistent size and appearance, making them ideally suited for comparison by human eye or computer vision software. Tomatoes of consistent size can be acquired, enabling easy comparison of mass loss. Their high water content is also ideal for this measurement. Tomatoes spoil on a timescale practical for this experiment, typically on the scale of a week, providing enough time to gather data while spoiling quickly enough to accommodate repeating the experiment within a doctorate-friendly timeframe. Tomatoes are easy to acquire all year round in the UK, where this research took place, making them ideal for repeats.

5.1.4 Aims and objectives

The overall aim of this chapter is to investigate whether [REDACTED] treatment can be used to extend shelf-life of fresh produce. This aim was addressed through the following three objectives:

- Assess the impact of [REDACTED] treatment on the spoilage of fast-spoiling high-value produce
- Quantify differential spoilage rates of [REDACTED]-treated and untreated vegetables
- Determine the potential for [REDACTED] treatment for affecting foodborne microbes within and on the vegetable using *Botrytis cinerea* R16 as a model fungus

5.2 Methods

5.2.1 Sample preparation and treatment

Pre-packed tomatoes were acquired from a local grocery store (Booths, Lancaster), both cherry tomatoes on the vine, and off-vine round tomatoes. The contents of each packet were divided equally between treatment and control groups to ensure like samples were compared. Tomatoes on the vine were carefully removed before treatment with a twisting motion whilst tomatoes in the control group remained on the vine in cold storage at 5°C for the duration of the [REDACTED] treatment and removed from the vine when the storage phase of the experiment began. Pre-packed grapes of Brazilian origin were acquired from a local grocery store (Booths, Lancaster) of the variety ARRA31. The contents of two punnets were divided equally between treatment and control groups. Grapes were carefully cut off the bunches, with pedicel attached. All loose grapes were excluded from the experiment.

5.2.2 [REDACTED] treatment

[REDACTED].

Following the [REDACTED] treatment, both treated and control tomatoes and grapes were stored in a well-ventilated growth room, on a shelving unit lit with strip lights to simulate supermarket shelf storage conditions. Strip lights were on a 16 hours/8 hours day/night cycle, with photosynthetically active radiation ~150 $\mu molm^{-2}s^{-1}$ at shelf height and 22°C room temperature during the day and 20°C at night. Humidity was not regulated but averaged approximately 65% RH. Samples were evenly spaced in seed trays lined with blue paper towel. Trays were cleaned with tap water and 70% ethanol prior to use.

Both tomatoes and grapes in control groups were stored at 5°C in a well-ventilated cold storage room while treatment groups were [REDACTED].

5.2.3 Shelf storage

Samples were regularly weighed on an electric balance during storage to determine mass loss over time. Tomatoes that became “unmarketable” due to exhibiting visible mould, splitting of the skin, blackening or internal sprouting of seeds were excluded

from further analysis. “Survival rate” refers to how many tomatoes were still remaining at a given point in time.

5.2.4 *Botrytis* growth and treatment

Botrytis cinerea R16 was grown from frozen samples on 10 cm diameter Petri dishes of potato glucose agar for 77 h in a Panasonic MLR-352-PE Versatile Test Chamber (Panasonic, Kadoma, Japan), at 21°C with 120 $\mu molm^{-2}s^{-1}$ light intensity on a 16h/8h day/night cycle. Potato glucose agar was prepared using Sigma-Aldrich brand potato glucose powder (product code: 101949178; Merck, Burlington, Massachusetts, USA) following packaging directions to suspend 39 g in 1 litre of water (reverse osmosis water was used) and immediately dissolve after boiling, then autoclave at 121°C for 15 mins and add 1 ml of 10% sterile lactic acid. Plugs (1 cm^2) were cut from these plates and used to seed a set of new plates. These were divided into two groups: treatment and control. Plates in the treatment group were treated with the same method as tomatoes and grapes [REDACTED], before having plugs removed for growth. After the treatment group had been treated, plugs were removed from the treated plates and control plates and used to seed new plates whose growth was observed over time. Twelve Plugs (1 cm^2) cut from each group were grown on fresh plates of agar and regularly photographed on a high contrast background to determine growth rate. The region of the plate covered by *B. cinerea* in each photograph was digitally filled in using an image manipulation program (GIMP 2.0, GIMP Development Team), and a pixel-counting MATLAB script was used to calculate the area of plate coverage. Contaminated plates were excluded from the experiment.

5.2.5 NIR spectroscopy

Tomatoes were scanned with a NIRvascan Nano (Allied Scientific Pro, Gatineau, Canada) immediately prior to shelf storage after samples in treatment groups had been treated. NIR spectra were not recorded from grapes due to their impractically small size. Each scan comprised the mean of six spectra. Twenty-five scans were recorded per tomato.

5.2.6 Data analysis

Linear regression was performed using the “fitlm” function in MATLAB R2024a (MathWorks, Portola Valley, USA), with the linear present and “robustops” set to off. Data were processed prior to fitting the linear model, using PCA on the second differential of the absorbance spectra.

5.3 Results

Tomato spoilage rates were reduced by [REDACTED] treatment

[REDACTED] treatment significantly increased the shelf-life of tomatoes, reducing the rate of spoilage (Figure 5.1). For cherry tomatoes on the vine, after 10 days almost all (91.7%) of the control group exhibited visible mould, splitting of the skin, or blackening rendering them unmarketable (Figure 5.2), while over half (58.3%) of treated tomatoes showed none of these symptoms remaining healthy. Treated tomatoes lasted 62% longer on average before being recorded as unmarketable on the basis of these symptoms, with a significant difference in shelf-life before exhibiting unmarketable defects between the control and [REDACTED]-treated groups (T-test P=0.0062). The shelf-life of off-vine round tomatoes was also significantly longer following [REDACTED] treatment, with only 25% (3) of the control group surviving 10 days on the shelf, while 100% (12) of the treated tomatoes remained healthy with no signs of unmarketable symptoms (T-test P=2.61e-05).

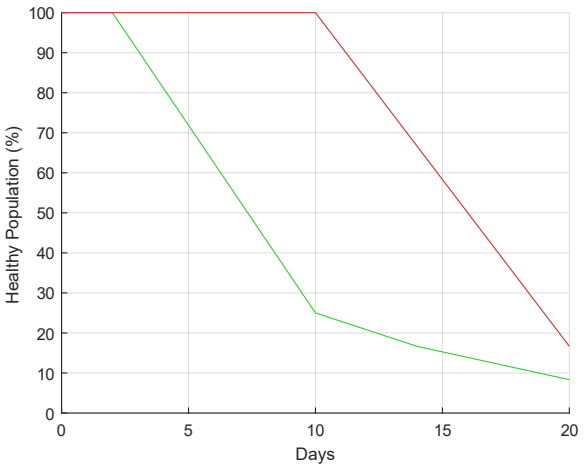

a

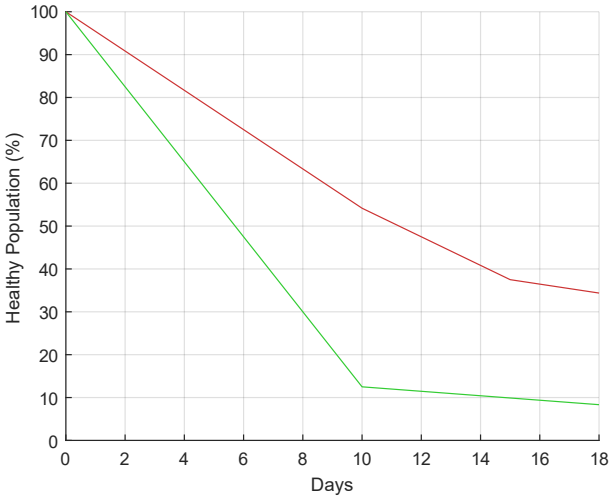

b

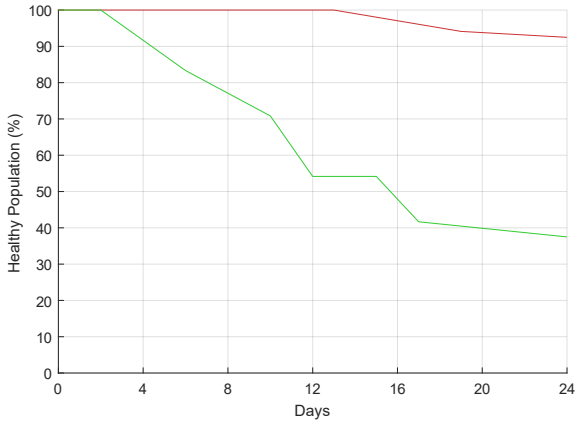

c

Figure 5.1 Survival rates of tomatoes between treatment and control. Red denotes control group, and green denotes treatment group.
a: Cherry tomatoes on the vine, n=48, measurements taken on days 0, 10,15,18. b: Off-vine round tomatoes, n=24, measurements taken on days 0, 2, 10, 14, 20. c: Off-vine round tomatoes, n=41, measurements take on days 0, 2, 4, 6, 10, 12, 15, 17, 24.

a b c

Figure 5.2 Examples of unmarketable tomato defects.
a: Mould. b: Splitting. c: Blackening.

5.3.1 Tomato mass loss provides an accurate measure of tomato shelf-life extension

Visible assessments of when a tomato is “unmarketable” have a subjective element and may be open to human bias. Water loss in tomatoes is closely linked to spoilage (Babaremu et al., 2019; Nunes & Emond, 2007), thus mass loss during the storage phase was also used to assess the impact of [REDACTED] treatment on tomato spoilage. Treated tomatoes lost significantly less mass than control tomatoes after 10 days of storage, in off-vine tomatoes (T-test P=7.9e-07) (Figure 5.3 a,b). Twenty-one tomatoes in the control group and 11 tomatoes in the treatment group showed visible unmarketability symptoms by 10 days. However, control tomatoes exhibiting visible defects lost considerably more water than treated tomatoes with similar defects (T-test P=1.87e-04) (Figure 5.3 c,d) suggesting that not only were defects more prevalent in control, but more severe. In contrast, there was no significant difference between mass loss in healthy control tomatoes and healthy treated tomatoes after 10 days (Figure 5.3 e,f), supporting the hypothesis that mass loss provides a reliable surrogate for spoilage.

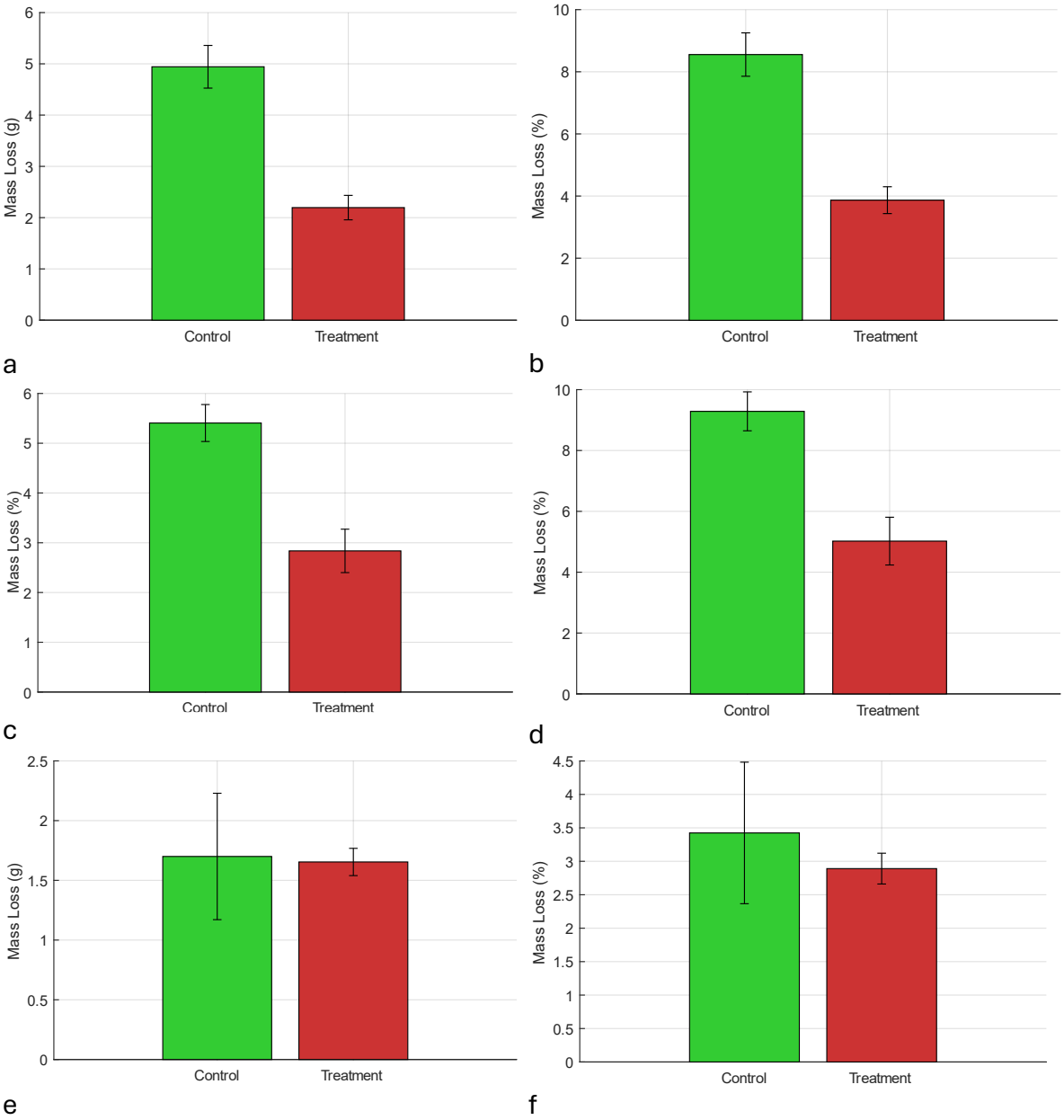

Figure 5.3 Mass loss in off-vine round tomatoes after 10 days storage, with or without [REDACTED] *treatment (n=48).*
P values calculated with Welch's T-test. a: Mass loss of all tomatoes after 10 days (P=7.4058e-07) (Control n=24, Treatment n=24). b: Mass loss as percentage of initial mass of all tomatoes after 10 days (P=7.8874e-07) (Control n=24, Treatment n=24). c: Mass loss of tomatoes showing visible defects after 10 days (P=1.8719e-04) (Control n=21, Treatment n=11). d: Mass loss as percentage of initial mass of tomatoes showing visible defects after 10 days (P=3.2914e-04) (Control n=21, Treatment n=11). e: Mass loss of tomatoes showing no defects after 10 days (P=0.8907) (Control n=3, Treatment n=13). f: Mass loss as percentage of initial mass of tomatoes showing no defects after 10 days (P=0.4343) (Control n=3, Treatment n=13).

5.3.2 NIR spectroscopy is not a good predictor of tomato shelf-life

Peaks in tomato absorbance spectra were identified via the zeros of the first differential at 980 nm, 1195 nm, 1445 nm, and 1624 nm. There also appears to be a weak peak at 929 nm but this is not reflected by a zero in the first differential (Figure 5.4). All of the peaks identified were also found in tuber spectra in Chapter 3. Table 2.7 describes the compounds associated with these peaks.

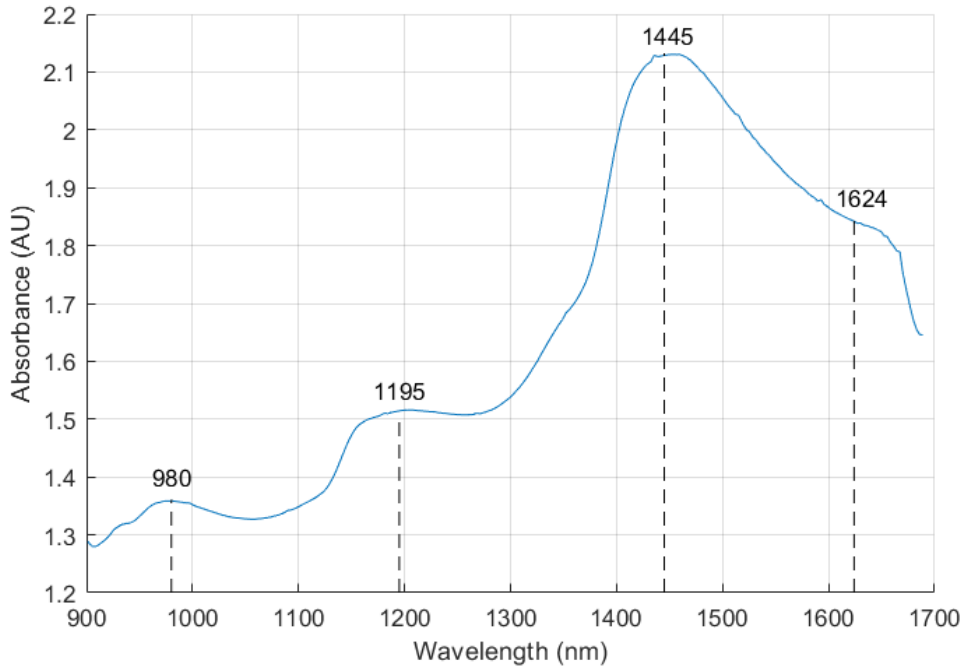

Figure 5.4 Peaks in NIR absorbance spectra of round tomatoes. Peak locations determined via zeros of first differential.

Linear regression was used to produce a model of tomato shelf-life for early spoilage prognosis with pre-storage NIR spectra. This model failed to predict shelf-life from NIR spectra with $R^2 = 0.00$ and RMSE = 14.866; Figure 5.5 shows that the model predicts a rough average for every value and fails to predict shelf-life.

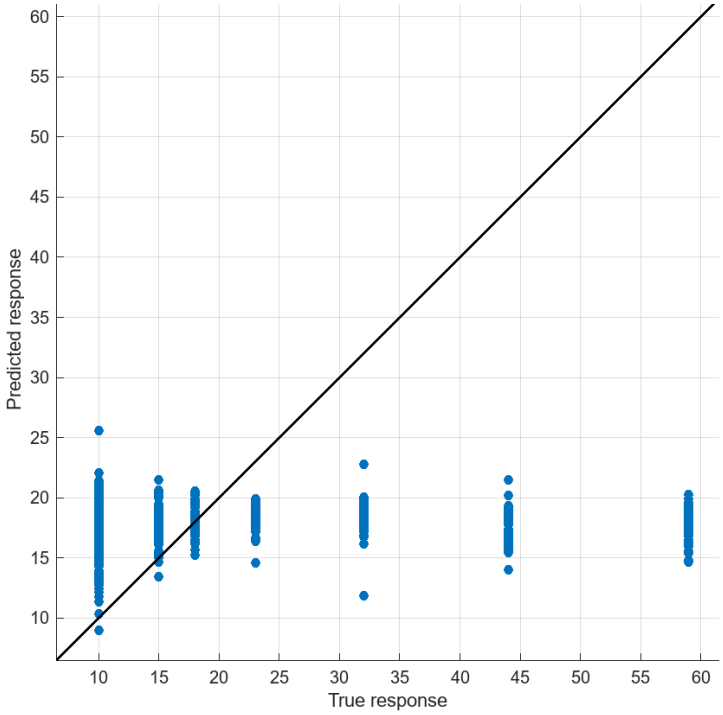

Figure 5.5 Linear process regression for predicting tomato shelf-life from pre-storage NIR spectra. R^2=0.00. No association found. Regression fitting was performed using MATLAB using PCA of the second differential of NIR absorbance spectra.

5.3.3 Grape spoilage rates were not affected by [REDACTED] treatment

Two punnets of grapes were used, with induvial grapes randomly distributed between two trays of equal mass with approximately 200 grapes per tray (counting the grapes in one tray yielded a population of 191). In contrast to tomato, [REDACTED] treatment had no effect on the shelf-life of grapes. There was no visible evidence of spoilage in either control or treated grapes following [REDACTED] of storage under supermarket shelf conditions. In addition, although the mass decreased in both groups over this period (stats), by 31% of total mass, there was no significant difference in mass loss between control and treated grapes (Table 6.1). Grapes did not biotically spoil, but rather shrivelled with no signs of mould or rot. The [REDACTED] treatment appears to be too [REDACTED] grapes and may be too extreme.

Table 5.1 Total mass of grapes pre and post 48 hours storage on supermarket shelf-like environment, without packaging on blue paper towel.

Grapes in treatment group were treated [REDACTED]. *Approximately 200 grapes in either group.*

	Control (g)	Treatment (g)
Pre-storage	411	412
Post-storage	286.6	285.4

5.3.4 [REDACTED] had no effect on *Botrytis* growth

In total, 20 plates were used, 12 treatment, 8 control. Plugs (1 cm^2) were taken from control and [REDACTED]-treated *Botrytis* colonies and used to seed fresh agar plates. There was no significant difference in area of the *Botrytis* colonies formed between control and treatment groups (Figure 5.6a; repeated measure ANOVA P=0.74). Similarly, there was no difference in average growth rate between control and treatment groups over the period studied (Welch's T-test P=0.209) (Figure 5.6b). In both cases, colonies completely covered all plates after ~80 h growth. However, there was a significant difference in initial growth rate following the transfer of control and treated plugs to the fresh agar plates; the treatment group grew significantly faster than controls (Figure 5.6a; Welch's T-test P=0.004). This difference was not maintained, as growth rate slowed due to factors independent of the treatment, i.e. reduction in available nutrients and space, such that the difference in later growth is less significant, as evidenced by a close correlation between the growth area of the control and treatment groups (Pearson's correlation coefficient, R=0.98, P=0.0033).

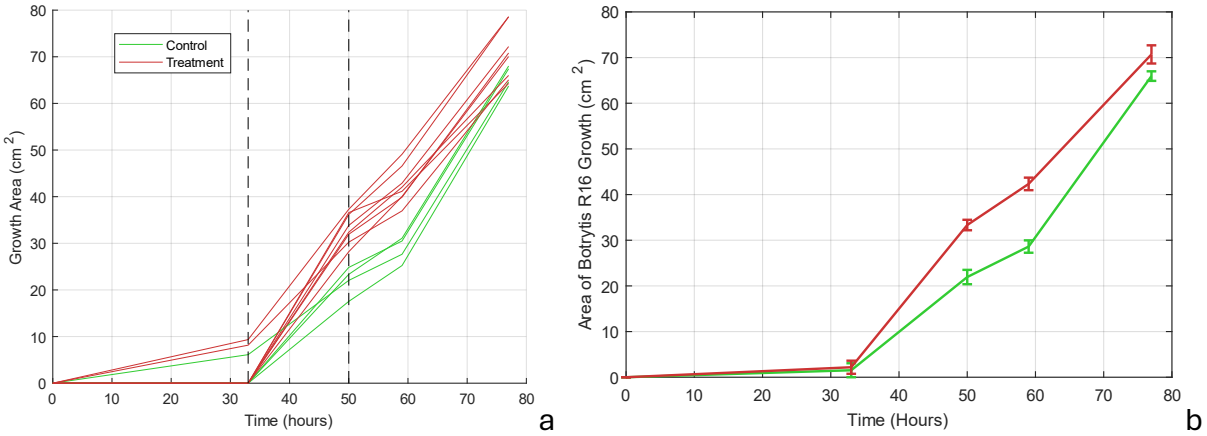

Figure 5.6 Area of growth of Botrytis cinerea R16 plugs cut from plates treated [REDACTED]*, compared with control.*
Control plates were propagated from untreated plugs. Total plate area = 78.5 cm^2. a: Growth individual plates, dotted lines denote initial growth period. Treatment group denoted by red, control by green. b: Group mean averages over time. Red denotes treatment, green denotes control.

5.4 Discussion

5.4.1 [REDACTED] treatment with [REDACTED] extends shelf-life of fresh tomatoes

[REDACTED] successfully extended the shelf-life of whole tomatoes, without the requirement for specialised packaging. Both the rate of mass loss and the prevalence of defects was significantly lower in the treatment groups compared to control (Figures 6.1 and 6.3). Having not directly compared [REDACTED] with modified atmosphere packaging, it is unclear whether there is significant difference in efficacy for shelf-life extension. However, having shown substantial improvements over control in mass loss reduction and spoilage delay without environmentally hazardous packaging or refrigeration suggests there is potential for this technology as a sustainable approach to shelf-life extension.

5.4.2 *Botrytis cinerea* does not pose elevated threat to treated tomatoes

Initial growth rate of *B. cinerea* was significantly faster in treated cultures than control, evidencing a lack of down-regulation of metabolism. These data may suggest that fungal pathogens could benefit from this treatment. However, treated tomatoes develop rot less frequently and more slowly than control, suggesting that the increase in growth rate of fungal pathogens is not sufficient to overwhelm the benefits to tomatoes. Senesced fruits are more vulnerable to fungal pathogens (Alkan & Fortes, 2015). Senescence is internally regulated by ripening-associated genes, although fruit–pathogen interactions may accelerate these processes (Figueroa et al., 2021). Senesced tomatoes being more vulnerable to pathogens, those with down-regulated metabolisms will have a delayed vulnerability to pathogens. Initial growth rate of *Botrytis* may exhibit greater inter-group separation at this stage as new cells are being produced by the treated plugs, whereas later in growth perimetral cells were not directly treated and thus not exhibiting effects of the treatment. Although *Botrytis* growth was unaffected by the [REDACTED] treatment, this cannot be extrapolated to bacterial pathogens that may [REDACTED] and may not represent all fungal pathogens accurately. [REDACTED] These effects, however, may not persist beyond the treatment period.

5.4.3 Variations in treatment protocol

[REDACTED]

5.4.4 Application of [REDACTED] in developing countries

In less economically developed regions, such as sub-Saharan Africa, tomato transit is often without refrigeration or controlled atmosphere, such as exposed baskets on motorcycles (Arah et al., 2015a). Here, losses of ~10% are experienced in the post-harvest pre-consumer stages of the supply chain (Sibomana et al., 2016). Such transit methods are not compatible with current approaches to produce metabolism management and may be ideal use cases for the [REDACTED] developed in this chapter. This treatment could be performed without electricity, [REDACTED].

Tomatoes are rich in lycopene and β-carotene, which are precursors to vitamin A (Rosati et al., 2000). Lycopene and β-carotene production is slower in modified atmosphere treated tomatoes compared to control (Hari Pranesh et al., 2022). Chromoplasts that produce these carotenoids in tomatoes arise from chloroplasts during ontogeny (Egea et al., 2011). Hari Pranesh et al. suggest that the observed slowing of lycopene and β-carotene production is due to a slowing of chromoplast biogenesis. Approximately a third of pre-school age children worldwide are vitamin A deficient, with the highest rates in sub-Saharan Africa and South-East Asia (WHO, 2009). Vitamin A deficiency causes over 600,000 deaths a year, predominantly of children and pregnant women (Burri, 2011). If [REDACTED] is to be used in sub-Saharan Africa or other developing regions it is of importance to test whether similar drops in vitamin A precursors also occur with this treatment. [REDACTED] could be used to extend the life of ripe picked tomatoes, which are allowed to reach full pro-vitamin A levels prior to treatment; the experiments conducted in this chapter were performed on already-ripe tomatoes, showing that this approach is impactful post-ripening.

Nutrient and antioxidant levels may become depleted in vegetables during storage (Murcia et al., 2009), although it is contested in the literature whether there is significant lowering of antioxidant capacity of fresh produce during storage (Kevers et al., 2007). Slowing metabolic rate may perhaps reduce the rate at which nutrients and antioxidants

are consumed for maintaining vegetable physiology, although further research would be needed to test whether this would make a significant effect after [REDACTED].

5.4.5 Quantification of spoilage

Spoilage of fresh produce can be non-destructively quantified in different ways, such as mass loss (Bovi et al., 2018; D'aquino et al., 2016), as used in this experiment (Figure 5.4), as well as firmness (Olveira-Bouzas et al., 2021), colour (Olveira-Bouzas et al., 2021; D'aquino et al., 2016) and visual appearance by human inspection (D'aquino et al., 2016). Gloss is a known marker of produce quality in various vegetables, reflecting both water content and consumer aesthetic preferences (Hao et al., 2024). An automated system of gloss determination was developed for this experiment, but due to jpeg compression and related issues (Figure 5.7) and hardware limitations of suboptimal image resolution and imaging device overheating the system was not used for this experiment. This system used the specular reflection of strip lights from overhead smartphone timelapse images but was not deployed in the final experiment; see Appendix 2 for system details.

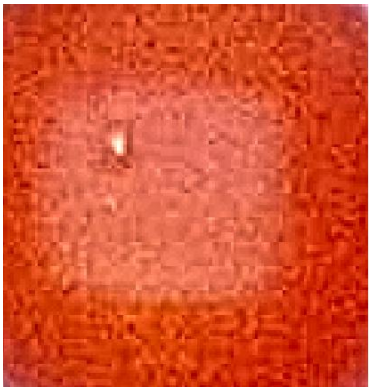

Figure 5.7 Photo of tomato automatically cropped to region surrounding reflection. Image sharpened to make jpeg compression clearer.

5.4.6 NIR spectroscopy did not predict shelf-life

The linear regression model trained on PCA of second differential pre-storage NIR absorbance spectra failed to predict tomato shelf-life (Figure 5.6), perhaps suggesting pre-shelf factors have less impact on tomato shelf-life than factors during shelf-life. Storage factors such as humidity, temperature and handling are known to impact

produce shelf-life (Arah et al., 2015a), although post-shelf precursors or predispositions to shelf spoilage may not be easily detectable until they advance, evidenced by blackheart being more detectable in its advanced stages, seen in Chapter 5, than in its early stages, seen in Chapter 4.

Tomatoes compared in this experiment were carefully selected to have no visible signs of spoilage, damage or disease prior to the experiment and acquired from a premium grocer. These standards may have led to skewing or clustering of pre-shelf factors, such that there was no significant variance to be detected by pre-shelf NIR spectroscopy.

5.5 Closing remarks

The experiments described in the preceding chapters have shown that novel approaches can be harnessed to better understand tuber defects throughout the fresh potato supply chain. The work described in this chapter has additionally demonstrated the potential of novel methods for reducing waste in the fresh produce supply chain through the prevention and improved management of produce defects. Although currently limited to tomato, it would be of interest to test how applicable the same approach is to a wider range of fresh produce.

6 Chapter 6: Discussion

This research aimed to find novel approaches to non-invasive non-destructive detection of internal potato defects. Experimental models were developed for internal defects and testing whether optical spectroscopy- and electrical impedance-based methods can be used to detect these defects. These methods were also used to test tubers provided from the project partner, Burgess Farms, for real defects as well as exploring if defect development can be detected early during growth or storage. [REDACTED] developing a method for extending the shelf life of tomatoes. The motivation for this work has been to reduce food waste and losses in the fresh produce supply chain.

6.1 NIR reflectance spectroscopy can be used for non-destructive defect detection

NIR reflectance spectroscopy showed great promise for non-destructive screening of blackheart and spraing in intact potatoes (Chapter 4). Models trained on tuber NIR reflectance spectra provided accurate classification of healthy tubers and those treated with blackheart-inducing stress. Variation in error costs while training classification models enabled tuneable adaptive screening of spraing (Table 4.2), adjustable to differing quality control standards to minimise healthy tuber losses. Rejection of harvest is a serious economic concern for farmers (Johnson et al., 2019), therefore tuneable screening methods that allow for healthy produce to be salvaged from otherwise rejected shipments could offer great financial security benefits for farmers.

6.1.1 Potential mechanisms responsible for observed changes and differences in spectra

6.1.1.1 Spectral absorbance peak associations

Presence of peaks in absorbance spectra can be used to make inferences about the chemistry of a sample. Different compounds, bonds and vibrations are known to absorb different wavelengths of light. By identifying which compounds are associated with the observed peaks in spectra, and which of those peaks change with experimental treatments, insight into the mechanisms underpinning these changes can be gleaned (Zahir et al., 2022).

There was consistency in the peaks of tuber spectra between experiments, mostly consisting of the same peaks with similar absorbances, as expected. However, the peak at 929 nm, as seen in the growth experiment (Figure 2.10), and the peak at 973 nm, as seen in the elevated CO_2 storage experiment (Figure 3.8), exhibited large variation between experiments. A weak peak at 929 nm can be seen in Figure 3.8, although not reflected in a zero of the differential, whereas the 973 nm peak is completely missing from Figure 2.10. The Orchestra variety of potato was used for both of these experiments; however, the tubers in the growth experiment (Chapter 2) were grown under drought conditions in the lab, while those in the elevated CO_2 experiment (Chapter 3) were grown outdoors by professional farmers for a premium potato supplier (Burgess Farms). The peak at 929 nm matches peaks for overtones of C–H bonds in methylene group lipids (Khodabux et al., 2007). Triglycerides, found in potatoes, fall within this category of compounds, and play a role in protecting cells from lipotoxicity under drought stress in ryegrass (Perlikowski et al., 2022). If a similar process occurs in potato plants this could explain the difference in the 929 nm peaks between commercial potatoes and those grown under severe drought stress in the lab. The peak at 973 nm could be related to the overtone of the O–H stretch in water (Khodabux et al., 2007), which would explain why it is not prominent in drought-stressed tubers, which likely have a lower water content than tubers not grown under severe drought stress. If this is the case, a prominent water peak in the tubers provided by Burgess Farms would suggest they were not grown under severe drought stress, supporting the analysis of the 929 nm peak. However, given the complexity of organic compounds and the enormous

range of compounds a vegetable or plant contains, it is not always clear which compounds are responsible for observed changes in spectra; some models using spectra are thus black boxes, with the underlying chemical interpretation unclear (Beć et al., 2021; Ribeiro, et al., 2025; Uwadaira et al., 2018). Further work could be done to confirm suspected chemical mechanisms through chemometric assays.

6.1.1.2 Spectral changes reflect stress-induced changes in tuber properties

Formation of biotic defects such as rots alters the chemistry of produce as it is broken down by the pathogen into products or end products of metabolic processes, altering the overall chemistry of a sample (Tournas, 2005). Most of the energy in a potato tuber is stored in starch, which makes up 66%–80% of the dry matter of a potato (Liu et al., 2007). Starch is cleaved by amylase into maltose, which is eventually hydrolysed into glucose (Tournas, 2005). The presence of more maltose or glucose than expected in a tuber may therefore be indicative of starch hydrolysis having occurred. Similarly, increases in amylase activity may also be indicative of starch hydrolysis occurring. Whilst FTIR has been used to determine amylase activity in a starch solution, by comparing two spectra with a 20-minute time interval (Krieg et al., 1996), this may not be directly applicable to intact tubers as the reaction may occur more slowly as behaviour of enzymes in non-physiological conditions may not reflect that inside a cell (van Eunen et al., 2012), and substantial periods between readings may be impractical for industrial application. In contrast, NIR spectroscopy could perhaps be used to measure the sugar content of intact produce. Liu et al. (2011) used NIR spectroscopy to measure the sugar content of chestnuts, with their model providing a correlation of 0.90 between spectroscopically estimated sugar levels and actual sugar levels in destructive samples, and a 0.83 correlation coefficient for intact samples. In potatoes, tuber glucose levels vary naturally during the first 14 to 16 weeks of storage (Cheng et al., 2010). However, fructose levels also vary during this time course, with close correlation to glucose, and the ratio between fructose and glucose is a function of storage temperature and time. Thus, fructose levels and storage time could be used to establish an expected baseline for tuber glucose content. Therefore, NIR spectroscopy could perhaps be used to measure the sugar content of intact potatoes as a marker for spoilage. Sugar content varies between varieties of potato; cultivars bred for frying

purposes have lower sugar content and fructose-to-glucose ratio than other varieties to minimise the browning from the Maillard reaction and acrylamide formation (Mestdagh et al., 2008). Thus, approaches focused on sugar content will require variety-specific calibration and may work less effectively on some varieties.

Some plant stress signals may alter the plant spectra. Damage-associated molecular pattern (DAMP) responses in plants involve a variety of compounds (Hou et al., 2019) that can alter NIR spectra including protein fragments, peptides (Siesler et al., 2008), nucleotides (Beć et al., 2019), and amino acids (Guorong et al., 2016; Siesler et al., 2008). Additionally, RAMAN spectroscopy has been used to detect signals of pathogen-associated molecular pathway (PAMP)-triggered immunity (PTI) in *Arabidopsis* and choy sum (Chung et al., 2021). Thus, some observed changes in spectra between healthy and defective potatoes may be due to immune responses of the tubers, either to physical or pathogenic stresses.

6.1.2 Alternative approaches to screening potatoes for defects

Spectroscopy-based approaches clearly afford opportunities for non-destructive screening of tubers, as evidenced by both the research conducted in this thesis and other work reported in the literature (López et al., 2013; Ren et al., 2025; Sanchez et al., 2020). However, mapping of the primary PC across the surface of tubers revealed that there is variation and localisation of spectral signals on the tuber surface (Figure 4.10). This led to the investigation of whether the differences between spectra spatially distributed across the surface of the same tuber can offer diagnostic insights that single or average spectra cannot. While the peak data of MIR spectra failed to offer detection of spraing, the skewness within spectra of each individual tuber of the primary principal component showed significant difference (Figure 4.13). Significant difference in skewness between healthy and spraing-affected tubers was also observed in NIR spectra (Figure 4.12). Interestingly, majority voting of MIR spectra failed to determine whether a tuber was healthy or affected by spraing, thus the difference between spectra within a sample may offer insights that individual or averaged spectra cannot. These data suggest there is locality to stress signals of spraing rather than being homogeneously or globally distributed across the tuber surface. Multiple spectra per test sample may be required in industrial screening to capture localised signals.

Skewness has been used as a measure in spectroscopy in previous work by Sanchez et al. (2017) assessing the skewness of peak emission intensity of fluorescence spectra for nanoparticle analysis. The use and application of skewness by Sanchez et al. (2017) is very distinct from that used in this thesis, but further research could perhaps illuminate further applications of skewness to spectroscopy. Skewness based approaches to spectroscopic vegetable assessment may have an advantage over machine learning and classification approaches. While classifier models need to be trained with large data sets for every defect of interest, and perhaps trained with multiple varieties to account for inter-variety variation in spectra, there may be a universality to skewness. If changes in skewness are shared across multiple defects, fewer models would be needed for defect detection potentially offering a universal indication of defectiveness. Although there are still benefits to defect specific models such as careful management of high-risk pathogenic defects.

Another spectroscopy method that entails multiple sample locations is spatially resolved spectroscopy (SRS) (Si et al., 2022), which differs from traditional methods by using optical fibres to sample scattered light at different positions relative to a singular light source. Photons take a banana-shaped path through the sample (Si et al., 2022; Xia et al., 2024), thus light that scatters further laterally will have penetrated deeper into the sample, providing a different penetration depth at each of the sampling locations. Progress has been made in recent years in applying spatially resolved spectroscopy to assessment of fruits and vegetables (Huang et al., 2020; Si et al., 2022; Xia et al., 2024). As this sampling method allows for spatially distributed sampling locations it could be compatible with PC skew analysis. However, entangling scattering data with surface variance data may reduce the effectiveness of skew analysis, although this requires experimental investigation.

6.2 Electrical spectroscopy could be an effective supplementary approach for vegetable quality assessment

Electrical spectroscopy offered an effective non-destructive means of detecting blackheart stress in intact potatoes and showed possible detection of simulated wireworm damage (Figure 4.14). While previous work on bioimpedance spectroscopy has explored the relationship between the real and imaginary parts of impedance

(resistance and reactance) (Van Haeverbeke et al., 2023), this research adopted a novel approach investigating the relationship between the real and imaginary parts of the analytic signal generated by the Hilbert transform of the recorded voltaic displacement signal of sweep responses. This revealed differences in the spread of the real components at each discretised imaginary value between healthy and RAC-stressed potatoes (Figure 4.19).

An increase in RMS voltage was found in sweep responses after simulated wireworm damage compared to pre-damage sweep responses from the same tubers (Figure 4.14). Phase was not altered by this treatment, suggesting the change was only in real resistance and not reactances, as reactances alter phase (Kuphaldt & Haughery, 2020). While the phase being measured here is in the Hilbert domain, it is expected that a change in real phase would be reflected by a change in phase in the Hilbert domain. Interestingly the RMS voltage increased after treatment, where a drop in RMS voltage would be expected for a loss in water content (Wang et al., 2001). This increase could perhaps be due to a decrease in resistance caused by the breaking of cell walls during mechanical damage, consistent with visible damage surrounding the wounds from wireworm simulation in Figure 6.1. However, damage to cell walls would alter the capacitance of the sample according to the Hayden model (Figure 1.1 a), which is not observed in the data. The underlying mechanism of this observed change in RMS voltage is unclear; further research is required to determine the basis of the changes observed in this study.

Figure 6.1 Bisected potato 3 days after simulated wireworm damage.
Each segment of the scalebar represents 1 cm.

Electrical behaviour of biological samples is largely governed by microstructure, as reflected in equivalent circuits such as the Hayden model and Cole–Cole model (Zhang et al., 1995), as well as network-equivalent circuits of plant tissue such as the Cauer and Foster networks (Kapoulea et al., 2020), whereas optical spectral characteristics are predominantly governed by chemical composition. Hence these two approaches could be used together in a complementary manner, providing different methods of assessing vegetable quality and the presence of defects, perhaps more accurately than either method alone.

Potatoes were stored in a 5°C and 2,000 ppm CO_2 environment in Chapter 3. PP and RMS voltages were recorded from passing sine and square oscillations through intact potatoes. An ensemble of linear discriminant classifiers trained on this electrical data were able to classify between pre- and post-storage potatoes with 82.6% accuracy (Figure 3.6). These measurements, however, were less effective at predicting storage time as a continuous duration via regression models. An LLS regression trained on the first differential of these electrical data provided predictions with R^2=0.47 and an RMSE of 46.3%. Greater performance in coarse categorical predictions suggest that there may be large biological variance between samples in how storage affects their electrical properties. There is large biological variance in post-harvest behaviour of produce including rate of senescence and responses to storage conditions (Hertog et al., 2007). As senescence is linked to water content (Ahlawat & Liu, 2021), soluble substance content (Zhu et al., 2020) and cell integrity (Ahlawat & Liu, 2021), which all impact the electrical properties of plant tissue, variance in the rate of senescence may modulate how storage time affects electrical properties. Whether changes in electrical properties are related more closely to meaningful impacts of storage than storage time itself will require further experimentation.

6.3 [REDACTED] treatment greatly extended the shelf life of intact tomatoes

Post-harvest losses are a major challenge to fresh tomato supply chains in both economically developed regions (Domínguez et al., 2025; Yadav et al., 2022) and in sub-Saharan Africa (Adeoye et al., 2009; Arah et al., 2015b; Emana et al., 2017). Cooling systems are used to reduce post-harvest losses in wealthy regions. However, storage

cooling systems are inaccessible in economically developing regions such as Nigeria, where tree shade or improvised cooling approaches are used (Arah et al., 2015b). More than 90% of African tomato farmers have no on-farm storage facilities (Arah et al., 2015b). Modified-atmosphere packaging and controlled-atmosphere storage are utilised further along the supply chain to reduce losses and improve tomato quality (Majidi et al., 2014). Modified-atmosphere packaging, however, requires use of plastic film packaging, contributing to the environmental impacts of plastic waste (Rigamonti et al., 2014). Plastic- and cooling-free approaches to tomato loss reduction or tomato quality support could be a valuable alternative to current approaches to reduce plastic waste and improve accessibility to less economically developed regions.

Tomatoes treated in a [REDACTED] developed fewer defects during subsequent shelf storage and lasted longer before spoiling compared to untreated tomatoes (Figure 5.3). This is a very exciting result and could be applied to extending the shelf life of fresh produce without refrigeration or plastic packaging. There do, however, seem to be applicability limits with this method. The shelf life of grapes was not enhanced, although the treatment may have been too severe for this fruit, and [REDACTED] is a large portion of the short post-harvest life span of fresh grapes. Treating Tenderstem™ broccoli was also attempted as a model for green vegetables, but the [REDACTED] of the treatment wilted the broccoli, making it unsuitable. Further research is therefore required to ascertain the optimal [REDACTED] for differing produce. Regression models trained on NIR spectra recorded from intact tomatoes following treatment failed to predict shelf life, suggesting the changes in tomatoes induced by this treatment did not alter fruit chemistry. This is consistent with the expected mechanism of metabolic and respiratory down-regulation, which may not alter spectra as there have been no published studies on NIR reflectance determination of plant respiration. Slowing of respiration rate, however, is linked to delayed senescence (Zhu et al., 2022).

Fungal rots account for a large amount of tomato spoilage and losses (Wani, 2011). Plugs cut from *Botrytis* R16, a common fungal pathogen of plants, treated with this method grew faster than plugs cut from cultures not treated, suggesting that the shelf-life extension treatment not only affects the produce, but may also affect pathogenic fungi within the produce. These data suggest that the increased shelf life of tomatoes is

likely not due to suppression of fungal pathogen growth but rather to slowed tomato senescence, although senescence increases vulnerability to fungal pathogens (Zhu et al., 2022).

6.4 Sustainability of methods

6.4.1 Spectroscopy

To be economically and environmentally valuable, screening approaches should save more energy and resources than they consume. NIR reflectance spectroscopy employs use of low-power source lighting and thus has low operating power, although it requires a computer to process data. It is difficult to ascertain how much energy would be consumed by the computer as the computational load required is not known. NIR reflectance spectrometers contain a diamond for dispersing wavelengths. These diamonds are lab grown to achieve required purity and optical characteristics, and to avoid many of the environmental impacts of mined diamonds such as habitat destruction. However, due to the energy intensiveness of the manufacturing process it emits large amounts of greenhouses gases. According to Trucost, growing 1 carat of diamond releases 511 kg of greenhouse gases on average (Trucost, 2019). The carbon footprint for potato production varies between 0.17 and 0.23 kg CO_2 eq kg^{-1} (Niu et al., 2023), so production of 1 carat generates the same greenhouses gas emissions as producing 2.5 tonnes of potatoes. In contrast, the production and running of spectroscopic potato screening equipment is likely not a significant environmental hazard.

6.4.2 Electrical data acquisition

Medical adhesive electrodes were used for electrical data collection. While this is practical and effective in the laboratory, such electrodes translate poorly to industry. Adhesive electrodes are slow to affix or remove, and the adhesive gel becomes dirty and less effective after multiple uses, resulting in a short lifespan. Clean metal electrodes may be more suitable for industrial applications, perhaps spring suspended to non-destructively fit produce, like that seen in Rehman et al.'s (2011) setup for mango impedance measurements. Single electrode setups could be more easily integrated into grading systems and remove the challenges and risks of closing electrodes around

tubers at high throughput without inducing damage. With a tuber as the terminator to a line, test signals could be reflected off this terminator to determine electrical properties; however, the variations in potato thickness will alter the time delay, and with a significant difference in properties between electrode and potato, there may be unwanted additional reflections at the tuber–electrode boundary.

6.4.3 Shelf-life extension

While [REDACTED] repurposing for vegetable [REDACTED] treatment to extend shelf life does not necessitate additional production. Additionally, an [REDACTED]is used for the [REDACTED] shelf-life treatment. While [REDACTED] was used to achieve this in Chapter 5, more environmentally friendly methods could be employed. Many of the regions most affected by food insecurity and lack of refrigeration access are equatorial, where [REDACTED]. [REDACTED]. Low-tech low-cost implementation of an [REDACTED] treatment could be applied at this stage, as temperatures rise, by farmers or buyers. Stones or clay acting as thermal batteries (Rempel et al., 2013) or insulation could perhaps be used to maintain adequate temperature at night. All experiments employing the [REDACTED] treatment used 25°C; this temperature was chosen to elevate above room temperature to increase enzymatic activity (Tjoelker et al., 2001) while not being too high as to course denaturing of compounds or heat damage to the tubers, which was noted to occur at 30°C. However, it is possible that this temperature might not be optimal for shelf-life extension, although factors such as produce variety or pre-treatment produce age could also affect the optimal temperature. Further experimentation would be needed to test this.

6.5 Other approaches

The potential of memristivity as a novel paradigm for electrical spectroscopy was also explored. The memristor, first described by Chau in 1971 (Chau, 1971), is the fourth fundamental two-terminal electronic component. Each of the fundamental components can be described as the differential of one electrical quantity with respect to another. Resistance is the differential of voltage with respect to current, capacitance is the differential of charge with respect to voltage, inductance is the differential of flux with respect to current, and memristivity is the differential of flux with respect to charge.

The resistance of a memristor can be altered by an excitation signal, resulting in a pinched-loop hysteresis curve in the I–V plane, allowing the memristor to act as a two-terminal memory component. Pinched loop hysteresis in the I–V plane, characteristic of memristivity, has been found in vegetables (Abdelrahman et al., 2021), including potatoes (Volkov et al., 2015; Volkov et al., 2016). The lobe area of the pinched loop is frequency dependent, approaching a single line as the input frequency tends to infinity. While the presence of memristive behaviour, and memfractive behaviour, a generalisation of two-terminal memory behaviour to include memory reactance and non-integer orders (Beasley et al., 2020), has been noted in vegetables, it is yet to be applied to vegetable quality assessment or vegetable defect detection. Research into the applications of memristive and memfractive measurements in intact produce could provide a novel paradigm of electrical spectroscopy. Although a setup for measuring hysteresis loops in intact potatoes was constructed, inspired by the AD844-based circuits used by Abdelrahman et al. (2021), with the addition of a summing amplifier for combining test and excitation signals, extensive measurements using this system were beyond the scope of the present study.

6.6 Applications of non-destructive defect detection and shelf-life extension

6.6.1 Reduced losses for producers and suppliers

Food losses threaten the livelihoods of farmers (Balana et al., 2022), especially in the face of worsening climate change (Verma & Sudan, 2021). Risk of rejection from suppliers and risk of market price not covering production costs are barriers to harvest, transportation and selling of produce that farmers face (Campbell & Munden-Dixon, 2018; Gillman et al., 2019; Johnson et al., 2019). Lack of non-destructive screening methods at supplier facilities limits the market value of mixed-quality harvests, as healthy and internally defective potatoes cannot be effectively separated. This leads to unnecessary rejection and undervaluation of produce, which negatively affects both suppliers and producers.

6.6.2 Societal impacts of shelf-life extension

Extension of fresh produce shelf life comes with many environmental and economic benefits; reduced waste incurs reduced production while maintaining effective supply. However, there may be additional nutritional and sociopolitical outcomes. A primary method for extending crop and food shelf life, is food processing: potato crisps last longer than potatoes, ketchup longer than tomatoes and canned fruit longer than fresh. However, food processing can negatively impact public health (Lane et al., 2020). Processed foods have reduced micronutritional content; vitamins, minerals, and other nutritionally valuable compounds such as polyphenols and flavonoids are being lost during refinement and processing (Coletro et al., 2023). Nutrient loss during processing should be considered a form of food waste, as nutrition is not making it from farm to fork. In addition to lack of nutritional content, high concentrations of refined sugars, fats and salt are added in food processing, alongside many direct and indirect additives or altered compounds, such as bisphenols and hydrogenated fats, incurring negative health impacts for consumers (Ma et al., 2019; Mozaffarian et al., 2004). Processed foods also contain higher levels of microplastics (Lin et al., 2022). Concern is rising over microplastics and nanoplastics in the human body as their health risks are unravelled (Tang et al., 2024). The NOVA food classification system proposed by Monteiro et al. (2019), subdivides processed food into processed food (PF) and ultra-processed food

(UPF), as well as describing two other categories: unprocessed/minimally processed food, and culinary ingredients. Both PF and UPF have significantly lower nutrient-rich food index (NRF) scores than unprocessed food (UF), with 61% of unprocessed food falling into the upper tertile, and 4% into the lower tertile, whereas 33.3% of PFs are in the upper tertile, and 22.2% in the lower tertile, and 17.5% of UPFs are in the upper tertile and 50.2% in the lower tertile (Gupta et al., 2019). This negative correlation has led critics of the NOVA scheme to suggest it is too close a proxy to NRF, and thus redundant (Drewnowski et al., 2020). UPF consumption is associated with non-communicable disease, all-cause mortality, and adult obesity (Lane et al., 2020). Shelf-life extension of fresh produce may therefore offer public health benefits by supporting consumption of unprocessed foods.

Processing of fresh produce into longer-lasting products facilitates cheaper transport, storage, and shelving, and reduction or elimination of consumer-performed preparation. Ketchup is cheaper than preparing homemade tomato sauce and is ready for immediate consumption; a microwaveable meal is typically cheaper than home cooking an equivalent dish and can be ready in only 5 minutes. These factors make processed food highly affordable and convenient, whereas fresh produce regularly comes with greater time and financial investments. PFs have largely displaced fresh produce across middle-income countries and the economically developed world (Baker & Friel, 2016; Monteiro et al., 2013), especially amongst lower economic classes (Dicken et al., 2023), although in newly developing countries, such as Argentina and regions of sub-Saharan Africa, higher income is associated with higher UPF consumption (Reardon et al., 2021; Zapata et al., 2023), as only the wealthier have access to such imported goods. UF, cost US$1.45/100 kcal in the USA in 2016, in contrast to $0.64/100 kcal for PF and $0.55 for UPF, this discrepancy having worsened over the subsequent years as the cost of UF rose by $0.41/100 kcal (39.4%) between 2004 and 2016, while PF and UPF rose by $0.13/100 kcal (25.5%) and $0.14/100 kcal (36.4%), respectively (Gupta et al., 2019), suggesting food displacement is a growing issue not only in newly industrialised regions, but also post-industrial countries. The units of $/100 kcal may exaggerate implications, however, since PF and UPF have a higher energy density than UF, so energy-based units might not be optimal or reflective

of nutrition and satiety. Consumption of UPF is inversely associated with consumption of fruits and vegetables (Cunha et al., 2018; Zapata et al., 2023), suggesting it may be displacing them from diets. Dietary sublimation from rural poverty dietary patterns to UPF drives the "double burden of malnutrition" (Reardon et al., 2021), where economically developing populations shift from shortage of traditional foods to UPF, from one form of malnutrition to another. Shelf-life extension (SLE) may have limited application in these food systems as access to UPF is not always limited, although SLE may facilitate diversification of UPFs or supplementary nutrition during famine. One factor limiting shelf life is refrigeration, which depends on supply of electricity. Seven hundred and sixty million people lacked access to electricity as of 2019 (Ritchie et al., 2024), which poses a barrier to refrigerator use. For example, in Africa, only 7.75% of the South Sudan population had electricity in 2021 (Ritchie et al., 2024). Alternative approaches to extending produce life may benefit populations lacking electricity and refrigeration, as well as supporting Africa's food supply and export chains. Transport is a critical stage for waste mitigation in the African tomato supply chain (Lin et al., 2022), so reduction in transport losses could yield great improvements in the African export and internal supply of tomatoes.

Improving the shelf life of fresh produce won't affect convenience but may lead to improvements in affordability, transport, storage, and shelving logistics. Improved affordability and access to fresh produce amongst economically disadvantaged communities, especially those living in food deserts, could yield public health and societal benefits beyond the reduction of food waste. There are, however, domains in which fresh produce, even with shelf-life extension, cannot compete against its tinned and hydrogenated competitors: marketing. It's easier to brand a breakfast cereal than a particular producer of wheat. To the consumer, a potato is a potato, but a Walkers is not a McCoy's. Advertising branded PF/UPF is more profitable than fresh produce, with more advertisements being run for high-sugar, high-fat, high-sodium PF/UPF (Fagerberg et al., 2019; Powell et al., 2010). These are issues my research cannot address. More affordable and accessible fresh produce has limitations to the degree it can solve problems of declining fresh produce consumption and consequential public health impacts. However, it may constitute a sufficient freshening of our food systems to

positively improve the lives and diets of those most victim to our food system's current failings.

Modified atmosphere packaging (MAP) is a standard technique for managing the respiration rate of fresh produce to extend shelf life and reduce pre-consumer waste (Mullan & McDowell, 2011). A requirement of MAP is packaging to contain the modified atmosphere, often constituted of plastic, posing an environmental challenge. Acute treatment for metabolic rate reduction would have fewer requirements and constraints on post-treatment packaging, enabling use of more sustainable packaging or elimination of individual unit packaging. Polyvinylidene chloride (PVdC), commonly used in MAP, contains twice the chlorine content as PVC, posing incineration issues (Marsh & Bugusu, 2007).

Refrigeration consumes 60% of the electricity use of supermarkets, open refrigerated shelving playing a major role in this consumption (Suzuki et al., 2011). If shelf-life extension can lower the need for refrigeration of some produce, this could lower the electricity consumption of supermarkets, saving supermarkets money and reducing their environmental impact.

6.6.3 Poverty and world hunger

While reductions in food waste and losses could have substantial benefits for hunger and poverty alleviation in the developing world (Galli et al., 2019; Munesue et al., 2015), technological solutions may have limited applicability in these regions. Technologies such as spectroscopy are highly applicable to industry in wealthy nations, but there may be challenges to implementation in the developing world. Adoption of agricultural technologies such as fertilisers and improved seed and management technologies in sub-Saharan Africa has faced many socioeconomic barriers (Arslan et al., 2022; Suri & Udry et al., 2022). Spectroscopic technologies require access to electricity, computers, expensive optical equipment and access to parts and expertise for maintenance, posing potential barriers to entry that may exclude much of the developing world. Spectroscopy solutions may be applicable to larger sorting and storage facilities in the developing world, however, enabling reduction of losses in the export market supporting

the local economy. Spectroscopy approaches may also be implementable in regions that provide humanitarian aid, allowing for more efficient food aid for those in need.

6.7 Are reductions in food waste and losses sufficient to end food insecurity?

Reductions in food waste and losses are valued as some of the most promising approaches to tackling food insecurity (Kummu et al., 2012; Santeramo & Lamonaca, 2021), but are reductions in waste and loss alone adequate to end world hunger? The SOFI report estimates that 746 million people live with severe food insecurity and that 2 billion people live with at least moderate food insecurity (FAO, 2019), although other estimates are higher than these. with Cooper et al. estimating 820 million for severe food insecurity and 2.5 billion for moderate food insecurity (Cooper et al., 2021). The 175 million tonnes of potato wasted or lost per year represents 2.6 billion days' (90 thousand lifetimes') worth of calories based on a 2000 kcal daily requirement. As around a third of all food is lost or wasted and less than a third of people are classified as hungry there is sufficient pre-losses food to feed all of humanity.

While the caloric and nutritional content of wasted food is more than enough to feed all hungry people, eliminating all food waste and losses is not a realistic goal, and logistical and sociopolitical challenges prevent food from being distributed in a manner that minimises global hunger. Approaches to hunger minimisation must be appropriate to the regions in which they are applied, for example rates of food waste are lower in sub-Saharan Africa and Southeast Asia, where food insecurity is most severe, compared to other regions (FAO, 2011). Food waste and loss reduction should be considered an essential component to tackling world hunger, but not a stand-alone solution.

6.8 Hidden food waste

Research in this thesis has been motivated by the reduction of food waste in the fresh potato supply chain. However, there may be forms of "hidden food waste" obscured by the metrics used to measure it. Food waste is typically measured by mass, and occasionally by monetary value or carbon emissions (Kafa & Jaegler, 2021). Although nutritional requirements of consumers are for individual nutrients rather than total food

mass, this may obfuscate the loss of nutritional content independent of total mass loss. Loss of nutritional content or its bioavailability during the supply chain, via senescence, or by processing and preparation, could be considered a form of food waste. While this is commonly included in definitions of food waste and losses, some proposed definitions take nutritional loss into account (Chaboud & Daviron, 2017).

Over-consumption of food is growing in the economically developed world. While consumption of excess food may play culinary, social or cultural purposes, it consumes agricultural products, increasing the environmental impact of our food systems without improving health or alleviation of world hunger. Thirty-eight percent of the global population are classified as overweight or obese, with higher rates in high-income regions (World Obesity Federation, 2023). While classification of overweight may not reflect overconsumption in all cases, globally the average human consumes 178 excess calories a day (Berners-Lee et al., 2018). The obesity epidemic is also increasing energy usage and carbon footprint in Europe (Koengkan & Fuinhas, 2021). Overconsumption could be considered a form of soft food waste, and its reduction may offer environmental benefits.

Another form of hidden food waste, more substantial than the previous two, is human edible food fed to livestock. Four calories of crop are required to produce one calorie of animal product (Berners-Lee et al., 2018; Pradhan et al., 2013), with both macronutrients and micronutrients lost in this conversion (Berners-Lee et al., 2018). Thirty-five percent of cropland on earth is used to grow crops that are fed to livestock (Foley et al., 2011). Replacement of crop-fed animal products with direct crop consumption would be a more efficient nutrient pathway from crop to human, reducing this form of food loss.

6.9 Conclusions

The research presented in this thesis successfully addressed all four objectives of the programme of research:

Optical and electrical spectroscopy showed great effectiveness for detecting internal potato defects, especially blackheart and spraing, achieving Objective 1 of using non-invasive techniques to detect internal potato defects.

The RAC system reliably induced blackheart development in a controlled and monitorable way, providing an excellent experimental model for testing non-destructive detection methods, achieving Objective 2. Chemical and mechanical void formation, however, proved unsuitable for this research.

Objective 3 was also achieved; simulated wireworm and lab-induced blackheart were both reflected in changes in optical and electrical properties of the treated tubers, showing that non-destructive methods were able to detect model defect analogues.

Objective 4 was achieved by developing an [REDACTED] based on [REDACTED], which showed great success in extending the shelf life of fresh tomatoes, demonstrating that the research conducted in this thesis can be translated into reductions in food waste and losses. Optical and electrical spectroscopy approaches to defect detection are also suited to tackling food losses at the storage and distribution stages of the potato supply chain.

Chapter 7: Appendix

7 Appendix 1: Potato art history manuscript

The manuscript contained in this appendix has been submitted to Plants, People and Planet, and is currently under peer review.

Using art history to explore society's changing connections with agriculture

Edward F. Hill-King, Michael R. Roberts, Martin R. McAinsh

Lancaster Environment Centre, Lancaster University, Lancaster LA1 4YQ, UK

E-mail:

e.hill-king@lancaster.ac.uk

m.r.roberts@lancaster.ac.uk

m.mcainsh@lancaster.ac.uk

Word Count: 5627

Figure Count: 10

Abstract

Societal Impact Statement

Food insecurity is a looming challenge that impacts, and will continue to impact, those least fortunate. Food systems cannot be effectively built without consideration of the communities they support, and the broader sociopolitical context in which they exist. Consumer food choices have a substantial impact on the sustainability of current food systems. Here, we use art as a lens through which to consider our contemporary and historical relationship to one of the world's most crucial crops, the potato, in the context of the perceived current disconnection between consumers and food production.

Summary

Climate change and food insecurity demand us to re-evaluate our perspectives on agriculture and our relationship with food and our planet. In a global food system, where many consumers have access to myriad foods from around the world, the choices of those consumers have significant impacts on sustainability of the food system. Unfortunately, many consumers in the developed world are disconnected from the way their food is produced, and food choices are commonly made without an understanding of their environmental consequences. It is often suggested, therefore, that reconnecting the public with agriculture is one way in which we can move towards a more sustainable food system. Societal attitudes are often reflected in the art of the time, and historical artworks thus offer a unique longitudinal perspective on cultural perceptions of their subjects. We have taken the potato as an example of an important global crop and examined its portrayal in a variety of different art forms across time. We compare artworks ranging from first millennium Moche pottery, where the potato was heralded as sacred, to contemporary audiovisual works, where it is presented as a source of comedy as often as a source of nourishment. Nineteenth-century European art depicts the potato as a representation of authentic rural living, whilst in the 20th century it became an object of propaganda. Thus, art provides a fascinating lens through which to evaluate society's changing connection to its sources of food.

Keywords

Art; Consumer awareness; Food security; Potato; Propaganda

Introduction

Reducing the impacts of anthropogenic climate change on food systems, along with combating food security and world hunger, are core components of the United Nations sustainable development goals (United Nations, 2015; Crippa, 2021). Whilst global dietary shifts can be harnessed to address both world hunger and climate change (Li, 2023; Willett et al, 2019; Hasegawa, 2019; Berners-Lee, 2018), achieving such shifts will require a major realignment of the food system, requiring action across a range of scales (Willett et al., 2019; Hoek et al., 2021; Biesbroek et al., 2023). Within this context, a better understanding of our relationship to food and agriculture can aid in tackling the dual issue of feeding a growing population without exacerbating the environmental impacts of agriculture.

In the developed world, there is a general lack of awareness of food production systems and of the different impacts resulting from the production and consumption of different food types (Hartmann and Siegrist, 2017; van Bussel et al., 2022). Hence, an individual's food choices are often not based on a consideration of the health and nutritional qualities of the products they are consuming, nor on their environmental impacts. Rather, they are made on the basis of affordability, availability and accessibility, alongside the influence of their wider cultural experiences and societal attitudes (Grunert et al., 2014; Leng et al., 2017). Reconnecting consumers with the sources of their food may, therefore, be one way in which the dietary shifts necessary to create a sustainable food system can be achieved.

The potato is the most cultivated non-grain vegetable in the world, with global annual production exceeding 370 million tonnes (Mishra, 2024). It is grown widely and consumed across all income levels, providing diverse perspectives through which to understand relationships between people and their food. Artistic representations of the potato appear as early as circa 200 CE, providing a wide temporal range over which to analyse these relationships. Here, we examine cultural views of the potato, as seen in art, as a lens through which to explore the changing relationships between society and agriculture.

The Sacred Potato in Ancient South America

Ancient civilisations of South America were the first to cultivate and domesticate the potato. Although many of these cultures left no written record, their abundant pottery provides insight into their practices and perceptions. Potatoes are a common theme amongst these pots. Whilst other crops such as maize, yuca and melon also appear (Mottl, 2015), the potato is distinguished by its curious and unique symbolism. Potato pots often feature deformed humans and potato–human hybrids (Figure 1a–c), this theme extending through several centuries.

Mutilation disappears from later pots, with Incan potato pottery typically featuring two potatoes connected by a bridge (Figure 1d). These bottles would often create a whistle sound when poured and be adorned by a creature at the spout.

a: https://tse2.mm.bing.net/th/id/OIP.gPYFa1MU9Lz-E66odKcg3wAAAA?pid=Api

b: https://www.tandfonline.com/cms/asset/0c7964aa-0d6a-4875-8cd4-7afd9959c764/rcab_a_1602449_f0017_c.jpg

c: https://o.quizlet.com/HN7YWuvRi7seaJH2Fl2A8Q.png

d: https://media.britishmuseum.org/media/Repository/Documents/2022_4/27_16/aa613278_9a05_4c56_b460_ae84010b6891/mid_ESA22594_0001.jpg

*FIGURE 1. Potatoes represented in ancient pottery. (a–c) Moche Stirrup bottles. (a) Mutilated human–potato hybrid, 200–600 CE (Museo Larco, Lima, Peru; id: ML007289); (b) Man straddling potato, 200–600 CE (Museo Larco, Lima, Peru; id: ML007284); (c) Human head potato, with potato eyes (Phoebe A. Hearst Museum of Anthropology, University of California; Specimen no. 4-2814); (d) Chimú-Inca Whistling Vessel 1470–1660 (The British Museum Images, id: 01613795909 *license required if published*).*

Many languages use the term for the visual organ “eye”, to name the sprouts on potatoes, such as English (and Spanish “ojos”), as well as many ancient South American languages such as the Quechuan “ñawi” (Trever, 2019). This comparison is expressed in Moche pots, where the eyes of human heads are replaced with the eyes of potatoes (Figure 1c), the tuberous nature of the figure confirmed by a lumpy geometry and further eyes throughout its form. This can be explained by potato eyes bearing resemblance to those of humans; however, there is perhaps further symbolism in the potato eye substitution of another facial feature. Mouths are often replaced by potato eyes as well, the leaflets and protrusions of a sprout bearing a somewhat toothy resemblance giving detail to the likeness. While the mouths of humans are replaced by those of potatoes, curiously those of potatoes are sometimes replaced by those of the jaguar. Redcliffe Salaman, the British biologist instrumental in the development of blight-resistant potatoes, suggested that as toothy sprouted potatoes were ideal for planting, the jaguar’s mouth represented the perfect seed potato (Salaman, 1985). In addition, Salaman posited that failure of a potato crop was believed to be due to “incapacity or weakness of the potato spirit”, and that human sacrifices were intended to “reinforce that spirit” and impart vigour to the potato (Salaman, 1985). The idea of the potato spirit was also ritualised in more pacifistic

manners, with potatoes being dressed as women to represent “Axo-mama”, the mother spirit of the potato.

Stirrup bottles are believed to have been used in funerary rituals (Trever, 2019), and be involved in religious beliefs, but the lack of written records leaves much uncertainty. Although one cannot be certain of the details of the potato’s symbolism in ancient South America, this symbolism is the defining trait that differentiates the cultural treatment of potatoes from other important crops. It is evident that the potato’s role extended beyond the agricultural into the sacred. White potatoes popular around the world today are pale in skin and cortex. However, many wild varieties and species of potato are red and flesh-like on both the inside and exterior. This fleshy appearance may have influenced the development of rituals and belief systems in South America. Human and non-human sacrifice have featured in potato rituals; Pedro Cieza de León details a potato ritual in his chronicles of Peru: “I then saw certain Indians taking up as much of the lamb’s blood as they could hold in their hands, and pouring it quickly amongst the potatoes in the bags” (Cieza de León, Markham). Bandelier accounts late-surviving elements of potato crop-enhancing rituals he witnessed in Titicaca and Koati in 1910. Bandelier reports chuño, a traditional freeze-dried potato food, being dipped in pools of blood and consumed by women following a homicide (Bandelier, p. 115). These practices demonstrate the connection between the potato and blood, perhaps linked to ideas of spirit.

Quechuan nobleman, Felipe Guamán Poma de Ayala, produced many artworks of South American life. Having been born two years after the Spanish conquest, his artworks capture the latter years of traditional South American life, although some artworks may be depicting historical scenes. The cultural crossroads at which Poma’s works lie is emphasised by a combination of South American and European art styles, and text in a combination of Spanish and Quechuan. Poma depicts the harvesting of potatoes by Incas using a digging tool called a “tacalla” (Figure 2). The men, discernible by their headdress, dig, while the women are seen gathering or planting potatoes. Poma’s drawings portray a sense of community, with beverages being brought to the diggers, and many differing roles fulfilled. These drawings evidence that the potato, and its cultivation, were a key part of South American culture surviving past the Spanish conquest.

https://www.researchgate.net/publication/373258958/figure/fig2/AS:11431281183003024@1692662444173/Figura-2-Meses-de-agosto-y-septiembre-Guaman-Poma-de-Ayala-1615-250-252-y-252.png

https://cdn.britannica.com/52/123952-050-B874EC13/men-women-Inca-cornfield-El-primer-nueva.jpg

https://www.researchgate.net/profile/Carlos-Bartesaghi-Koc/publication/215584431/figure/fig1/AS:305950037692423@1449955581398/An-engraving-made-by-the-Peruvian-chronicler-Guaman-Poma-de-Ayala-1556-1644-depicting.png

FIGURE 2. Drawings of potato farming by Felipe Guamán Poma de Ayala, 16th Century.

Botanical Curiosity in 16th–17th Century Europe

When first introduced to Europe following the Spanish invasion of South America, the potato was solely an artefact of botanical curiosity; its culinary potential was not initially recognised in Europe. Two tubers and a fruit were brought to Carolus Clusius, the former director of the Holy Roman Emperor's Garden, sent by Phillipe De Sivry (Wilson, 1993). A year later in 1589, these specimens were paired with a watercolour featuring the aerial parts of the plant (Figure 3a). The plant is portrayed as a botanical specimen, with little inclination towards agriculture, and free of the symbolism of the land from which it was taken. The work is produced for explicit communication of the plant's morphology; although the artist's enthusiasm for botanical beauty is evident, there is no abstract commentary in the piece. The arrangement is unidealised, suggesting a faithful reproduction of a sample. Clusius later authored the *Rariorum Plantarum Historia* in 1601, detailing the potato under the synonym *"Papas peruanorum",* with an accompanying illustration (Figure 3b). By this time, some curiosity regarding the culinary value of the potato was developing in Europe. Clusius describes tasting the potato raw, as rough and bitter, but tender as a chestnut once roasted (Clusius, 1601). European potato cooking practices had not yet developed, exemplified by Clusius first tasting the tubers raw.

a: https://upload.wikimedia.org/wikipedia/commons/thumb/f/f9/Aardappelplant%2C_anoniem%2C_Museum_Plantin-Moretus_%28Antwerpen%29.jpg/960px-Aardappelplant%2C_anoniem%2C_Museum_Plantin-Moretus_%28Antwerpen%29.jpg?20181005081817

b: https://www.researchgate.net/profile/Marie-Christine-Daunay/publication/237536956/figure/fig18/AS:298989531484163@1448296067397/Potato-from-Clusius-Rariorum-plantarum-historia-LIIII-plxxix-1601.png

c: https://www.caburdenraremaps.com/wp-content/uploads/2025/03/D3272.jpg

FIGURE 3. Early European botanical illustrations of the potato plant. (a) Watercolour of potato plant delivered to Phillipe De Sivry, 1589. (b) Drawing of aerial potato and root system, Rariorum Plantarum Historia, 1601. (c) Illustration of potato plant with thyme and lemon thyme, Hortus Eystettensis, 1613.

Hortus Eystettensis, a 1613 florilegium by Basilius Besler, detailed the plants in the first botanical garden in Germany, at the palace of the Prince-Bishop of Eichstätt (Besler, 1613). The potato appears in this florilegium, evidencing it to have featured in the botanical garden and thus being of botanical interest. Accompanying a botanical description is a vibrant illustration of a potato plant, paired with thyme and lemon thyme. In contrast to the watercolour received by Clusius (Figure 3a), the illustration in *Hortus Eystettensis* shows a flourishing plant, depicted in a grand manner. Tuber morphology reveals the subject in *Hortus Eystettensis* to be of a distinct cultivar or species to the other works in Figure 3, suggesting multiple germlines to be present in Europe by this time.

From Curio to Cuisine

Plants of the nightshade family, to which the potato belongs, hold a reputation of malice, many being poisonous and bearing menacing names like “deadly nightshade”. This created a stigma around the potato during its initial spread across Europe. It was believed that the compound atropine, found in many nightshades, enabled witches to concoct ointments that granted the power to fly. This association with witchcraft added to potato stigma (Graves, 2001).

Amongst the population of Elizabethan England, the sweet potato (*Ipomoea batatas*) was considered an aphrodisiac, with lesser attention towards culinary use. In a series of pamphlets telling the tales of thieves, published in 1592 as “*The Complete Cony-Catching”*, Robert Greene recalls a debate between a foist and a traffic on “whether a whore or a thief is more prejudicial”. The foist, arguing for the economic benefits of “whores”, posits that without whores “the apothecaries would have surfling water and potato-roots lie dead on their hands” (Greene, 1592), demonstrating the erotic association of the sweet potato. Thersites, in *Troilus and Cressida*, cries “How the devil luxury, with his fat rump and potato-finger, tickles these together! Fry lechery, fry!” (Shakespeare, Troilus and Cressida, Act V, Scene II). Referring to luxury as a devil, the lovers’ activities are implied as sinful indulgence, alluding to the elicit associations of the sweet potato. Shakespeare authored *Troilus and Cressida* in 1602, prior to the popularisation of the white potato in England, but the white potato inherited the sweet potato’s reputation upon introduction to Britain.

Elizabethan England was not the only culture to ascribe a sexual element to potatoes. Twin potatoes, where one tuber merges into another, are considered fertility symbols in South American folklore, surviving to the Spanish invasion and the modern day. However, the same symbolism is also tied to twin maize. The reputation that preceded the potato garnered great resistance to its popularisation; Scottish clergymen banned the potato as it did not feature in the Bible (Singh, 2014). The 'Society for the Prevention of an Unwholesome Diet' campaigned against the potato in Britain during the 17th century, citing lust amongst the many ailments they believed the potato to cause (Singh, 2014), and the belief that they caused leprosy led to the banning of potatoes in France.

Frederick the Great of Prussia was instrumental in the popularisation and destigmatisation of the potato in Europe. Fearing potential famine, he performed publicity stunts promoting the potato and implored his citizens to cultivate and consume it. Prussia fought in the Seven Years' War, where Antione-Augustine Parmentier served as a medic for the opposing French military. Becoming a prisoner of war to the Prussians he developed a passion for potatoes. On return to France, Parmentier promoted the potato and strived for its legalisation. In fashion with his once captor, Parmentier performed a series of stunts promoting the potato in France. Members of French and global powers were invited to a potato banquet, where both French royalty and George Washington enjoyed various forms of potato dishes.

The Paris metro station bearing Parmentier's namesake holds a replica statue of Parmentier presenting a potato to a peasant farmer (Figure 4a). Parmentier is presented in this work almost messianically, elevated above the peasant with an erect posture contrasting with the peasant being slightly hunched in gratitude. Being a hero of the potato meant being a hero of one's nation. Similar in composition and theme to the Parmentier Station statue, "The King Everywhere" by Robert Muller (Figure 4b) depicts Frederick the Great visiting a potato harvest. Frederick has one glove removed, as was etiquette when meeting people, to prepare to shake their hands (Walton, 2014). Although the potato farmers are portrayed as poor, they're portrayed as people worthy of the King's respect. This work depicts all ages, amongst both the farmers and the nobles, creating the impression of inclusion and unity in the striving to feed Prussia.

Both Frederick the Great and Parmentier were celebrated in artworks long after their deaths. "The King Everywhere", painted in 1886, over a century after Frederick's death, may not reflect perspectives contemporary to Frederick, perhaps with revelry for an idealised past.

a: https://fabricofparis.com/assets/images/parmentier-statue.jpg

b: https://pure-potential.co.uk/wp-content/uploads/2023/03/Frederick-2-Frederick-the-Great-Potatoes.jpg

FIGURE 4. Promoting the potato as a food crop in Europe. (a) Statue in Parmentier Station, Paris Metro (Clicsouris [CC BY-SA 3.0] via Wikimedia Commons. (b) Robert Muller, The King Everywhere (Frederick the Great of Prussia examines the potato harvest), 1886, German Historical Museum, Berlin, Germany. Wikimedia Commons (public domain).

The Common Vegetable of Europe

The first edition of *Encyclopaedia Britannica* details how to cultivate potatoes, describing them as "one of the most useful roots" cultivated in Britain (Encyclopaedia Britannica Volume 1, 1771, p. 66), illustrating that the potato had become well adopted as a food crop in Britain by the late 18th century. *Encyclopaedia Britannica* First Edition mentions both white and red potatoes, and while it is unclear whether "red" refers to sweet potatoes or a red variety of *Solanum tuberosum*, 'white' confirms that *S. tuberosum* is being discussed (*Encyclopaedia Britannica* Volume 1, 1771, p. 66).

By the Victorian Era, potatoes had gained great popularity in Britain, as well as in North America and continental Europe. This enthusiasm for the potato culminated in international potato shows in London, the first held in 1874 at the Alexandra Palace (Wilson, 1993). Fuelled by the mass appeal of the potato, and fear of repeating blight and other crop failures, both amateur and professional breeders cultivated an enormous variety of germ lines. Along with exhibiting exciting varieties, dishes made from these potatoes were in great abundance, with exhibits featuring over 1500 dishes. These shows, however, did not last, disappearing in the mid-1880s (Wilson, 1993).

The potato continued to feature in artworks from this period. The realist movement of the 19th century rejected romanticism and the snobbery of salons. The core of the realist movement was to paint the real world and ordinary people. Gustave Corbet, considered the father of realism, is quoted as saying "Show me an angel and I'll paint one" (Van Gogh, 1885; translated, Pomerans, 1996). Their subjects included humble farmers and peasants, perceiving them as more authentic than the nobles and angels of prior romantic canvasses. Millet's 1850s work "The Angelus" (Figure 5a), originally entitled "Prayer for the Potato Crop", depicts two farmers in earthy tones, connecting them to the earth they farmed. There is a contrasting light in the background; whether this is hope or the distance of hope is unclear, such uncertainty reflecting the uncertainty of, and their dependence upon, the harvest.

In letters to this brother Theo, Vincent Van Gogh writes in 1885 of his soon-to-be-completed work, “The Potato Eaters”: “… eating their potatoes by the light of their little lamp, [they] have tilled the earth themselves with these hands they are putting in the dish, and so it speaks of manual labour and — that they have thus honestly earned their food” (Van Gogh, 1885). Van Gogh saw the lives of peasants as containing a realness lacking in his well-off upbringing. He elaborates that “A peasant girl is more beautiful than a lady” (Van Gogh, 1885) and that her genuineness were to be lost if she donned a lady’s dress. Romanticising the foibles of the peasants he wishes to capture in this piece, Van Gogh declares it would be wrong “to give a peasant painting a certain conventional smoothness” (Van Gogh, 1885). The characterful imperfections of this painting reflect the sentiments articulated in Van Gogh’s letters, tying ideas of authenticity and peasantry to the potato (Figure 5b).

The viewpoint of “The Potato Eaters” is of someone not seated at the table, as if to witness these potato eaters from an outsider’s perspective. Van Gogh, born to a wealthy family and well educated, was certainly an outsider to the potato eaters in this respect.

“The Potato Eaters” was not Van Gogh’s only piece to depict the potato. He also produced three still lifes, one in the later iconic style he is today famous for (Figure 5c–e). Dutch still lifes of the period typically featured diverse arrays of luxury and imported goods, whereas these three of Van Gogh’s feature only potatoes and their vessels. There is a sense of Van Gogh’s rejection of high culture, and idealisation of peasanty, but also a sense of elevating the potato to the status of the goods frequently included in still lifes of the era.

a: https://uploads7.wikiart.org/images/jean-francois-millet/the-angelus-1859.jpg

b: https://uploads1.wikiart.org/images/vincent-van-gogh/the-potato-eaters-1885.jpg!Large.jpg

c: https://cdn.gallerix.asia/sr/_EX/280359500/5658.jpg

d: https://uploads5.wikiart.org/images/vincent-van-gogh/basket-of-potatoes-1885(1).jpg!Large.jpg

e: https://uploads1.wikiart.org/images/vincent-van-gogh/still-life-potatoes-in-a-yellow-dish-1888.jpg

FIGURE 5. The potato in 19th-century European art. (a) The Angelus, Jean-François Millet, 1857–59, Musee d’Orsay, Paris, France. (b) The Potato Eaters, Vincent Van Gogh, 1885. (c, d, e) Potato Still Lifes, Vincent Van Gogh. (f) Saison d’Octobre, oil on canvas, Jules Bastien-Lepage, 1878.

Jules Bastien-Lepage, while not strictly a realist, employed a strikingly well-rendered naturalist style. Naturalism is distinguished from realism; where realism is an art movement, naturalism is a visual style, representing subjects in a natural and realistic manner, often employing perspective techniques. Bastien-Lepage's 1878 oil on canvas "Saison d'Octobre" (October), also known by "Récolte des Pommes de Terre" (Picking Potatoes; Figure 5f), depicts French peasants gathering the potato harvest. The apron adorning the lady in the foreground blends almost seamlessly into the sack into which she pours her potatoes, giving a strong sense of connection between gatherer and the potato. The potato is portrayed as lowly, but not as beneath the artist; there is a dignity and beauty to the humility of the potato and farmers. With the farm spanning the entire canvas, there is a sense that not only is potato farming the whole painting, but perhaps the subjects' whole lives. The potato's representation in realist and related works demonstrate a strong association between the potato and peasant farmers. The artists portray such farmers positively, although this may not have reflected broader societal attitudes.

Famine in Ireland

The print in Figure 6a, produced in 1847 for the *Illustrated London News*, captures the abject poverty and suffering experienced by the victims of famine in Ireland (Illustrated London News, 1847). The cottier class of 19th-century Ireland were wholly dependent upon the potato. Unable to buy land, they rented off landlords, typically an intermediate landlord subletting small plots termed "conacres". Conacres, often 1 acre, were just big enough to feed and house one family and pay their rent. After eating and rent, there would be little to nothing left. Some families would fall short and beg to feed their children; surviving on such a slim margin left an entire class of Irish people vulnerable. The 1841 census classified the lowest class in terms of housing as mud huts of a single room. Twenty-four percent of the population were ascribed to this class (Census, 1841).

a: https://upload.wikimedia.org/wikipedia/commons/9/97/Skibbereen_by_James_Mahony%2C_1847.JPG

b: https://www.irishcentral.com/uploads/article/127016/GettyImages-996291592_famine_memorial_dublin___getty.jpg?t=1762509848

c: https://morningstaronline.co.uk/sites/default/files/styles/desktop/public/ART%20IN%20THE%20OPEN%20-%20IRISH%20FAMINE%20SEPT%20webpic.jpg.webp?itok=I5Mf5u9k

FIGURE 6. The Irish Famine. (a) Print of victims of the Irish famine gathering potatoes (Illustrated London News, 20th Feb 1847) (b, c) Irish Famine Memorial Statues, Dublin, Sculpted by Rowan Gillespie.

The potato, drawing a thin line between poverty and starvation, was becoming as vulnerable as those who depended on it. Throughout Ireland there had been numerous crop failures in the decades prior to the great famine, in 1816–1818, 1822 and 1831 (Lidwell-Durnin, 2020). The precariousness of this monocrop food system was evident, but cottiers had little in the way of alternatives, without the land or resources for diversity of investment. When the great famine came in 1845–1852, the line between poverty and starvation was erased. Starvation and resulting disease claimed one million lives (UK Parliament, 2024). With an Irish population of 8.175m in 1841 and 6.552m in 1851, the population fell by 20% in a decade (Grada, 1979). This rapid depopulation was partly due to mass emigration as people fled famine, but approximately one in seven of the Irish population was killed. A workhouse scheme was set up to provide shelter and employment to once-cottiers. However, harsh conditions and famine-weakened immune systems enabled a plethora of infectious diseases to lay waste to densely populated workhouses; in April 1847, around 7% of workhouse inmates died in a single week (Edwards, 1994, p. 251). Bronze figures cast by Irish sculptor Rowan Gillespie (Figure 6b,c), graphically portray the hunger and displacement faced by victims of the Irish famine.

Wartime Potato Propaganda

During the Second World War, food systems saw radical change. Imports were limited, supplies shipped to the front lines, and rationing placed on previously abundant products. These shifts occurred at both industrial and domestic levels. Governmental campaigns were launched in both Britian and the United States to endorse the domestic consumption of potatoes as a replacement for bread, to avoid wheat imports and to allow wheat to be supplied to soldiers. British “Field Marshal Potato Pete”, an anthropomorphic potato, touted the benefits to body and country of eating potatoes (Figure 7a). Cooking potatoes was portrayed as just as essential to battle as firing arms, and the language of military conflict was used in this campaign. Militaristic slogans such as “Attack with me” (Figure 7b) are juxtaposed by culinary claims of “I make good soup” (Figure 7c).

Both British and US wartime propaganda urged civilians to eat at least one pound of potatoes per day. A United States Department of Agriculture poster asks the rhetorical “Have you eaten your pound of potatoes today?” (Figure 7d). The Ministry of Food in Britian launched “the potato

plan" campaign, stating "Doctors say 'eat at least 1 lb. of potatoes every day'" (Figure 7e). These programmes demonstrate the importance the potato held during World War II.

Amongst the schemes of Potato Pete, a recipe book was published, focusing on making the most of rations when combined with potatoes (Figure 7f). Although a dish seldom portrays a statement or a social commentary beyond aesthetics or status signals, dishes can inform us of the chef's or consumer's relationship with food and produce. Militaristic language continues into the cookery book, the contents page reading "the more you serve me the better I can serve you", connecting the domestic and military aspects of wartime. To eat a potato was to support the troops on the frontline; it was a patriotic and proper thing to do.

Potato Pete material was not limited to visual media, but also included a song with the lyrics: "Potatoes new, potatoes old, Potato (in a salad) cold, Potatoes baked or mashed or fried, Potatoes whole, potato pied, Enjoy them all, including chips, Remembering spuds don't come in ships!" These lyrics overtly present the motive and mode of the programme, encouraging potato consumption as an alternative to imports.

Patriotism of potato consumption is a theme also seen in US material. "BE PATRIOTIC!" proclaims the poster in Figure 7g, with a saluting potato-headed waiter carrying a large plate of steaming potatoes. The dual use of the term "serve" for both culinary and military service seen in The Potato Pete Cookbook appears also on the US poster in Figure 7g; "at your service" says the potato man with a proud smile.

a: https://encrypted-tbn0.gstatic.com/images?q=tbn:ANd9GcQ8x_cynnNbO5uqXqpmbqT1hV4UBpRINE9ZOA&s

b: https://www.mediastorehouse.com/p/497/wwii-poster-c1943-attack-says-potato-pete-13642768.jpg.webp

c: https://media.iwm.org.uk/ciim5/176/503/large_000000.jpg

d: https://www.nal.usda.gov/exhibits/speccoll/files/original/5c92bcee837eda7d85d4450adc16aa5b.jpg

e: https://history-commons.net/artifacts/2615447/the-potato-plan/3638057/

f: https://digital.nls.uk/ministry-of-food/archive/247739218?mode=fullsize page 2 and 3

g: https://th-thumbnailer.cdn-si-edu.com/6Ugxh46EzudJw_r8OM8F0EgM5Oc=/1000x750/filters:no_upscale()/https://tf-cmsv2-smithsonianmag-media.s3.amazonaws.com/filer/Here-Sir-Potato-war-food-poster-3.jpg

FIGURE 7. World War II potato propaganda. (a, b, c) Posters based on the "Potato Pete" character. (d) USDA potato propaganda. (e) British Potato Plan Poster. (f) Contents page of Potato Pete Recipe Book, UK Ministry of Food. (g) United States potato propaganda poster.

The War Against the Potato Beetle

In the wake of World War II, many nations were struggling to rebuild. The potato had served Eastern Europe well in the prior years, holding an important agricultural position in countries like Germany and Russia. Although the war had ended, a new threat stifled their recovery; an outbreak of Colorado potato beetles began decimating potato crops. The beetles, native to the United States, were assumed to be an instrument of war. The United States was accused of dispersing them by plane, although there is insufficient evidence to either substantiate or refute these allegations (Santini et al., 2023). Nevertheless, potato beetles with star-spangled wing cases appeared on German posters, in a similar fashion to the adversarial troops vilified on wartime posters (Figure 8). In the same way that a US wartime poster compared Nazis to malaria-ridden mosquitos (Figure 8a), German propaganda now framed the American insect in a similar manner (Figure 8). To threaten the potato was to threaten the nation. Pressures of crippled food systems and international tensions, brought on by the potato beetle, almost incurred further military conflict. Although not an abject war, the war against the potato beetle adopted the aesthetics and the culture of the recent conflict. Use of martial language like "zwalczajcie", meaning "fight", evidences the militarised framing of the potato beetle. A sense of national pride is present in much of this potato beetle propaganda, all ages within Germany uniting to fight off a threat to their country.

FIGURE 8. German post-war potato beetle posters. (a) poster indicating US origin of Colorado potato beetle. (b) US propaganda poster likening enemy troops to malaria-carrying mosquitoes. (c, d) Posters encouraging citizens to control potato beetle.

The Potato Kingdom of Asia

Decades later, the potato was again used as a crop that could protect a nation from food insecurity created by external factors, this time in North Korea. The collapse of the Soviet Union

in 1991 brought with it the collapse of North Korean agriculture. Highly dependent on Soviet imports of fertiliser and water pumps, and with an already wounded economy, North Korea entered famine. The Arduous March of 1994–1998 claimed between 240,000 and 420,000 lives (Spoorenberg, 2012). Without food, and without hope, the potato was offered. Kim Il-Sung brought promise of the "Potato Kingdom of Asia", a nation built from ashes and loam, that would blossom on the potato. To promise a future of potatoes was to promise a future of prosperity. Kim Il-Sung launched the "gamja hyeongmyeong" meaning "potato revolution", to save both his country and his power. Artworks featuring the leader and loyal subjects with bountiful potato harvests were commissioned.

North Korean propaganda can only be understood within the context of the national ideology of "Juche". Juche derives from Marxist-Leninism, although is differentiated by the incorporation of extreme nationalism and pseudoreligious leader worship. The ideals of Juche are captured in the "Ten Principles for the Establishment of a Monolithic Ideological System", first listed in a speech by eternal leader Kim Il-Sung to the Supreme People's Assembly in 1967 and became official in 1974 (Lim, 2015). The degree to which leader worship is emphasised is made clear by every one of the 10 principles, including the leader's name. The leader is an embodiment of the state, and such artworks featuring leaders with potatoes evidence a relationship between state and potato.

North Korean paintings share a theme with prior works from other cultures, that of a leader and peasant potato farmers (Figure 9a). This motif is seen with Frederick the Great and Parmentier (Figure 4). Whilst Parmentier was not a head of state, he was a leader in French agriculture and socially higher than peasant farmers. These works invoke the idea of the good king, a leader providing for their people, the potato a symbol of both peasantry but also prosperity.

Amongst North Korean propaganda, the potato became a symbol of prosperity and sustenance. "The Long-Awaited Meeting in Taehongdan", painted by Kim Song Min in 2009 (Figure 9a), depicts Kim Il-Sung sharing guidance and potatoes with farmers by a campfire (Lea-Henry). Kim Il-Sung is portrayed as presenting the potatoes to the very farmers who grew them, suggesting that the prosperity that enabled them to farm was a gift from their leader, potatoes representing all their leader has allegedly done for them.

Taehongdan County has been set as a model for potato farming by Kim Jong-il (Kim, 2017). The print by Hwang In Je: "The Potato Flower Fragrance of Taehongdan County" (Figure 9b), uses a simple and striking colour palette invoking unity and patriotism, the white shirts and green khakis of the soldiers matching the blooms and green of the potato fields. As they march

through the potatoes, a symbol of pride and prosperity, they are immersed within the state and its portrayed glory. Red flags are carried by the soldiers. According to Kim Il-Sung, "The red colour of the flag symbolises the anti-Japanese fervour, the red blood shed by the Korean patriots and the invincible might of our people firmly united to support the Republic" (Tertitskiy, 2014). The military is a major part of North Korean patriotism and ideology, with the "Songun" policy putting great emphasis on the country's military. This work further evidences the potato's role in North Korean Nationalism at the close of the 20th century.

a: https://preview.redd.it/my-other-post-of-kim-jong-il-giving-potatoes-a-while-ago-v0-69fse539padb1.jpg?width=640&crop=smart&auto=webp&s=001b7311b55626ec34e4cf6c9d9a0a8c570f2631

b: https://www.northcountrypublicradio.org/arts/brushnk/gallery/nk03.jpg

FIGURE 9. North Korean propaganda – The Potato Kingdom of Asia. (a) The Long-Awaited Meeting in Taehongdan, Song Ming, 2009. (b) The Potato Flower Fragrance of Taehongdan County, Hwang In Je, 1999.

Accompanying visual works, a musical campaign starring a patriotic ode to the potato entitled "감자자랑" or "Potato Pride" was launched. The song tells the tale of how people who once lived in struggle have been brought to "paradise on earth" by the fuel of the potato and the guidance of their leader. The nation having recently faced famine, boasting longevity of potato eaters is a running theme, with lyrics translating to: "The old man from the long-lived family" … "In our village an old man on the day of potato distribution" … "The old man who ate a lot and lived to a ripe age" and "Engage in much potato agriculture and live to an old age". The idea of potatoes feeding people into old age speaks both of potatoes as a way to survival and nationalistic pride of prosperity.

From Hero to Veteran

The anthropomorphic Potato Pete character from World War II was soon supplanted by another tuber: Mr. Potato Head. Mr. Potato Head is a children's toy from Hasbro™ (Figure 10a), where plastic facial features and accessories are pinned to a potato to produce an amusing character. While Potato Pete's message was one of scarcity and victory, Mr. Potato Head presents the potato as humorous, common, and perhaps disposable. Although potatoes largely escaped rationing and their liberal consumption was promoted during World War II, rationing produced a

strong culture against food waste. The idea of adopting a non-food use for the potato, which might previously have been considered wasteful, and turning it into a popular toy, marks a post-war shift in people's relationship with the potato in the West.

Not only was Mr. Potato Head an art kit but also made art history by being the first toy to receive a television advert. The advert presents the potato not as a potato *per se*, but as what it can become. With a variety of options of facial features and accessories, the Mr. Potato Head kits capture the versatility of the potato, and how this versatility captures the values and expression of those who utilise the potato. In 1964, Mr. Potato Head turned plastic, chiefly over concerns of child safety with sharp parts required for puncturing vegetables, and vegetable toys rotting in children's bedrooms. Although no longer an actual potato, preserving the appearance and namesake of the potato, our perceptions of the toy still reflected those of the potato. Mr. Potato Head saw a revival in popularity when he arrived on the silver screen in "Toy Story" (Toy Story, 1995).

https://www.antiquetrader.com/uploads/MTc5NjQ3NDQ4NDg5MTQyMDkw/original-mr-p.jpg?format=auto&optimize=high&width=1920

https://tse3.mm.bing.net/th/id/OIP.ot3UVQIrbTTQjv1FOlT4wHaR7?cb=ucfimg2&pid=Api&ucfimg=1

FIGURE 10. Anthropomorphic potato representations. (a) Post-war anthropomorphic potato, Mr. Potato Head. (b) Marilyn Monroe potato sack dress.

The potato's shift from an instrument of war to one of peace, reflected by the introduction of Mr. Potato Head, is furthered by Marilyn Monroe's potato sack dress (Figure 10b). The potato sack is used as a symbol of humility and something typically devoid of glamour. The garment is a statement that if Monroe can make a potato sack appear fashionable, she can do so for anything.

Conclusions

Examining the portrayal of the potato in art produced by different societies over time provides a fascinating insight into how this important vegetable crop has been viewed over the past two millennia. Personification of a potato spirit is a cross-cultural trend, manifest either by linking its significance to existing people or via origination of anthropomorphic characters. Europe and North Korea linked the potato to peasants and the "Eternal" Leader, respectively, whereas

ancient South America and wartime Britian created pottery and Potato Pete to represent the spirit of the potato. Despite aesthetic similarities between Mr. Potato Head and the potato-human hybrids of Moche pots, they reflect distinct relationships with the potato. The synthesis of human and potato in Moche vessels is born from a spiritual connection and reliance upon the crop, whereas Mr. Potato Head marks relief from reliance upon the potato, enabling diversification of its utility beyond sustenance. This difference represents two disparate positions within a landscape of perspectives through which the potato has been represented in art throughout history. The early deification of the potato by the Incas and other South American civilisations reflects the central importance of agriculture to the existence of these societies. In later South American art, we see the emergence of an attitude of respect and appreciation for the potato and those who grow it, as reflected in the works of Poma de Ayala, although some of the ancient rituals based on the potato were still practised at this time. A similar attitude is also seen in the later European works of Millet and van Gogh. In times of need, the image of the potato as a robust, reliable source of sustenance has been exploited by governments to unite nations, in the West, during and after World War II, and later in the East, in North Korea. In the modern Western world, however, the potato is now often taken for granted as a rather basic, common food item and is held in low esteem.

The reverence and respect with which the potato was viewed in earlier cultures is associated with a much closer relationship between society and the production of food than exists in many of today's industrialised societies. Here, individuals often have little connection with, or understanding of, the sources of their food (van Bussel et al., 2022). There is little awareness or information on land use, water use, pesticides, pre-consumer waste, or other environmental and sociological factors. This is reflected in the wider issue of a general lack of appreciation of the importance of plants in the natural world, recognised as "plant blindness", or more recently, "plant awareness disparity" (Wandersee and Schussler, 1999; Parsley, 2020). To extend this concept, there appears also to be a disparity between the awareness for produce and crop, and in the case of processed foods, between product and crop. Such "crop blindness" breeds a disconnect from the processes and consequences of agriculture. This can pose a range of potential challenges to the creation of sustainable food systems, such as resource overuse, food waste, devaluation of local agriculture and a loss of traditional culture and practice, and a reinforcement of policies that favour large-scale intensive agriculture (Hartmann and Siegrist, 2017; Macdiarmid, Douglas and Campbell, 2016; O'Kane, 2012; Reisch, Eberle and Lorek, 2013; Conrad and Blackstone, 2021).

As recognised in the EAT-*Lancet* report (Willett et al., 2019), the generation of a sustainable global food system that ensures food security for the majority of people on the planet requires, amongst other things, a shift in the awareness of crop and food production systems and subsequent consumer behaviours. There is a clear consensus that change is needed across a range of scales, encompassing both education and information, but also introduction of new (inter)national policies and economic tools (Willett et al., 2019; Hoek et al., 2021; Biesbroek et al., 2023;). Whilst this is not an easy task, our study of the art history of the potato illustrates that national campaigns can successfully change society's appreciation of a simple staple food.

Acknowledgements

We thank BBSRC and Waitrose Collaborative Training Programme for funding Edward F. Hill-King's PhD study. Proofreader: Louise Hill-King, LHK Ltd.

Author Contribution

Edward F. Hill-King conceived the study, carried out research, and wrote the main draft. Michael R. Roberts and Martin R. McAinsh acquired funding and revised and edited the manuscript.

Data Availability Statement

Data sharing is not applicable to this article as no new data were created or analysed in this study.

Conflict of Interest Statement

The authors declare no conflict of interest.

References

Encyclopaedia Britannica, First edition. (1771) Smellie, W. (ed.) Edinburgh: Colin Macfarquhar & Andrew Bell.

Bandelier, A. F. (1910) The islands of Titicaca and Kaoti. New York: The Hispanic Society of America.

Berners-Lee, M., Kennelly, C., Watson, R. & Hewitt, C. N. (2018) Current global food production is sufficient to meet human nutritional needs in 2050 provided there is radical societal adaptation. Elementa: Science of the Anthropocene, 6, 52.

Besler, B. (1640) Hortus Eystettensis, sive, Diligens et accurata omnium plantarum, florum, stirpium : ex variis orbis terrae partibus, singulari studio collectarum, quae in celeberrimis viridariis arcem episcopalem ibidem cingentibus, olim conspiciebantur delineatio et ad vivum repraesentatio et advivum repraesentatio opera. Nuremberg.

Biesbroek, S., Kok, F. J., Tufford, A. R., Bloem, M. W., Darmon, N., Drewnowski, A., Fan, S., Fanzo, J., Gordon, L. J., Hu, F. B., Lähteenmäki, L., Nnam, N., Ridoutt, B. G., Rivera, J., Swinburn, B. & Veer, P. V. T. (2023) Toward healthy and sustainable diets for the 21st century: Importance of sociocultural and economic considerations. Proceedings of the National Academy of Sciences, 120(26), e2219272120.

Cieza De Leon, P. (1883) The Second Part of the Chronicle of Peru. London: The Hakluyt Society.

Clusius, C. (1601) Rariorum Plantarum Historia. Antwerp: Ioannem Moretum.

Conrad, Z. & Blackstone, N. T. (2021) Identifying the links between consumer food waste, nutrition, and environmental sustainability: a narrative review. Nutrition Reviews, 79(3), 301-314.

Crippa, M., Solazzo, E., Guizzardi, D., Monforti-Ferrario, F., Tubiello, F. N. & Leip, A. (2021) Food systems are responsible for a third of global anthropogenic GHG emissions. Nature Food, 2(3), 198-209.

Grada, C. O. (1979) The population of Ireland 1700-1900: A survey. Annales de Démographie Historique, 281-299.

Graves, C. (ed.) (2001) The Potato, Treasure of the Andes. Lima: International Potato Centre.

Greene, R. (1592) The Complete Cony-Catching. Ex-classics Project, 2017. Exclassics.com.

Grunert, K. G., Hieke, S. & Wills, J. (2014) Sustainability labels on food products: Consumer motivation, understanding and use. Food Policy, 44**,** 177-189.

Hartmann, C. & Siegrist, M. (2017) Consumer perception and behaviour regarding sustainable protein consumption: A systematic review. Trends in Food Science & Technology, 61**,** 11-25.

Hasegawa, T., Havlík, P., Frank, S., Palazzo, A. & Valin, H. (2019) Tackling food consumption inequality to fight hunger without pressuring the environment. Nature Sustainability, 2(9)**,** 826-833. 10.1038/s41893-019-0371-6.

Hoek, A. C., Malekpour, S., Raven, R., Court, E. & Byrne, E. (2021) Towards environmentally sustainable food systems: decision-making factors in sustainable food production and consumption. Sustainable Production and Consumption, 26**,** 610-626.

Jon-Il, K. (2017) Biography. Pyongyang: Foreign Languages Publishing House.

Lasseter, J. (Dir.) (1995) *Toy Story*. United States: Pixar Animation Studios.

Lea-Henry, J. (2018) Potato Propaganda: A Very North Korean Revolution. Available at: https://jrleahenry.medium.com/potato-propaganda-a-very-north-korean-revolution-cda895fa63c5 [Accessed 06/02/25 2025].

Leng, G., Adan, R. a. H., Belot, M., Brunstrom, J. M., De Graaf, K., Dickson, S. L., Hare, T., Maier, S., Menzies, J., Preissl, H., Reisch, L. A., Rogers, P. J. & Smeets, P. a. M. (2017) The determinants of food choice. Proceedings of the Nutrition Society*,* 76(3)**,** 316-327.

Li, Y., He, P., Shan, Y., Li, Y., Hang, Y., Shao, S., Ruzzenenti, F. & Hubacek, K. (2024) Reducing climate change impacts from the global food system through diet shifts. Nature Climate Change*,* 14(9)**,** 943-953.

Lidwell-Durnin, J. (2020) Cultivating famine: data, experimentation and food security, 1795–1848. The British Journal for the History of Science*,* 53(2)**,** 159-181.

Lim, J.-C. (2015) Leader Symbols and Personality Cult in North Korea: The Leader State. Abingdon: Routledge.

Macdiarmid, J. I., Douglas, F. & Campbell, J. (2016) Eating like there's no tomorrow: Public awareness of the environmental impact of food and reluctance to eat less meat as part of a sustainable diet. Appetite*,* 96**,** 487-493.

Mishra, P., Alhussan, A. A., Khafaga, D. S., Lal, P., Ray, S., Abotaleb, M., Alakkari, K., Eid, M. M. & El-Kenawy, E.-S. M. (2024) Forecasting Production of Potato for a Sustainable Future: Global Market Analysis. Potato Research, 67(4), 1671-1690.

Mottl, K. M. (2015) Re-examined and Re-defined: an Exploration and Comparative Analysis of Moche Ceramic Vessels in the Milwaukee Public Museum Collections. MSc thesis, University of Wisconsin-Milwaukee.

United Nations (2015) Transforming our World: The 2030 Agenda for Sustainable Development.

O'Kane, G. (2012) What is the real cost of our food? Implications for the environment, society and public health nutrition. Public Health Nutrition, 15(2), 268-276.

Parsley, K. M. (2020) Plant awareness disparity: A case for renaming plant blindness. Plants People Planet, 2(6), 598-601.

Reisch, L., Eberle, U. & Lorek, S. (2013) Sustainable food consumption: an overview of contemporary issues and policies. Sustainability: Science, Practice and Policy, 9(2), 7-25.

Salaman, R. N. (1985) The History and Social Influence of the Potato. Revised impression, edited with new introduction by J.G Hawkes. Cambridge: Cambridge University Press.

Santini, A., Maresi, G., Richardson, D. M. & Liebhold, A. M. (2023) Collateral damage: military invasions beget biological invasions. Frontiers in Ecology and the Environment, 21(10), 469-478.

Spoorenberg, T. & Schwekendiek, D. (2012) Demographic Changes in North Korea: 1993–2008. Population and Development Review, 38(1), 133-158.

Trever, L. (2019) A Moche Riddle in Clay: Object Knowledge and Art Work in Ancient Peru. The Art Bulletin, 101(4), 18-38.

Van Bussel, L. M., Kuijsten, A., Mars, M. & Van 'T Veer, P. (2022) Consumers' perceptions on food-related sustainability: A systematic review. Journal of Cleaner Production, 341, 130904.

Van Gogh, V. (1997) The Letters of Vincent Van Gogh. Penguin Classics.

Wandersee, J. H. & Schussler, E. E. (1999) Preventing Plant Blindness. The American Biology Teacher, 61(2), 82-86.

Willett, W., Rockström, J., Loken, B., Springmann, M., Lang, T., Vermeulen, S., Garnett, T., Tilman, D., Declerck, F., Wood, A., Jonell, M., Clark, M., Gordon, L. J., Fanzo, J., Hawkes, C., Zurayk, R., Rivera, J. A., De Vries, W., Majele Sibanda, L., Afshin, A., Chaudhary, A., Herrero, M.,

Agustina, R., Branca, F., Lartey, A., Fan, S., Crona, B., Fox, E., Bignet, V., Troell, M., Lindahl, T., Singh, S., Cornell, S. E., Srinath Reddy, K., Narain, S., Nishtar, S. & Murray, C. J. L. (2019) Food in the Anthropocene: the EAT–Lancet Commission on healthy diets from sustainable food systems. The Lancet, 393(10170), 447-492.

Wilson, A. (1993) The Story of the Potato Through Illustrated Varieties. Wisbech: A. Wilson.

8 Appendix 2: Automated Gloss Measurement System

An automated system was developed for non-destructive measurement of surface gloss of potatoes and tomatoes. Glossiness was determined from photographs via computer vision software I developed. Glossiness is defined the spread of reflected light, a matte surface diffusing reflections in all directions and an ideal glossy surface reflected an undistorted image like a mirror (Figure *7.2.*1).

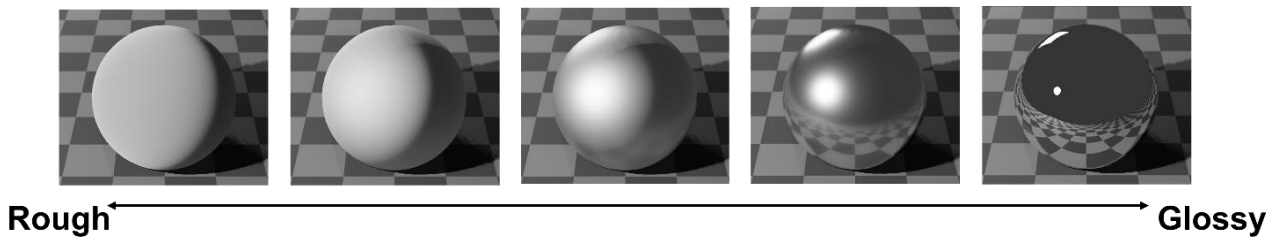

Figure 7.2.1 Visualisation of glossiness scale rendered in Blender (Blender Foundation, Amsterdam, Netherlands)

Glossiness of flat surfaces is conventionally measured via a glossmeter; however, this is not applicable to round 3-dimension produce without destructive peeling (Nussinovitch et al., 1996). To acquire images for non-destructive gloss determination a contraption was constructed to rotate and photograph samples in darkness, illuminated only by a columnated light source. This was constructed from a wooden base, with aluminium struts to hold up a light blocking cloth placed over the contraption during imaging. Both sample rotation and imaging were controlled by an Arduino MEGA microcontroller (Arduino, Monza, Italy). A lazy Susan bearing, and servo motor were used to rotate a plate which holds the sample, the plate is rotated by a fixed angle between each image. Imaging was performed using a Canon EOS 500D DLSR camera (Canon, Tokyo, Japan) with a zoom lens. The camera was controlled via an optoisolator controlled by the Arduino MEGA to close the camera's clicker circuit with a long hold for automatic focus.

This contraption however proved impractical for the shelf-life experiment (see Chapter 6), having to remove all samples from the shelving environment and handle them for every reading, introducing excess mechanical stress on the samples. To address these issues, smartphones were mounted above the strip lights of the shelving unit to gather timelapse images. Another piece of software was developed to use the reflection of the

strip lights on the samples for gloss determination. Kondo et al. took a similar approach for grading aubergines (Konda et al., 2010), using multiple camera in a rotating fruit inspection machine to assess glossiness from reflections of strip lights. Kondo et al. however do not detail the method used to analyse the images in their paper.

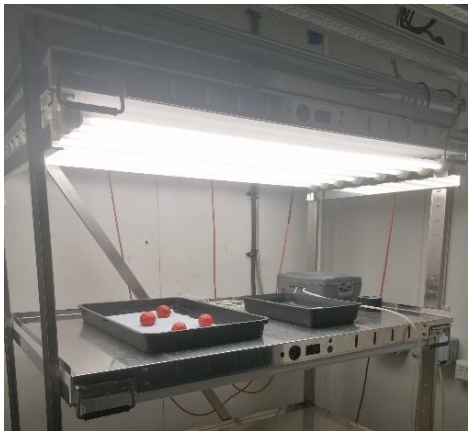
a


b


c

Figure 7.2.2 Photographs of tomatoes in shelf like environment with strip lights. a: Shelf where trays of samples were monitored. b: 2 trays of tomatoes on shelf under strip lights. c: Strip lights as seen from below.

Multiple samples feature in each photograph; thus photographs are divided by sample; samples are placed in a grid to accommodate this, and samples removed due to spoilage are replaced with dummies to enable correct counting. Tomatoes were placed on blue paper towel to maximise background contrast and to absorb moisture. To isolate individual samples the blue channel was subtracted from the red channel and converted to binary based on a threshold level. From this binary image a region detection algorithm was used to find circular regions above a minimum size, this

detects the red tomatoes on the blue background. Determination of glossiness was computed via a human written algorithm; machine learning was not used as a large dataset with supervisory gloss levels determined by another means would be required. Sharpness of the edge of the specular strip light reflection was used as the metric of glossiness.

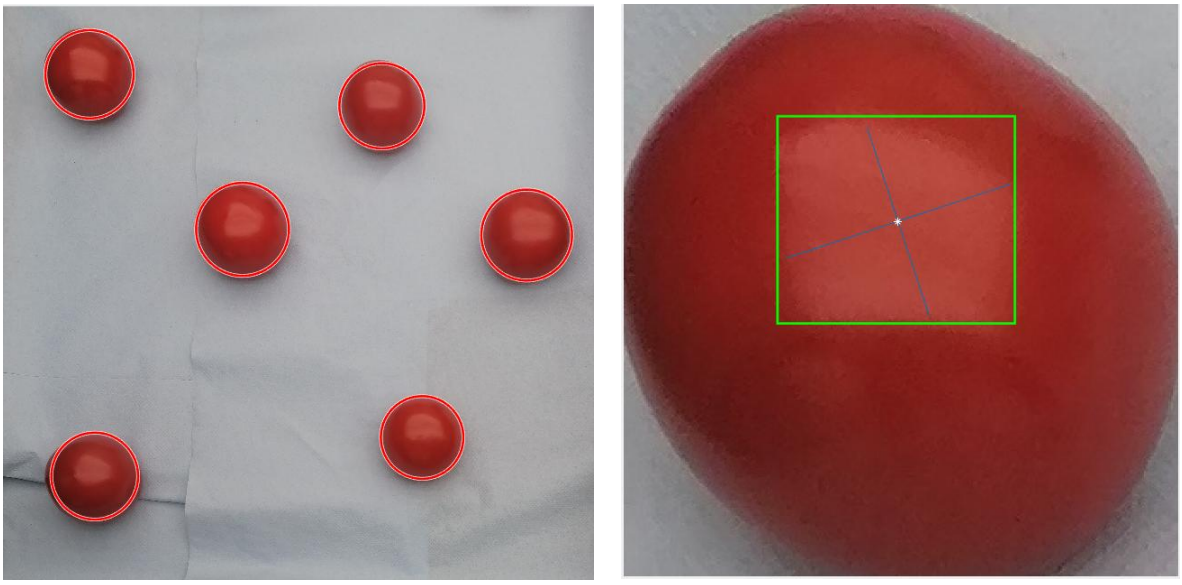

a b

Figure 7.2.3 Tests of glossopteris. a: Tomato detection test locating 6 tomatoes randomly spaces, b: strip light reflection detection locating reflection on isolated tomato.

Assuming the camera is aligned with the axis of the strip lights, the fall off of the edge of the reflection is measured vertically at both top and bottom and averaged across the width of the reflection. Fall off is measured in pixels as the same camera at the same distance with the same light source is used for all images, however if these factors were to vary the edge of the tomato should be used for calibration, fall offs from the original sample rotating contraption with a DLSR were in the region of 1000px, much greater than ~30px of these tomato images.

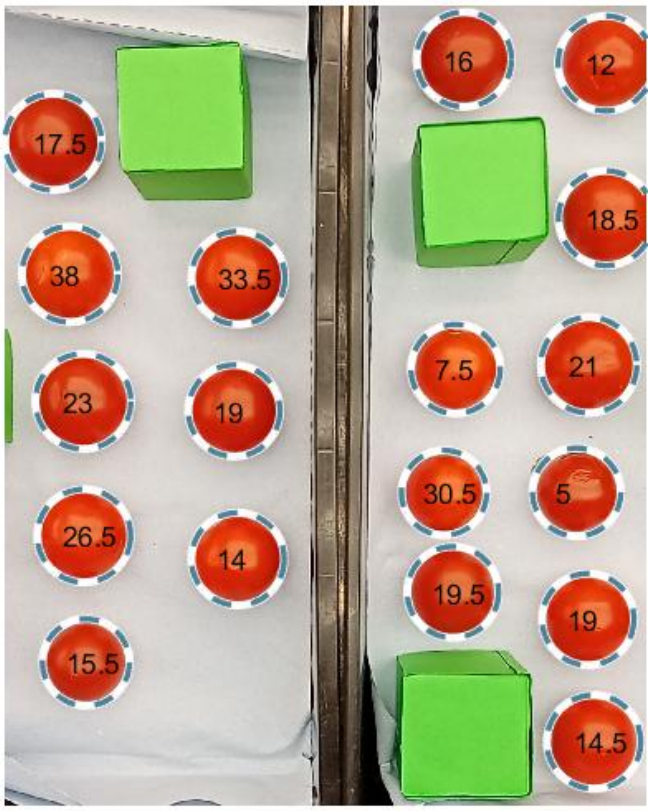

Figure 7.2..4 Example of Glossopteris system detecting tomatoes and assigning gloss scores. Green cubes are dummies to replace tomatoes removed due to spoilage.

Tomatoes in Figure *7.2.4* have been assigned roughness scores, roughness being the inverse of glossiness. The tomatoes with lower roughness scores appear to have glossier surfaces.

Unfortunately, the mobile app used to record timelapses saved all frames as jpeg files. Low resolution of cropped isolated tomato images along with jpeg compression (Figure 5.7) rendered the edges of specular reflections very noisy, making this gloss system not applicable to the images collected.

9 Appendix 3: Basics of Reflectance Spectroscopy

Reflectance spectroscopy is based on comparing the frequency composition of light reflected off a sample to the composition of the light source. White light is shined on the sample and the reflected light is split using a diamond prism (Figure 9.1). The light intensity across the spectrum of the reflected light will vary from the source light, as the sample absorbs light. The more of a certain frequency of light the sample absorbs the lower the intensity of that frequency will be in the reflected light. As differing chemical compounds, bonds, bends and vibrations absorbs different frequencies of light more or less effectively, the change in frequency composition of the light after reflecting off the sample provides information about the chemistry of that sample.

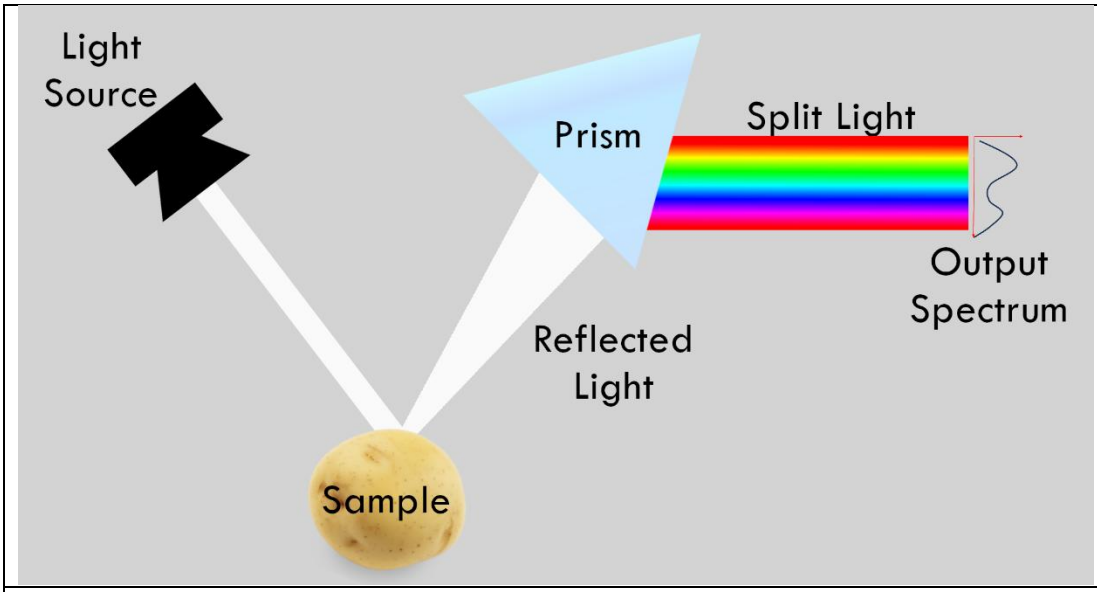

Figure 9.1 Diagram of reflectance spectroscopy.

Absorbance spectra were collected during this thesis primarily in an NIR bandwidth of 900-1700 nm wavelength. These NIR spectra were collected using a handheld Nirvascan ASP-NIR-M-Reflect (Allied Scientific Pro, Gatineau, Canada) (Figure 9.2).


a


b


c

Figure 9.2 Nirvascan ASP-NIR-M-Reflect handheld spectrometer used for NIR spectra collection in this thesis. Image credit: Allied Scientific Pro https://www.alliedscientificpro.com/nirvascan

10 Glossary

ANOVA – Analysis of Variance

C_i – Internal Carbon Dioxide Concentration

DS – Drought Stressed

EIS – Electrical Impedance Spectroscopy

FAO – Food and Agriculture Organization of The United Nations

FET – Fischer's Exact Text

FTIR – Fourier Transform InfraRed

GPR – Gaussian Process Regression

LLS – Linear Least Squares

MIR – Mid Infrared

NIR – Near Infrared

PC – Principal Component

PCA – Principal Component Analysis

PP – Peak to Peak

RAC – Rapid Anaerobic Chamber

RMS – Root Mean Squared

SOFI – The State of Food Security and Nutrition in the World

SRS – Spatially Resolved Spectroscopy

SVM – Support Vector Machine

UN – United Nations

WHO – World Health Organization

WW – Well-Watered

11 Bibliography

Abbas, S., Haider, A., Kousar, S., Lu, H., Lu, S., Liu, F., Li, H., Miao, C., Feng, W., Ahamad, M. I., Mehmood, M. S., & Zulqarnain, R. M. (2025). Climate variability, population growth, and globalization impacting food security in Pakistan. *Scientific Reports*, *15*(1), 4225.

Abbasi, T., Jaafarzadeh Haghighi Fard, N., Madadizadeh, F., Eslami, H., & Ebrahimi, A. A. (2023). Environmental impact assessment of low-density polyethylene and polyethylene terephthalate containers using a life cycle assessment technique. *Journal of Polymers and the Environment*, *31*(8), 3493-3508.

Abdelrahman, D. K., Mohammed, R., Fouda, M. E., Said, L. A., & Radwan, A. G. (2021). Memristive bio-impedance modeling of fruits and vegetables. *IEEE Access*, *9*, 21498-21506.

Adams, M. J. (1975). Potato tuber lenticels: development and structure. *Annals of Applied Biology*, *79*(3), 265-273.

Adams, S. S., & Stevenson, W. R. (1990). Water management, disease development, and potato production. *American Potato Journal*, *67*, 3-11.

Adeoye, I. B., Odeleye, O. M. O., Babalola, S. O., & Afolayan, S. O. (2009). Economic analysis of tomato losses in Ibadan metropolis, Oyo State, Nigeria. *African Journal of Basic and Applied Sciences*, *1*(5-6), 87-92.

Ahlawat, Y., & Liu, T. (2021). Varied expression of senescence-associated and ethylene-related genes during postharvest storage of brassica vegetables. *International Journal of Molecular Sciences*, *22*(2), 839.

Agrawal, M. (2005). Effects of air pollution on agriculture: an issue of national concern. *National Academy Science Letters*, *28*(3/4), 93-106.

Agricrops. (2020). Potato Variety Database. https://potatoes.agricrops.org/varieties/view/ORCHESTRA (Accessed 26/04/2025).

Akinro, A. O., Ikumawoyi, O. B., Yahaya, O., & Ologunagha, N. M. (2012). Environmental impacts of polyethylene generation and disposal in Akure City, Nigeria. *Global Journal of Science Frontier Research Agriculture and Biology*, *12*(3), 1-8.

Abdelrahman, D. K., Mohammed, R., Fouda, M. E., Said, L. A., & Radwan, A. G. (2021). Memristive bio-impedance modeling of fruits and vegetables. *IEEE Access*, *9*, 21498-21506.

Aliche, E. B., Oortwijn, M., Theeuwen, T. P., Bachem, C. W., Visser, R. G., & van der Linden, C. G. (2018). Drought response in field grown potatoes and the interactions between canopy growth and yield. *Agricultural Water Management*, *206*, 20-30.

Al-Dairi, M., Pathare, P. B., Al-Yahyai, R., & Opara, U. L. (2022). Mechanical damage of fresh produce in postharvest transportation: current status and future prospects. *Trends in Food Science & Technology*, *124*, 195-207.

Alkan, N., & Fortes, A. M. (2015). Insights into molecular and metabolic events associated with fruit response to post-harvest fungal pathogens. *Frontiers in Plant Science*, *6*, 889.

Alsabri, A., Tahir, F., & Al-Ghamdi, S. G. (2022). Environmental impacts of polypropylene (PP) production and prospects of its recycling in the GCC region. *Materials Today: Proceedings*, *56*(4), 2245-2251.

Ampatzidis, Y., De Bellis, L., & Luvisi, A. (2017). iPathology: robotic applications and management of plants and plant diseases. *Sustainability*, *9*(6), 1010.

Ando, Y., Mizutani, K., & Wakatsuki, N. (2014). Electrical impedance analysis of potato tissues during drying. *Journal of Food Engineering*, *121*, 24-31.

Arah, I. K., Amaglo, H., Kumah, E. K., & Ofori, H. (2015a). Preharvest and postharvest factors affecting the quality and shelf life of harvested tomatoes: a mini review. *International Journal of Agronomy*, *2015*(1), 478041.

Arah, I. K., Kumah, E. K., Anku, E. K., & Amaglo, H. (2015b). An overview of post-harvest losses in tomato production in Africa: causes and possible prevention strategies. *Journal of Biology, Agriculture and Healthcare*, *5*(16), 78-88.

Arslan, A., Floress, K., Lamanna, C., Lipper, L., & Rosenstock, T. S. (2022). A meta-analysis of the adoption of agricultural technology in Sub-Saharan Africa. *PLOS Sustainability and Transformation*, *1*(7), e0000018.

Awasthi, L. P., & Verma, H. N. (2017). Current status of viral diseases of potato and their ecofriendly management -A critical review. *Virology: Research & Reviews*, *1*(4), 1-16.

Azzarello, E., Masi, E., & Mancuso, S. (2012). Electrochemical impedance spectroscopy. In: *Plant electrophysiology: Methods and cell electrophysiology* (pp. 205-223). Berlin, Heidelberg: Springer Berlin Heidelberg.

Babaremu, K. O., Adekanye, T. A., Okokpujie, I. P., Fayomi, J., & Atiba, O. E. (2019). The significance of active evaporative cooling system in the shelf life enhancement of vegetables (red and green tomatoes) for minimizing post-harvest losses. *Procedia Manufacturing*, *35*, 1256-1261.

Baker, P., & Friel, S. (2016). Food systems transformations, ultra-processed food markets and the nutrition transition in Asia. *Globalization and Health*, *12*, 1-15.

Balana, B. B., Aghadi, C. N., & Ogunniyi, A. I. (2022). Improving livelihoods through postharvest loss management: evidence from Nigeria. *Food Security*, *14*(1), 249-265.

Bantadjan, Y., Rittiron, R., Malithong, K., & Narongwongwattana, S. (2020). Rapid starch evaluation in fresh cassava root using a developed portable visible and near-infrared spectrometer. *ACS Omega*, *5*(19), 11210-11216.

Battersby-Lennard, J., Fincham, R., Frayne, B., & Haysom, G. (2009). Urban food security in South Africa: case study of Cape Town, Msunduzi and Johannesburg. *Development Planning Division Working Paper Series*, *15*, 115-129.

Bartholomew, E. T. (1913). Blackheart of potatoes. *Phytopathology*, *3*, 180-182.

Bartholomew, E. T. (1914). A pathological and physiological study of the black heart of potato tubers. University of Wisconsin–Madison, USA.

Beasley, A. E., Abdelouahab, M. S., Lozi, R., Powell, A. L., & Adamatzky, A. (2020). On memfractance of plants and fungi. *arXiv*, 2005.10500.

Beć, K. B., Grabska, J., Ozaki, Y., Czarnecki, M. A., & Huck, C. W. (2019). Simulated NIR spectra as sensitive markers of the structure and interactions in nucleobases. *Scientific Reports*, *9*(1), 17398.

Beć, K. B., Grabska, J., & Huck, C. W. (2021). NIR spectroscopy of natural medicines supported by novel instrumentation and methods for data analysis and interpretation. *Journal of Pharmaceutical and Biomedical Analysis*, *193*, 113686.

Berners-Lee, M., Kennelly, C., Watson, R., & Hewitt, C. N. (2018). Current global food production is sufficient to meet human nutritional needs in 2050 provided there is radical societal adaptation. *Elementa: Science of the Anthropocene*, *6*, 52.

Bera, T. K., Bera, S., Kar, K., & Mondal, S. (2016). Studying the variations of complex electrical bio-impedance of plant tissues during boiling. *Procedia Technology*, *23*, 248-255.

Bethke, P. C., Sabba, R., & Bussan, A. J. (2009). Tuber water and pressure potentials decrease and sucrose contents increase in response to moderate drought and heat stress. *American Journal of Potato Research*, *86*, 519-532.

Bethke, P.C. (2023). Potato tuber lenticels: a review of their development, structure, function, and disease susceptibility. *American Journal of Potato Research,* 100, 253-264.

Bindraban, P. S., van der Velde, M., Ye, L., van den Berg, M., Materechera, S., Kiba, D. I., Tamene, L., Ragnarsdóttir, K. V., Jongschaap, R., Hoogmoed, M., Hoogmoed, W., van Beek, C. & van Lynden, G. (2012). Assessing the impact of soil degradation on food production. *Current Opinion in Environmental Sustainability*, *4*(5), 478-488.

Bjerring Jensen, N., Vrobel, O., Akula Nageshbabu, N., De Diego, N., Tarkowski, P., Ottosen, C. O., & Zhou, R. (2024). Stomatal effects and ABA metabolism mediate differential regulation of leaf and flower cooling in tomato cultivars exposed to heat and drought stress. *Journal of Experimental Botany*, *75*(7), 2156-2175.

Boccaletti, S., Kurths, J., Osipov, G., Valladares, D. L., & Zhou, C. S. (2002). The synchronization of chaotic systems. Physics reports, 366(1-2), 1-101.

Bonierbale, M., Grüneberg, W., Amoros, W., Burgos, G., Salas, E., Porras, E., & zum Felde, T. (2009). Total and individual carotenoid profiles in *Solanum phureja* cultivated potatoes: II. Development and application of near-infrared reflectance spectroscopy (NIRS) calibrations for germplasm characterization. *Journal of Food Composition and Analysis*, *22*(6), 509-516.

Bošković, M. Č., Šekara, T. B., Lutovac, B., Daković, M., Mandić, P. D., & Lazarević, M. P. (2017, June). Analysis of electrical circuits including fractional order elements. In *2017 6th Mediterranean Conference on Embedded Computing (MECO)* (pp. 1-6). IEEE.

Bovi, G. G., Caleb, O. J., Klaus, E., Tintchev, F., Rauh, C., & Mahajan, P. V. (2018). Moisture absorption kinetics of FruitPad for packaging of fresh strawberry. *Journal of Food Engineering*, *223*, 248-254.

Brancoli, P., Rousta, K., & Bolton, K. (2017). Life cycle assessment of supermarket food waste. *Resources, Conservation and Recycling*, *118*, 39-46.

Brodribb, T. J., McAdam, S. A., & Carins Murphy, M. R. (2017). Xylem and stomata, coordinated through time and space. *Plant, Cell & Environment*, *40*(6), 872-880.

Brown, C. R., Mojtahedi, H., Santo, G. S., Hamm, P., Pavek, J. J., Corsini, D., Love, S., Crosslin, J. M. & Thomas, P. E. (2000). Potato germplasm resistant to corky ringspot disease. *American Journal of Potato Research*, *77*, 23-27.

Brown, C. R., Mojtahedi, H., Crosslin, J. M., James, S., Charlton, B., Novy, R. G., Love, S. L., Vales, S. I., & Hamm, P. (2009). Characterization of resistance to corky ringspot disease in potato: a case for resistance to infection by tobacco rattle virus. *American Journal of Potato Research*, *86*, 49-55.

Brunt, K., & Drost, W. C. (2010). Design, construction, and testing of an automated NIR in-line analysis system for potatoes. Part I: Off-line NIR feasibility study for the characterization of potato composition. *Potato Research*, *53*, 25-39.

Burney, J., & Ramanathan, V. (2014). Recent climate and air pollution impacts on Indian agriculture. *Proceedings of the National Academy of Sciences*, *111*(46), 16319-16324.

Burri, B. J. (2011). Evaluating sweet potato as an intervention food to prevent vitamin A deficiency. *Comprehensive Reviews in Food Science and Food Safety*, *10*(2), 118-130.

Cabrera-López, J. J., & Velasco-Medina, J. (2019). Structured approach and impedance spectroscopy microsystem for fractional-order electrical characterization of vegetable tissues. *IEEE Transactions on Instrumentation and Measurement*, *69*(2), 469-478.

CALU. (June 2011). Crop walking: an introduction. CALU factsheet. Ref: 080301. http://www.calu.bangor.ac.uk/Technical%20leaflets/080301%20CALU%20crop%20walking.pdf.

Campbell, D., & Munden-Dixon, K. (2018). On-farm food loss: farmer perspectives on food waste. *The Journal of Extension*, *56*(3), 23.

Cartwright, K. V. (2007). Determining the effective or RMS voltage of various waveforms without calculus. *The Technology Interface*, *8*(1). https://tiij.org/issues/issues/fall2007/30_Cartwright/Cartwright-Waveforms.pdf.

Cassman, K. G., Wood, S., Choo, P. S., Cooper, H. D., Devendra, C., Dixon, J., Gaskell, J., Khan, Y., Lal, R., Lipper, L., Pretty, J., Primavera, J., Ramankutty, N., Viglizzo, E., Wiebe, K., Kadungure, S., Kanbar, N., Khan, Z., Leakey, R., Porter, S., Sebastian, K. & Tharme, R. (2005). Chapter 26. Cultivated Systems. In: *Ecosystems and Human Well-Being: Current State and Trends*, the Millennium Ecosystem Assessment. 1. https://www.millenniumassessment.org/documents/document.295.aspx.pdf.

Campoy-Muñoz, P., Cardenete, M. A., & Delgado, M. C. (2017). Economic impact assessment of food waste reduction on European countries through social accounting matrices. *Resources, Conservation and Recycling*, *122*, 202-209.

Chaboud, G., & Daviron, B. (2017). Food losses and waste: navigating the inconsistencies. *Global Food Security*, *12*, 1-7.

Chandel, R. S., Chandla, V. K., Verma, K. S., & Pathania, M. (2022). Insect pests of potato in India: biology and management. In: *Insect pests of potato* (pp. 371-400). Academic Press.

Chapman, L. (2018). Understanding the post harvest disorder blackheart in Solanum tuberosum. Doctoral dissertation, University of Oxford, UK.

Chen, J. Y., Miao, Y., Zhang, H., & Matsunaga, R. (2004). Non-destructive determination of carbohydrate content in potatoes using near infrared spectroscopy. *Journal of Near Infrared Spectroscopy*, *12*(5), 311-314.

Chen, J. Y., Zhang, H., Miao, Y., & Asakura, M. (2010). Nondestructive determination of sugar content in potato tubers using visible and near infrared spectroscopy. *Japan Journal of Food Engineering*, *11*(1), 59-64.

Cheng, J., Yu, P., Huang, Y., Zhang, G., Lu, C., & Jiang, X. (2022). Application status and prospect of impedance spectroscopy in agricultural product quality detection. *Agriculture*, *12*(10), 1525.

Chourasia, M. K., Maji, P., Baskey, A., & Goswami, T. K. (2005). Estimation of moisture loss from the cooling data of potatoes. *Journal of Food Process Engineering*, *28*(4), 397-416.

Chua, L. O. (1971). Memristor—the missing circuit element. *IEEE Transactions on Circuit Theory*, *CT-18*, 507-519.

Chung, P. J., Singh, G. P., Huang, C. H., Koyyappurath, S., Seo, J. S., Mao, H. Z., Diloknawarit, P., Ram, R. J., Sarojam, R., & Chua, N. H. (2021). Rapid detection and quantification of plant innate immunity response using Raman spectroscopy. *Frontiers in Plant Science*, *12*, 746586.

Cohen, L., Loughlin, P., & Vakman, D. (1999). On an ambiguity in the definition of the amplitude and phase of a signal. Signal Processing, 79(3), 301-307.

Coletro, H. N., Bressan, J., Diniz, A. P., Hermsdorff, H. H. M., Pimenta, A. M., Meireles, A. L., de Deus Mendonça R., & Carraro, J. C. C. (2023). Habitual polyphenol intake of foods according to NOVA classification: implications of ultra-processed foods intake (CUME study). *International Journal of Food Sciences and Nutrition*, *74*(3), 338-349.

Cooper, M., Müller, B., Cafiero, C., Bayas, J. C. L., Cuaresma, J. C., & Kharas, H. (2021). Monitoring and projecting global hunger: are we on track?. *Global Food Security*, *30*, 100568.

Corrado, S., & Sala, S. (2018). Food waste accounting along global and European food supply chains: state of the art and outlook. *Waste Management*, *79*, 120-131.

Cotrozzi, L., Couture, J. J., Cavender-Bares, J., Kingdon, C. C., Fallon, B., Pilz, G., Pellegrini, E., Nali, C. & Townsend, P. A. (2017). Using foliar spectral properties to assess the effects of drought on plant water potential. *Tree Physiology*, *37*(11), 1582-1591.

Crippa, M., Solazzo, E., Guizzardi, D., Monforti-Ferrario, F., Tubiello, F. N., & Leip, A. J. N. F. (2021). Food systems are responsible for a third of global anthropogenic GHG emissions. *Nature Food*, *2*(3), 198-209.

Cunha, D. B., da Costa, T. H. M., da Veiga, G. V., Pereira, R. A., & Sichieri, R. (2018). Ultra-processed food consumption and adiposity trajectories in a Brazilian cohort of adolescents: ELANA study. *Nutrition & Diabetes*, *8*, 28.

Cunnington, A. (2023). Developments in automated potato storage management. *Potato Research*, *66*(4), 1305-1314.

Dacal-Nieto, A., Formella, A., Carrión, P., Vazquez-Fernandez, E., & Fernández-Delgado, M. (2011). Non–destructive detection of hollow heart in potatoes using hyperspectral imaging. In: *Computer Analysis of Images and Patterns: 14th International Conference, CAIP 2011, Seville, Spain, 29-31 August 2011, Proceedings, Part II 14* (pp. 180-187). Springer Berlin Heidelberg.

Dardić, M. I. L. E., & Dimitrić, R. A. T. K. O. (2009). Influence of variety, seed tuber mass and number of sprouts on potato yield. *Savremena Poljoprivreda*, *58*(3-4), 23-29.

Davis, W. B. “Physiological Investigation of Black Heart of Potato Tuber.” Botanical Gazette, vol. 81, no. 3, 1926, pp. 323-38. JSTOR.

D’aquino, S., Mistriotis, A., Briassoulis, D., Di Lorenzo, M. L., Malinconico, M., & Palma, A. (2016). Influence of modified atmosphere packaging on postharvest quality of cherry tomatoes held at 20 °C. *Postharvest Biology and Technology*, *115*, 103-112.

Department for Environment, Food & Rural Affairs, UK Government. (2024). United Kingdom Food Security Report 2021: Theme 2: UK Food Supply Sources. https://www.gov.uk/government/statistics/united-kingdom-food-security-report-2021/united-kingdom-food-security-report-2021-theme-2-uk-food-supply-sources (Accessed 08/05/2025).

Díaz, A. J. P., Romero, M. A. P., & Jaramillo, I. L. C. (2025). Implementation of an automated *Solanum tuberosum* grading system using image processing. *Cientifica*, *29*(1), 2594-2921.

Dicken, S. J., Qamar, S., & Batterham, R. L. (2023). Who consumes ultra-processed food? A systematic review of sociodemographic determinants of ultra-processed food consumption from nationally representative samples. *Nutrition Research Reviews*, *37*, 416-456.

Divakaruni, A. S., Paradyse, A., Ferrick, D. A., Murphy, A. N., & Jastroch, M. (2014). Chapter Sixteen—Analysis and interpretation of microplate-based oxygen consumption and pH data. *Methods in Enzymology*, *547*, 309-354.

Domínguez, I., del Río, J. L., Ortiz-Somovilla, V., & Cantos-Villar, E. (2025). Technological innovations for reducing tomato loss in the agri-food industry. *Food Research International*, *203*, 115798.

Dospatliev, L., Katrandzhiev, N., & Kostadinova, G. (2013). Use of nearinfrared spectroscopy technology for assessment of the internal quality of some fruits and vegetables. Review. *Science and Technologies, III*(3*)*, 39-48.

Driesen, E., Van den Ende, W., De Proft, M., & Saeys, W. (2020). Influence of environmental factors light, CO_2, temperature, and relative humidity on stomatal opening and development: a review. *Agronomy*, *10*(12), 1975.

Eiasu, B. K., Soundy, P., & Hammes, P. S. (2007). Response of potato (*Solarium tuberosum*) tuber yield components to gel-polymer soil amendments and irrigation regimes. *New Zealand Journal of Crop and Horticultural Science*, *35*(1), 25-31.

Egea, I., Bian, W., Barsan, C., Jauneau, A., Pech, J. C., Latché, A., Li, Z., & Chervin, C. (2011). Chloroplast to chromoplast transition in tomato fruit: spectral confocal

microscopy analyses of carotenoids and chlorophylls in isolated plastids and time-lapse recording on intact live tissue. *Annals of Botany*, *108*(2), 291-297.

Elbatawi, I. E., Ebaid, M. T., & Hemeda, B. E. (2008a). Determination of potato water content using NIR diffuse reflection method. *Misr Journal of Agricultural Engineering*, *25*(4), 1279-1292.

Elbatawi, I. E. (2008b). An acoustic impact method to detect hollow heart of potato tubers. *Biosystems Engineering*, *100*(2), 206-213.

English, A. & Tobi, R. (2023). Food Prices and Profits During the Cost of Living Crisis. *The Food Foundation Report*. https://foodfoundation.org.uk/sites/default/files/2023-09/TFF_PROFIT%20BRIEFING_Final.pdf.

Emana, B., Afari-Sefa, V., Nenguwo, N., Ayana, A., Kebede, D., & Mohammed, H. (2017). Characterization of pre-and postharvest losses of tomato supply chain in Ethiopia. *Agriculture & Food Security*, *6*, 3.

Erb, K. H., Gaube, V., Krausmann, F., Plutzar, C., Bondeau, A., & Haberl, H. (2007). A comprehensive global 5 min resolution land-use data set for the year 2000 consistent with national census data. *Journal of Land Use Science*, *2*(3), 191-224.

Erb, K. H., Lauk, C., Kastner, T., Mayer, A., Theurl, M. C., & Haberl, H. (2016). Exploring the biophysical option space for feeding the world without deforestation. *Nature Communications*, *7*(1), 11382.

Ericksen, P. J., Ingram, J. S., & Liverman, D. M. (2009). Food security and global environmental change: emerging challenges. *Environmental Science & Policy*, *12*(4), 373-377.

Escuredo, O., Seijo-Rodriguez, A., Rodríguez-Flores, M. S., Míguez, M., & Seijo, M. C. (2018). Influence of weather conditions on the physicochemical characteristics of potato tubers. *Plant, Soil and Environment, 64*(7), 317-323.

Escuredo, O., Meno, L., Rodríguez-Flores, M. S., & Seijo, M. C. (2021). Rapid estimation of potato quality parameters by a portable near-infrared spectroscopy device. *Sensors*, *21*(24), 8222.

Esposito, V. J., Fortenberry, R. C., Boersma, C., & Allamandola, L. J. (2024). Assigning the CH stretch overtone spectrum of benzene and naphthalene with extension to anthracene and tetracene using 2-and 3-quanta anharmonic quantum chemical computations. *The Journal of Chemical Physics*, *160*(21), 211101.

European Commission: Directorate-General for Environment. (2011). Preparatory study on food waste across EU 27 – Final report. Publications Office. https://data.europa.eu/doi/10.2779/85947.

Fagerberg, P., Langlet, B., Oravsky, A., Sandborg, J., Löf, M., & Ioakimidis, I. (2019). Ultra-processed food advertisements dominate the food advertising landscape in two Stockholm areas with low vs high socioeconomic status. Is it time for regulatory action? *BMC Public Health*, *19*, 1717.

FAO. (2011). Global food losses and food waste – Extent, causes and prevention. https://www.fao.org/4/mb060e/mb060e00.pdf.

FAO. (2019). Ultra-processed foods, diet quality, and health using the NOVA classification system. https://openknowledge.fao.org/server/api/core/bitstreams/5277b379-0acb-4d97-a6a3-602774104629/content.

FAO, IFAD, UNICEF, WFP and WHO. (2020). The State of Food Security and Nutrition in the World 2020. Transforming food systems for affordable healthy diets. https://openknowledge.fao.org/server/api/core/bitstreams/9a0fca06-5c5b-4bd5-89eb-5dbec0f27274/content.

FAO, IFAD, UNICEF, WFP, & WHO. (2022). The State of Food Security and Nutrition in the World 2022: Repurposing food and agricultural policies to make healthy diets more affordable. https://openknowledge.fao.org/server/api/core/bitstreams/67b1e9c7-1a7f-4dc6-a19e-f6472a4ea83a/content.

Farber, J. M. (1991). Microbiological aspects of modified-atmosphere packaging technology - a review. *Journal of Food Protection*, *54*()1, 58-70.

Fawole, W. O., Ilbasmis, E., & Ozkan, B. (2015). Food insecurity in Africa in terms of causes, effects and solutions: a case study of Nigeria. In: *2nd ICSAE 2015, International*

Conference on Sustainable Agriculture and Environment, 30 September – 3 October 2025, Konya, Turkey (pp. 6-11). Proceedings book.

Feng, L., Hou, T., & Zhang, B. (2021). A noninvasive method for detecting frozen injuries in potatoes based on electrical impedance spectroscopy. *Journal of Food Process Engineering*, *44*(5), e13682.

Fiers, M., Edel-Hermann, V., Chatot, C., Le Hingrat, Y., Alabouvette, C., & Steinberg, C. (2012). Potato soil-borne diseases. A review. *Agronomy for Sustainable Development*, *32*(1), 93-132.

Fernández-Ahumada, E., Garrido-Varo, A., Guerrero-Ginel, J. E., Wubbels, A., Van der Sluis, C., & Van der Meer, J. M. (2006). Understanding factors affecting near infrared analysis of potato constituents. *Journal of Near Infrared Spectroscopy*, *14*(1), 27-35.

Figueroa, C. R., Jiang, C. Z., Torres, C. A., Fortes, A. M., & Alkan, N. (2021). Regulation of fruit ripening and senescence. *Frontiers in Plant Science*, *12*, 711458.

Filonchyk, M., Peterson, M. P., Zhang, L., Hurynovich, V., & He, Y. (2024). Greenhouse gases emissions and global climate change: examining the influence of CO_2, CH_4, and N_2O. *Science of The Total Environment*, *935*, 173359.

Foley, J. A., Ramankutty, N., Brauman, K. A., Cassidy, E. S., Gerber, J. S., Johnston, M., Mueller, N. D., O'Connell, C., Ray, D. K., West, P. C., Balzer, C., Bennett, E. M., Carpenter, S. R., Hill, J., Monfreda, C., Polasky, S., Rockström, J., Sheehan, J., Siebert, S., Tilman, D., & Zaks, D. P. M. (2011). Solutions for a cultivated planet. *Nature*, *478*(7369), 337-342.

Fox, C. (1957). A generalization of the Cauchy principal value. *Canadian Journal of Mathematics*, *9*, 110-117.

Fox, T. (2013). Global food: waste not, want not. Institution of Mechanical Engineers report. https://www.imeche.org/policy-and-press/reports/detail/global-food-waste-not-want-not.

Franco, O. L., Rigden, D. J., Melo, F. R., & Grossi-de-Sá, M. F. (2002). Plant α-amylase inhibitors and their interaction with insect α-amylases: structure, function and potential for crop protection. *European Journal of Biochemistry*, *269*(2), 397-412.

Fuentes, A., Vázquez-Gutiérrez, J. L., Pérez-Gago, M. B., Vonasek, E., Nitin, N., & Barrett, D. M. (2014). Application of nondestructive impedance spectroscopy to determination of the effect of temperature on potato microstructure and texture. *Journal of Food Engineering*, *133*, 16-22.

Galli, F., Cavicchi, A., & Brunori, G. (2019). Food waste reduction and food poverty alleviation: a system dynamics conceptual model. *Agriculture and Human Values*, *36*, 289-300.

Gillman, A., Campbell, D. C., & Spang, E. S. (2019). Does on-farm food loss prevent waste? Insights from California produce growers. *Resources, Conservation and Recycling*, *150*, 104408.

Gao, Y., Alyokhin, A., Prager, S. M., Reitz, S., & Huseth, A. (2024). Complexities in the implementation and maintenance of integrated pest management in potato. *Annual Review of Entomology*, *70*(1), 45-63.

Gascon, M., Cirach, M., Martínez, D., Dadvand, P., Valentín, A., Plasència, A., & Nieuwenhuijsen, M. J. (2016). Normalized difference vegetation index (NDVI) as a marker of surrounding greenness in epidemiological studies: the case of Barcelona city. *Urban Forestry & Urban Greening*, *19*, 88-94.

Gatto, A., & Chepeliev, M. (2024). Global food loss and waste estimates show increasing nutritional and environmental pressures. *Nature Food*, *5*(2), 136-147.

Gervais, T., Creelman, A., Li, X. Q., Bizimungu, B., De Koeyer, D., & Dahal, K. (2021). Potato response to drought stress: physiological and growth basis. *Frontiers in Plant Science*, *12*, 698060.

Ghosh, S. C., Asanuma, K. I., Kusutani, A., & Toyota, M. (2000). Effects of temperature at different growth stages on nonstructural carbohydrate, nitrate reductase activity and yield of potato. *Environment Control in Biology*, *38*(4), 197-206.

Gleick, P. H., & Cooley, H. (2021). Freshwater scarcity. *Annual Review of Environment and Resources*, *46*(1), 319-348.

Goffart, J. P., Haverkort, A., Storey, M., Haase, N., Martin, M., Lebrun, P., Ryckmans, D., Florins, D., & Demeulemeester, K. (2022). Potato production in northwestern Europe (Germany, France, the Netherlands, United Kingdom, Belgium): characteristics, issues, challenges and opportunities. *Potato Research*, *65*(3), 503-547.

Gowda, P., Steiner, J. L., Olson, C., Boggess, M., Farrigan, T., & Grusak, M. A. (2018). Chapter 10: Agriculture and rural communities. In: *Impacts, risks, and adaptation in the United States: Fourth National Climate Assessment*, *II*, 391-437. https://nca2018.globalchange.gov/chapter/10/.

Gracia, A., & Gomez, M. I. (2020). Food sustainability and waste reduction in Spain: consumer preferences for local, suboptimal, and/or unwashed fresh food products. *Sustainability*, *12*(10), 4148.

Grudzińska, M. & Mańkowski, D. (2018). Losses during storage of potato varieties in relation to weather conditions during the vegetation period and temperatures during long-term storage. *American Journal of Potato Research*, *95*, 130-138

Guenthner, J. F., Wiese, M. V., Pavlista, A. D., Sieczka, J. B., & Wyman, J. (1999). Assessment of pesticide use in the US potato industry. *American Journal of Potato Research*, *76*, 25-29.

Guo, Y., Zhang, L., He, Y., Lv, C., Liu, Y., Song, H., Lv, H, & Du, Z. (2024). Online inspection of blackheart in potatoes using visible-near infrared spectroscopy and interpretable spectrogram-based modified ResNet modeling. *Frontiers in Plant Science*, *15*, 1403713.

Guorong, D., Yanjun, M., Li, M., Jun, Z., & Yue, H. (2016). Exploring the use of NIR reflectance spectroscopy in prediction of free L-asparagine in solanaceae plants. *International Journal of Biological Macromolecules*, *91*, 426-430.

Gupta, S., Hawk, T., Aggarwal, A., & Drewnowski, A. (2019). Characterizing ultra-processed foods by energy density, nutrient density, and cost. *Frontiers in Nutrition*, *6*, 70.

Haase, N. U. (2011). Prediction of potato processing quality by near infrared reflectance spectroscopy of ground raw tubers. *Journal of Near Infrared Spectroscopy*, *19*(1), 37-45.

Hafez, S. L., Palanisamy, S., & MacGuidwin, A. E. (2020). Nematode management. In: *Potato Production Systems*, 259-282. Springer. https://link.springer.com/chapter/10.1007/978-3-030-39157-7_10.

Hao, Y., Luo, H., Wang, Z., Lu, C., Ye, X., Wang, H., & Miao, L. (2024). Research progress on the mechanisms of fruit glossiness in cucumber. *Gene*, *927*, 148626.

Hari Pranesh, G., Ganapathy, S,, Sudha, P., & Anand, M. (2022). Modified atmospheric packaging of transported and stored tomatoes at cooling temperature. *The Pharma Innovation Journal*, *11*(9S), 1310-1316.

Hassankhani, R., & Navid, H. (2012). Quantitative sorting of potatoes by means of machine vision system. *The Journal of Agricultural Science*, *4*(5), 235-244.

Hayden, R. I., Moyse, C. A., Calder, F. W., Crawford, D. P., & Fensom, D. S. (1969). Electrical impedance studies on potato and alfalfa tissue. *Journal of Experimental Botany*, *20*(2), 177-200.

He, J., Zhu, S., Chu, B., Bai, X., Xiao, Q., Zhang, C., & Gong, J. (2019). Nondestructive determination and visualization of quality attributes in fresh and dry *Chrysanthemum morifolium* using near-infrared hyperspectral imaging. *Applied Sciences*, *9*(9), 1959.

Heinemann, P. H., Pathare, N. P., & Morrow, C. T. (1996). An automated inspection station for machine-vision grading of potatoes. *Machine Vision and Applications*, *9*, 14-19.

Hermansyah, D., & Romli, M. (2025). Critical safety points in handling fresh fruits and vegetables throughout the supply chain. *IOP Conference Series: Earth and Environmental Science*, *1460*, 012055.

Hertog, M. L., Lammertyn, J., Scheerlinck, N., & Nicolai, B. M. (2007). The impact of biological variation on postharvest behaviour: the case of dynamic temperature conditions. *Postharvest Biology and Technology*, *43*(2), 183-192.

Hijmans, R. J. (2003). The effect of climate change on global potato production. *American Journal of Potato Research*, *80*, 271-279.

Holgado, R., & Magnusson, C. (2012). Nematodes as a limiting factor in potato production in Scandinavia. *Potato Research*, *55*(3), 269-278.

Holman, R. T., & Edmondson, P. R. (1956). Near-infrared spectra of fatty acids and some related substances. *Analytical Chemistry*, *28*(10), 1533-1538.

Hopkins, E. F. (1924). Relation of low temperatures to respiration and carbohydrate changes in potato tubers. *Botanical Gazette*, *78*(3), 311-325.

Hou, S., Liu, Z., Shen, H., & Wu, D. (2019). Damage-associated molecular pattern-triggered immunity in plants. *Frontiers in Plant Science*, *10*, 646.

Hsieh, C., & Lee, Y. (2005). Applied visible/near-infrared spectroscopy on detecting the sugar content and hardness of pearl guava. *Applied Engineering in Agriculture*, *21*(6), 1039-1046.

Hu, J., Ma, X., Liu, L., Wu, Y., & Ouyang, J. (2017). Rapid evaluation of the quality of chestnuts using near-infrared reflectance spectroscopy. *Food Chemistry*, *231*, 141-147.

Hu, Q., Xiang, M., Chen, D., Zhou, J., Wu, W., & Song, Q. (2020). Global cropland intensification surpassed expansion between 2000 and 2010: a spatio-temporal analysis based on GlobeLand30. *Science of the Total Environment*, *746*, 141035.

Huang, Y., Si, W., Chen, K., & Sun, Y. (2020). Assessment of tomato maturity in different layers by spatially resolved spectroscopy. *Sensors*, *20*(24), 7229.

Hussain, T. (2016). Potatoes: ensuring food for the future. *Advances in Plants & Agriculture Research*, *3*(6), 178-182.

Ibba, P. (2021). *Fruit quality evaluation using electrical impedance spectroscopy.* Doctoral dissertation, Free University of Bozen-Bolzano, Italy.

Ingle, P. D., Christian, R., Purohit, P., Zarraga, V., Handley, E., Freel, K., & Abdo, S. (2016). Determination of protein content by NIR spectroscopy in protein powder mix products. *Journal of AOAC International*, *99*(2), 360-363.

Imanian, K., Pourdarbani, R., Sabzi, S., García-Mateos, G., Arribas, J. I., & Molina-Martínez, J. M. (2021). Identification of internal defects in potato using spectroscopy and computational intelligence based on majority voting techniques. *Foods*, *10*(5), 982.

Islam, S., Eusufzai, T. K., Ansarey, F. H., Hasan, M. M., & Nahiyan, A. S. M. (2022). A breeding approach to enhance late blight resistance in potato. *The Journal of Horticultural Science and Biotechnology*, *97*(6), 719-729.

Janatabadi, F., Newing, A., & Ermagun, A. (2024). Social and spatial inequalities of contemporary food deserts: a compound of store and online access to food in the United Kingdom. *Applied Geography*, *163*, 103184.

Jesus, I. S., Machado, J. T., & Cunha, J. B. (2006). Fractional electrical dynamics in fruits and vegetables. *IFAC Proceedings Volumes*, *39*(11), 308-313.

Jiang, X., Zhu, B., & Zhu, M. (2023). An overview on the recycling of waste poly (vinyl chloride). *Green Chemistry*, *25*(18), 6971-7025.

Johansson, M. (1999). The Hilbert transform. Mathematics Master's Thesis. Växjö University, Sweden.

Johnson, D. A., & Cummings, T. F. (2015). Effect of extended crop rotations on incidence of black dot, silver scurf, and Verticillium wilt of potato. *Plant Disease*, *99*(2), 257-262.

Johnson, L. K., Bloom, J. D., Dunning, R. D., Gunter, C. C., Boyette, M. D., & Creamer, N. G. (2019). Farmer harvest decisions and vegetable loss in primary production. *Agricultural Systems*, *176*, 102672.

Kabasa, J. D., & Sage, I. (2009). Climate change and food security in Africa. In: *Climate Change in Africa: Adaptation, Mitigation and Governance Challenges (CIGI Special Report*), pp. 21-25. Waterloo, Canada: The Centre for International Governance Innovation. https://www.cigionline.org/sites/default/files/climate_change_in_africa_0.pdf.

Kader, A. A., & Saltveit, M. E. (2002). Atmosphere modification. In: *Postharvest physiology and pathology of vegetables* (pp. 274-294). CRC Press.

Kafa, N., & Jaegler, A. (2021). Food losses and waste quantification in supply chains: a systematic literature review. *British Food Journal*, *123*(11), 3502-3521.

Kandasamy, P. (2022). Respiration rate of fruits and vegetables for modified atmosphere packaging: a mathematical approach. *Journal of Postharvest Technology*, *10*(1), 88-102.

Kapoulea, S., Psychalinos, C., & Elwakil, A. S. (2020). Realization of Cole–Davidson function-based impedance models: application on plant tissues. *Fractal and Fractional*, *4*(4), 54.

Karanth, S., Feng, S., Patra, D., & Pradhan, A. K. (2023). Linking microbial contamination to food spoilage and food waste: the role of smart packaging, spoilage risk assessments, and date labeling. *Frontiers in Microbiology*, *14*, 1198124.

Kathayat, K., & Rawat, M. (2019). Physiological disorders in vegetable crops. *Advances in Horticultural Crop Management and Value Addition*, pp. 307-316.

Keiser, A., Häberli, M., & Stamp, P. (2012a). Drycore appears to result from an interaction between *Rhizoctonia solani* and Wireworm (*Agriotes* ssp.)—Evidence from a 3-Year Field Survey. *Potato Research*, 55, 59-67.

Keiser, A., Häberli, M., & Stamp, P. (2012b). Quality deficiencies on potato (*Solanum tuberosum* L.) tubers caused by *Rhizoctonia solani*, wireworms (*Agriotes* ssp.) and slugs (*Deroceras reticulatum*, *Arion hortensis*) in different farming systems. *Field Crops Research*, *128*, 147-155.

Kevers, C., Falkowski, M., Tabart, J., Defraigne, J. O., Dommes, J., Pincemail, J. (2007). Evolution of antioxidant capacity during storage of selected fruits and vegetables. *Journal of Agricultural and Food Chemistry*, *55*(21*)*, 8596-8603.

Khaled, D. E., Novas, N., Gazquez, J. A., Garcia, R. M., & Manzano-Agugliaro, F. (2015). Fruit and vegetable quality assessment via dielectric sensing. *Sensors*, 15(7), 15363-15397.

Khan, S., Latif, N., Adnan, H., & Khosa, I. (2022, December). A portable real time health inspection system for cotton and potato crop using drone. In: *2022 International*

Conference on Emerging Trends in Electrical, Control, and Telecommunication Engineering (ETECTE) (pp. 1-5). https://ieeexplore.ieee.org/document/10007247.

Khanal, B., & Uprety, D. (2014). Effects of storage temperature on post-harvest of potato. *International Journal of Research*, *1*(4), 903-909.

Kikuchi, A., Huynh, H. D., Endo, T., & Watanabe, K. (2015). Review of recent transgenic studies on abiotic stress tolerance and future molecular breeding in potato. *Breeding Science*, *65*(1), 85-102.

Khodabux, K., L'Omelette, M. S. S., Jhaumeer-Laulloo, S., Ramasami, P., & Rondeau, P. (2007). Chemical and near-infrared determination of moisture, fat and protein in tuna fishes. *Food Chemistry*, *102*(3), 669-675.

Kiaitsi, E. (2015). Physiological and biochemical changes in potato stocks with different susceptibility to blackheart disorder. Cranfield University, UK.

Kohli, K., Prajapati, R., Shah, R., Das, M., & Sharma, B. K. (2024). Food waste: environmental impact and possible solutions. *Sustainable Food Technology*, *2*(1), 70-80.

Kondo, N., Ninomiya, K., Kamata, J., Chong, V. K. (2010). Eggplant grading system including rotary tray assisted machine vision whole fruit inspection. *Trends in Food Science & Technology*, *21*(3), 147.

Krausz, E. (2013). Selective and differential optical spectroscopies in photosynthesis. *Photosynthesis research*, *116*(2), 411-426.

Krieg, P., Lendl, B., Vonach, R., & Kellner, R. (1996). Determination of α-amylase activity using Fourier transform infrared spectroscopy. *Fresenius' Journal of Analytical Chemistry*, *356*, 504-507.

Kummu, M., de Moel, H., Porkka, M., Siebert, S., Varis, O., & Ward, P. J. (2012). Lost food, wasted resources: global food supply chain losses and their impacts on freshwater, cropland, and fertiliser use. *Science of the Total Environment*, *438*, 477-489.

Kuphaldt, T.R., & Haughery, J.R. (2020). Applied Industrial Electricity: Theory and Application. Ames: Iowa State University Digital Press. https://www.iastatedigitalpress.com/plugins/books/31/.

Kschischang, F. R. (2006). The Hilbert Transform. University of Toronto, Canada.

Kudenov, M. W., Scarboro, C. G., Altaqui, A., Boyette, M., Yencho, G. C., & Williams, C. M. (2021). Internal defect scanning of sweetpotatoes using interactance spectroscopy. *PloS One*, *16*(2), e0246872.

Kumar, D., Singh, B. P., & Kumar, P. (2004). An overview of the factors affecting sugar content of potatoes. *Annals of Applied Biology*, *145*(3), 247-256.

Kummu, M., De Moel, H., Porkka, M., Siebert, S., Varis, O., & Ward, P. J. (2012). Lost food, wasted resources: global food supply chain losses and their impacts on freshwater, cropland, and fertiliser use. *Science of the Total Environment*, *438*, 477-489.

Kyprianidis, K., & Skvaril, J. (Eds.). (2017). *Developments in Near-Infrared Spectroscopy*. https://www.intechopen.com/books/5437.

Lal, M. K., Kumar, A., Jena, R., Dutt, S., Thakur, N., Parmar, V., Kumar, V., & Singh, B. (2020). Lipids in potato. In: *Potato: Nutrition and Food Security*, pp. 73-85. Springer Nature.

Lane, M. M., Davis, J. A., Beattie, S., Gómez-Donoso, C., Loughman, A., O'Neil, A., Jacka, F., Berk, M., Page, R., Marx, W., & Rocks, T. (2020). Ultraprocessed food and chronic noncommunicable diseases: a systematic review and meta-analysis of 43 observational studies. *Obesity Reviews*, *22*(3), e13146.

Iannetta, P. P. M., Begg, G. S., Valentine, T. A., & Wishart, J. (2010). Sustainable disease control using weeds as indicators: *Capsella bursa-pastoris* and Tobacco Rattle Virus. *Weed Research*, *50*(6), 511-514.

Li, G., Bartram, S., Guo, H., Mithöfer, A., Kunert, M., & Boland, W. (2019b). SpitWorm, a herbivorous robot: mechanical leaf wounding with simultaneous application of salivary components. *Plants*, *8*(9), 318.

Li, J., Xu, Y., Zhu, W., Wei, X., & Sun, H. (2019a). Maturity assessment of tomato fruit based on electrical impedance spectroscopy. *International Journal of Agricultural and Biological Engineering*, *12*(4), 154-161.

Li, M., Han, D., & Liu, W. (2019c). Non-destructive measurement of soluble solids content of three melon cultivars using portable visible/near infrared spectroscopy. *Biosystems Engineering*, *188*, 31-39.

Liang, P. S., Haff, R. P., Hua, S. S. T., Munyaneza, J. E., Mustafa, T., & Sarreal, S. B. L. (2018). Nondestructive detection of zebra chip disease in potatoes using near-infrared spectroscopy. *Biosystems Engineering*, *166*, 161-169.

Lin, Q., Zhao, S., Pang, L., Sun, C., Chen, L., & Li, F. (2022). Potential risk of microplastics in processed foods: preliminary risk assessment concerning polymer types, abundance, and human exposure of microplastics. *Ecotoxicology and Environmental Safety*, *247*, 114260.

Liu, Q., Tarn, R., Lynch, D., & Skjodt, N. M. (2007). Physicochemical properties of dry matter and starch from potatoes grown in Canada. *Food Chemistry*, *105*(3), 897-907.

Liu, J., Li, X., Li, P., Wang, W., Zhou, W., & Zhang, J. (2010). Determination of moisture in chestnuts using near infrared spectroscopy. *Transactions of the Chinese Society of Agricultural Engineering*, *26*(2), 338-341.

Liu, X. (2006). Electrical impedance spectroscopy applied in plant physiology studies. Doctoral dissertation, RMIT University, Australia.

Liu, J., Li, X., Li, P., Wang, W., Zhang, J., Zhou, W., & Zhou, Z. (2011). Non-destructive measurement of sugar content in chestnuts using near-infrared spectroscopy. In: *Computer and Computing Technologies in Agriculture IV: 4th IFIP TC 12 Conference, CCTA 2010, Nanchang, China, 22-25 October 2010, Selected Papers, Part IV 4* (pp. 246-254). Springer Berlin Heidelberg.

Lobell, D. B., Hammer, G. L., McLean, G., Messina, C., Roberts, M. J., & Schlenker, W. (2013). The critical role of extreme heat for maize production in the United States. *Nature Climate Change*, *3*(5), 497-501.

Lohumi, S., Lee, S., Lee, W. H., Kim, M. S., Mo, C., Bae, H., & Cho, B. K. (2014). Detection of starch adulteration in onion powder by FT-NIR and FT-IR spectroscopy. *Journal of Agricultural and Food Chemistry*, *62*(38), 9246-9251.

Loizou, E., Karelakis, C., Galanopoulos, K., & Mattas, K. (2019). The role of agriculture as a development tool for a regional economy. *Agricultural Systems*, *173*, 482-490.

López, A., Arazuri, S., García, I., Mangado, J., & Jarén, C. (2013). A review of the application of near-infrared spectroscopy for the analysis of potatoes. *Journal of Agricultural and Food Chemistry*, *61*(23), 5413-5424.

López, M. G., García-González, A. S., & Franco-Robles, E. (2017). Carbohydrate analysis by NIRS-Chemometrics. *Developments in Near-Infrared Spectroscopy*, *10*, 67208.

López-Maestresalas, A. (2016). Near-infrared spectroscopy and hyperspectral imaging for non-destructive quality inspection of potatoes. Doctoral thesis, The Public University of Navarre: Pamplona, Spain.

Lutaladio, N., & Castaldi, L. (2009). Potato: the hidden treasure. *Journal of Food Composition and Analysis*, *22*(6), 491-493.

Ma, Y., Liu, H., Wu, J., Yuan, L., Wang, Y., Du, X., Wang, R., Marwa, P. W., Petlulu, P., Chen, X., Zhang, H. (2019). The adverse health effects of bisphenol A and related toxicity mechanisms. *Environmental Research*, *176*, 108575.

Mahalanobis, P. C. (1936). Reprinted (2018). On the generalized distance in statistics. *Sankhyā: The Indian Journal of Statistics, Series A (2008-)*, *80*, S1-S7.

Majidi, H., Minaei, S., Almassi, M., & Mostofi, Y. (2014). Tomato quality in controlled atmosphere storage, modified atmosphere packaging and cold storage. *Journal of Food Science and Technology*, *51*, 2155-2161.

Makhal, A., Robertson, K., Thyne, M., & Mirosa, M. (2021). Normalising the “ugly” to reduce food waste: exploring the socialisations that form appearance preferences for fresh fruits and vegetables. *Journal of Consumer Behaviour*, *20*(5), 1025-1039.

Mangaraj, S., Goswami, T. K., & Mahajan, P. V. (2009). Applications of plastic films for modified atmosphere packaging of fruits and vegetables: a review. *Food Engineering Reviews*, *1*, 133-158.

Mao, H. B., Zhang, M., Liu, J. H., Sun, H., Li, M., & Yang, W. (2016). Effect of spectra preprocessing method on winter wheat chlorophyll content detection. In *2016 ASABE Annual International Meeting* (p. 1). American Society of Agricultural and Biological Engineers.

Marks & Spencer. Tomato innovation - greener energy for the Isle of Wight. https://corporate.marksandspencer.com/tomato-innovation-greener-energy-isle-wight (Accessed 23/02/2025).

Maroušek, J., Rowland, Z., Valášková, K., & Král, P. (2020). Techno-economic assessment of potato waste management in developing economies. *Clean Technologies and Environmental Policy*, *22*, 937-944.

Marsh, K., & Bugusu, B. (2007). Food packaging—roles, materials, and environmental issues. *Journal of Food Science*, *72*, R39-55.

Martínez-Vilalta, J., & Garcia-Forner, N. (2017). Water potential regulation, stomatal behaviour and hydraulic transport under drought: deconstructing the iso/anisohydric concept. *Plant, Cell & Environment*, *40*(6), 962-976.

Matsuki, A., Kori, H. & Kobayashi, R. An extended Hilbert transform method for reconstructing the phase from an oscillatory signal. Sci Rep 13, 3535 (2023). https://doi.org/10.1038/s41598-023-30405-5

Matson, P. A., Parton, W. J., Power, A. G., & Swift, M. J. (1997). Agricultural intensification and ecosystem properties. *Science*, *277*(5325), 504-509.

Mauser, W., Klepper, G., Zabel, F., Delzeit, R., Hank, T., Putzenlechner, B., & Calzadilla, A. (2015). Global biomass production potentials exceed expected future demand without the need for cropland expansion. *Nature Communications*, *6*(1), 8946.

Meadows, J., Montano, M., Alfar, A. J., Başkan, Ö. Y., De Brún, C., Hill, J., McClatchey, R., Kallfa, N. & Fernandes, G. S. (2024). The impact of the cost-of-living crisis on population health in the UK: rapid evidence review. *BMC Public Health*, *24*(1), 561.

Mestdagh, F., De Wilde, T., Castelein, P., Németh, O., van Peteghem, C., & de Meulenaer, B. (2008). Impact of the reducing sugars on the relationship between acrylamide and Maillard browning in French fries. *European Food Research and Technology*, *227*, 69-76.

Midler, E. (2022). Environmental degradation: impacts on agricultural production. IEEP-Policy Brief. https://ieep.eu/publications/environmental-degradation-impacts-on-agricultural-production/.

Mishra, R. K. (2023). Fresh water availability and its global challenge. *British Journal of Multidisciplinary and Advanced Studies*, *4*(3), 1-78.

Mishra, P., Alhussan, A. A., Khafaga, D. S., Lal, P., Ray, S., Abotaleb, M., Alakkari, K., Eid, M. M. & El-Kenawy, E. S. M. (2024). Forecasting production of potato for a sustainable future: global market analysis. *Potato Research*, *67*(4), 1671-1690.

Mølgaard, J. P., & Nielsen, S. L. (1996). Influence of post harvest temperature treatments, storage period and harvest date on development of spraing caused by tobacco rattle virus and potato mop-top virus. *Potato Research*, 39, 571-579.

Monteiro, C. A., Moubarac, J. C., Cannon, G., Ng, S. W., & Popkin, B. (2013). Ultra-processed products are becoming dominant in the global food system. *Obesity Reviews*, *14*, 21-28.

Moscetti, R., Monarca, D., Cecchini, M., Haff, R. P., Contini, M., & Massantini, R. (2014). Detection of mold-damaged chestnuts by near-infrared spectroscopy. *Postharvest Biology and Technology*, *93*, 83-90.

Mozaffarian, D., Rimm, E. B., King, I. B., Lawler, R. L., McDonald, G. B., & Levy, W. C. (2004). Trans fatty acids and systemic inflammation in heart failure. *The American Journal of Clinical Nutrition*, *80*(6), 1521-1525.

Mullan, M., & McDowell, D. (2011). Modified atmosphere packaging. In: *Food and Beverage Packaging Technology*, pp. 263-294. Wiley-Blackwell.

Muluneh, M. G. (2021). Impact of climate change on biodiversity and food security: a global perspective—a review article. *Agriculture & Food Security*, *10*(1), 36.

Munesue, Y., Masui, T., & Fushima, T. (2015). The effects of reducing food losses and food waste on global food insecurity, natural resources, and greenhouse gas emissions. *Environmental Economics and Policy Studies*, *17*, 43-77.

Mumia, B. I., Muthomi, J. W., Narla, R. D., Nyongesa, M., & Olubayo, F. M. (2017). Effect of seed potato tuber storage methods on occurrence of potato diseases. *International Journal of Research in Agricultural Sciences*, *4*(4), 192-201.

Munesue, Y., Masui, T., & Fushima, T. (2015). The effects of reducing food losses and food waste on global food insecurity, natural resources, and greenhouse gas emissions. *Environmental Economics and Policy Studies*, *17*, 43-77.

Murcia, M. A., Jiménez, A. M., & Martínez-Tomé, M. (2009). Vegetables antioxidant losses during industrial processing and refrigerated storage. *Food Research International*, *42*(8), 1046-1052.

Nasir, M. W., & Toth, Z. (2022). Effect of drought stress on potato production: a review. *Agronomy*, *12*(3), 635.

Nielsen, G. G. B., Kjær, A., Klösgen, B., Hansen, P. L., Simonsen, A. C., & Jørgensen, B. (2016). Dielectric spectroscopy for evaluating dry matter content of potato tubers. *Journal of Food Engineering*, *189*, 9-16.

Ni, Y., Mei, M., & Kokot, S. (2011). Analysis of complex, processed substances with the use of NIR spectroscopy and chemometrics: classification and prediction of properties—the potato crisps example. *Chemometrics and Intelligent Laboratory Systems*, *105*(2), 147-156.

Niu, K.-y., Guo, H., & Liu, J. (2023). Can food security and low carbon be achieved simultaneously? —An empirical analysis of the mechanisms influencing the carbon

footprint of potato and corn cultivation in irrigation areas. *Journal of Integrative Agriculture*, *22*(4), 1230-1243.

Nunes, C. N., & Emond, J. P. (2007, December). Relationship between weight loss and visual quality of fruits and vegetables. *Proceedings of the Florida State Horticultural Society*, *120*, 235-245.

Nussinovitch, A., Ward, G., & Mey-Tal, E. (1996). Gloss of fruits and vegetables. *LWT-Food Science and Technology*, *29*(1-2), 184-186.

Obidiegwu, J. E., Bryan, G. J., Jones, H. G., & Prashar, A. (2015). Coping with drought: stress and adaptive responses in potato and perspectives for improvement. *Frontiers in Plant Science*, *6*, 542.

Olayemi, F. F., Adegbola, J. A., Bamishaiye, E. I., & Daura, A. M. (2010). Assessment of post-harvest challenges of small scale farm holders of tomotoes, bell and hot pepper in some local government areas of Kano State, Nigeria. *Bayero Journal of Pure and Applied Sciences*, *3*(2), 39-42.

Olveira-Bouzas, V., Pita-Calvo, C., Vázquez-Odériz, M. L., & Romero-Rodríguez, M. Á. (2021). Evaluation of a modified atmosphere packaging system in pallets to extend the shelf-life of the stored tomato at cooling temperature. *Food Chemistry*, *364*, 130309.

Omolayo, Y., Feingold, B. J., Neff, R. A., & Romeiko, X. X. (2021). Life cycle assessment of food loss and waste in the food supply chain. *Resources, Conservation and Recycling*, *164*, 105119.

Oren, R., Sperry, J. S., Ewers, B. E., Pataki, D. E., Phillips, N., & Megonigal, J. P. (2001). Sensitivity of mean canopy stomatal conductance to vapor pressure deficit in a flooded *Taxodium distichum* L. forest: hydraulic and non-hydraulic effects. *Oecologia*, *126*, 21-29.

Osborne, B. G., Fearn, T., & Hindle, P. H. (1993). *Practical NIR spectroscopy with applications in food and beverage analysis*. Harlow: Longman Scientific and Technical.

Palmer, M. W., Cooper, J., Tétard-Jones, C., Średnicka-Tober, D., Barański, M., Eyre, M., Shotton, P. N., Volakakis, N., Cakmak, C., Ozturk, L., Leifert, C., Wilcockson, S. J., &

Bilsborrow, P. E. (2013). The influence of organic and conventional fertilisation and crop protection practices, preceding crop, harvest year and weather conditions on yield and quality of potato (*Solanum tuberosum*) in a long-term management trial. *European Journal of Agronomy*, *49*, 83-92.

Paraschivu, M., Cotuna, O., Matei, G., & Sărățeanu, V. (2022). Are food waste and food loss a real threat for food security? *Scientific Papers Series "Management, Economic Engineering in Agriculture and Rural Development"*, *22*(1). https://www.cabidigitallibrary.org/doi/pdf/10.5555/20220202801.

Parfitt, J., Barthel, M., & Macnaughton, S. (2010). Food waste within food supply chains: quantification and potential for change to 2050. *Philosophical Transactions of the Royal Society B: Biological Sciences*, *365*(1554), 3065-3081.

Parker, W. E., & Howard, J. J. (2001). The biology and management of wireworms (*Agriotes* spp.) on potato with particular reference to the UK. *Agricultural and Forest Entomology*, *3*(2), 85-98.

Partington, J. C., & Bolwell, G. P. (1996). Purification of polyphenol oxidase free of the storage protein patatin from potato tuber. *Phytochemistry*, *42*(6), 1499-1502.

Pedreschi, F., Mery, D., & Marique, T. (2016). Grading of potatoes. In: *Computer vision technology for food quality evaluation* (pp. 369-382). Academic Press.

Pérez, E. E., Weingartner, D. P., McSorley, R., & Littell, R. (2003). Estimates of sample size for detection and estimation of incidence and severity of corky ringspot of potato. *American Journal of Potato Research*, *80*, 117-124.

Perlikowski, D., Lechowicz, K., Skirycz, A., Michaelis, Ä., Pawłowicz, I., & Kosmala, A. (2022). The role of triacylglycerol in the protection of cells against lipotoxicity under drought in *Lolium multiflorum*/*Festuca arundinacea* introgression forms. *Plant and Cell Physiology*, *63*(3), 353-368.

Pikovsky, A. S., Rosenblum, M. G., Osipov, G. V., & Kurths, J. (1997). Phase synchronization of chaotic oscillators by external driving. Physica D: Nonlinear Phenomena, 104(3-4), 219-238.

Pison, G. (2019, June). How many humans tomorrow? The United Nations revises its projections. *The Conversation*, 1-6. https://theconversation.com/how-many-humans-tomorrow-the-united-nations-revises-its-projections-118938.

Pllana, M., Merovci, N., Jashari, M., Tmava, A., & Shaqiri, F. (2018). Potato market and consumption. *International Journal of Sustainable Economies Management*, *7*(3), 19-29.

Polder, G., Blok, P. M., De Villiers, H. A., Van der Wolf, J. M., & Kamp, J. (2019). Potato virus Y detection in seed potatoes using deep learning on hyperspectral images. *Frontiers in Plant Science*, *10*, 209.

Powell, L. M., Szczypka, G., & Chaloupka, F. J. (2010). Trends in exposure to television food advertisements among children and adolescents in the United States. *Archives of Pediatrics & Adolescent Medicine*, *164*(9), 794-802.

Pradhan, P., Lüdeke, M. K., Reusser, D. E., & Kropp, J. P. (2013). Embodied crop calories in animal products. *Environmental Research Letters*, *8*(4), 044044.

Prananto, J. A., Minasny, B., & Weaver, T. (2020). Near infrared (NIR) spectroscopy as a rapid and cost-effective method for nutrient analysis of plant leaf tissues. *Advances in Agronomy*, *164*, 1-49.

Qian, J., Zhou, J., Di, B., Liu, Y., Zhang, G., & Yang, X. (2021). Using electrical impedance tomography for rapid determination of starch and soluble sugar contents in Rosa hybrida. *Scientific Reports*, *11*(1), 2871.

Qu, P., Zhang, M., Fan, K., & Guo, Z. (2022). Microporous modified atmosphere packaging to extend shelf life of fresh foods: a review. *Critical Reviews in Food Science and Nutrition*, *62*(1), 51-65.

Quick, R. A., Cimrhakl, L., Mojtahedi, H., Sathuvalli, V., Feldman, M. J., & Brown, C. R. (2020). Elimination of *Tobacco rattle virus* from viruliferous *Paratrichodorus allius* in greenhouse pot experiments through cultivation of castle russet. *Journal of Nematology*, *52*, e2020-11.

Ramachandran, P., & Varoquaux, G. (2011). Mayavi: 3D Visualization of Scientific Data. IEEE Computing in Science & Engineering, *13*(2), 40-51.

Ray, D. K., Sloat, L. L., Garcia, A. S., Davis, K. F., Ali, T., & Xie, W. (2022). Crop harvests for direct food use insufficient to meet the UN's food security goal. *Nature Food*, *3*(5), 367-374.

Razmjooy, N., Mousavi, B. S., & Soleymani, F. (2012). A real-time mathematical computer method for potato inspection using machine vision. *Computers & Mathematics with Applications*, *63*(1), 268-279.

Reardon, T., Tschirley, D., Liverpool-Tasie, L. S. O., Awokuse, T., Fanzo, J., Minten, B., Vos, R., Dolislager, M., Sauer, C., Dhar, R., Vargas, C., Lartey, A., Raza, A., & Popkin, B. M. (2021). The processed food revolution in African food systems and the double burden of malnutrition. *Global Food Security*, *28*, 100466.

Rehman, M., Abu Izneid, B. A. J. A., Abdullah, M. Z., & Arshad, M. R. (2011). Assessment of quality of fruits using impedance spectroscopy. *International Journal of Food Science & Technology*, *46*(6), 1303-1309.

Rempel, A. R., & Rempel, A. W. (2013). Rocks, clays, water, and salts: highly durable, infinitely rechargeable, eminently controllable thermal batteries for buildings. *Geosciences*, *3*(1), 63-101.

Ren, W., Jiang, Q., & Qi, W. (2025). Research progress in near-infrared spectroscopy for detecting the quality of potato crops. *Chemical and Biological Technologies in Agriculture*, *12*(1), 32.

Ribeiro, P., Barbosa, M. I., Sousa, C., & Rodrigues, P. M. (2025). Near-infrared spectroscopy machine-learning spectral analysis tool for blueberries (*Vaccinium corymbosum*) cultivar discrimination. *Foods*, *14*(8), 1428.

Rigamonti, L., Grosso, M., Møller, J., Sanchez, V. M., Magnani, S., & Christensen, T. H. (2014). Environmental evaluation of plastic waste management scenarios. *Resources, Conservation and Recycling*, *85*, 42-53.

Ripple, W. J., Wolf, C., Newsome, T. M., Barnard, P., & Moomaw, W. R. (2020). World scientists' warning of a climate emergency. *BioScience*, *70*(1), 8-12.

Ritchie, H., Rosado, P., & Roser, M. (2024). Access to Energy. Data compiled from multiple sources by World Bank – with minor processing by Our World in Data. "Share of the population with access to electricity – World Bank" [dataset]. World Bank, "World Bank World Development Indicators" [original data]. https://ourworldindata.org/energy-access?trk=public_post_comment-text (Accessed 30/01/2024).

Robinson, E. (2023). Obesity and the cost of living crisis. *International Journal of Obesity*, *47*(2), 93-94.

Rosa, L. (2022). Adapting agriculture to climate change via sustainable irrigation: biophysical potentials and feedbacks. *Environmental Research Letters*, *17*(6), 063008.

Rosati, C., Aquilani, R., Dharmapuri, S., Pallara, P., Marusic, C., Tavazza, R., Bouvier, F., Camara, B., & Giuliano, G. (2000). Metabolic engineering of beta-carotene and lycopene content in tomato fruit. *The Plant Journal*, *24*(3), 413-420.

Sato, T., Kawano, S., & Iwamoto, M. (1991). Near infrared spectral patterns of fatty acid analysis from fats and oils. *Journal of the American Oil Chemists Society*, *68*, 827-833.

Sanchez, S. R., Bachilo, S. M., Kadria-Vili, Y., & Weisman, R. B. (2017). Skewness analysis in variance spectroscopy measures nanoparticle individualization. *The Journal of Physical Chemistry Letters*, *8*(13), 2924-2929.

Sanchez, P. D. C., Hashim, N., Shamsudin, R., & Nor, M. Z. M. (2020). Applications of imaging and spectroscopy techniques for non-destructive quality evaluation of potatoes and sweet potatoes: a review. *Trends in Food Science & Technology*, *96*, 208-221.

Sandhya. (2010). Modified atmosphere packaging of fresh produce: current status and future needs. *LWT-Food Science and Technology*, *43*(3), 381-392.

Sankaran, S., Mishra, A., Ehsani, R., & Davis, C. (2010). A review of advanced techniques for detecting plant diseases. *Computers and Electronics in Agriculture*, *72*(1), 1-13.

Santeramo, F. G., & Lamonaca, E. (2021). Food loss–food waste–food security: a new research agenda. *Sustainability*, *13*(9), 4642.

Sarma, H. H., & Paul, A. (2024). Turning waste into wealth: exploring strategies for effective agricultural waste management. *Vigyan Varta*, *5*(5), 322-330.

Scholz, K., Eriksson, M., & Strid, I. (2015). Carbon footprint of supermarket food waste. *Resources, Conservation and Recycling*, *94*, 56-65.

Scialabba, N. (2015). Food wastage footprint & climate change. FAO. https://openknowledge.fao.org/server/api/core/bitstreams/7fffcaf9-91b2-4b7b-bceb-3712c8cb34e6/content (Accessed: 24/05/2025).

Ścibisz, I., Reich, M., Bureau, S., Gouble, B., Causse, M., Bertrand, D., & Renard, C. M. (2011). Mid-infrared spectroscopy as a tool for rapid determination of internal quality parameters in tomato. *Food Chemistry*, *125*(4), 1390-1397.

Semyalo, D., Kim, Y., Omia, E., Arief, M. A. A., Kim, H., Sim, E.-Y., Kim, M. S., Baek, I. & Cho, B. K. (2024). Nondestructive identification of internal potato defects using visible and short-wavelength near-infrared spectral analysis. *Agriculture*, *14*(11), 2014.

Si, W., Xiong, J., Huang, Y., Jiang, X., & Hu, D. (2022). Quality assessment of fruits and vegetables based on spatially resolved spectroscopy: a review. *Foods*, *11*(9), 1198.

Sibomana, M. S., Workneh, T. S., & Audain, K. J. F. S. (2016). A review of postharvest handling and losses in the fresh tomato supply chain: a focus on sub-Saharan Africa. *Food Security*, *8*, 389-404.

Siesler, H. W., Ozaki, Y., Kawata, S., & Heise, H. M. (Eds.). (2008). *Near-infrared spectroscopy: principles, instruments, applications*. John Wiley & Sons.

Sinabell, F. (2009). *Roles of Agriculture in the Rural Economy: An Exploration Exemplified by Austria, Vienna*. https://epub.boku.ac.at/obvbokhs/content/titleinfo/1930890/full.pdf.

Singh, B. P., Agnihotri, S., Singh, G., & Gupta, V. K. (Eds.). (2023). *Postharvest Management of Fresh Produce: Recent Advances*. Academic Press.

Slorach, P. C., Jeswani, H. K., Cuéllar-Franca, R., & Azapagic, A. (2019). Environmental and economic implications of recovering resources from food waste in a circular economy. *Science of the Total Environment*, *693*, 133516.

Sobotka, J., Krejčí, J., & Blahovec, J. (2006). Electric permittivity of potato during compression test. In: *The Hidden and the Masked in Agricultural and Biological Engineering. Czech University of Agriculture in Prague*, pp. 89-94.

Sperry, J. S., Venturas, M. D., Anderegg, W. R., Mencuccini, M., Mackay, D. S., Wang, Y., & Love, D. M. (2017). Predicting stomatal responses to the environment from the optimization of photosynthetic gain and hydraulic cost. *Plant, Cell & Environment*, *40*(6), 816-830.

Stancu, V., Haugaard, P., & Lähteenmäki, L. (2016). Determinants of consumer food waste behaviour: two routes to food waste. *Appetite*, *96*, 7-17.

Stuart, T. (2009). *Waste: Uncovering the global food scandal*. WW Norton & Company.

Su, W. H., He, H. J., & Sun, D. W. (2017). Non-destructive and rapid evaluation of staple foods quality by using spectroscopic techniques: a review. *Critical Reviews in Food Science and Nutrition*, *57*(5), 1039-1051.

Su, W. H., & Xue, H. (2021). Imaging spectroscopy and machine learning for intelligent determination of potato and sweet potato quality. *Foods*, *10*(9), 2146.

Suri, T., & Udry, C. (2022). Agricultural technology in Africa. *Journal of Economic Perspectives*, *36*(1), 33-56.

Suzuki, Y., Yamaguchi, Y., Shiraishi, K., Narumi, D., & Shimoda, Y. (2011). Analysis and modeling of energy demand of retail stores. In *Proceedings of Building Simulation 2011: 12th Conference of International Building Performance Simulation Association*. pp. 1824-1831. https://publications.ibpsa.org/proceedings/bs/2011/papers/bs2011_1591.pdf.

Tahmasbian, I., Morgan, N. K., Hosseini Bai, S., Dunlop, M. W., & Moss, A. F. (2021). Comparison of hyperspectral imaging and near-infrared spectroscopy to determine nitrogen and carbon concentrations in wheat. *Remote Sensing*, *13*(6), 1128.

Tan, D., Adedoyin, F. F., Alvarado, R., Ramzan, M., Kayesh, M. S., & Shah, M. I. (2022). The effects of environmental degradation on agriculture: evidence from European countries. *Gondwana Research*, *106*, 92-104.

Tang, K. H. D., Li, R., Li, Z., & Wang, D. (2024). Health risk of human exposure to microplastics: a review. *Environmental Chemistry Letters*, *22*, 1155–1183.

Taylor, C. J., Pedregal, D. J., Young, P. C. and Tych, W. (2007). Environmental time series analysis and forecasting with the Captain toolbox. *Environmental Modelling and Software*, *22*, 797-814.

Thybo, A. K., Jespersen, S. N., Lærke, P. E., & Stødkilde-Jørgensen, H. J. (2004). Nondestructive detection of internal bruise and spraing disease symptoms in potatoes using magnetic resonance imaging. *Magnetic Resonance Imaging*, *22*(9), 1311-1317.

Thygesen, L. G., Engelsen, S. B., Madsen, M. H., & Sørensen, O. B. (2001). NIR spectroscopy and partial least squares regression for the determination of phosphate content and viscosity behaviour of potato starch. *Journal of Near Infrared Spectroscopy*, *9*(2), 133-139.

Teigiserova, D. A., Hamelin, L., & Thomsen, M. (2020). Towards transparent valorization of food surplus, waste and loss: clarifying definitions, food waste hierarchy, and role in the circular economy. *Science of the Total Environment*, *706*, 136033.

Terry, L. A. (2015). Blackheart - an emerging problem for the GB potato packing industry. *Potato Council Agriculture & Horticulture Development Board*. https://projectblue.blob.core.windows.net/media/Default/Sector%20pages/Potaotes/R456%20CU%20Literature%20Review.pdf.

Tjoelker, M. G., Oleksyn, J., & Reich, P. B. (2001). Modelling respiration of vegetation: evidence for a general temperature-dependent Q10. *Global Change Biology*, *7*(2), 223-230.

Torres, I., Sánchez, M.-T., Entrenas, J.-A., Garrido-Varo, A., & Pérez-Marín, D. (2019). Monitoring quality and safety assessment of summer squashes along the food supply chain using near infrared sensors. *Postharvest Biology and Technology*, *154*, 21-30.

Tort, Ö. Ö., Vayvay, Ö., & Çobanoğlu, E. (2022). A systematic review of sustainable fresh fruit and vegetable supply chains. *Sustainability*, *14*(3), 1573.

Tournas, V. H. (2005). Spoilage of vegetable crops by bacteria and fungi and related health hazards. *Critical Reviews in Microbiology*, *31*(1), 33-44.

Tsolakis, N., & Kumar, M. (2019). Investigating wastage and associated mitigation scenarios across fresh potato supply chains in the UK: a critical literature synthesis. https://papers.ssrn.com/sol3/papers.cfm?abstract_id=3422067.

Trucost. (2019). The Socioeconomic and Environmental Impact of Large-Scale Diamond Mining. https://www.spglobal.com/marketintelligence/en/documents/the-socioeconomic-and-environmental-impact-of-large-scale-diamond-mining_dpa_02-may-2019.pdf.

UN General Assembly. (2015). Transforming our world: the 2030 Agenda for Sustainable Development, A/RES/70/1, 21 October 2015. https://www.refworld.org/legal/resolution/unga/2015/en/111816 (Accessed 07/05/2025).

United Nations Environment Programme (2024). Food Waste Index Report 2024. Think Eat Save: Tracking Progress to Halve Global Food Waste. https://wedocs.unep.org/20.500.11822/45230.

UNFCCC Secretariat. (2024). Nationally determined contributions under the Paris Agreement. Synthesis report by the secretariat [FCCC/PA/CMA/2024/10]. https://unfccc.int/process-and-meetings/the-paris-agreement/nationally-determined-contributions-ndcs/2024-ndc-synthesis-report (Accessed 15/05/2025).

Urban, J., Ingwers, M., McGuire, M. A., & Teskey, R. O. (2017). Stomatal conductance increases with rising temperature. *Plant Signaling & Behavior*, *12*(8), e1356534.

Urugo, M. M., Teka, T. A., Gemede, H. F., Mersha, S., Tessema, A., Woldemariam, H. W., & Admassu, H. (2024). A comprehensive review of current approaches on food waste reduction strategies. *Comprehensive Reviews in Food Science and Food Safety*, *23*(5), e70011.

Uwadaira, Y., Sekiyama, Y., & Ikehata, A. (2018). An examination of the principle of non-destructive flesh firmness measurement of peach fruit by using VIS-NIR spectroscopy. *Heliyon*, *4*(2), e00531.

van Dijk, M., Morley, T., Rau, M. L., & Saghai, Y. (2021). A meta-analysis of projected global food demand and population at risk of hunger for the period 2010–2050. *Nature Food*, *2*(7), 494-501.

van Eunen, K., Kiewiet, J. A., Westerhoff, H. V., & Bakker, B. M. (2012). *Testing biochemistry* revisited: how *in vivo* metabolism can be understood from *in vitro* enzyme kinetics. *PLoS Computational Biology*, *8*(4), e1002483.

van Groenigen, J. W., Mutters, C. S., Horwath, W. R., & van Kessel, C. (2003). NIR and DRIFT-MIR spectrometry of soils for predicting soil and crop parameters in a flooded field. *Plant and Soil*, *250*, 155-165.

Van Haeverbeke, M., De Baets, B., & Stock, M. (2023). Plant impedance spectroscopy: a review of modeling approaches and applications. *Frontiers in Plant Science*, *14*, 1187573.

Venkat, K. (2011). The climate change and economic impacts of food waste in the United States. *International Journal on Food System Dynamics*, *2*(4), 431-446.

Vernon, B., & van Herk, W. (2022). Wireworms as pests of potato. In: *Insect pests of potato* (pp. 103-148). Academic Press.

Verma, S., & Sudan, F. K. (2021). Impact of climate change on marginal and small farmers' livelihood and their adaptation strategies-a review. *Regional Economic Development Research*, *2*(2), 96-112.

Volkov, A. G., Nyasani, E. K., Blockmon, A. L., & Volkova, M. I. (2015). Memristors: memory elements in potato tubers. *Plant Signaling & Behavior*, *10*(10), e1071750.

Volkov, A. G., & Markin, V. S. (2016). Chapter 4: Memristors in biomembranes. In: *Advances in Biomembranes and Lipid Self-Assembly*, Volume 24, pp. 91-117. Academic Press.

Wang, C. S., Kuo, S. Z., Kuo-Huang, L. L., & Wu, J. S. B. (2001). Effect of tissue infrastructure on electric conductance of vegetable stems. *Journal of Food Science*, *66*(2), 284-288.

Wang, Y., Bussan, A.J. & Bethke, P.C. (2012). Stem-end defect in chipping potatoes (*Solanum tuberosum* L.) as influenced by mild environmental stresses. *American Journal of Potato Research, 89*, 392-399.

Wang, L., Xiong, Z., Gao, D., Shi, G., Zeng, W., & Wu, F. (2015). High-speed hyperspectral video acquisition with a dual-camera architecture. In *Proceedings of the IEEE Conference on Computer Vision and Pattern Recognition* (pp. 4942-4950).

Wang, H., Xiong, J., Li, Z., Deng, J., & Zou, X. (2016). Potato grading method of weight and shape based on imaging characteristics parameters in machine vision system. *Transactions of the Chinese Society of Agricultural Engineering*, *32*(8), 272-277.

Wang, Y., Ying, H., Stefanovski, D., Shurson, G. C., Chen, T., Wang, Z., Yin, Y., Zheng, H., Nakaishi, T., Li, J., Cui, Z. & Dou, Z. (2025). Food waste used as a resource can reduce climate and resource burdens in agrifood systems. *Nature Food*, *6*, 478-490.

Wani, A. H. (2011). An overview of the fungal rot of tomato. *Mycopath*, *9*(1), 33-38.

Wei, Q., Zheng, Y., Chen, Z., Huang, Y., Chen, C., Wei, Z., Zhou, S., Sun, H. & Chen, F. (2024). Nondestructive perception of potato quality in actual online production based on cross-modal technology. *International Journal of Agricultural and Biological Engineering*, *16*(6), 280-290.

Welthungerhilfe (WHH), Concern Worldwide, & Institute for International Law of Peace and Armed Conflict (IFHV). (2024). 2024 Global Hunger Index: How Gender Justice Can Advance Climate Resilience and Zero Hunger. https://www.globalhungerindex.org/pdf/en/2024.pdf.

Wenninger, E. J., & Rashed, A. (2024). Biology, ecology, and management of the potato psyllid, *Bactericera cockerelli* (Hemiptera: Triozidae), and zebra chip disease in potato. *Annual Review of Entomology*, *69*(1), 139-157.

Weyer, L. G., & Lo, S. C. (2002). Spectra–structure correlations in the near-infrared. *Handbook of Vibrational Spectroscopy*, *3*, 1817-1837.

Wijesinha-Bettoni, R., & Mouillé, B. (2019). The contribution of potatoes to global food security, nutrition and healthy diets. *American Journal of Potato Research*, *96*, 139-149.

Willersinn, C., Mack, G., Mouron, P., Keiser, A., & Siegrist, M. (2015). Quantity and quality of food losses along the Swiss potato supply chain: stepwise investigation and the influence of quality standards on losses. *Waste Management*, *46*, 120-132.

Willersinn, C., Mouron, P., Mack, G., & Siegrist, M. (2017). Food loss reduction from an environmental, socio-economic and consumer perspective – The case of the Swiss potato market. *Waste Management*, *59*, 451-464.

World Health Organization. (1996). Indicators for Assessing Vitamin A Deficiency and Their Application in Monitoring and Evaluating Intervention Programmes. https://www.who.int/publications/i/item/WHO-NUT-96.10.

World Obesity Federation. (2023). World Obesity Atlas 2023. https://data.worldobesity.org/publications/?cat=19.

World Resources Institute. (2019). Creating a sustainable food future: a menu of solutions to feed nearly 10 billion people by 2050. Final report. https://research.wri.org/sites/default/files/2019-07/WRR_Food_Full_Report_0.pdf.

WRAP. (2012). Reducing supply chain and consumer potato waste. https://www.wrap.ngo/sites/default/files/2020-10/WRAP-Amcor%20project%20report%20final%2C%2003%20Jan%202012.pdf (Accessed: 24/05/2025).

Wu, C. T. (2010). An overview of postharvest biology and technology of fruits and vegetables. *AARDO Workshop on Technology on reducing post-harvest losses and maintaining quality of fruits and vegetables*. https://www.tari.gov.tw/df_inc/get_content.asp?t=p&n=/publication3/index%E2%80%941.asp?Parser=99,9,54,,,,99,145.

Wurr, D. C. E. (1978). Studies of the measurement and interpretation of potato sprout growth. *The Journal of Agricultural Science*, *90*(2), 335-340.

Wyman, O. (2013). Getting fresh: lessons from the global leaders in fresh food. http://www.oliverwyman.com/content/dam/oliver-wyman/europe/germany/de/insights/publications/2015/jan/OW_POV_Getting%20Fresh.pdf (Accessed: 10/04/2025).

Xia, Y., Liu, W., Meng, J., Hu, J., Liu, W., Kang, J., Luo, B., Zhang, H., & Tang, W. (2024). Principles, developments, and applications of spatially resolved spectroscopy in agriculture: a review. *Frontiers in Plant Science*, *14*, 1324881.

Xu, S., Huang, X., & Lu, H. (2023). Advancements and applications of Raman spectroscopy in rapid quality and safety detection of fruits and vegetables. *Horticulturae*, *9*(7), 843.

Yadav, J., Rani, A., Singh, V., & Murari, B. M. (2015). Prospects and limitations of non-invasive blood glucose monitoring using near-infrared spectroscopy. *Biomedical Signal Processing and Control*, *18*, 214-227.

Yadav, A., Kumar, N., Upadhyay, A., Sethi, S., & Singh, A. (2022). Edible coating as postharvest management strategy for shelf-life extension of fresh tomato (*Solanum lycopersicum* L.): an overview. *Journal of Food Science*, *87*(6), 2256-2290.

Yang, C., Everitt, J. H., Du, Q., Luo, B., & Chanussot, J. (2012). Using high-resolution airborne and satellite imagery to assess crop growth and yield variability for precision agriculture. *Proceedings of the IEEE*, *101*(3), 582-592.

Yang, Z., Sun, W., Liu, F., Zhang, Y., Chen, X., Wei, Z., & Li, X. (2024). Field collaborative recognition method and experiment for thermal infrared imaging of damaged potatoes. *Computers and Electronics in Agriculture*, *223*, 109096.

Yencho, G. C., McCord, P. H., Haynes, K. G., & Sterrett, S. R. (2008). Internal heat necrosis of potato—a review. *American Journal of Potato Research*, *85*, 69-76.

Yarullina, L. G., Akhatova, A. R., & Kasimova, R. I. (2016). Hydrolytic enzymes and their proteinaceous inhibitors in regulation of plant–pathogen interactions. *Russian Journal of Plant Physiology*, *63*, 193-203.

Ye, L., Qi, C., Hong, J., & Ma, X. (2017). Life cycle assessment of polyvinyl chloride production and its recyclability in China. *Journal of Cleaner Production*, *142*, 2965-2972.

Ye, D., Sun, L., Tan, W., Che, W., & Yang, M. (2018). Detecting and classifying minor bruised potato based on hyperspectral imaging. *Chemometrics and Intelligent Laboratory Systems*, *177*, 129-139.

Yuan, X., Wang, Y., Ji, P., Wu, P., Sheffield, J., & Otkin, J. A. (2023). A global transition to flash droughts under climate change. *Science*, *380*(6641), 187-191.

Zahir, S. A. D. M., Omar, A. F., Jamlos, M. F., Azmi, M. A. M., & Muncan, J. (2022). A review of visible and near-infrared (Vis-NIR) spectroscopy application in plant stress detection. *Sensors and Actuators A: Physical*, *338*, 113468.

Zapata, M. E., Arrieta, E., Beltramo, B., & Rovirosa, A. (2023). Ultra-processed food consumption in Argentina according to income level and its association with the intake of healthy foods. *Nutrition Bulletin*, *48*(3), 317-328.

Zhang, M. I. N., Stout, D. G., & Willison, J. H. M. (1990). Electrical impedance analysis in plant tissues: symplasmic resistance and membrane capacitance in the Hayden model. *Journal of Experimental Botany*, *41*(224), 371-380.

Zhang, M. I. N., & Willison, J. H. M. (1992). Electrical impedance analysis in plant tissues: the effect of freeze-thaw injury on the electrical properties of potato tuber and carrot root tissues. *Canadian Journal of Plant Science*, *72*(2), 545-553.

Zhang, M. I. N., Repo, T., Willison, J. H. M., & Sutinen, S. (1995). Electrical impedance analysis in plant tissues: on the biological meaning of Cole-Cole α in Scots pine needles. *European Biophysics Journal*, *24*, 99-106.

Zhang, N., Xiong, J., Zhong, J., & Leatham, K. (2018, June). Gaussian process regression method for classification for high-dimensional data with limited samples. In *2018 Eighth*

International Conference on Information science and technology (ICIST) (pp. 358-363). IEEE.

Zhang, G., Tang, R., Niu, S., Si, H., Yang, Q., Bizimungu, B., Regan, S., & Li, X. Q. (2020). Effects of earliness on heat stress tolerance in fifty potato cultivars. *American Journal of Potato Research*, *97*, 23-32.

Zhang, B., Dong, Z., Sui, X., Gao, J., & Feng, L. (2024). Detection of water content in tomato stems by electrical impedance spectroscopy: preliminary study. *Computers and Electronics in Agriculture*, *219*, 108755.

Zhou, Y., Vroegop-Vos, I., Schuurink, R. C., Pieterse, C. M., & Van Wees, S. C. (2017). Atmospheric CO_2 alters resistance of Arabidopsis to *Pseudomonas syringae* by affecting abscisic acid accumulation and stomatal responsiveness to coronatine. *Frontiers in Plant Science*, *8*, 700.

Zhu, Y., Du, M., Jiang, X., Huang, M., & Zhao, J. (2022). Nitric oxide acts as an inhibitor of postharvest senescence in horticultural products. *International Journal of Molecular Sciences*, *23*(19), 11512.